

~~OFFICIAL USE ONLY~~

Mission Research Corporation

MRC/COS-R-1311/R1 - SAN
Copy ~~1~~

HEMP SIMULATION TESTS [REDACTED]

FINAL TEST REPORT, Sanitized Version

W. A. Bereuter
S. M. Dunivin

Revised 10 September 1992

Prepared for: Director
Defense Nuclear Agency
6801 Telegraph Road
Alexandria, VA 22310-3398
Contract No. DNA001-91-C-0093
CDRL Item No. 16

Prepared by: MISSION RESEARCH CORPORATION
4935 North 30th Street
Colorado Springs, CO 80919

This work sponsored by the Defense Nuclear Agency
RDT&E RMSS CODE: B 4662 D RV RD 00128 3400 A AF

19981106129

PORTIONS OF DOCUMENT(S) RELEASED
UNDER THE FREEDOM OF INFORMATION ACT
DSWA CASE NO. 97-033

~~OFFICIAL USE ONLY~~

Reproduced From
Best Available Copy

5 U.S.C. 552 (b)(2) and (b)(3)
FOIA Exemptions 2 and 3,
apply to this document.

MRC/COS-R-1311/R1
Copy

HEMP SIMULATION TESTS

FINAL TEST REPORT

**W. A. Bereuter
S. M. Dunivin**

Revised 10 September 1992

Prepared for: Director
Defense Nuclear Agency
6801 Telegraph Road
Alexandria, VA 22310-3398
Contract No. DNA001-91-C-0093
CDRL Item No. 16

Prepared by: MISSION RESEARCH CORPORATION
4935 North 30th Street
Colorado Springs, CO 80919

**This work sponsored by the Defense Nuclear Agency
RDT&E RMSS CODE: B 4662 D RV RD 00128 3400 A AF**

THIS PAGE INTENTIONALLY LEFT BLANK

[Redacted address line]			
1. AGENCY USE ONLY (Leave Blank)	2. REPORT DATE	3. REPORT TYPE AND DATES COVERED	
		Technical	920229 - 920814
4. TITLE AND SUBTITLE HEMP Simulation Tests	5. FUNDING NUMBERS B 4662 D RV RD 00128		
6. AUTHOR(S) Wolfgang A. Bereuter, Stephen M. Dunivin			
7. PERFORMING ORGANIZATION NAME(S) AND ADDRESS(ES) Mission Research Corporation 4935 North 30th Street Colorado Springs, CO 80919	8. PERFORMING ORGANIZATION REPORT NUMBER MRC/COS-R-1311/R1		
9. SPONSORING/MONITORING AGENCY NAME(S) AND ADDRESS(ES) Defense Nuclear Agency 6801 Telegraph Road Alexandria, VA 22310-3398 RAEE/Rooney	10. SPONSORING/MONITORING AGENCY REPORT NUMBER		
11. SUPPLEMENTARY NOTES			
12a. DISTRIBUTION/AVAILABILITY STATEMENT	12b. DISTRIBUTION CODE		
13. ABSTRACT (Maximum 200 words) This report documents the results of the HEMP simulation tests conducted at the [redacted] during May and June 1992. The following tests were performed: [redacted] communications antennas were illuminated with CW fields and the field-to-antenna coupling transfer functions were measured.			
14. SUBJECT TERMS HEMP, MIL-STD-188-125, Long Pulse, Intermediate Pulse, MHD-EMP	15. NUMBER OF PAGES		
	16. PRICE CODE		
17. SECURITY CLASSIFICATION OF REPORT Unclassified	18. SECURITY CLASSIFICATION OF THIS PAGE Unclassified	19. SECURITY CLASSIFICATION OF ABSTRACT Unclassified	20. LIMITATION OF ABSTRACT Unlimited

~~CLASSIFIED BY:~~

~~DECLASSIFY ON:~~

SECURITY CLASSIFICATION OF THIS PAGE

~~Unclassified~~

PREFACE

This work was sponsored by the Defense Nuclear Agency under the Advanced FGBC4I EMP Testing (AFEMPT) program. The DNA project officer for this effort is MAJ Michael R. Rooney.

CONVERSION TABLE

Conversion factors for U.S. Customary to metric (SI) units of measurement



angle	1.000×10^{-10}	radians (rad)
atmosphere (standard)	$1.013 25 \times 10^{-4}$	bite Pascal (bPa)
bar	$1.000 000 \times 10^{-4}$	bite Pascal (bPa)
barn	$1.000 000 \times 10^{-28}$	barn ² (m^2)
British Thermal unit (Thermodynamic)	$1.054 359 \times 10^{-9}$	joule (J)
coulomb (Thermodynamic)	$1.000 000$	joule (J)
cal (Thermodynamic)/cm ²	$1.000 000 \times 10^{-4}$	megajoule/m ² (MJ/m^2)
calorie	$1.000 000 \times 10^{-4}$	megajoule (MJ)
degree (angle)	$1.000 000 \times 10^{-4}$	radian (rad)
degree Fahrenheit	$7.23 = (F^\circ - 459.67)/1.8$	degree Kelvin (K)
electron volt	$1.000 19 \times 10^{-10}$	joule (J)
erg	$1.000 000 \times 10^{-7}$	joule (J)
erg/second	$1.000 000 \times 10^{-7}$	watt (W)
foot	$1.000 000 \times 10^{-1}$	meter (m)
foot-pound-force	$1.333 816$	joule (J)
gallon (U.S. liquid)	$1.000 412 \times 10^{-3}$	cubic meter (m^3)
inch	$2.500 000 \times 10^{-2}$	meter (m)
jerk	$1.000 000 \times 10^{-9}$	joule (J)
joule/kilogram (J/kg) (radiation dose absorbed)	$1.000 000$	Gray (Gy)
kilowatt	4.000	terajoules
kilop (1000 lbf)	$4.448 222 \times 10^{-3}$	newton (N)
kilobarn ² (barn)	$6.094 757 \times 10^{-10}$	bite Pascal (bPa)
kilop	$1.000 000 \times 10^{-4}$	newton-meter/ m^2 $(N\cdot m/m^2)$
liter	$1.000 000 \times 10^{-4}$	meter (m)
mi	$2.500 000 \times 10^{-3}$	meter (m)
mi (international)	$1.000 344 \times 10^{-3}$	meter (m)
ounce	$2.834 952 \times 10^{-2}$	kilogram (kg)
pound-force (lbs standard)	$4.448 222$	newton (N)
pound-force inch	$1.129 844 \times 10^{-1}$	newton-meter (Nm)
pound-force/feet	$1.751 266 \times 10^{-2}$	bite Pascal (bPa)
pound-force/feet ²	$4.708 026 \times 10^{-2}$	bite Pascal (bPa)
pound-force/inch ² (psi)	$6.094 757$	kilogram (kg)
pound-force (lbs international)	$4.535 924 \times 10^{-1}$	kilogram-meter ² $(kg\cdot m^2)$
pound-force-inch ² (moment of inertia)	$4.214 011 \times 10^{-2}$	kilogram/meter ³ (kg/m^3)
psquare-millimeter/inch ²	$1.001 046 \times 10^{-1}$	megray (Gy)
rad (radiation dose absorbed)	$1.000 000 \times 10^{-2}$	centilamb/kilogram (C/kg)
remington		second (s)
sphere	$2.579 760 \times 10^{-4}$	kilogram (kg)
slug	$1.499 390 \times 10^{-1}$	bite Pascal (bPa)
torr (in Hg, °F, °C)	$1.333 22 \times 10^{-1}$	

* The becquerel (Bq) is the SI unit of radioactivity; 1 Bq = 1 event/s.

** The Gray (Gy) is the SI unit of absorbed radiation.

TABLE OF CONTENTS

Section	Page
1 INTRODUCTION	1
2 LONG PULSE CURRENT (E3) INJECTIONS	6
2.1 [REDACTED]	6
2.2 [REDACTED]	13
[REDACTED]	13
[REDACTED]	16
[REDACTED]	27
3 INTERMEDIATE PULSE INJECTION [REDACTED]	35
3.1 COMMON MODE INJECTION	35
3.2 WIRE-TO-GROUND INJECTION	53
4 HEMP COUPLING MEASUREMENTS TO [REDACTED] ANTENNAS	76
4.1 OBJECTIVES AND OVERVIEW OF DATA ACQUIRED	76
4.2 [REDACTED] ANTENNAS TESTED	76
4.2.1 [REDACTED]	83
4.2.2 [REDACTED]	83
4.2.3 [REDACTED]	88
4.2.4 [REDACTED]	88
4.2.5 [REDACTED]	88
4.3 DESCRIPTION OF THE TESTS AND DATA PROCESSING	88
4.3.1 Horizontally Polarized Illumination	88
4.3.2 Vertically Polarized Illumination	94
4.4 HEMP INDUCED ANTENNA CURRENTS	96
4.4.1 Representative Results for Each Antenna	97
4.4.2 Antenna Impedance	97
4.4.3 Measured Stresses vs. Test Requirements	107
5 CONCLUSIONS AND RECOMMENDATIONS	118
6 REFERENCES	122

FIGURES

Figure	Page
Figure 1-1. E2 pulser short circuit current	4
Figure 1-2. E3 pulser short circuit current	5
Figure 2-1. [REDACTED] current injected at [REDACTED] pulser voltage (file 3C000ABC)	7
Figure 2-2. [REDACTED] current injected at [REDACTED] pulser voltage; expanded time scales (file 3C000ABC)	8
Figure 2-3. [REDACTED]	8
Figure 2-4. [REDACTED]	10
Figure 2-5. [REDACTED]	10
Figure 2-6. [REDACTED]	11
Figure 2-7. [REDACTED]	11
Figure 2-8. [REDACTED]	11
Figure 2-9. [REDACTED]	12
Figure 2-10. [REDACTED], current injected at [REDACTED] pulser voltage (file G17900AC)	12
Figure 2-11. [REDACTED] current injected at [REDACTED] pulser voltage, expanded time scale (file G17900AC)	14
Figure 2-12. [REDACTED]	15
Figure 2-13. E3 common mode injection, [REDACTED] (file 3C0024AV)	17
Figure 2-14. E3 common mode injection, [REDACTED], expanded time scale (file 3C0024AV)	17
Figure 2-15. [REDACTED] (file 3C0024AC)	18
Figure 2-16. [REDACTED] (file 3C0024AC)	18
Figure 2-17. E3 common mode injection, [REDACTED] (file 3C0025AC)	19
Figure 2-18. E3 common mode injection, [REDACTED], expanded time scale (file 3C0025AC)	19

FIGURES

Figure

Page

Figure 2-19.	20
Figure 2-20.	E3 wire-to-ground injection, input current (file 3A0021AC)	21
Figure 2-21.	E3 wire-to-ground injection, input current expanded time scale (file 3A0021AC)	21
Figure 2-22.	E3 wire-to-ground injection, [REDACTED] (file 3A0025BC)	22
Figure 2-23.	[REDACTED] expanded	22
Figure 2-24.	E3 wire-to-ground injection, [REDACTED] (file 3A0026BC)	23
Figure 2-25.	E3 wire-to-ground injection, [REDACTED] expanded	23
Figure 2-26.	E3 wire-to-ground injection, input current (file 3A0021CC)	24
Figure 2-27.	E3 wire-to-ground injection, input current expanded time scale (file 3A0021CC)	24
Figure 2-28.	E3 wire-to-ground injection, [REDACTED] (file 3A0027BC)	25
Figure 2-29.	E3 wire-to-ground injection, [REDACTED] expanded	25
Figure 2-30.	E3 wire-to-ground injection, [REDACTED] (file 3A0028BC)	26
Figure 2-31.	E3 wire-to-ground injection, [REDACTED] expanded	26
Figure 2-32.	[REDACTED]	28
Figure 2-33.	[REDACTED]	30
Figure 2-34.	[REDACTED]	30
Figure 2-35.	[REDACTED]	31
Figure 2-36.	[REDACTED]	31
Figure 2-37.	[REDACTED]	32
Figure 2-38.	[REDACTED]	32
Figure 2-39.	[REDACTED]	33
Figure 2-40.	[REDACTED]	33
Figure 2-41.	[REDACTED]	34

FIGURES

Figure	Page
Figure 2-42.	34
Figure 3-1.	37
Figure 3-2.	39
Figure 3-3.	40
Figure 3-4.	41
Figure 3-5.	42
Figure 3-6.	43
Figure 3-7.	44
Figure 3-8.	45
Figure 3-9.	46
Figure 3-10.	47
Figure 3-11.	48
Figure 3-12.	49
Figure 3-13.	50
Figure 3-14.	51
Figure 3-15.	52
Figure 3-16.	55
Figure 3-17.	56
Figure 3-18.	57
Figure 3-19.	58
Figure 3-20.	59
Figure 3-21.	60
Figure 3-22.	61
Figure 3-23.	62
Figure 3-24.	63
Figure 3-25.	64
Figure 3-26.	65

FIGURES

Figure

Page

Figure 3-27.	66
Figure 3-28.	67
Figure 3-29.	68
Figure 3-30.	69
Figure 3-31.	70
Figure 3-32.	71
Figure 3-33.	72
Figure 3-34.	73
Figure 3-35.	74
Figure 3-36.	75
Figure 4-1.	82
Figure 4-2.	84
Figure 4-3.	85
Figure 4-4.	86
Figure 4-5.	87
Figure 4-6.	89
Figure 4-7.	90
Figure 4-8.	91
Figure 4-9.	92
Figure 4-10.	95
Figure 4-11.	98
Figure 4-12.	99
Figure 4-13.	100
Figure 4-14.	101
Figure 4-15.	102
Figure 4-16.	103

FIGURES

Figure

Page

Figure 4-17.	104
Figure 4-18.	105
Figure 4-19.	106
Figure 4-20. Coupling path and equivalent circuit	107
Figure 4-21.	108
Figure 4-22.	109
Figure 4-23.	111
Figure 4-24.	112
Figure 4-25.	113
Figure 4-26.	114
Figure 4-27.	115
Figure 4-28.	116
	117

TABLES

Table	Page
Table 2-1.	7
Table 2-2.	9
Table 2-3.	13
Table 2-4	16
Table 2-5.	28
Table 3-1.	38
Table 3-2.	53
Table 4-1.	77
Table 4-2.	83
Table 4-3.	109

SECTION 1

INTRODUCTION

This report documents the results from the tests conducted [REDACTED]

[REDACTED] 3 May to 17

June 1992.

The overall purpose of the test was to acquire test data to support the further development of MIL-STD-188-125 (Reference 1), and to demonstrate the test requirements in this standard in practice. The tests addressed the following objectives:

1. [REDACTED]

2. [REDACTED]

3. [REDACTED]

5. Measure the HEMP field coupling transfer functions to [redacted] communications antennas.

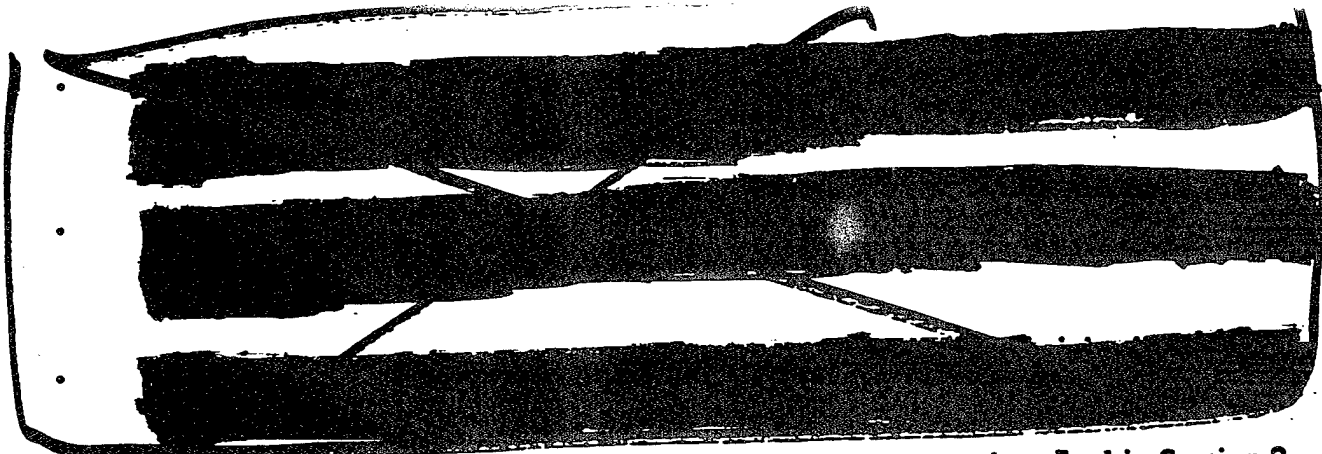
- To define waveforms for injecting antenna lines, and thus verify the hardness of radio equipment against HEMP, measurements at typical antennas are necessary to ensure that the waveforms properly represent the induced threat transients.
- Useful measurements at all antennas were acquired for this purpose.

DOD-STD-2169A specifies the HEMP field environments in terms of three time regimes: The early time (E1) field pulse, the intermediate time (E2) field pulse, and the late time (E3) field pulse.

All three environments induce current pulses on exposed electrical lines. MIL-STD-188-125 defines generic current pulses for each environment: The E1 field environment produces the Short Pulse, the E2 environment produces the Intermediate Pulse, and E3 produces the Long Pulse. [redacted]

Unfortunately, the terminology of DOD-STD-2169A is now also widely used when referring to the coupled currents. For example, the Long Pulse is also known as "E3"; the corresponding pulser is called the "E3 pulser." This short-hand presumably does no harm as long as environments (in Volts/meter) and coupled currents (in Amps) are not confused.

The test [redacted] addressed all three HEMP time regimes:


The tests and measurements acquired for objectives 1, 2, and 3 are described in Section 2.
The Intermediate Pulse test data (objective 4) are contained in Section 3.

Section 4 documents the antenna coupling measurements (objective 5). The conclusions and recommendations are summarized in Section 5. For detailed descriptions of the test activities see Reference 2.

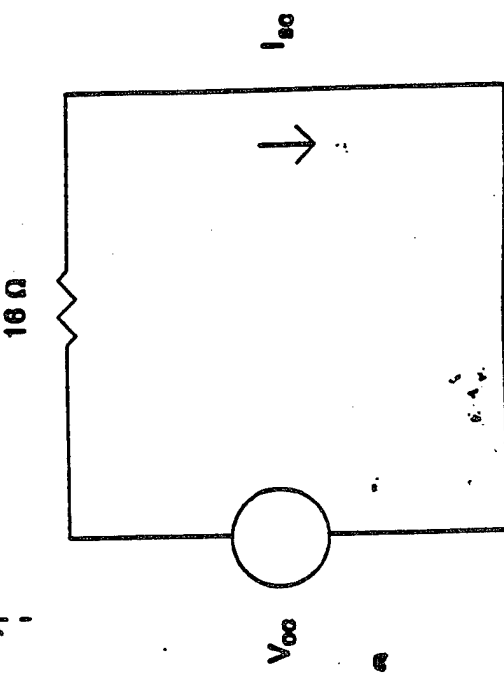
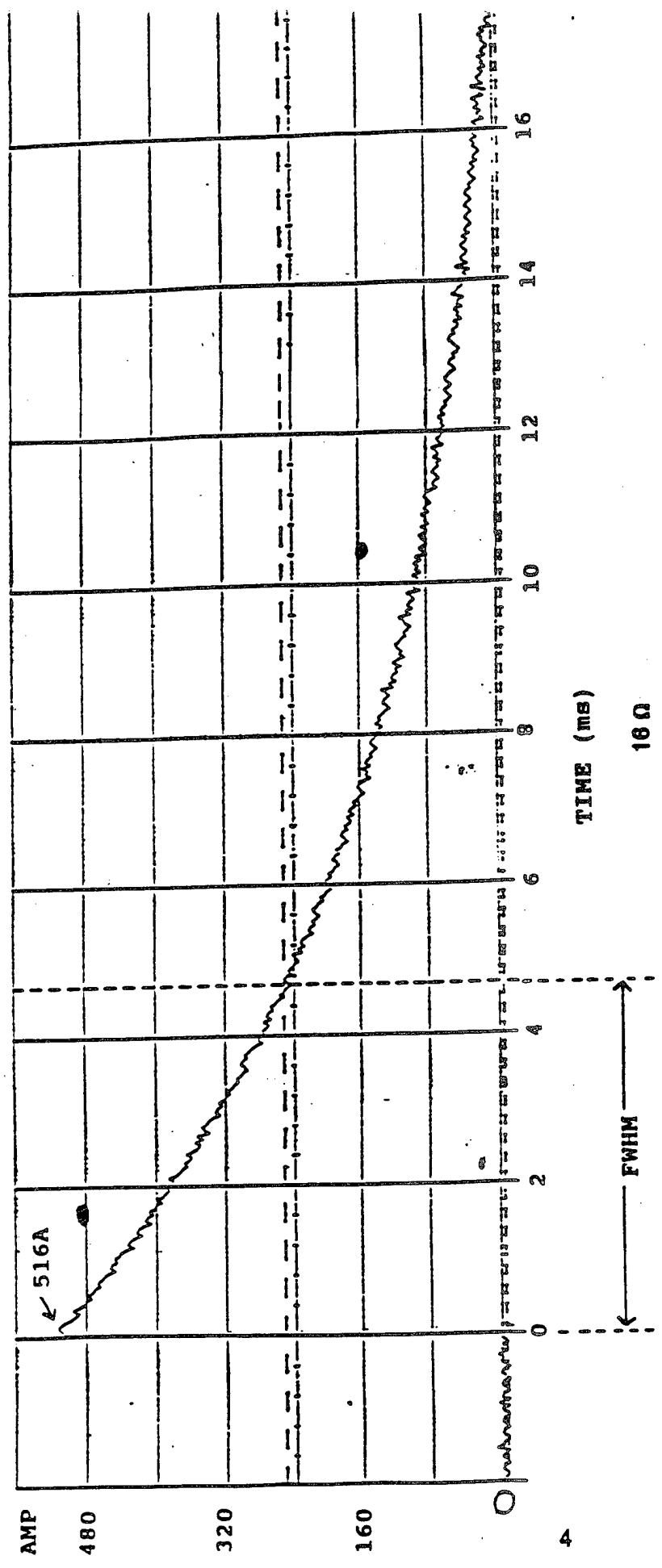


Figure 1-1. E2 pulser short circuit current.

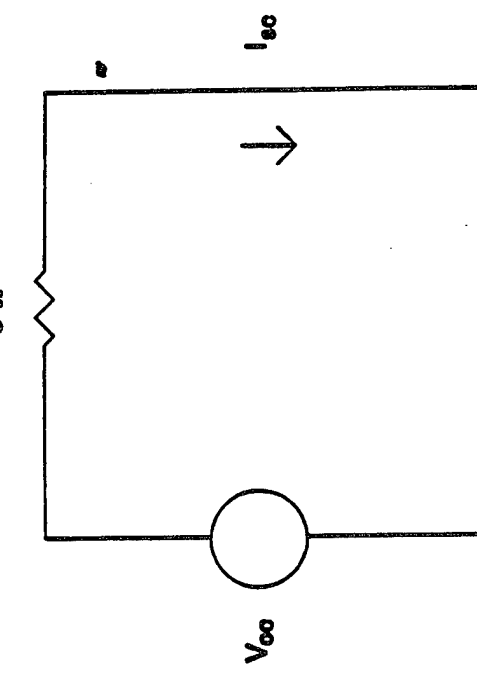
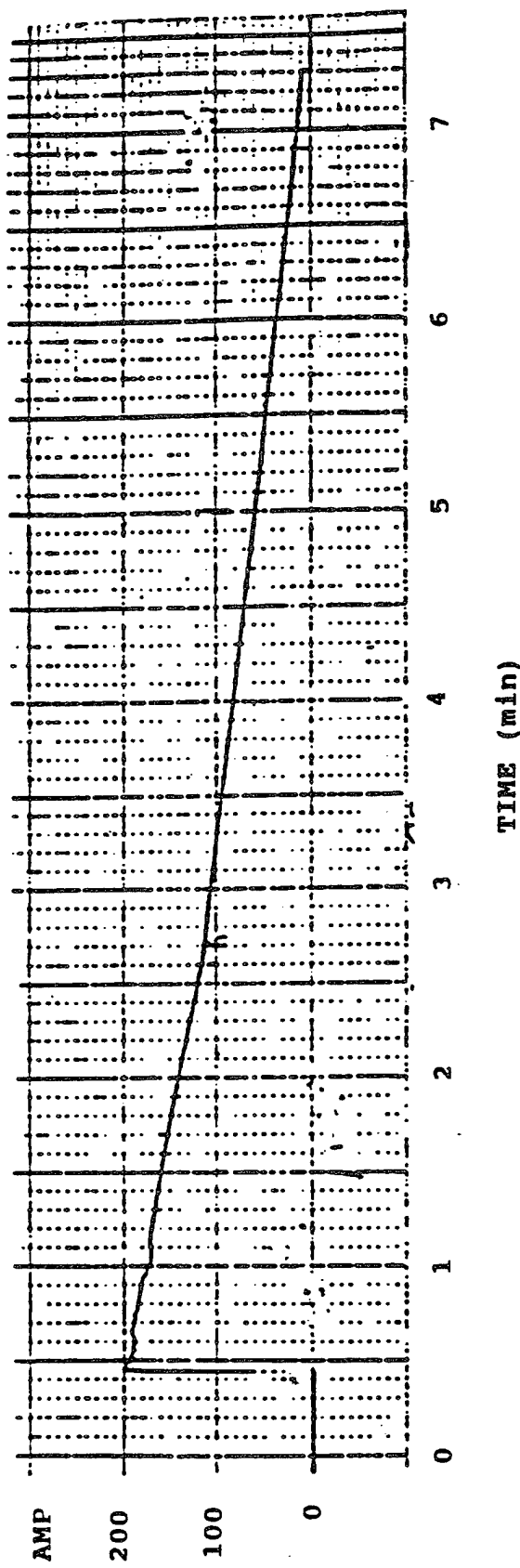


Figure 1-2. E3 pulser short circuit current.

SECTION 2

LONG PULSE CURRENT (E3) INJECTIONS

The current waveform induced by MHD-EMP is specified in MIL-STD-188-125 as a double exponential waveform (200 A peak, less than 0.5 seconds rise time, and at least 100 seconds full-width-at-half-max). The waveform provided by the E3 pulser (Reference 3) meets these requirements.

2.1

[REDACTED] Injections were performed with the pulser output connected [REDACTED]. The injected current was increased stepwise as a precaution as shown in Table 2-1. [REDACTED] The first column lists the pulser voltage for each shot. The second and third columns are the measured peak currents on the pulser output cable and on the return, respectively.

Since the return current is equal to the pulser output current, all coulombs are properly accounted for; i.e., Kirchhoff's circuit equations are satisfied. The last column is the estimated path resistance (R_{path}). It is in series with the pulser source impedance (5 ohms by design). R_{path} can be estimated from the peak pulser voltage V_p and the measured peak input or return current I_{med} as follows:

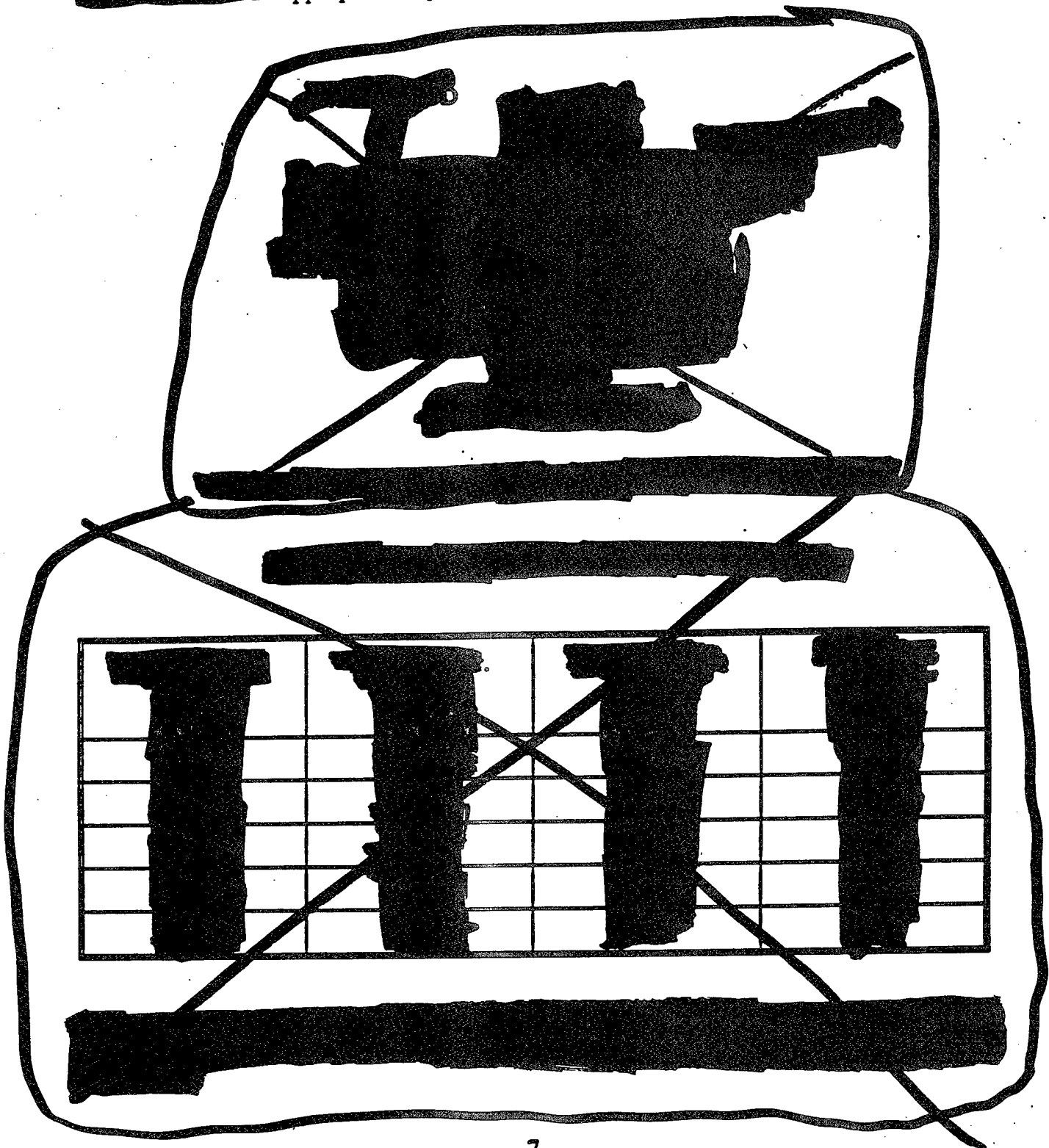
$$R_{PATH} = \frac{V_p}{I_{med}} - 5 \quad (\Omega) \quad (2-1)$$

The calculated values in the last column of Table 2-1 indicate that the path resistance is less than 1 ohm. [REDACTED]

The waveforms were recorded [REDACTED]. The transients were generally sampled every 1 ms. Thus, for a full E3 measurement, there are 360000 samples (9 Mbytes). Consequently, the full time history of the measurements cannot be plotted in a useful manner; instead, narrow time windows were selected in all following displays.

[REDACTED] Figure 2-3 is the same pulse, but with the time scale expanded. The ripples on the E3 pulse

(evident on the blowup of the early time portion)



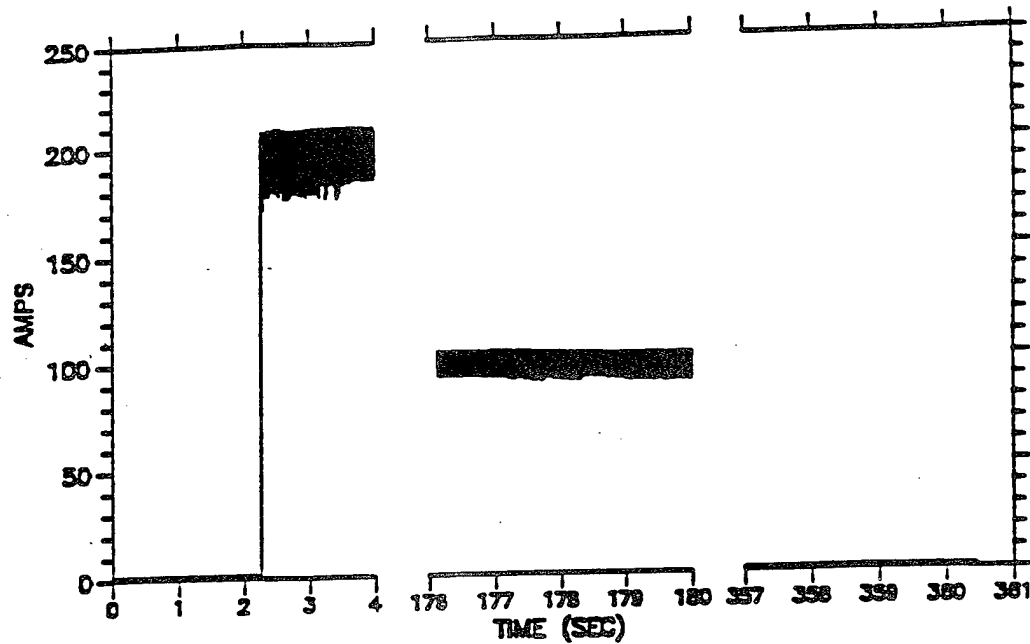


Figure 2-2. [REDACTED] current injected at [REDACTED] pulser voltage (file 3C000ABC).

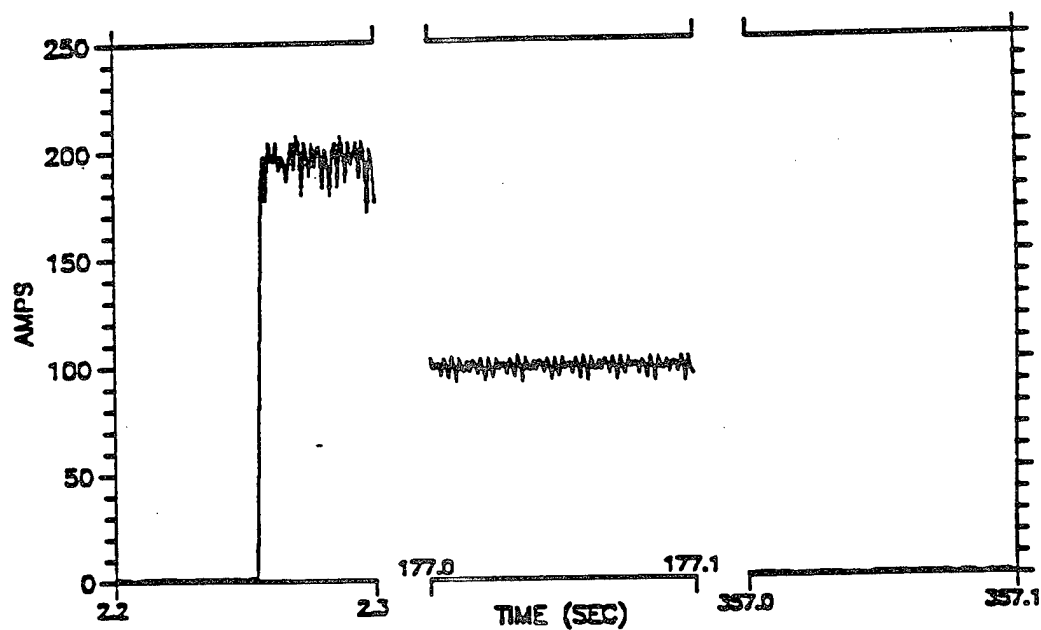


Figure 2-3. [REDACTED] current injected at [REDACTED] pulser voltage; expanded time scales (file 3C000ABC).

Pages 9-13 removed
in its entirety.

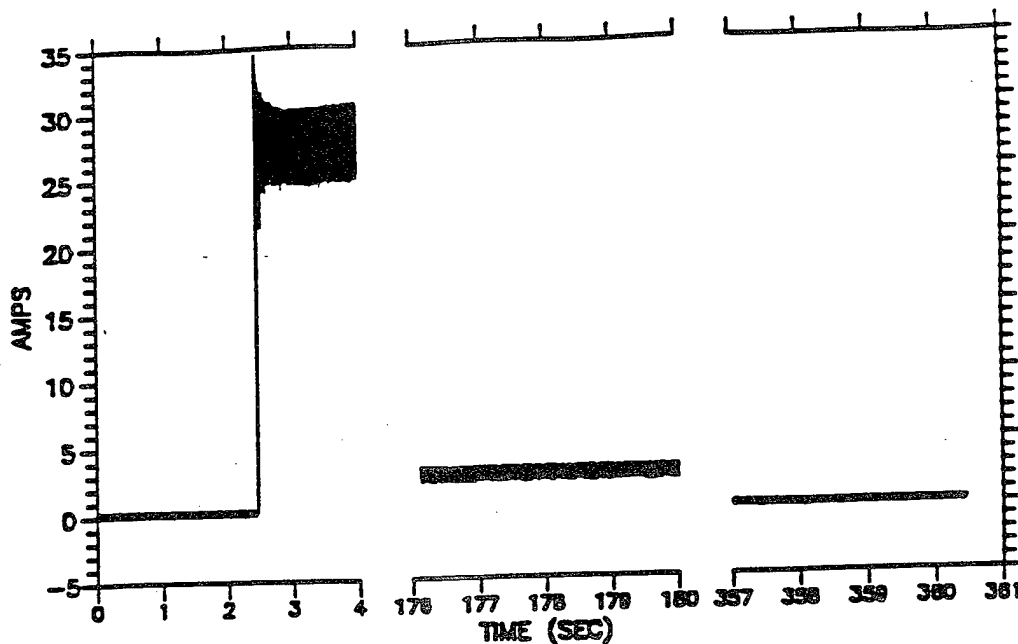


Figure 2-10. [REDACTED] current injected at [REDACTED] pulser voltage (file G17900AC).

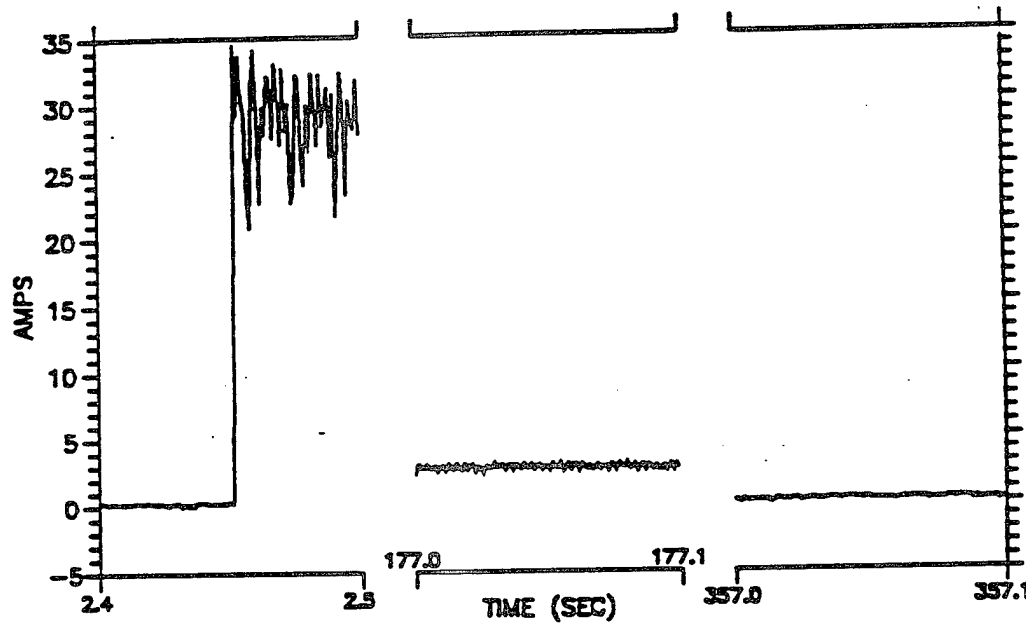


Figure 2-11. [REDACTED] current injected at [REDACTED] pulser voltage, expanded time scale (file G17900AC).

Figures 15 & 16
removed in their
entirety.

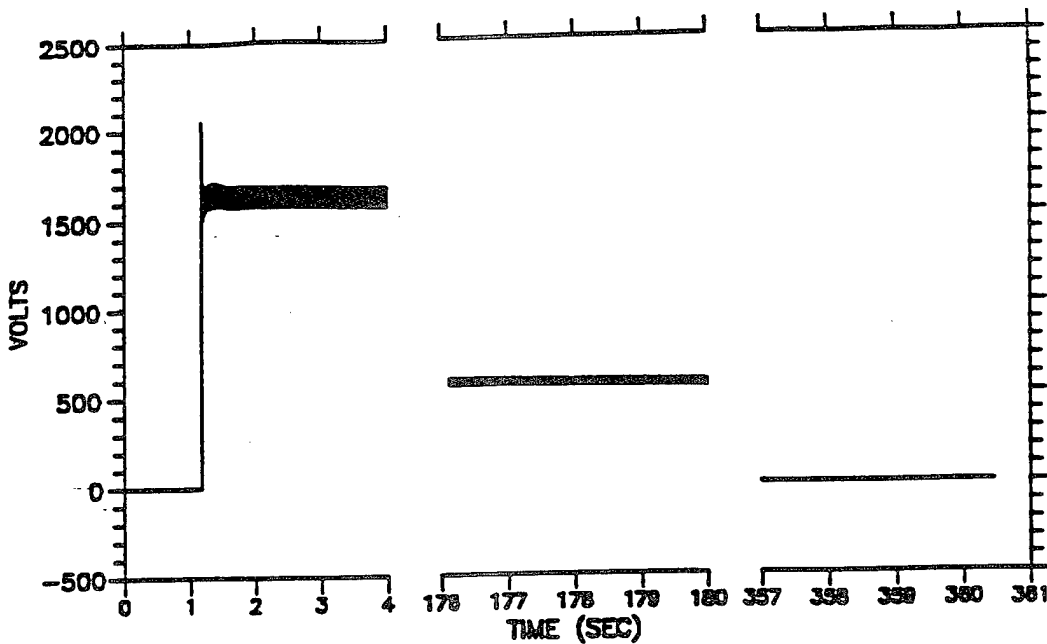


Figure 2-13. E3 common mode injection, [REDACTED] (file 3C0024AV).

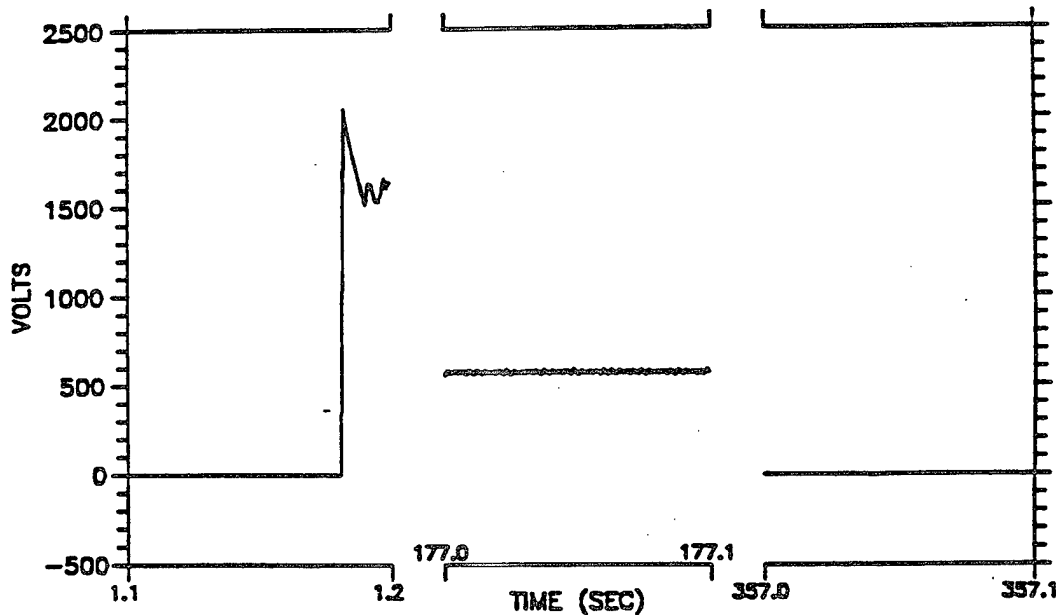


Figure 2-14. E3 common mode injection, [REDACTED], expanded time scale (file 3C0024AV).

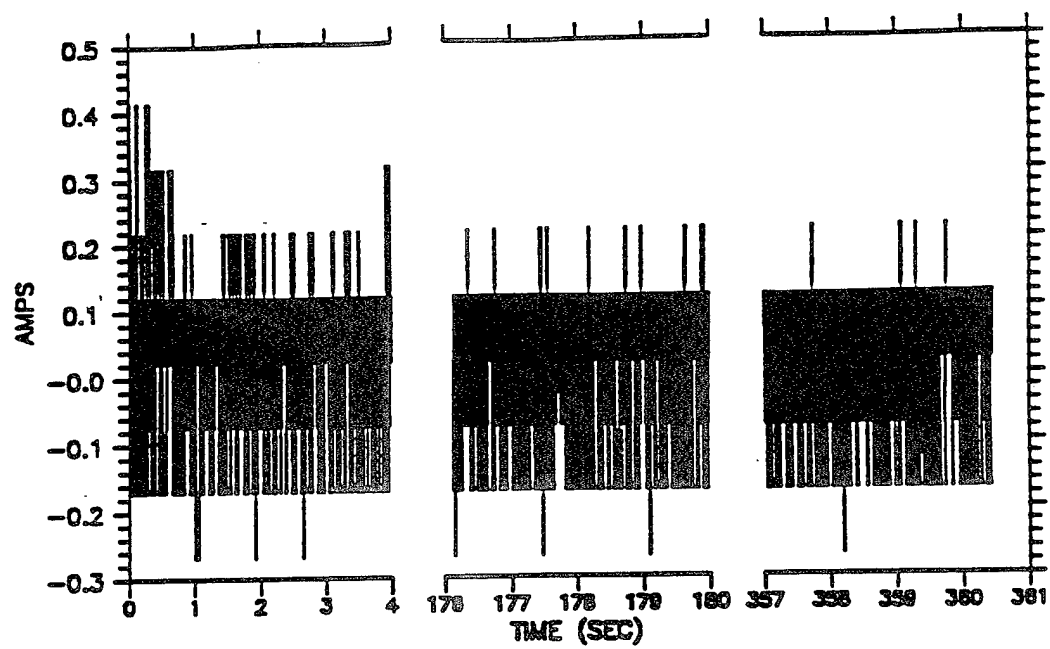


Figure 2-15. [REDACTED] (file 3C0024AC).

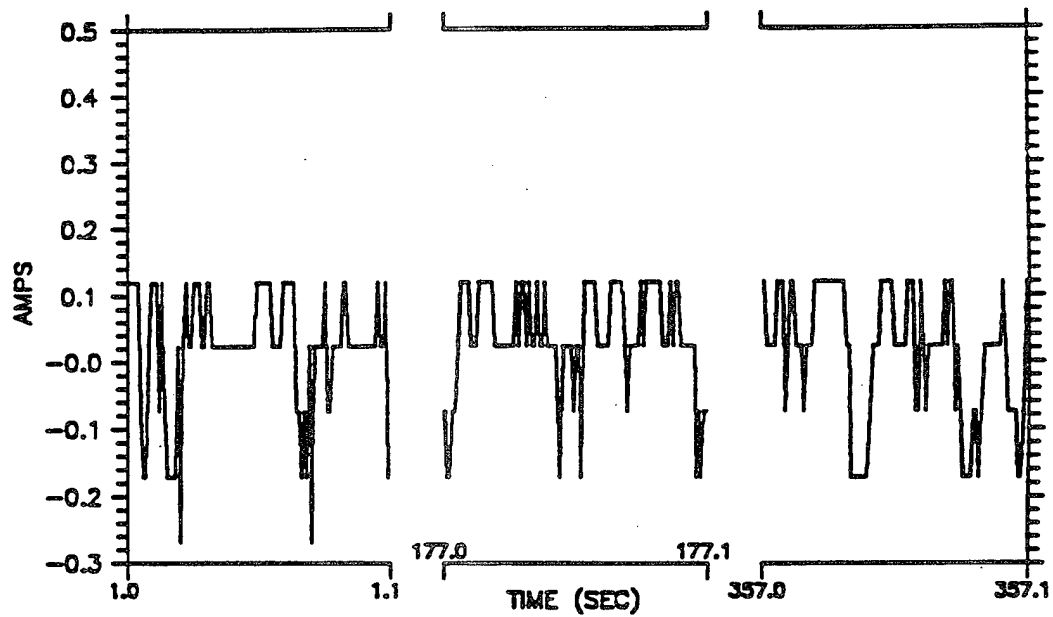


Figure 2-16. [REDACTED] (file 3C0024AC).

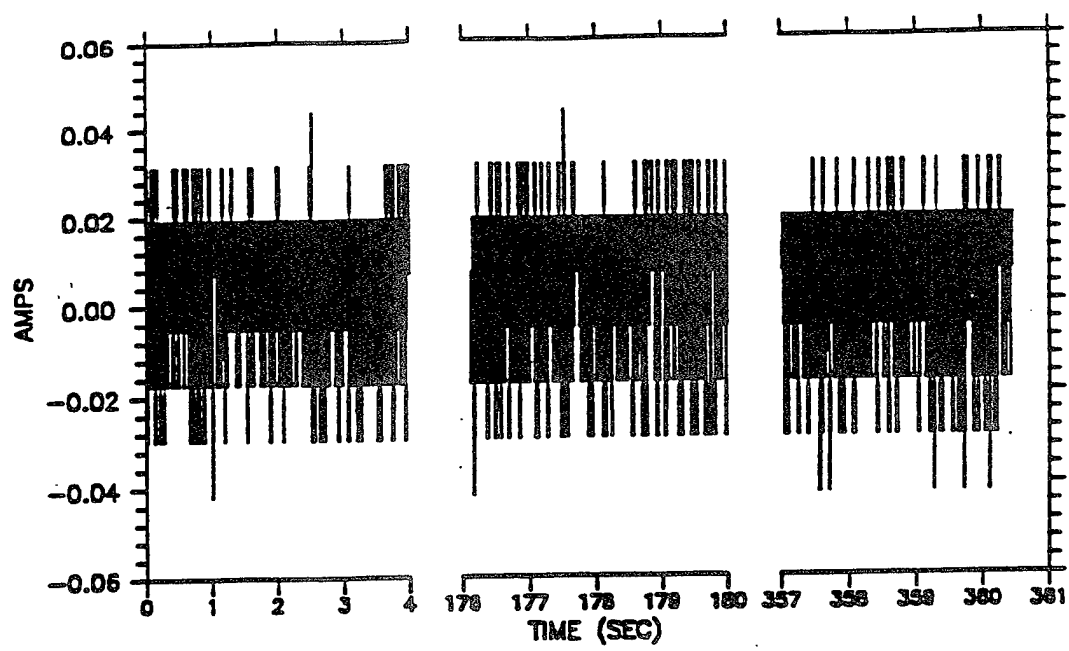


Figure 2-17. E3 common mode injection [REDACTED] file 3C0025AC).

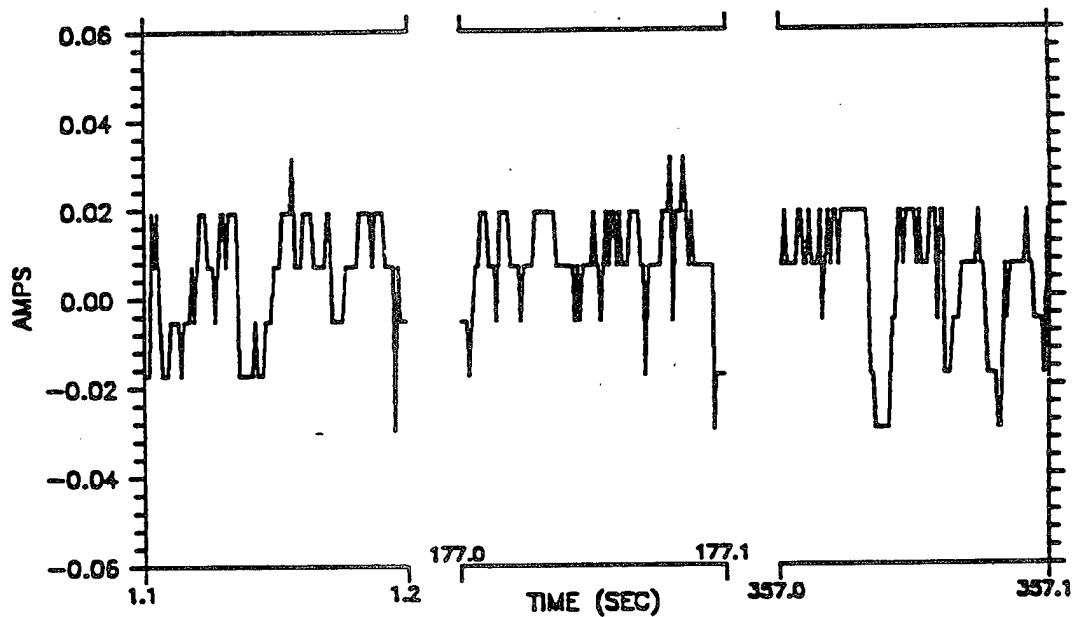


Figure 2-18. E3 common mode injection [REDACTED] expanded time scale (file 3C0025AC).

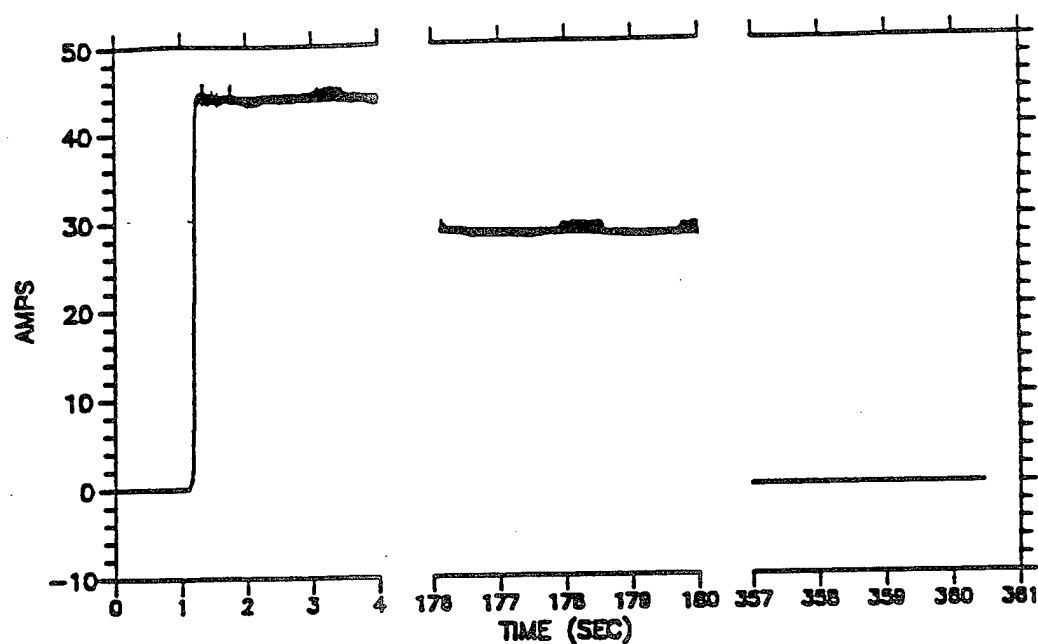


Figure 2-20. E3 wire-to-ground injection, input current (file 3A0021AC).

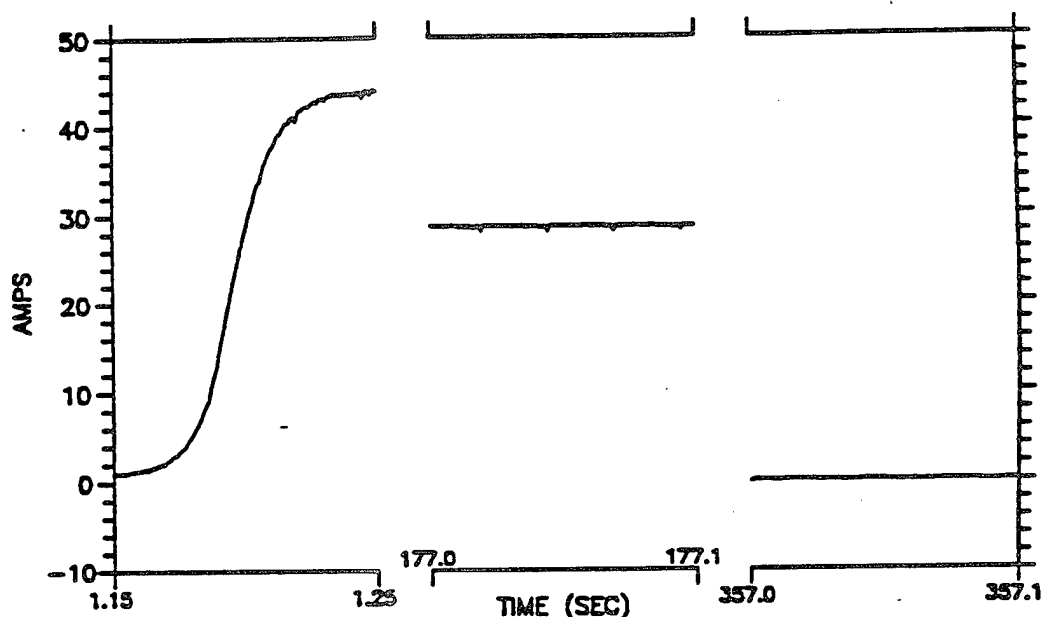


Figure 2-21. E3 wire-to-ground injection, input current expanded time scale (file 3A0021AC).

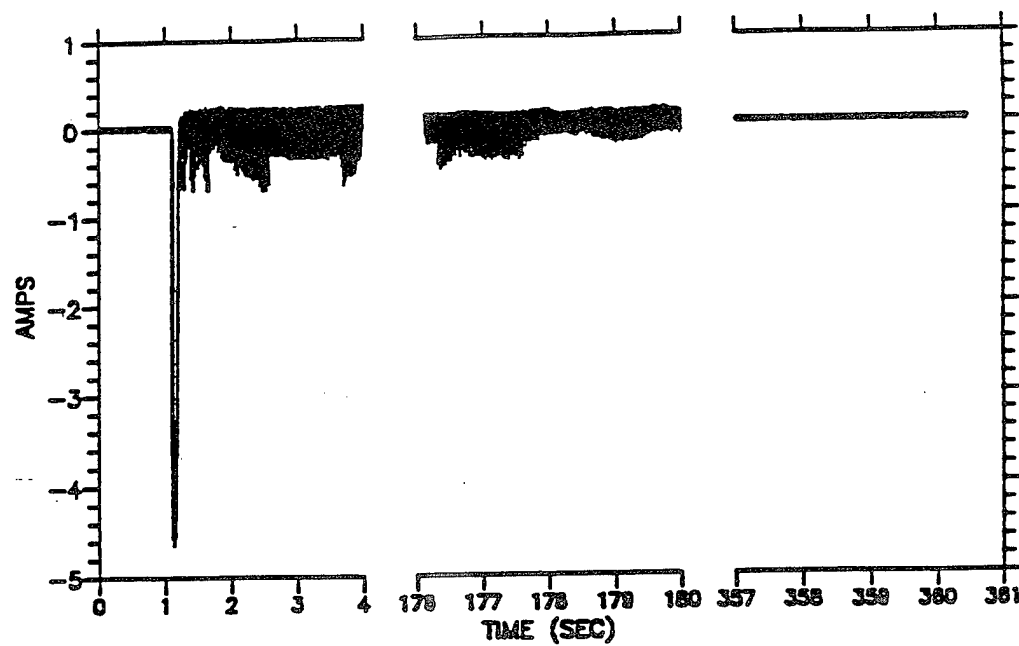


Figure 2-22. E3 wire-to-ground injection [REDACTED] (file 3A0025BC).

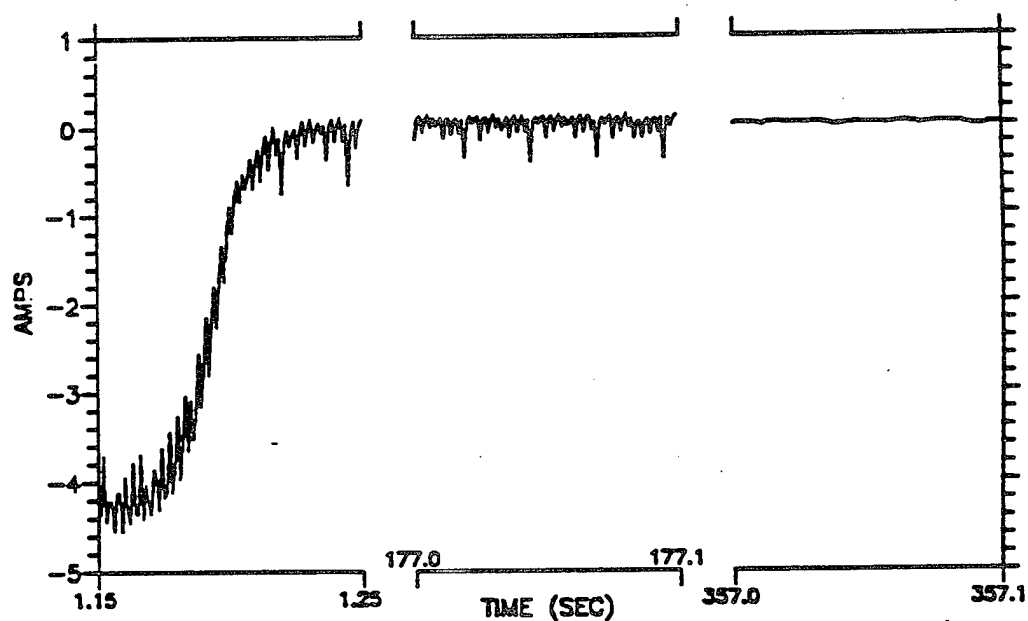


Figure 2-23. E3 wire-to-ground injection, [REDACTED], expanded time scale (file 3A0025BC).

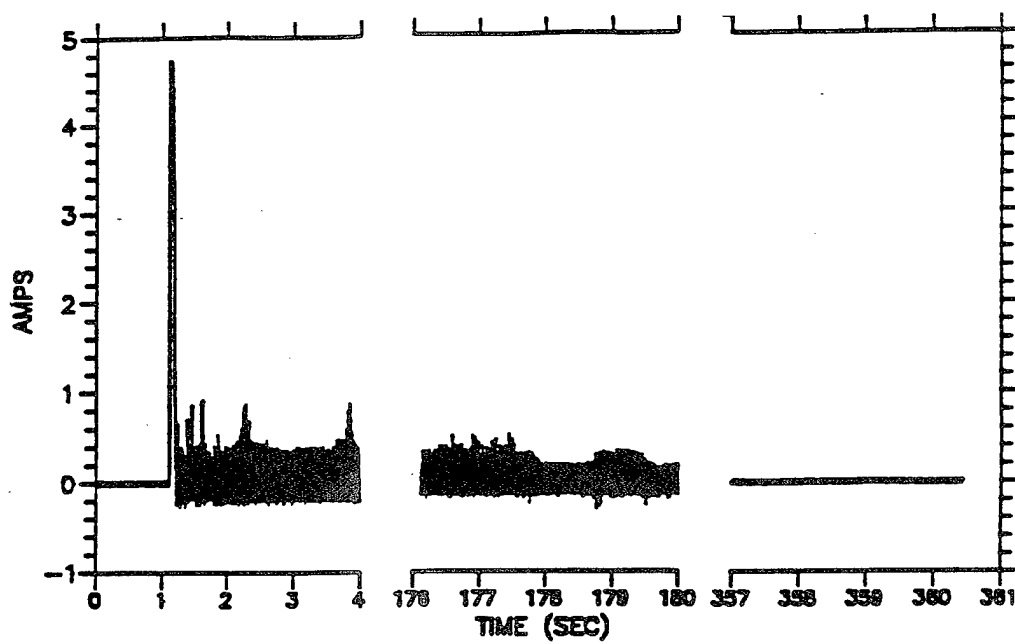


Figure 2-24. E3 wire-to-ground injection, [REDACTED] file 3A0026BC).

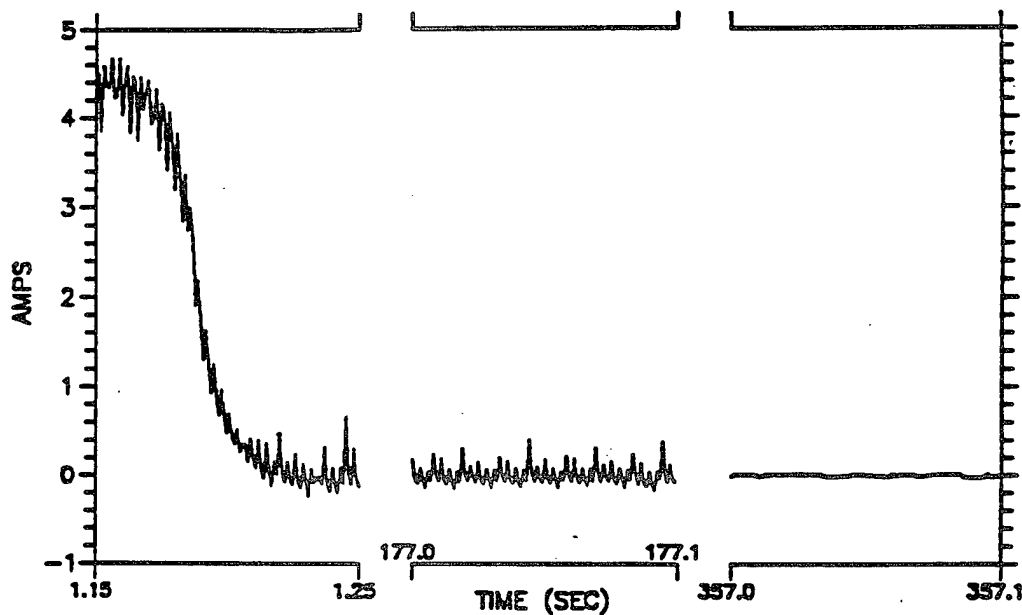


Figure 2-25. E3 wire-to-ground injection, [REDACTED] → expanded time scale (file 3A0026BC).

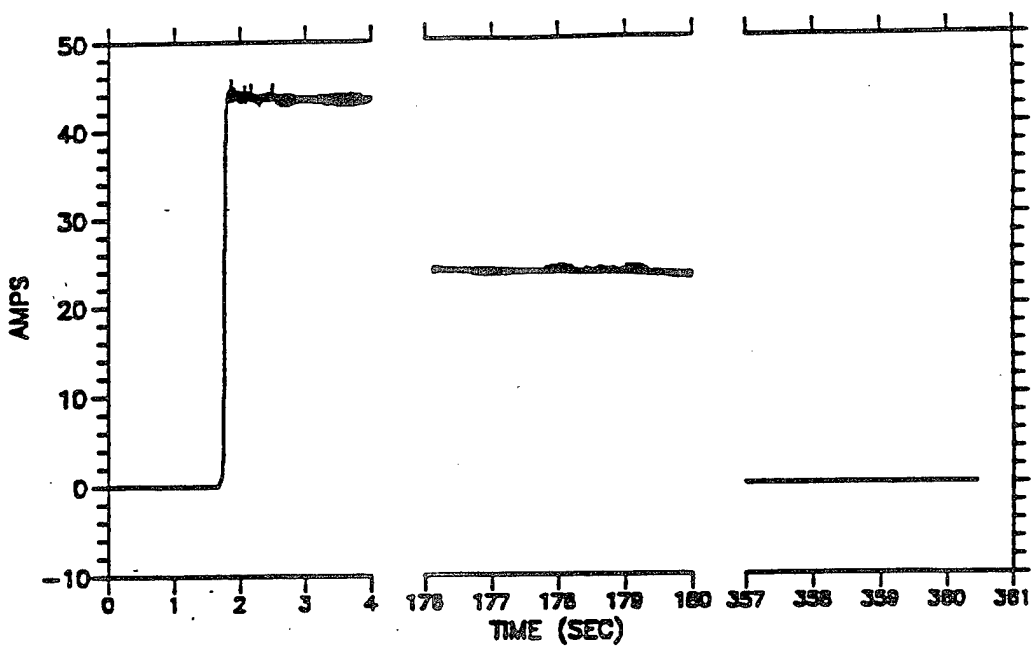


Figure 2-26. E3 wire-to-ground injection, input current (file 3A0021CC).

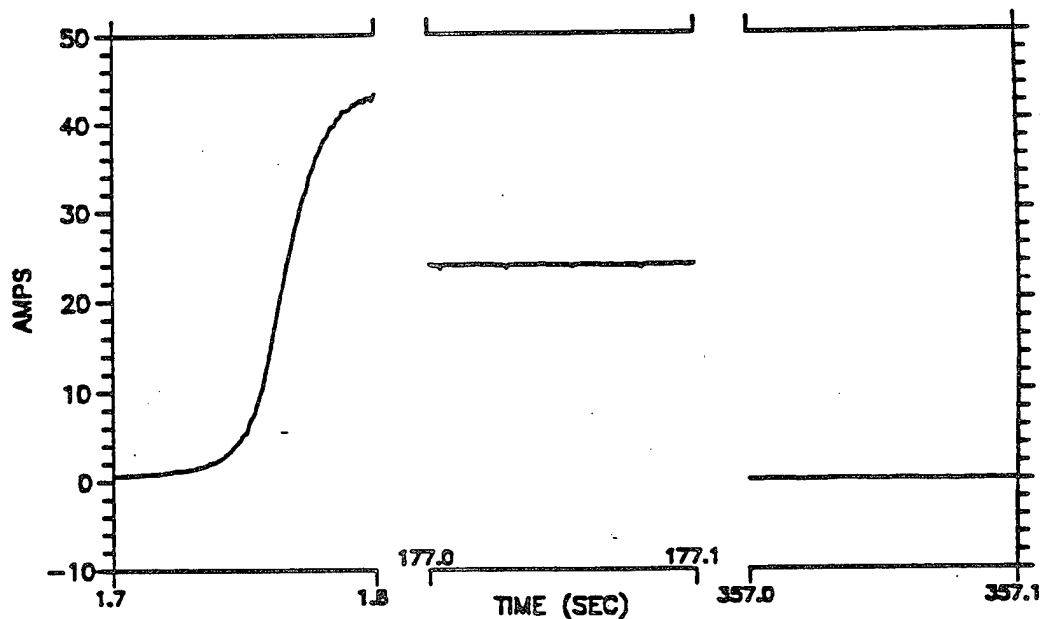


Figure 2-27. E3 wire-to-ground injection, input current expanded time scale (file 3A0021CC).

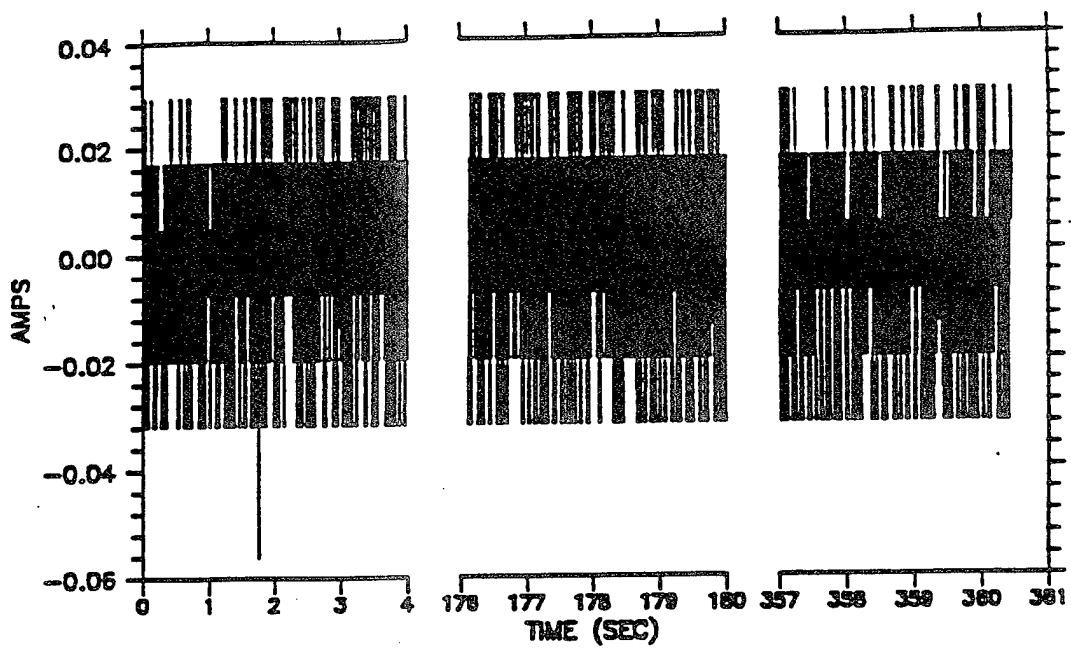


Figure 2-28. E3 wire-to-ground injection, [REDACTED] file 3A0027BC).

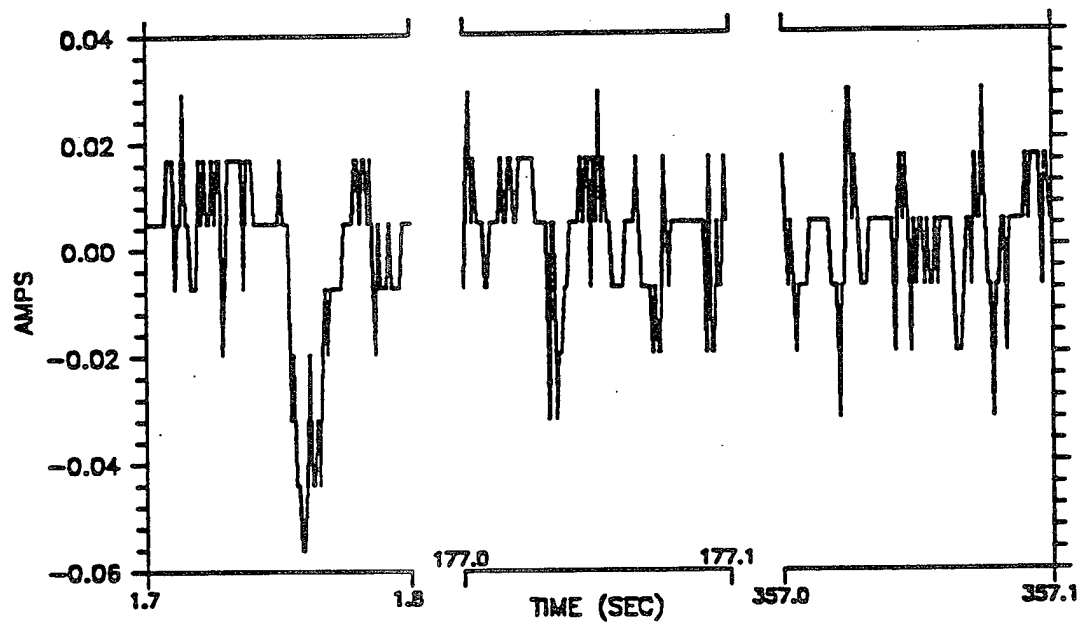


Figure 2-29. E3 wire-to-ground injection, [REDACTED] expanded time scale (file 3A0027BC).

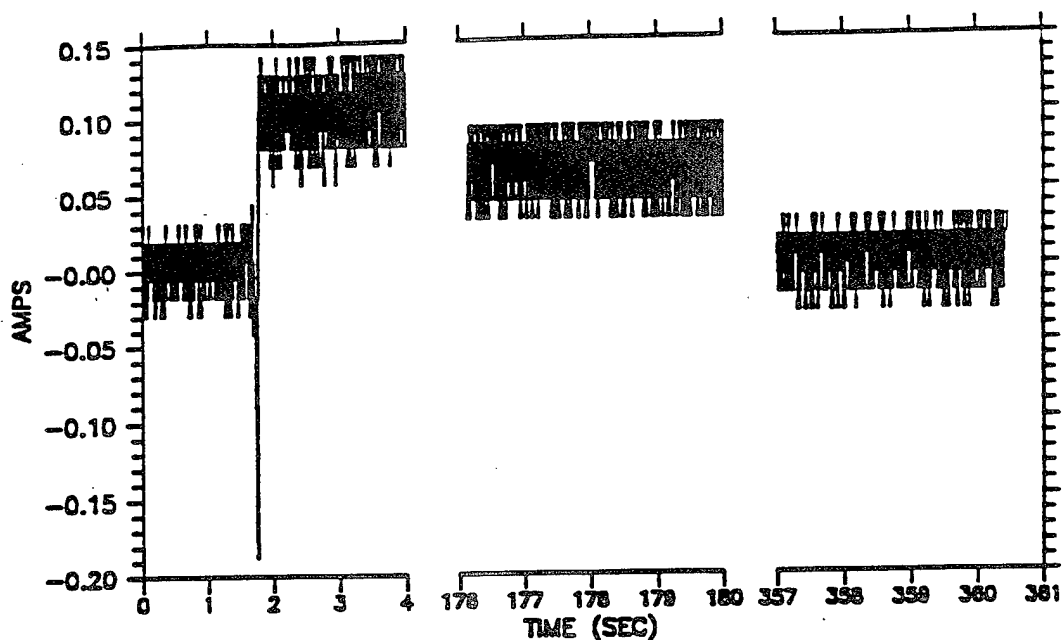


Figure 2-30. E3 wire-to-ground injection, [REDACTED] (file 3A0028BC).

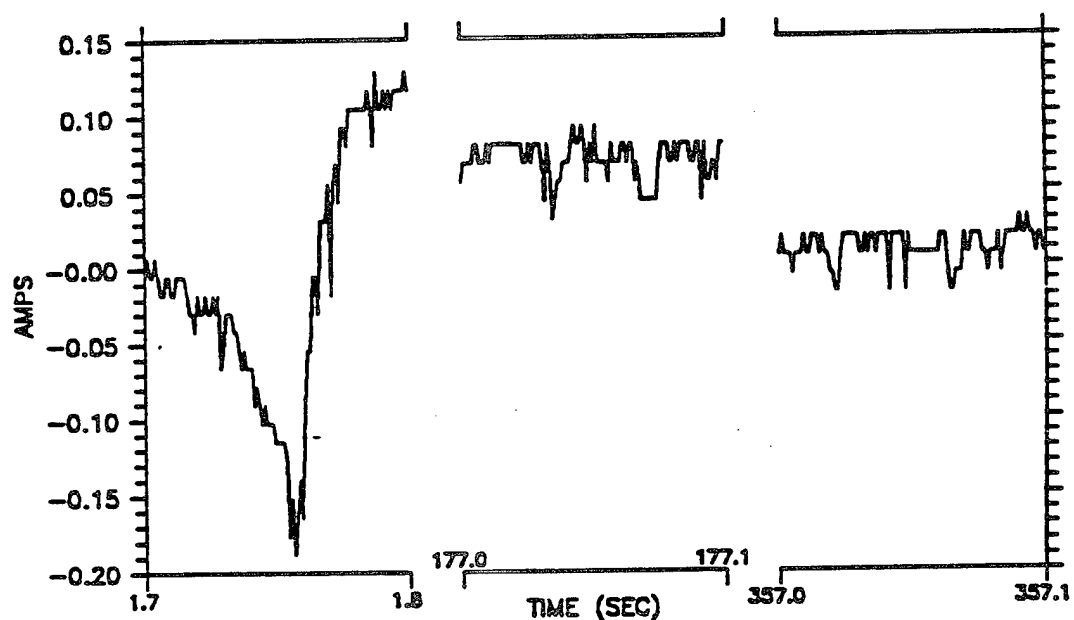
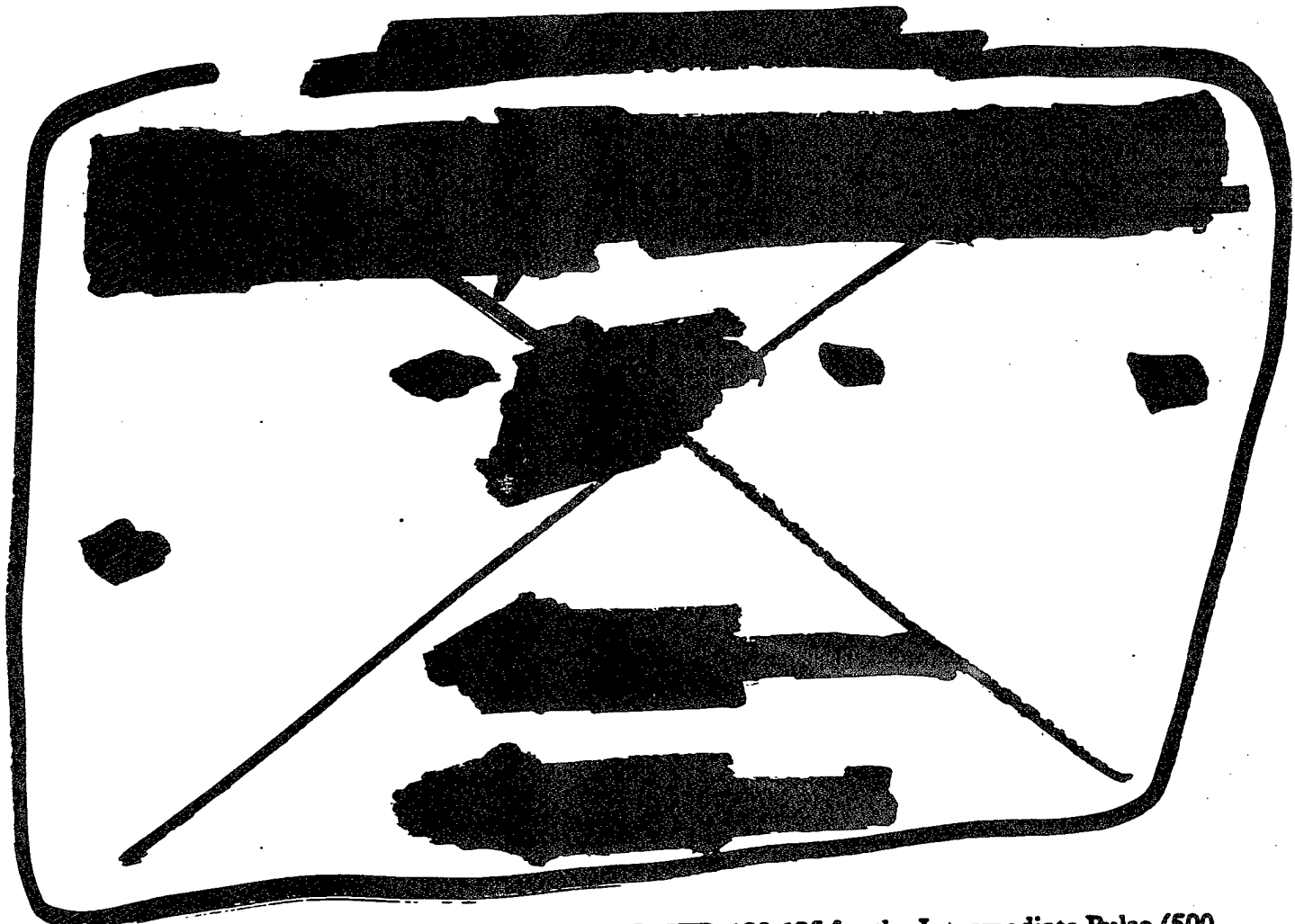


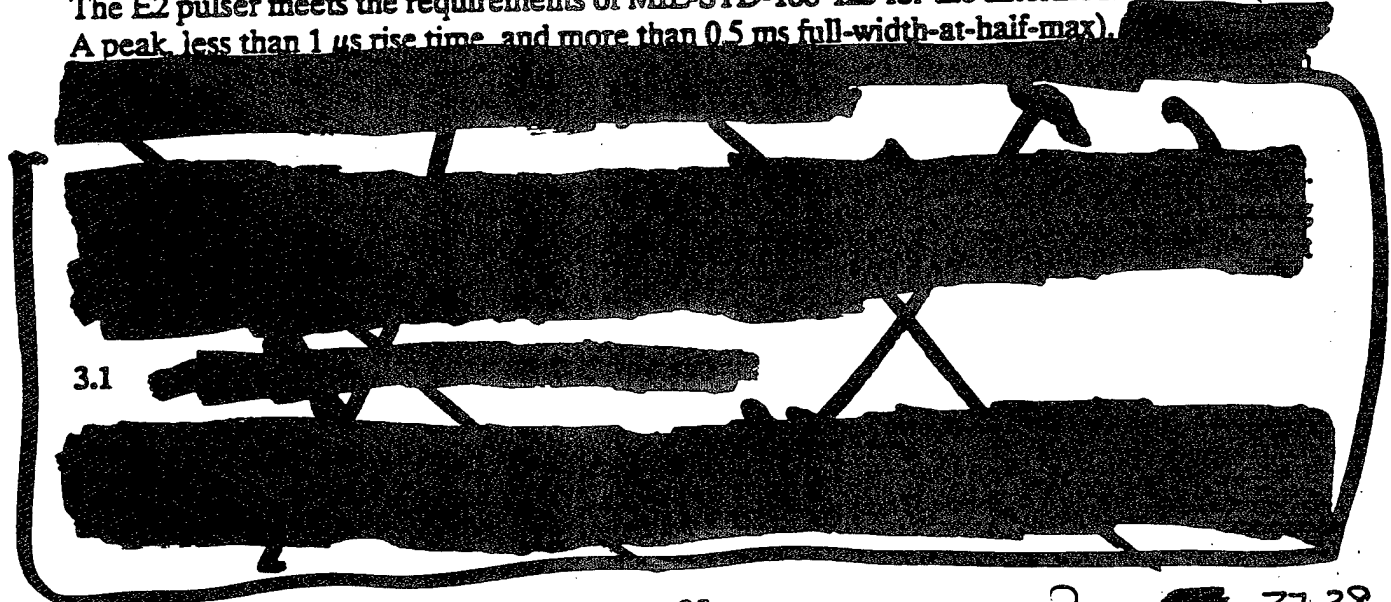
Figure 2-31. E3 wire-to-ground injection, [REDACTED] expanded time scale (file 3A0028BC).

Pages 27-34
removed in their
entirety,

SECTION 3



The E2 pulser meets the requirements of MIL-STD-188-125 for the Intermediate Pulse (500 A peak, less than 1 μ s rise time, and more than 0.5 ms full-width-at-half-max).



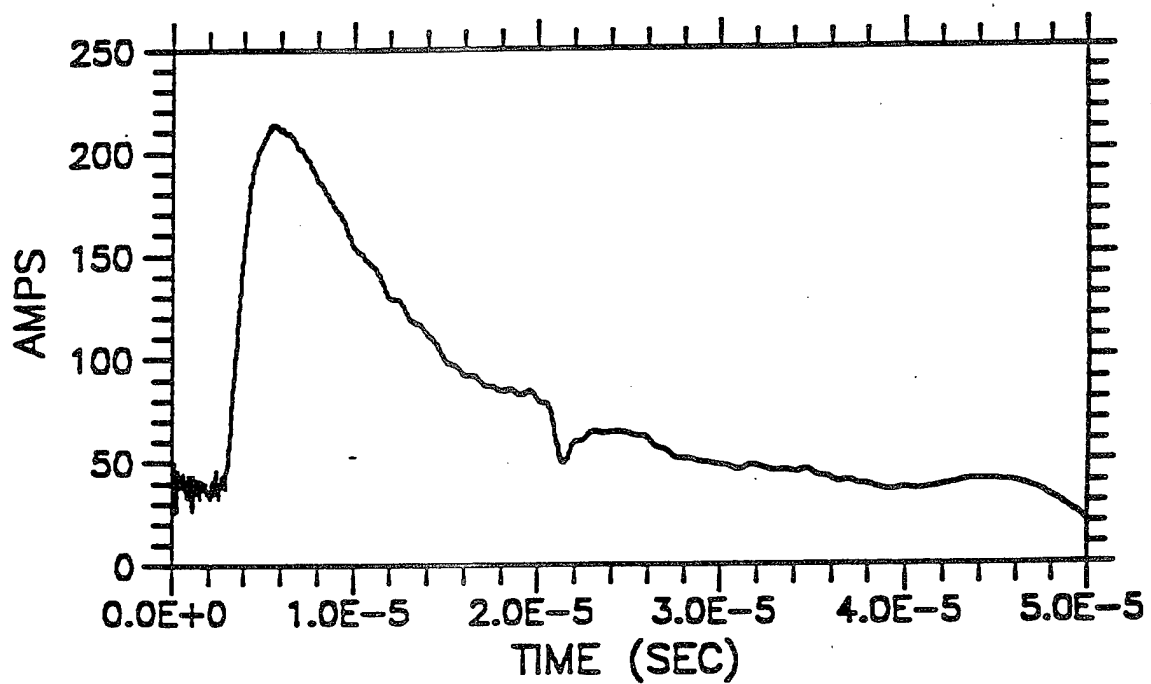
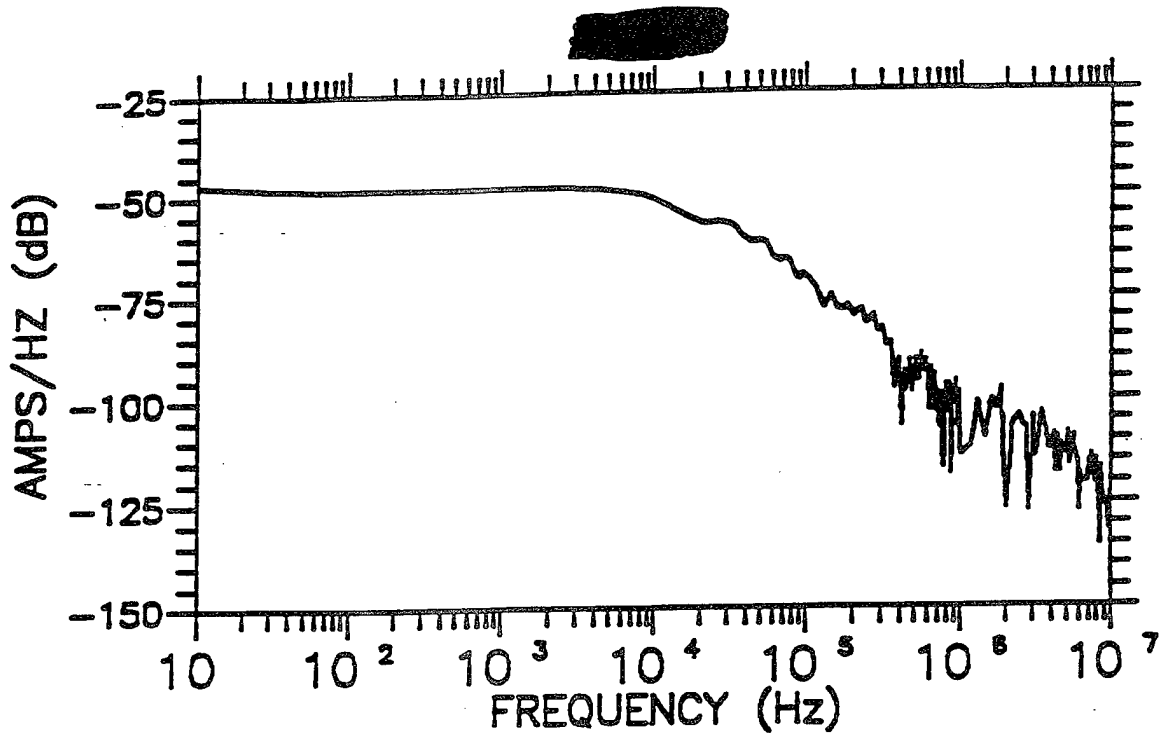


Figure 3-2.

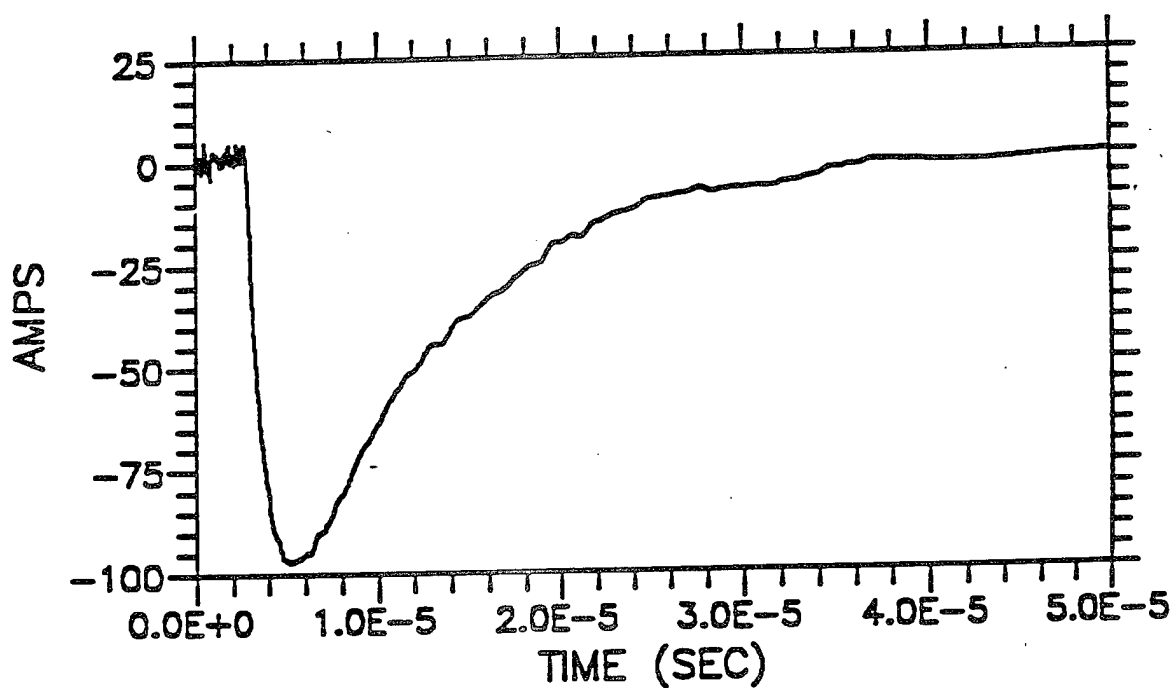
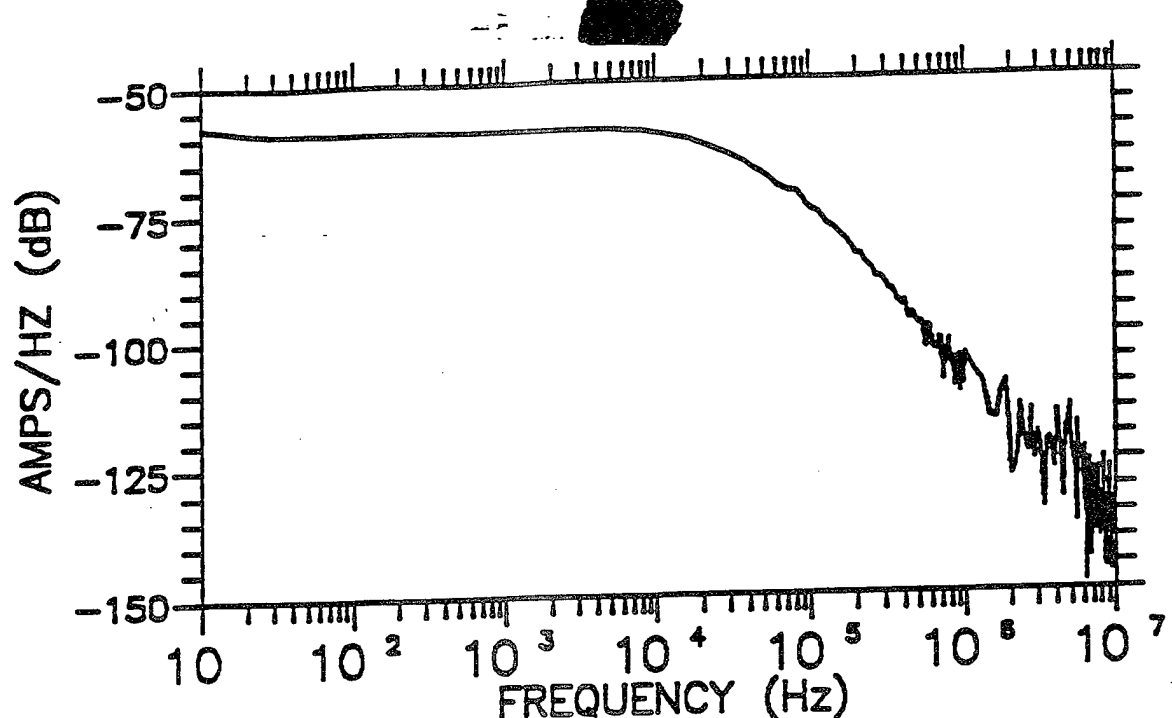


Figure 3-3. [REDACTED] (b).

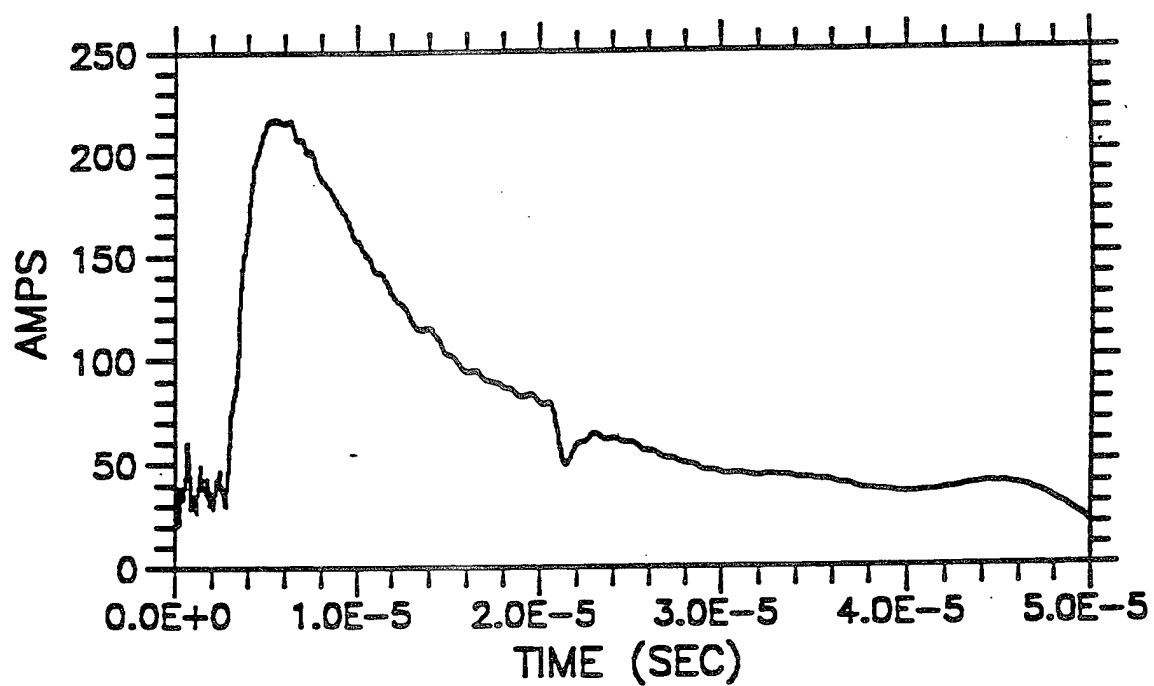
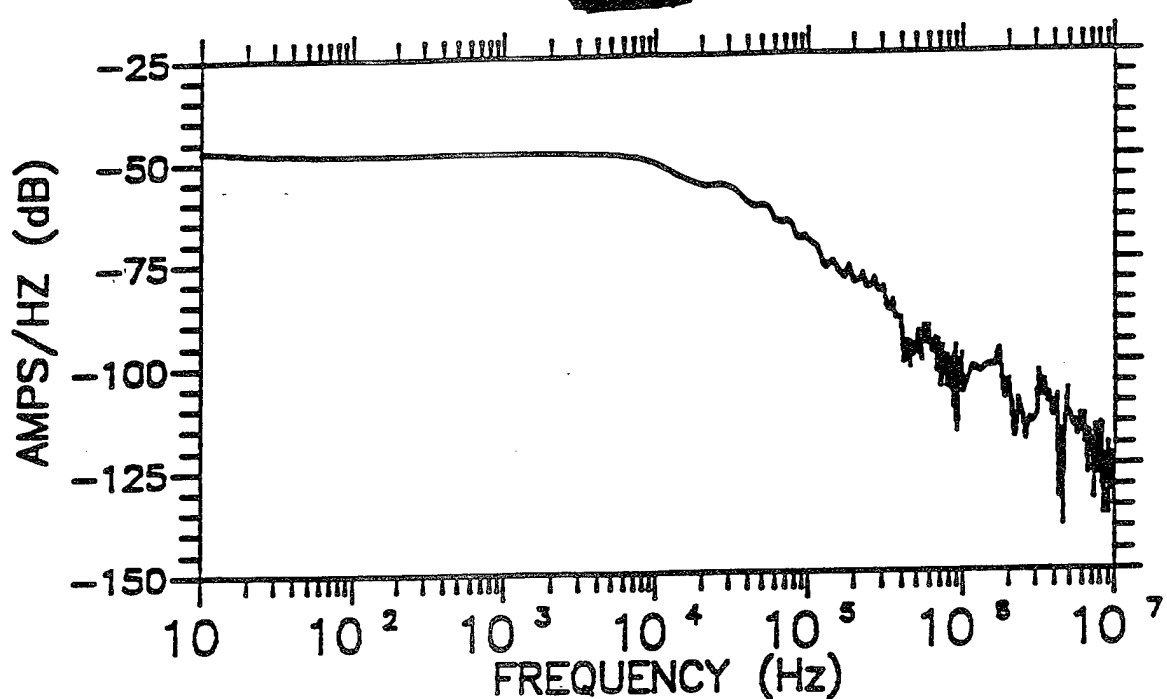


Figure 3-4.

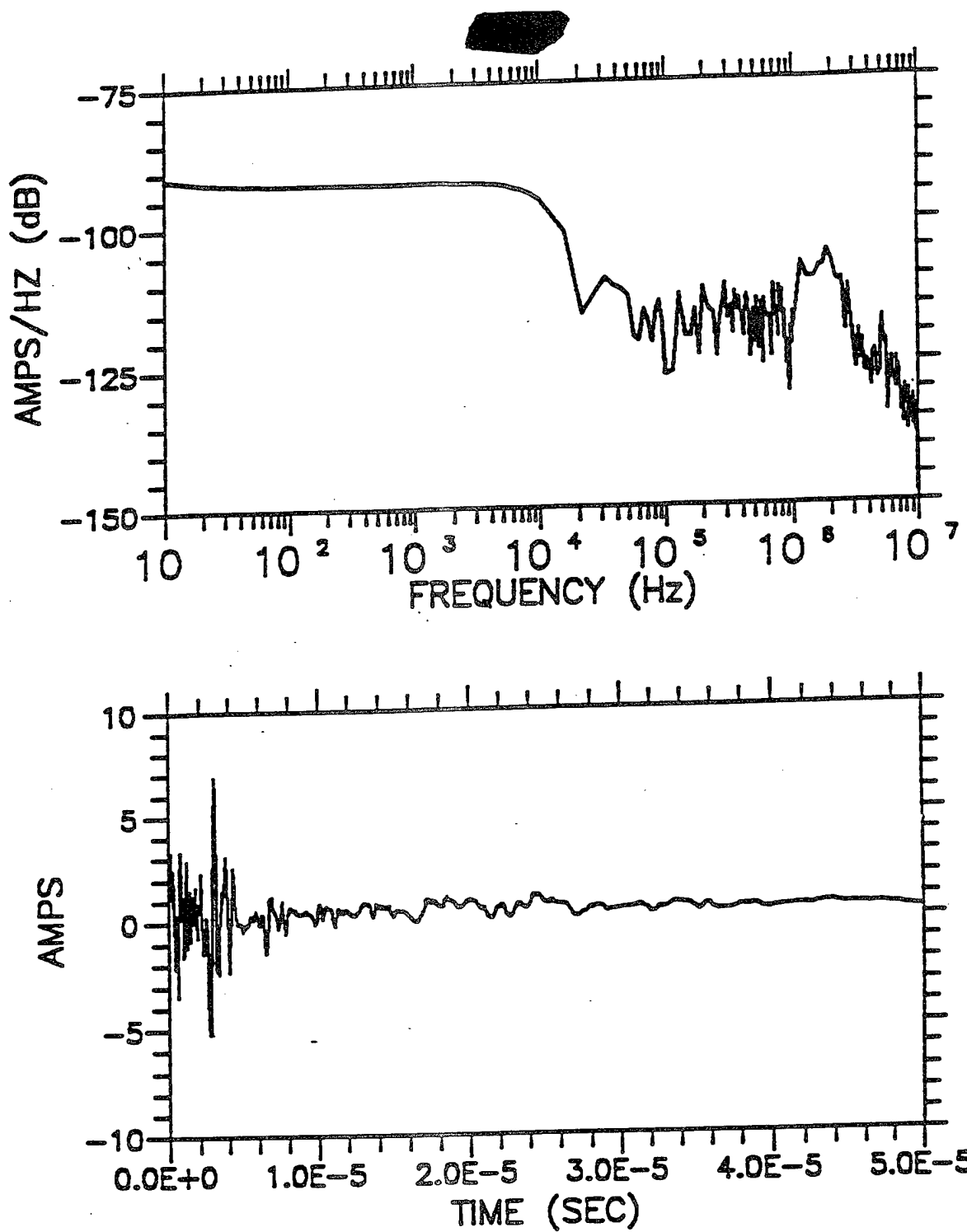


Figure 3-5.

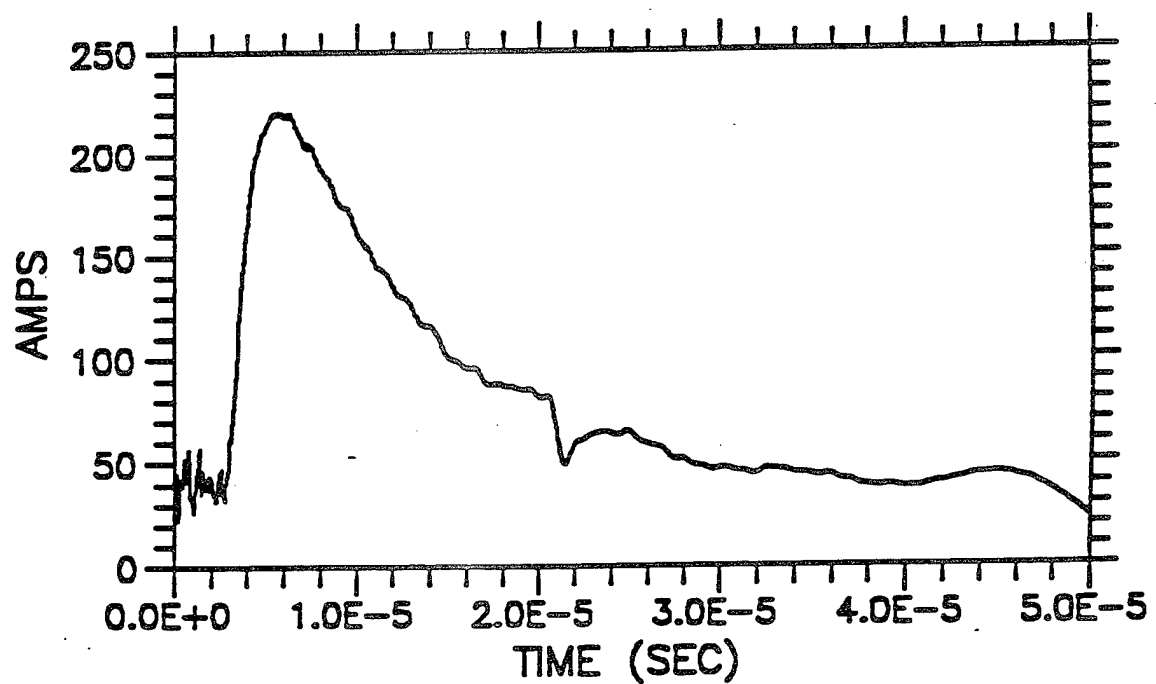
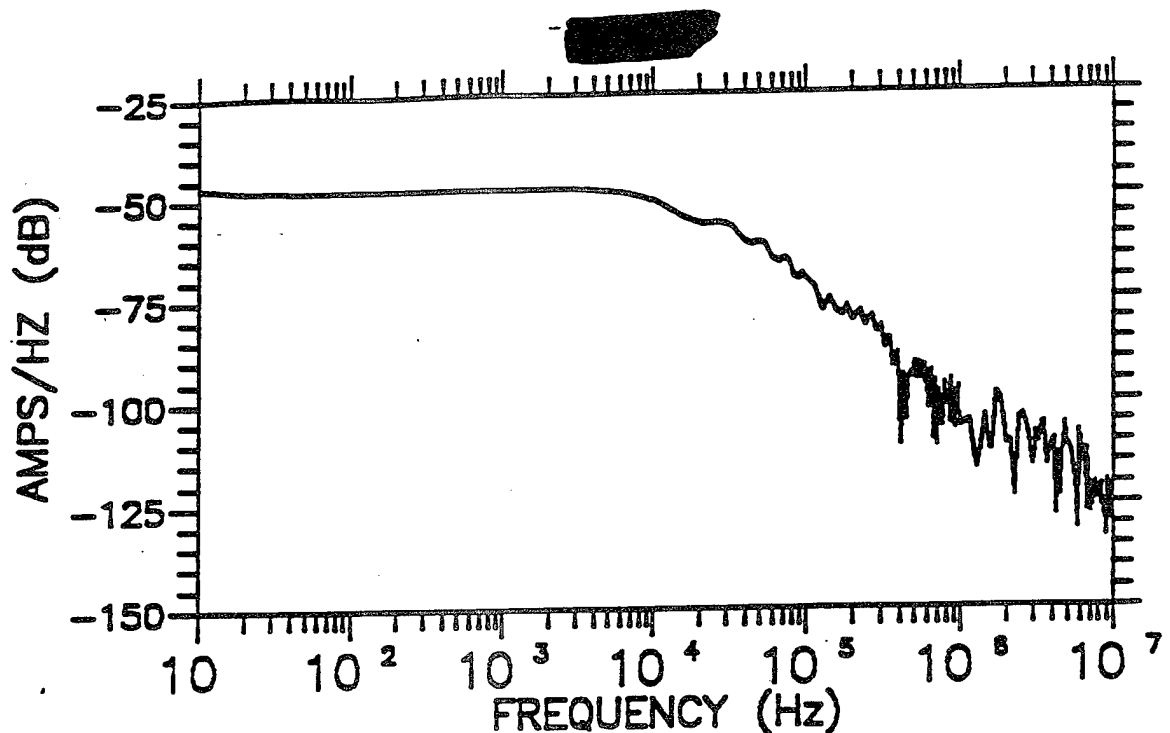
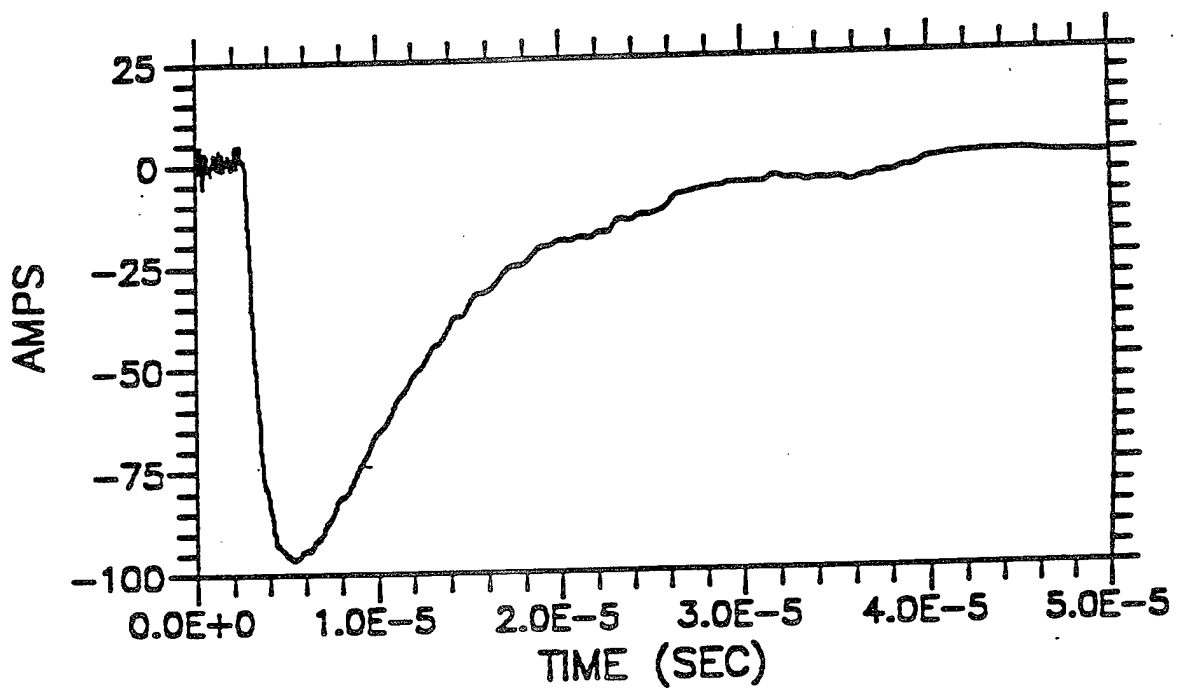
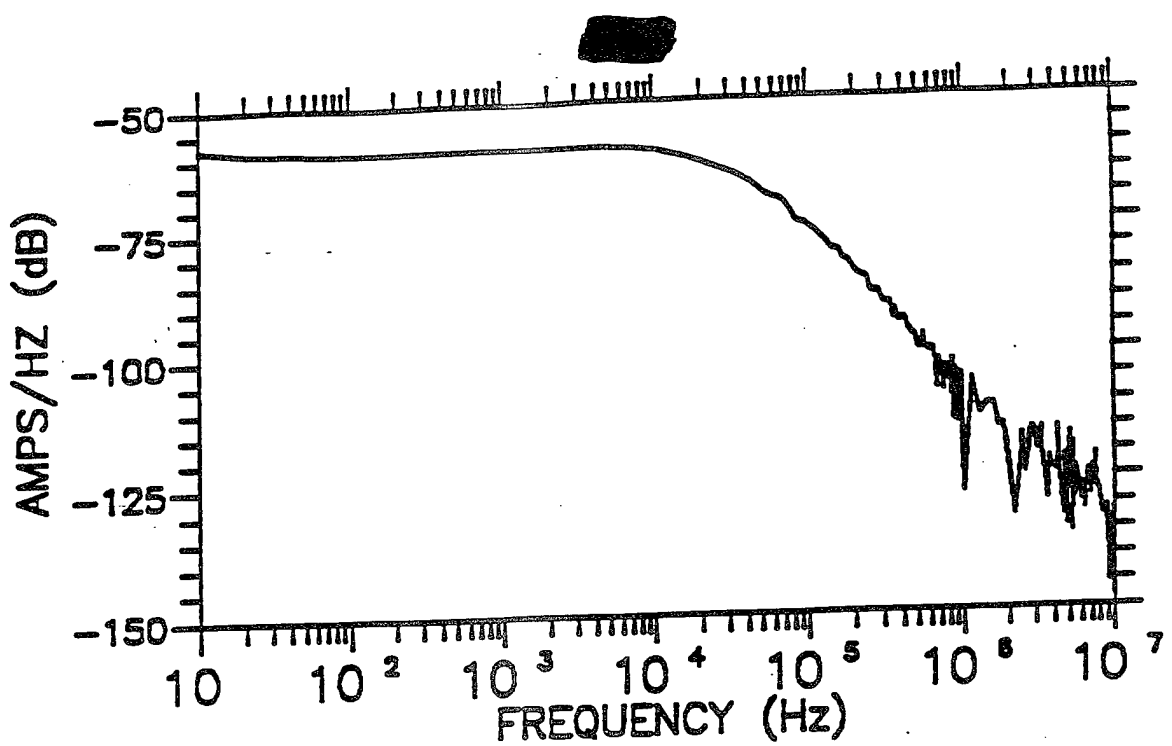


Figure 3-6.



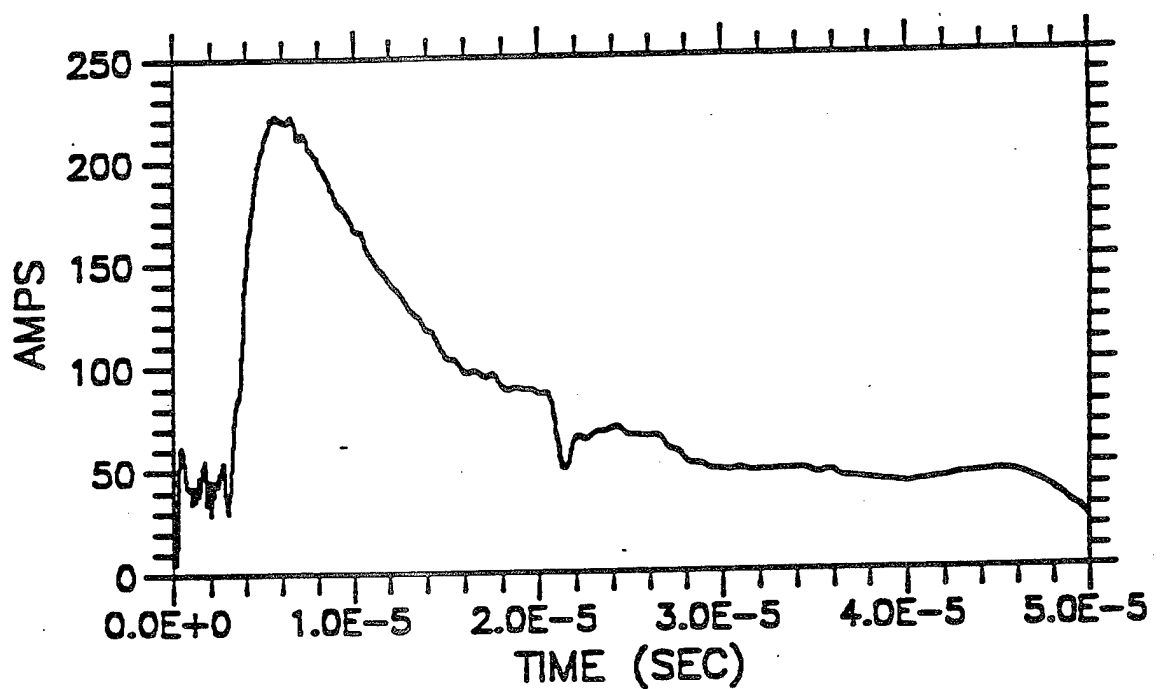
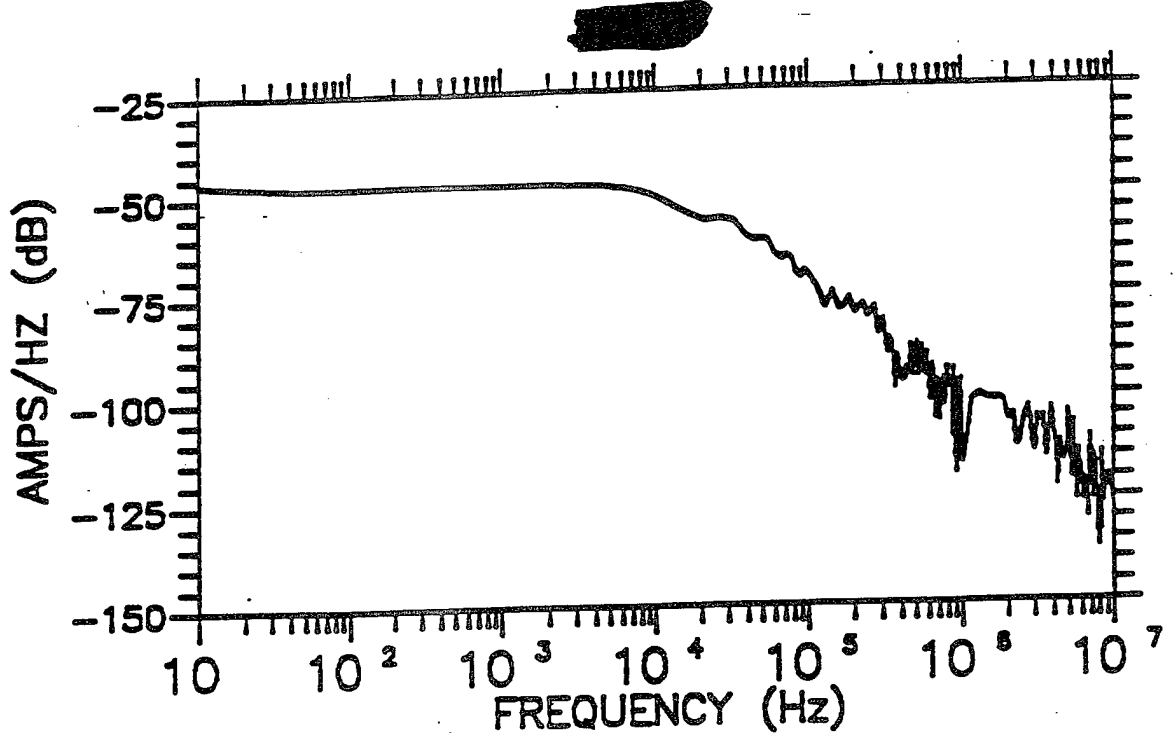


Figure 3-8.

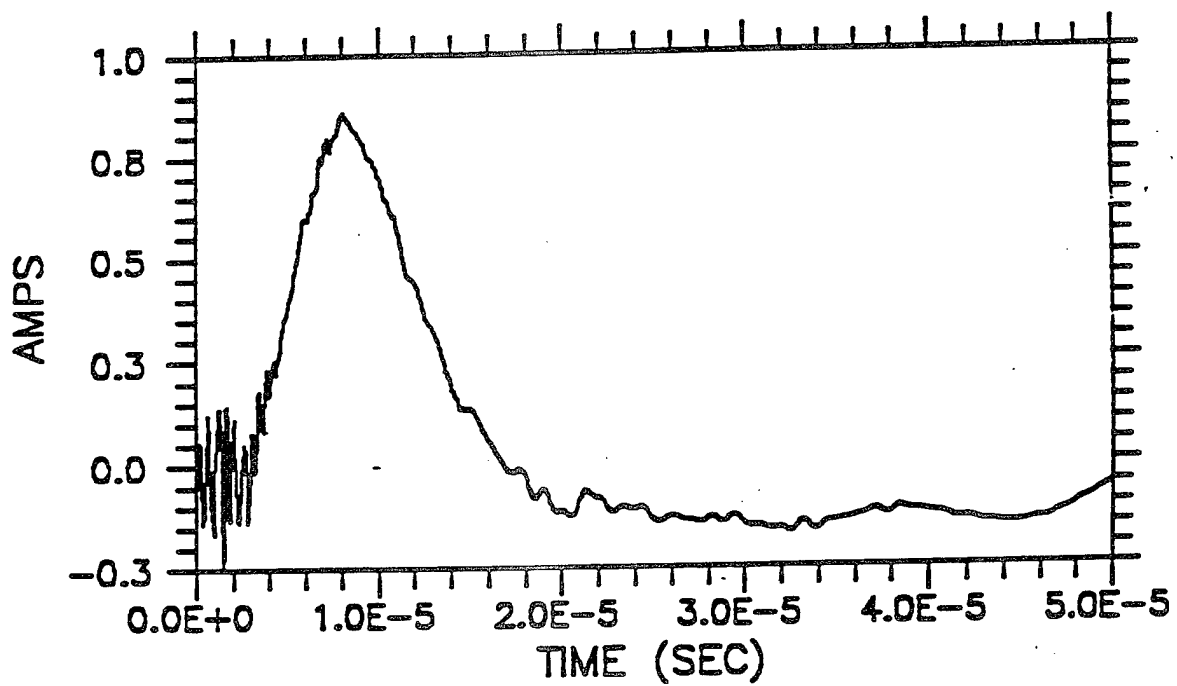
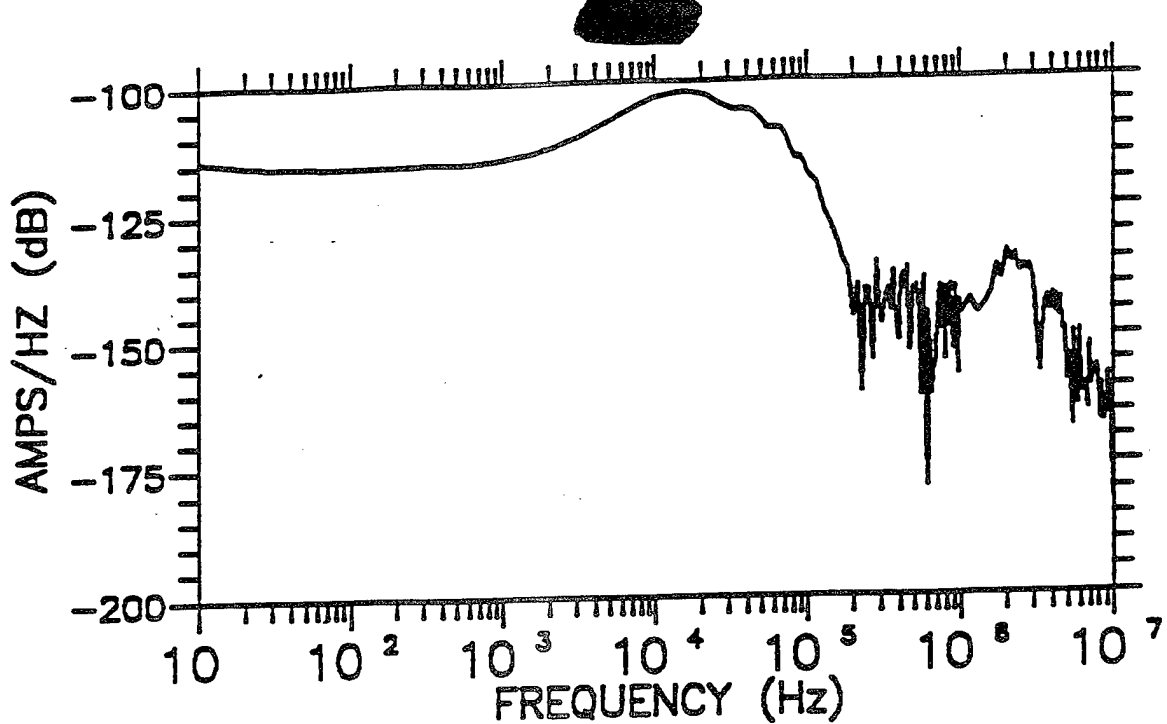


Figure 3-9.

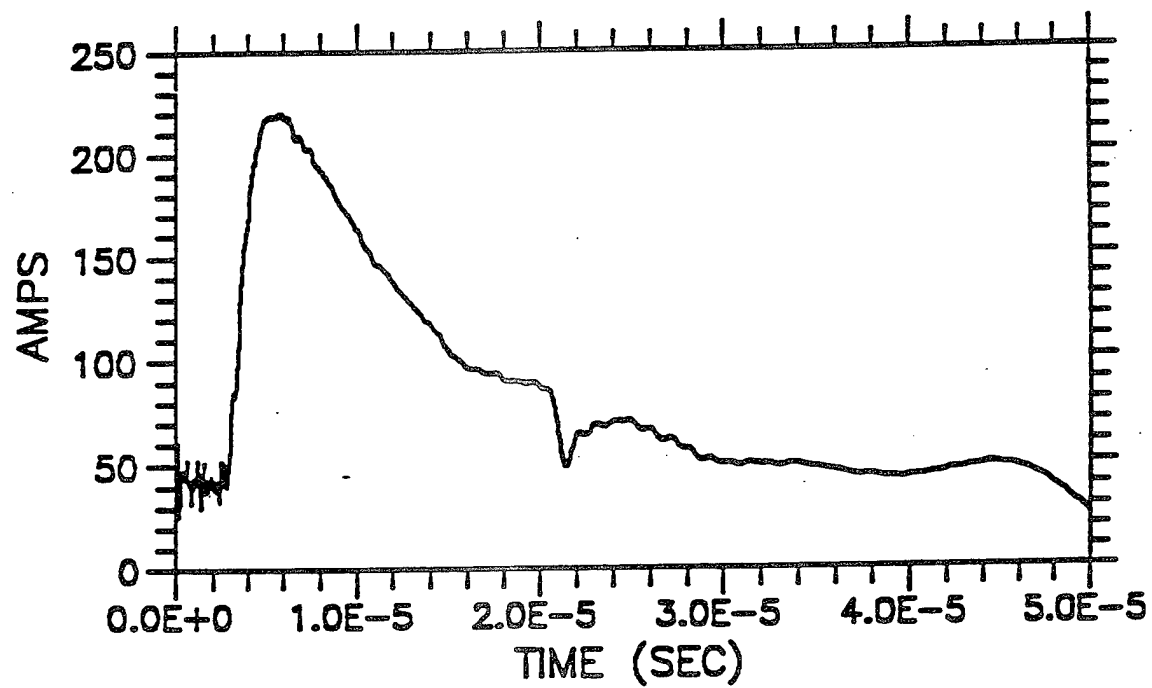
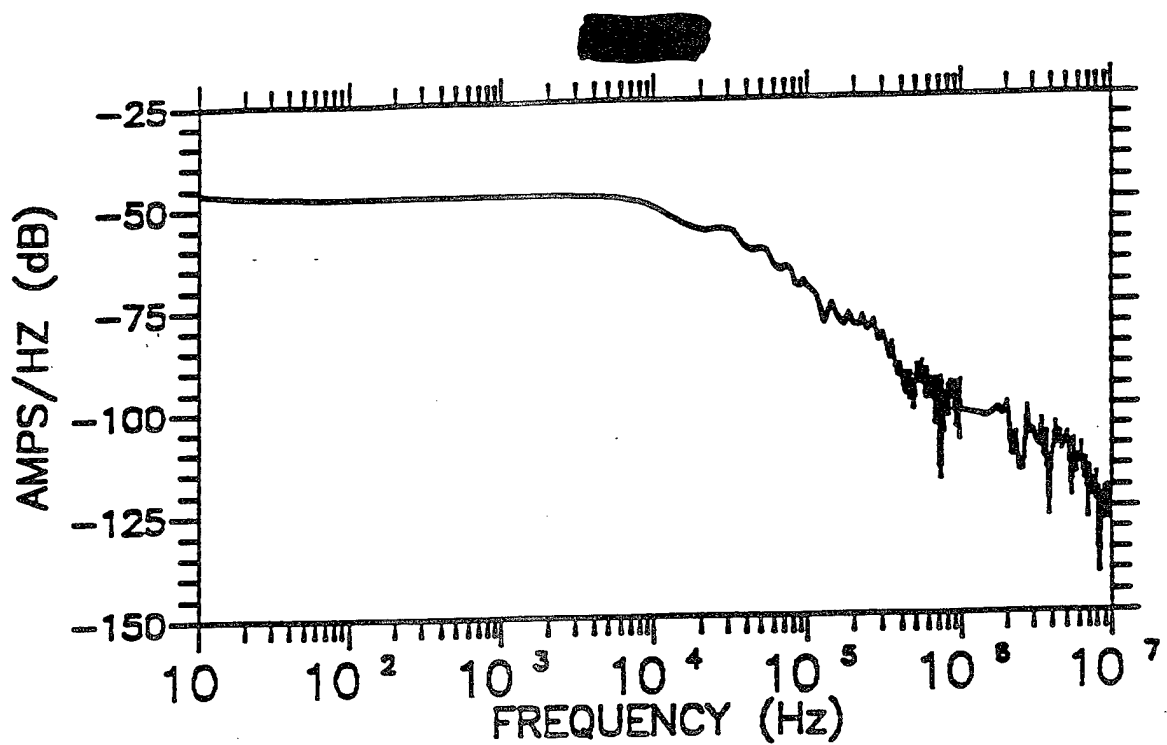


Figure 3-10.

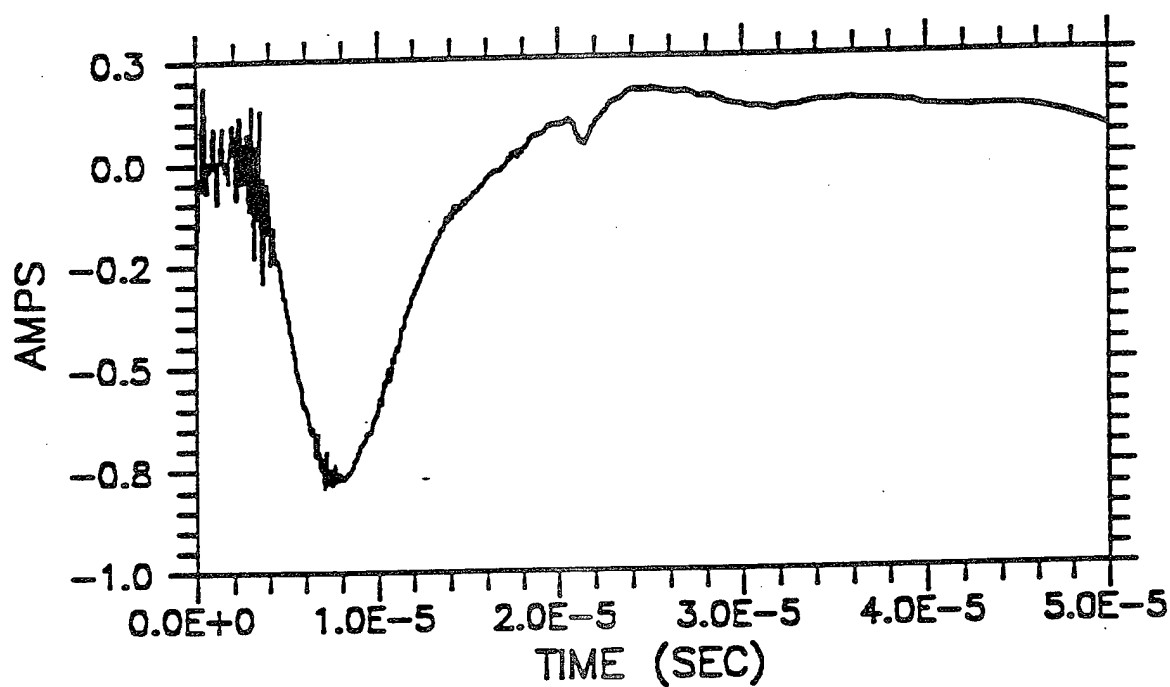
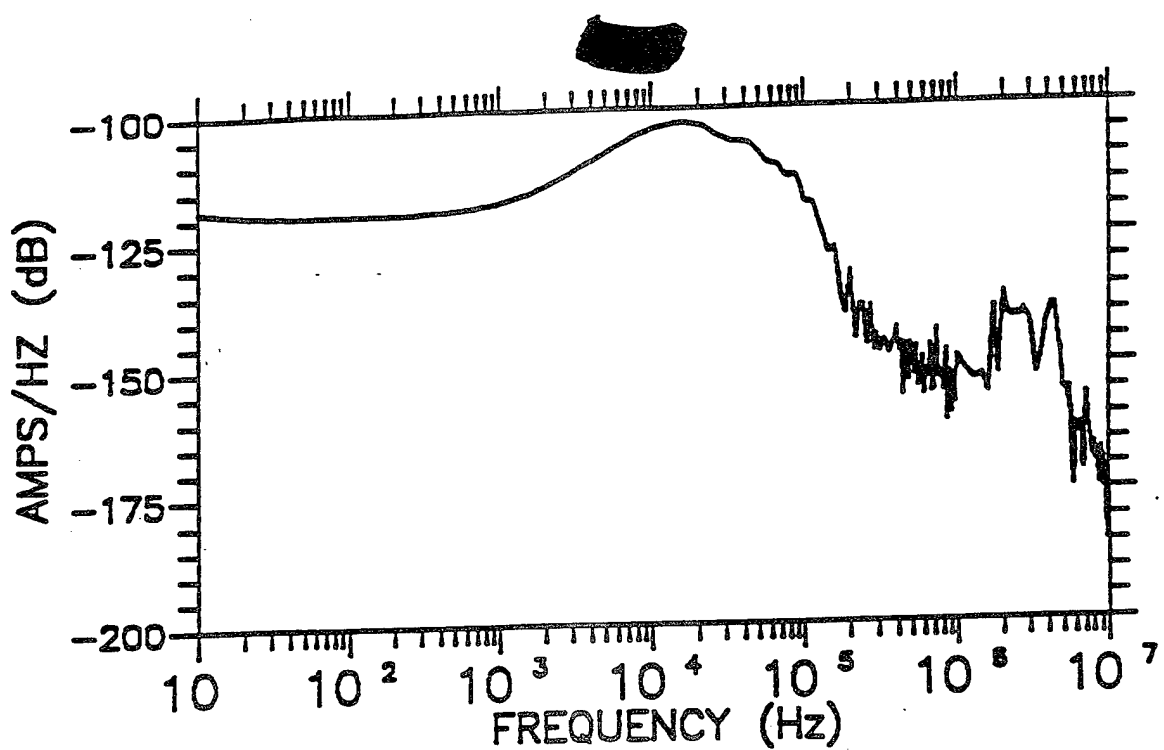


Figure 3-11.

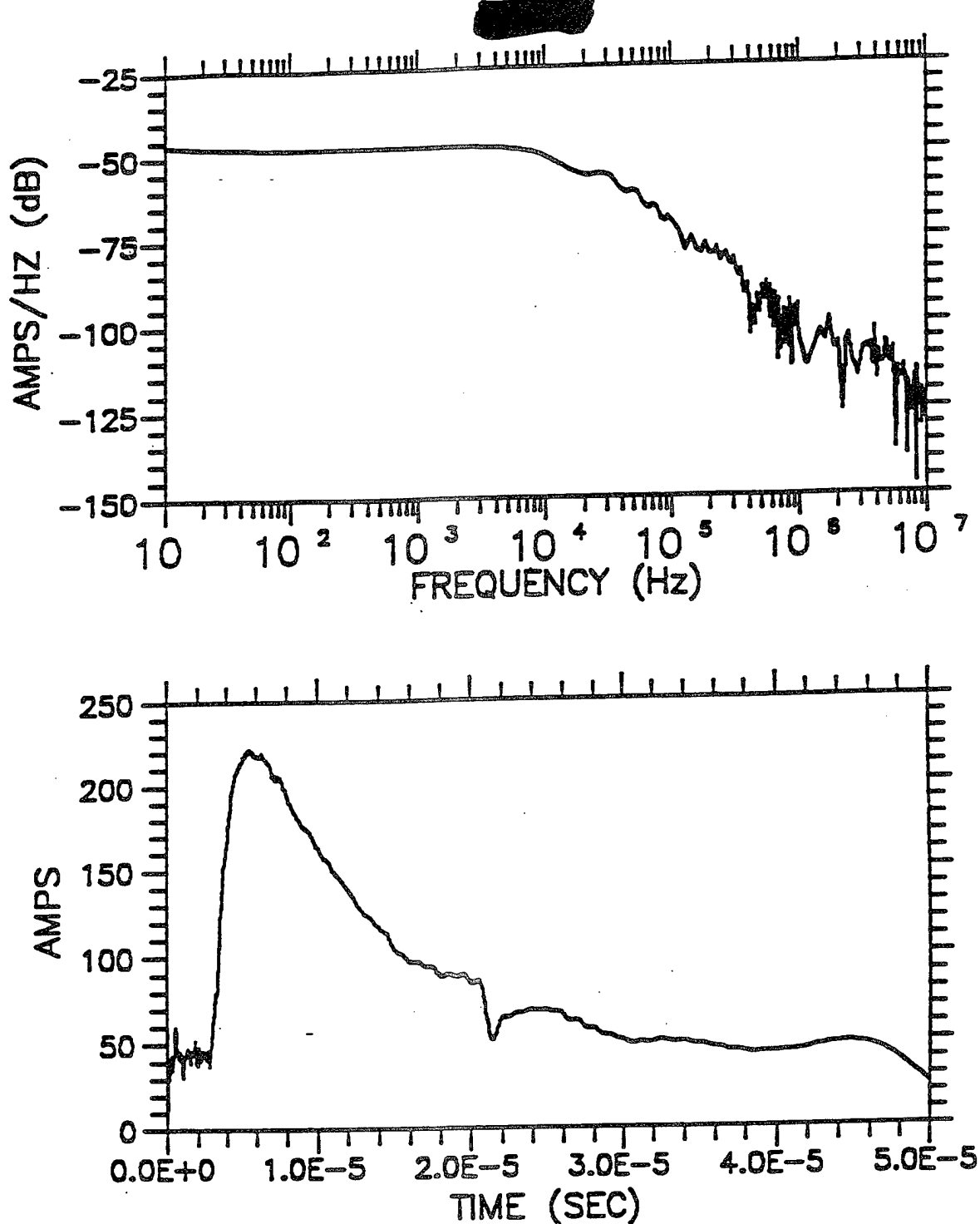


Figure 3-12.

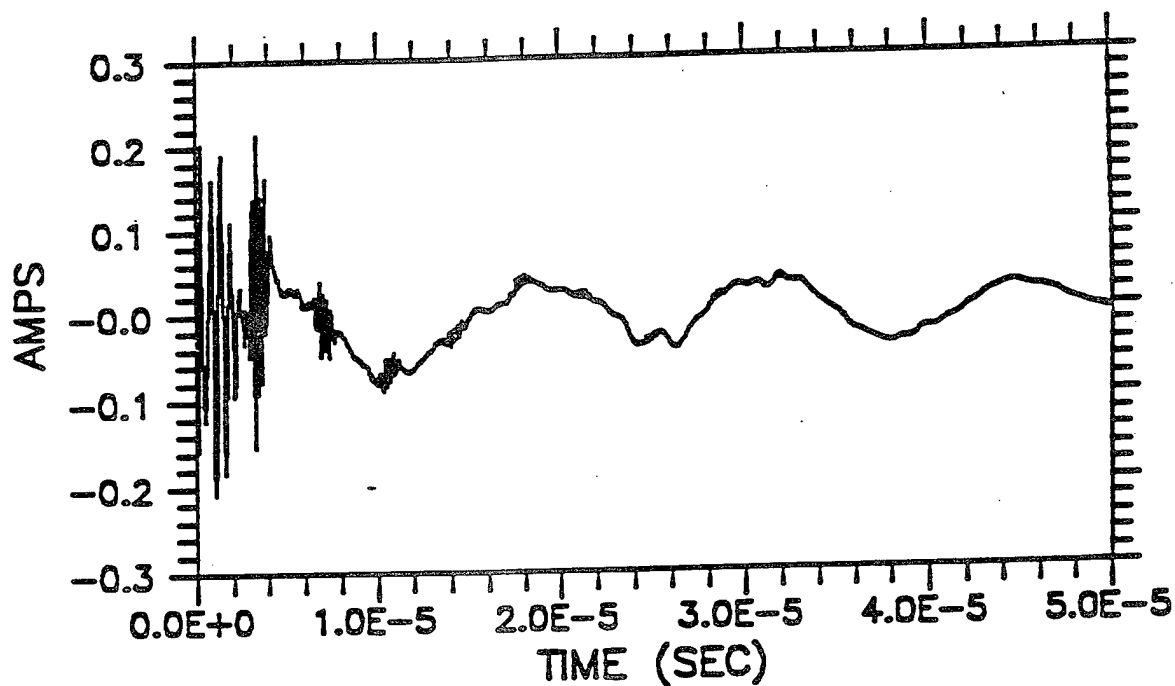
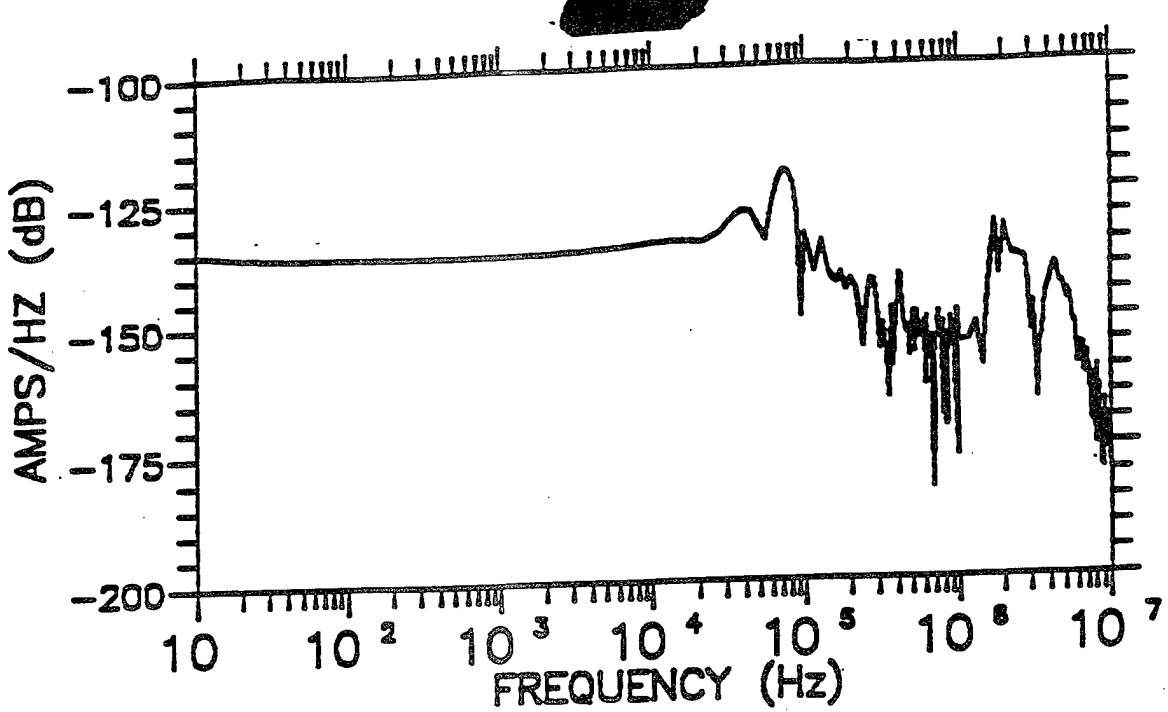


Figure 3-13.

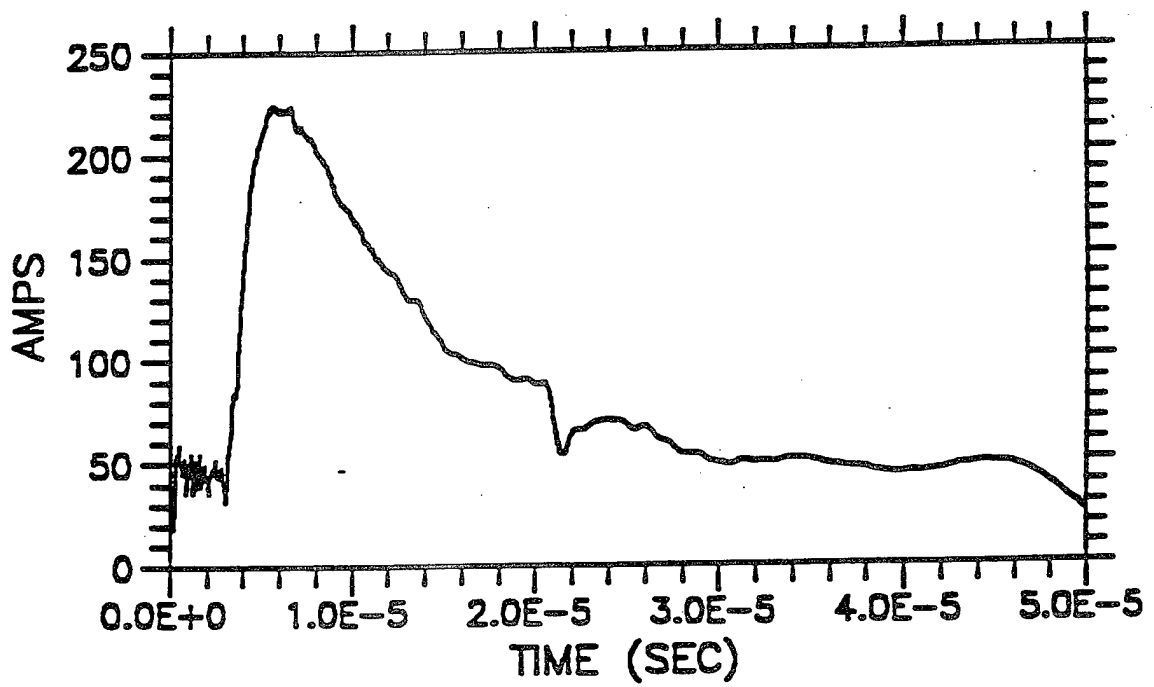
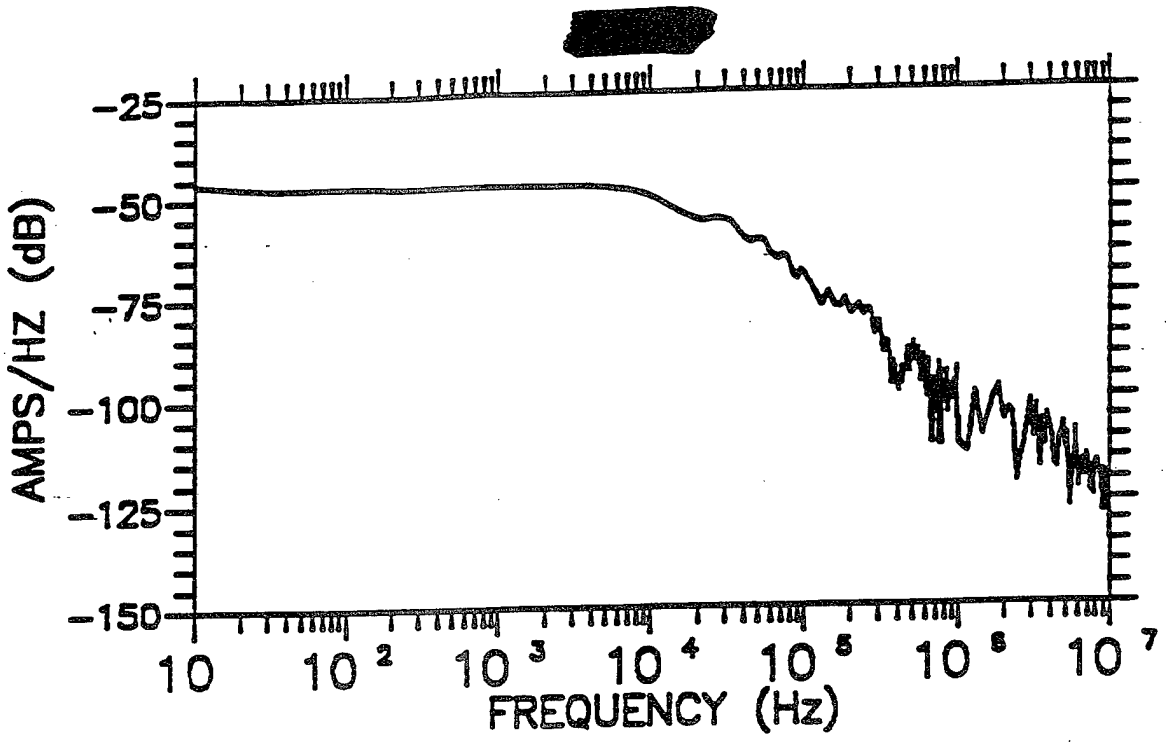


Figure 3-14.

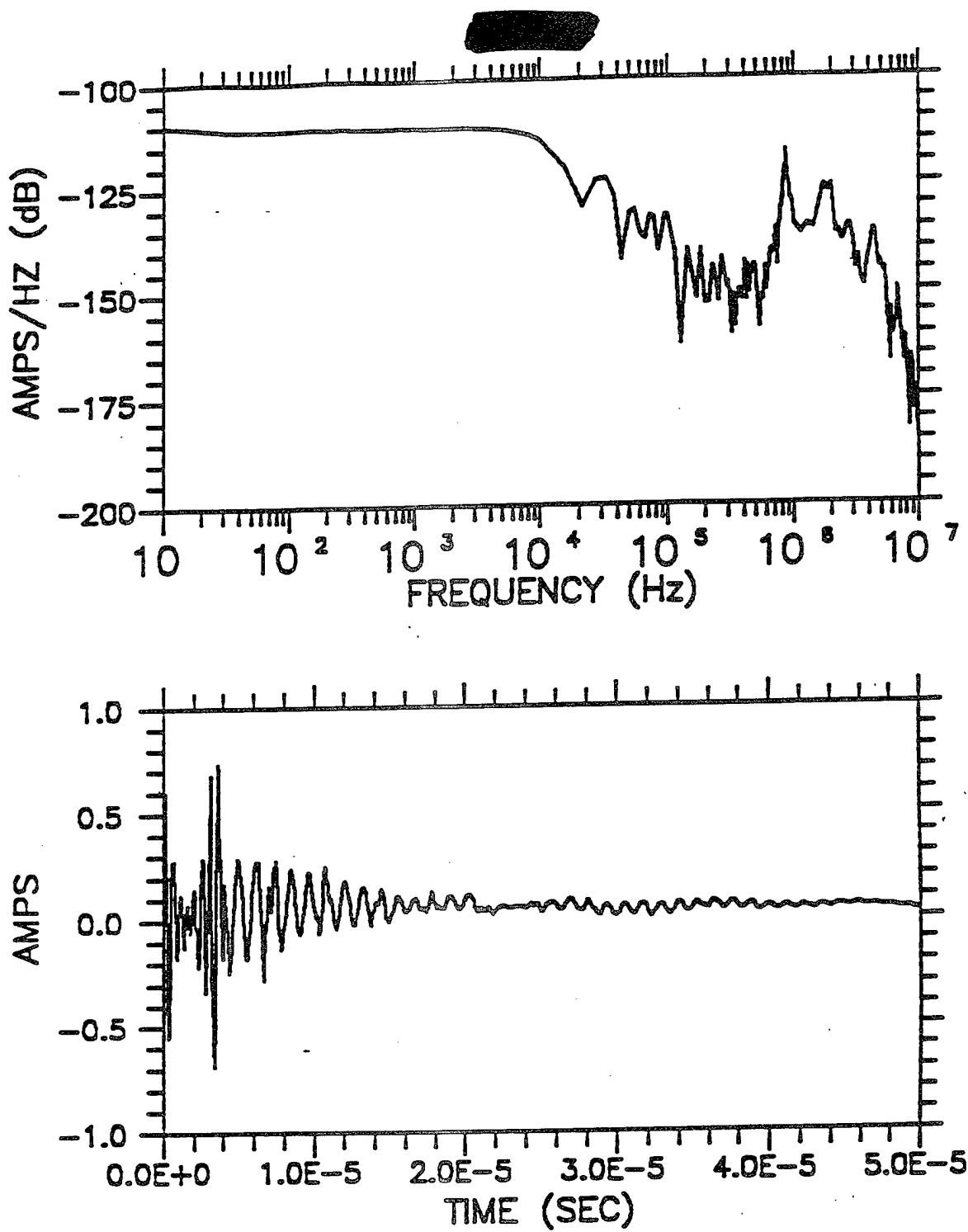


Figure 3-15.

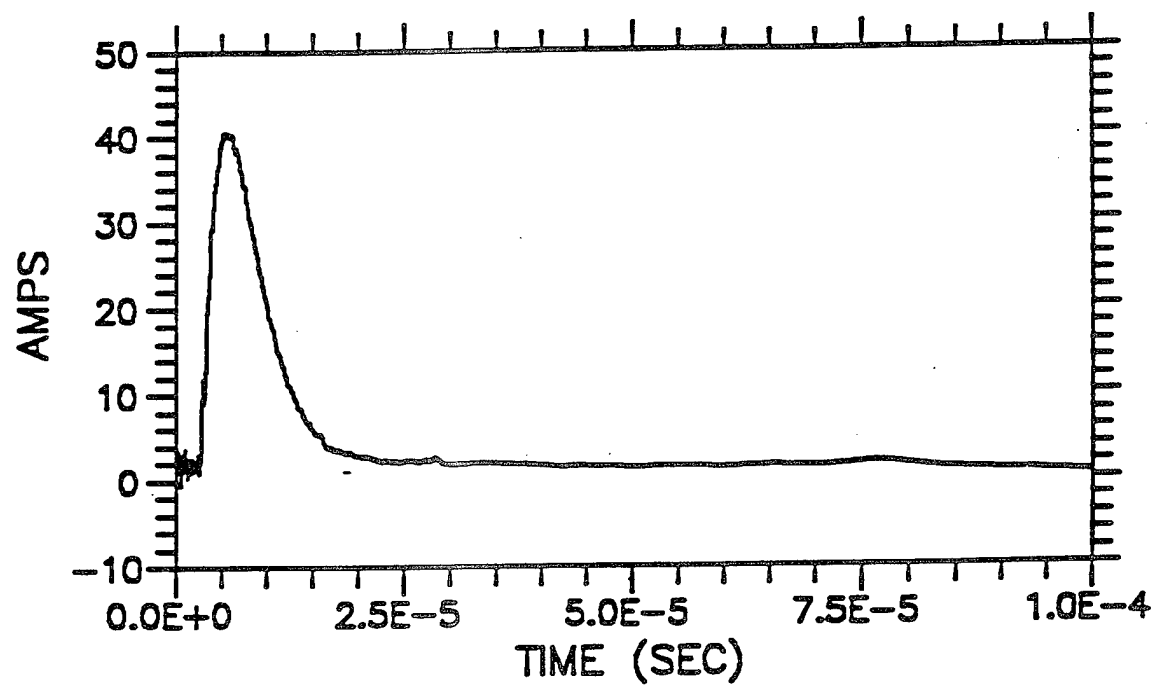
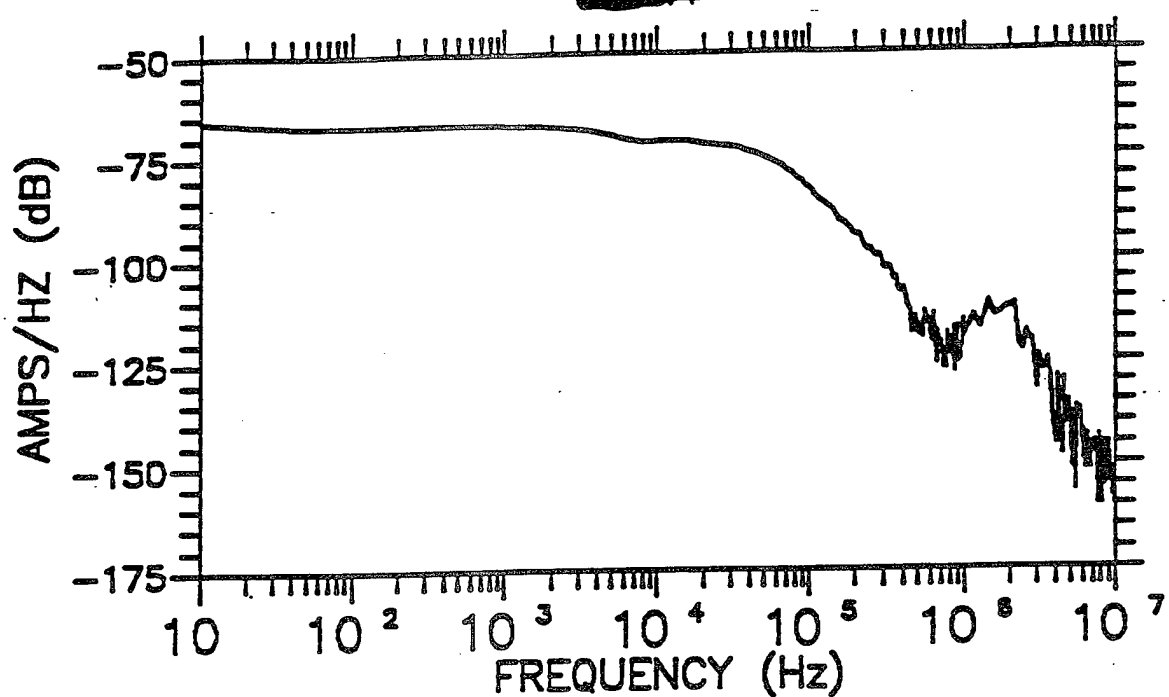


Figure 3-17

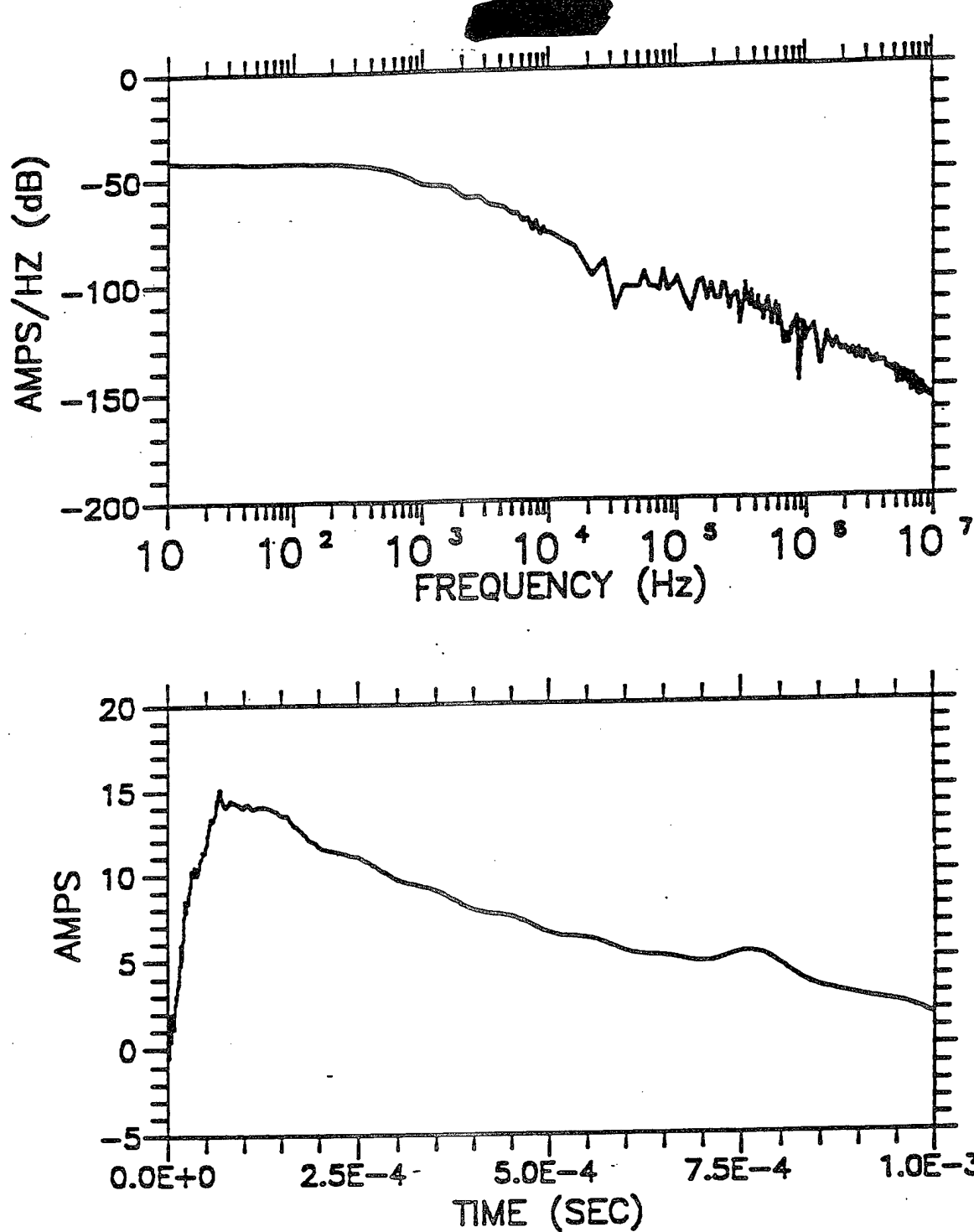
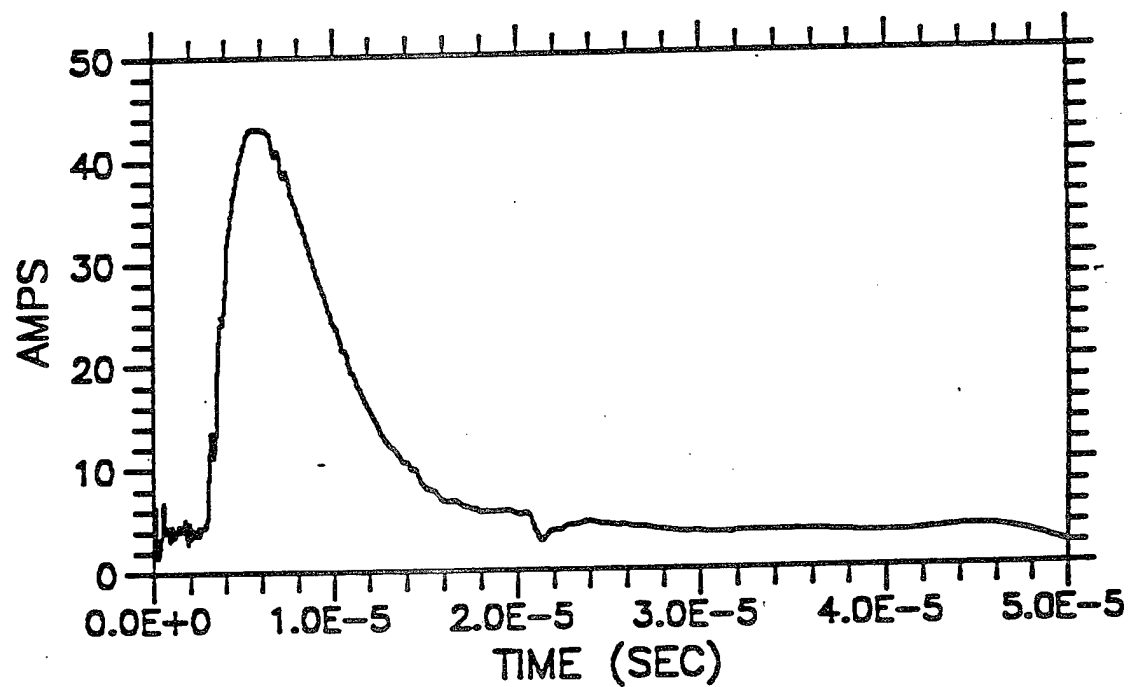
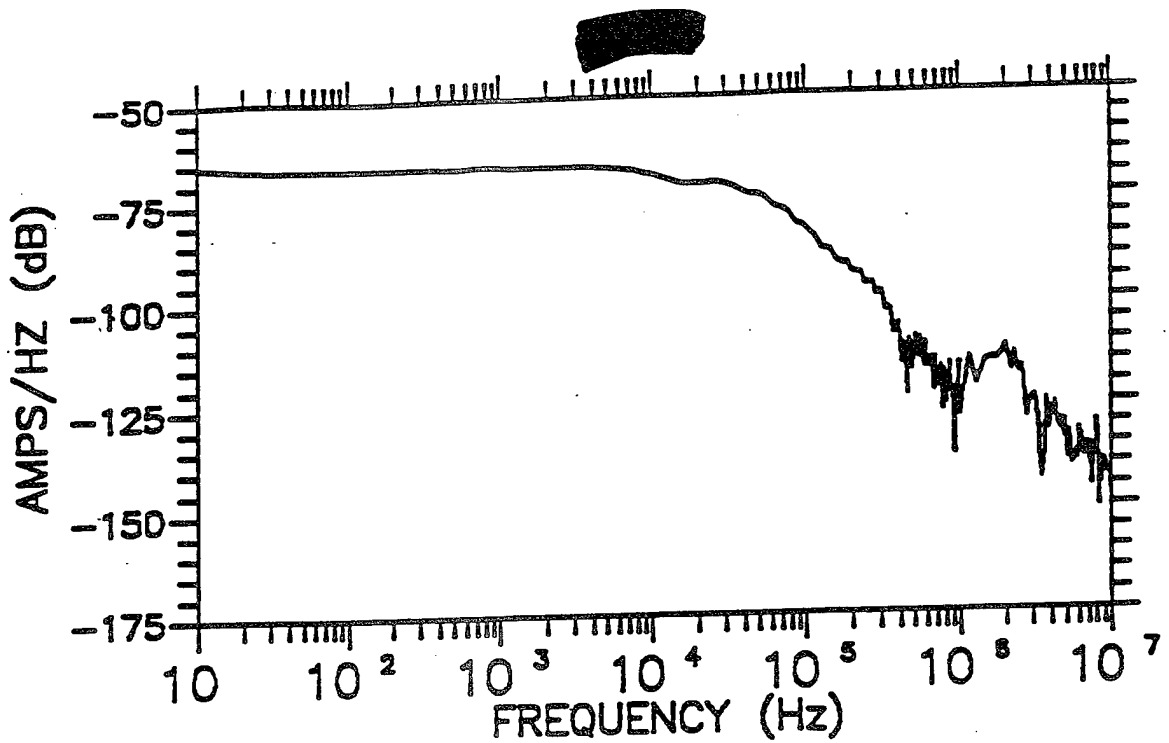
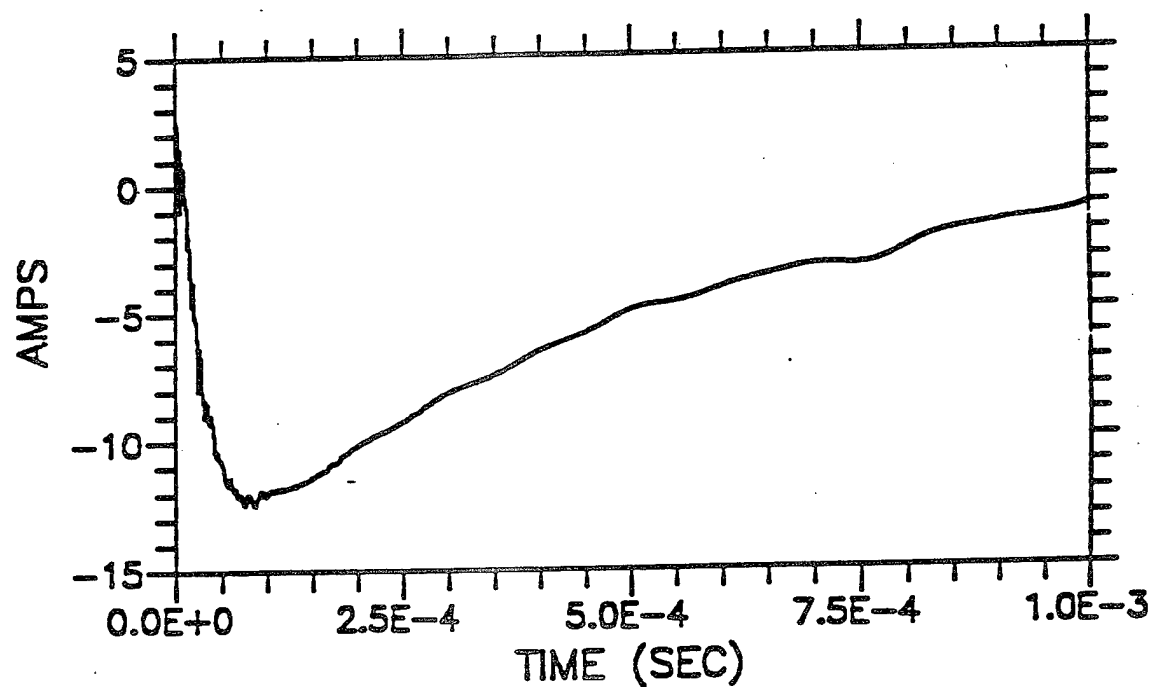
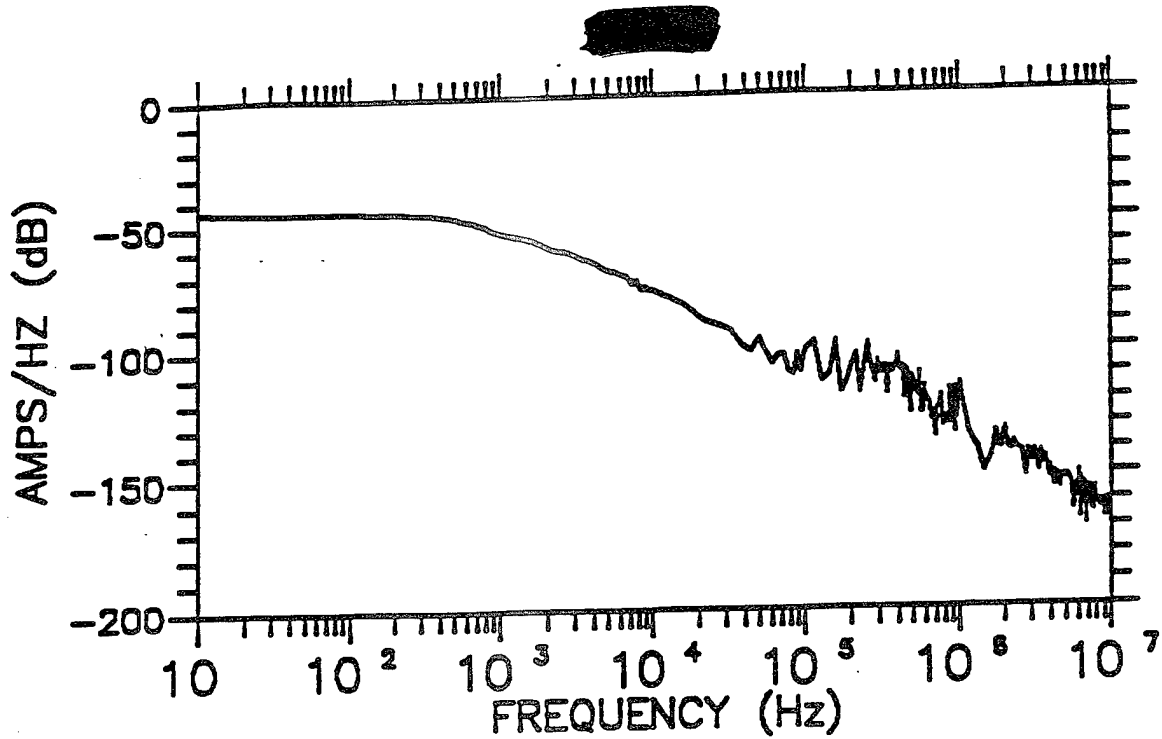
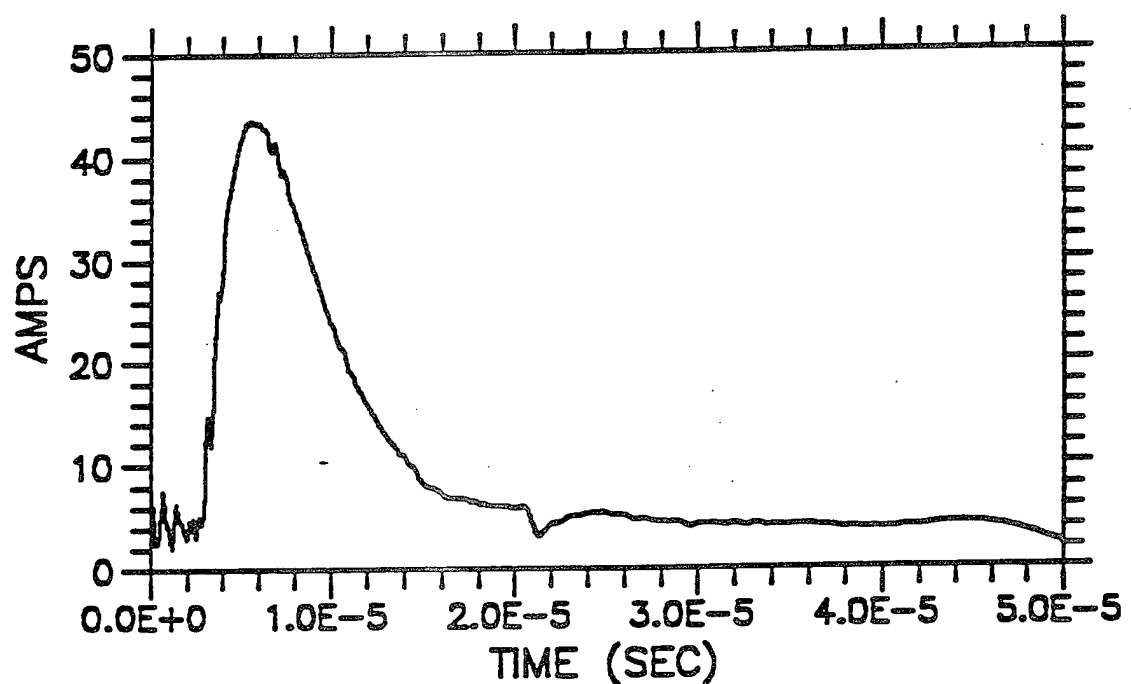
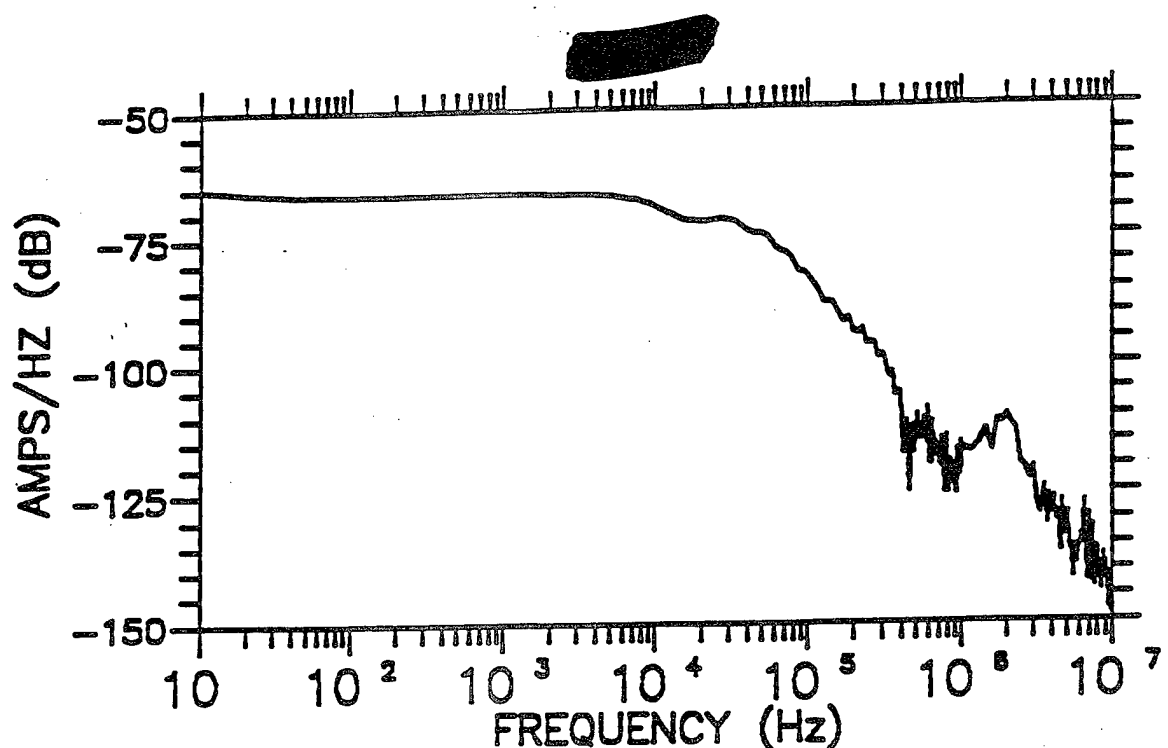
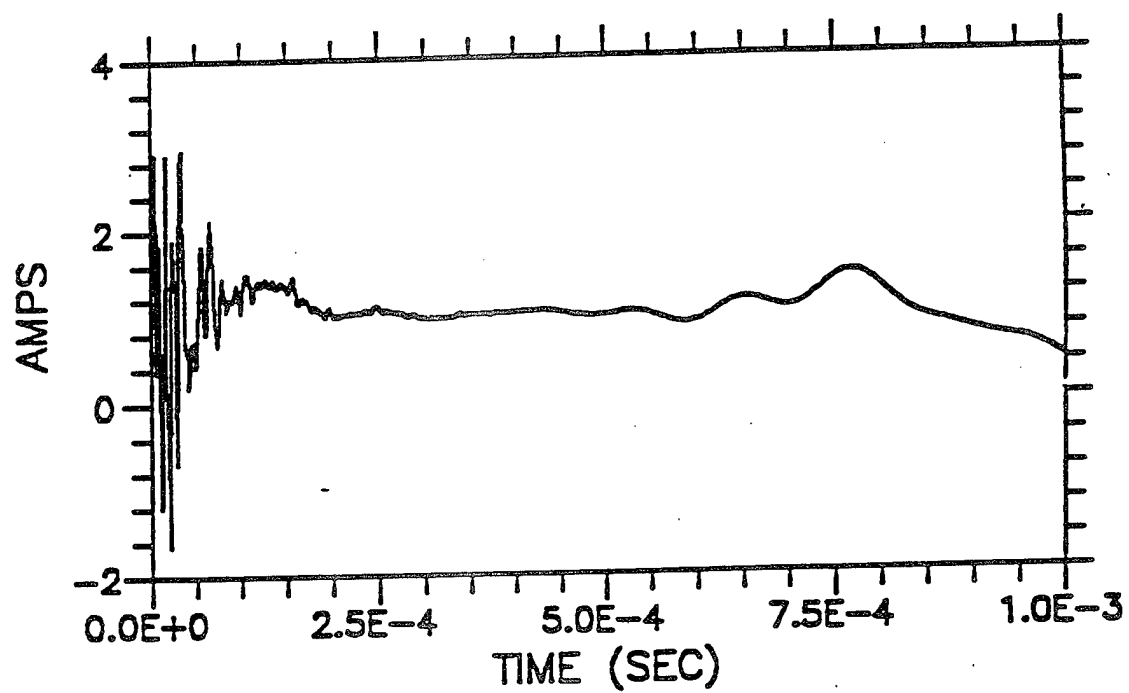
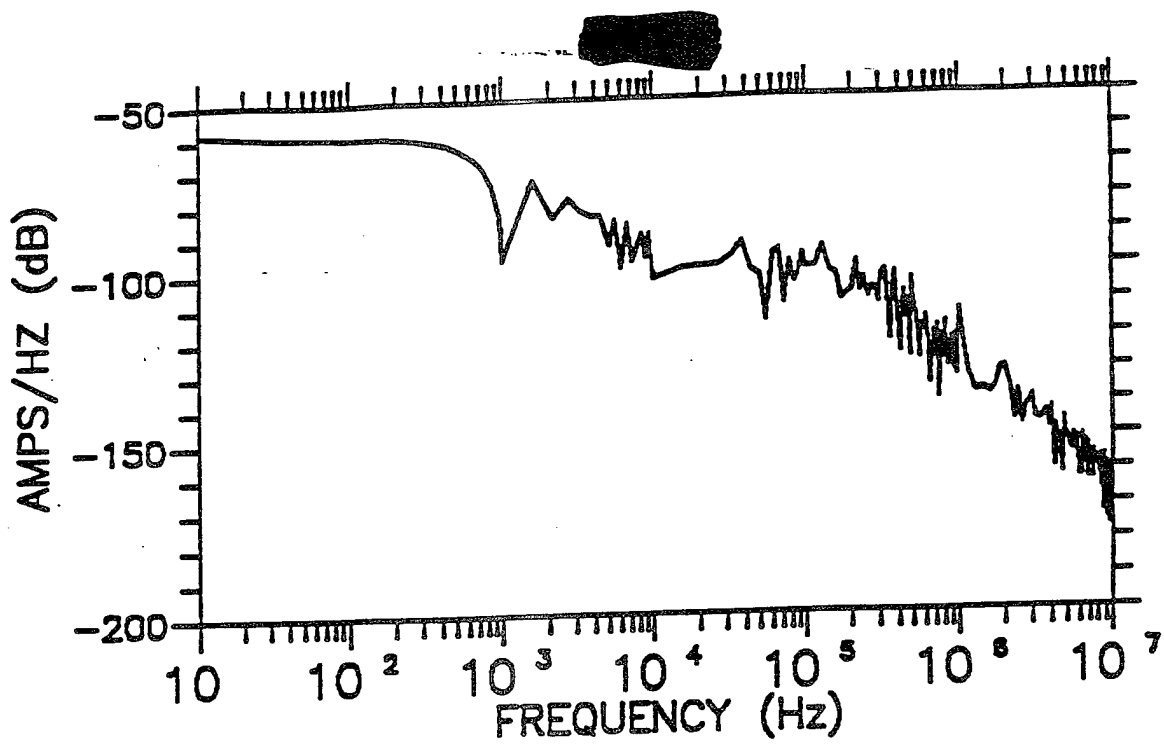


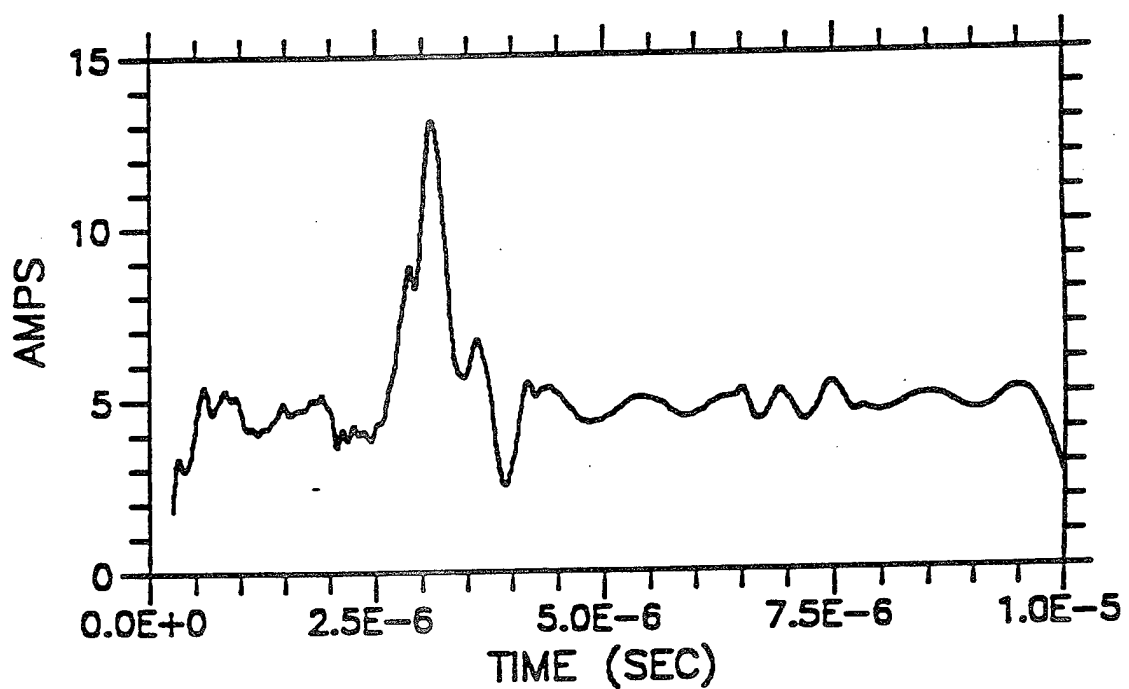
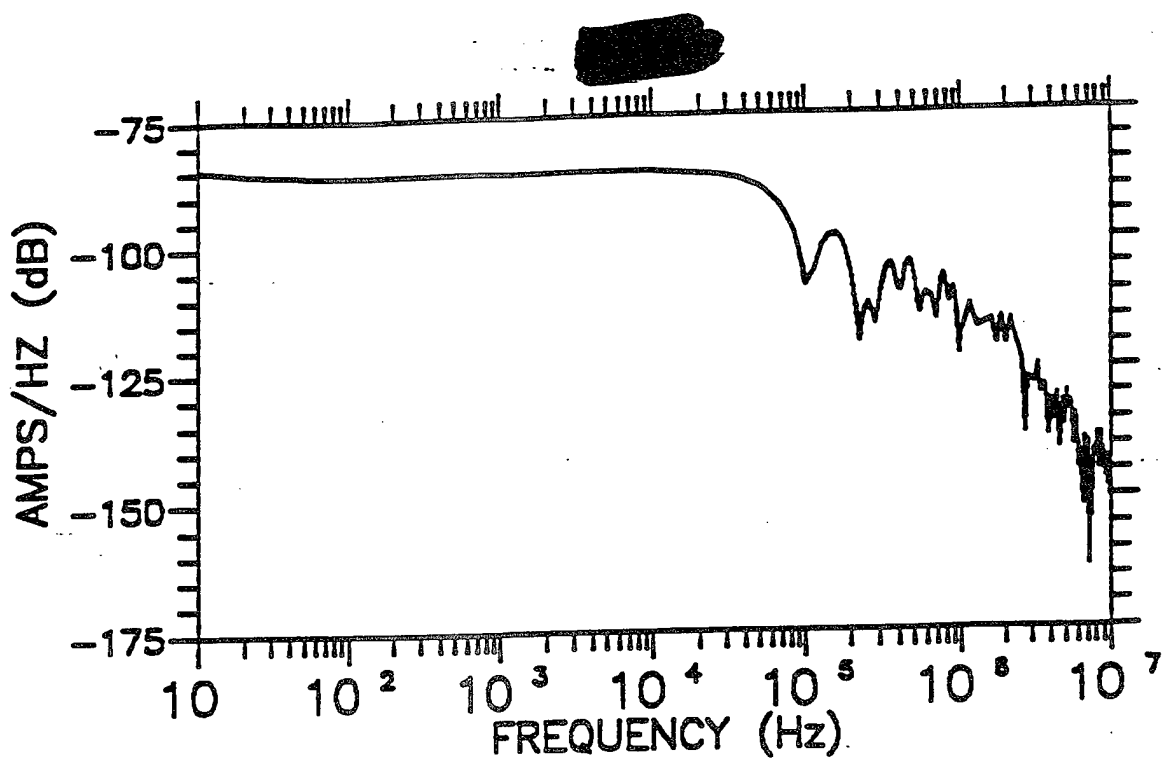
Figure 3-18.

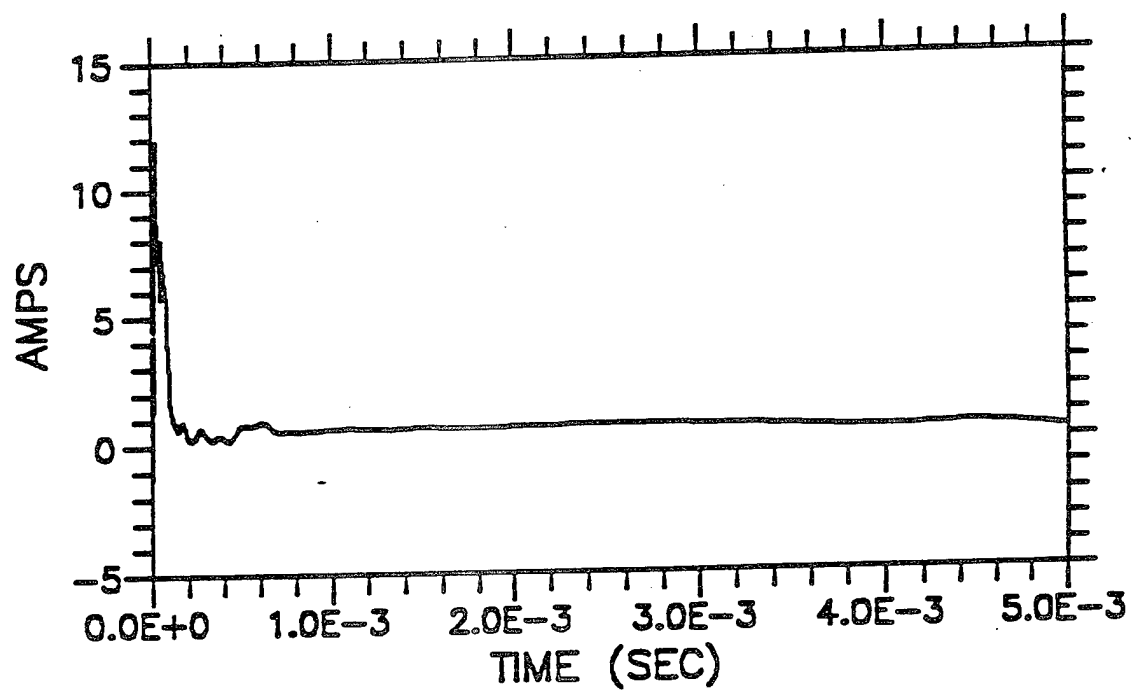
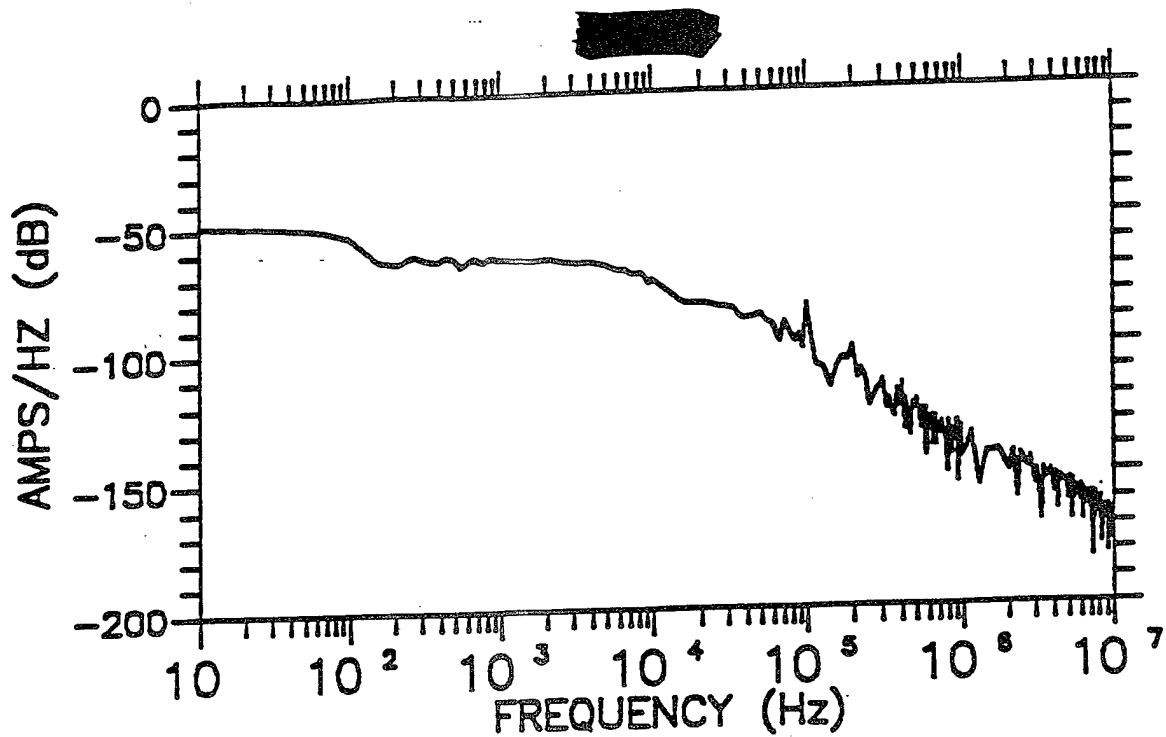


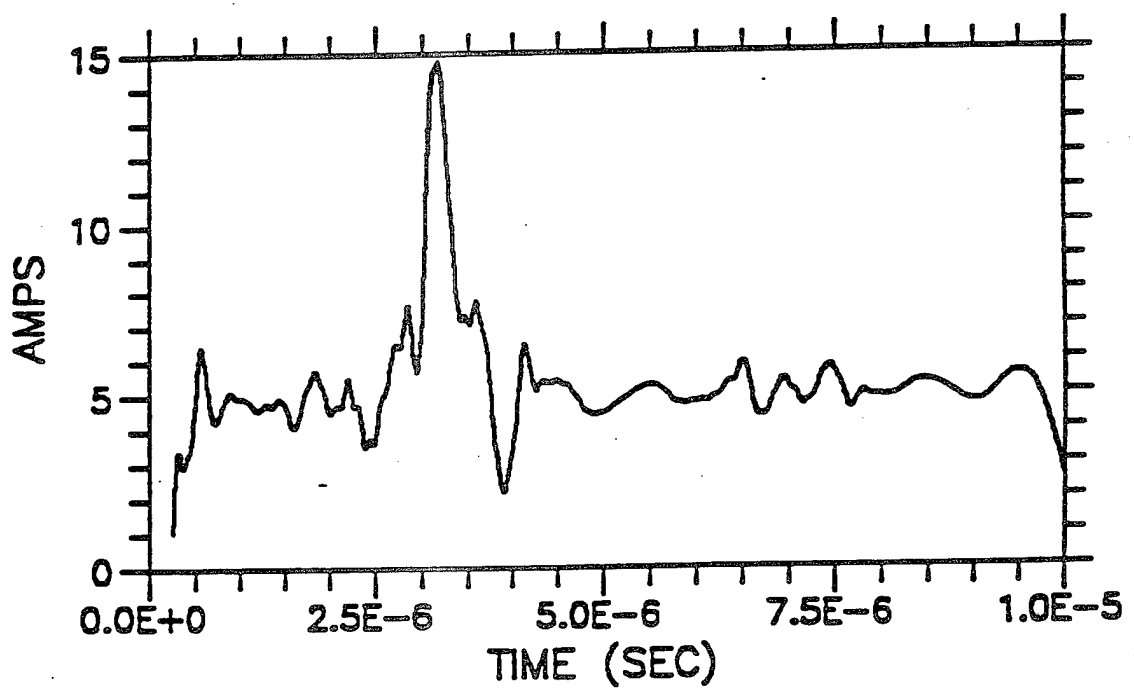
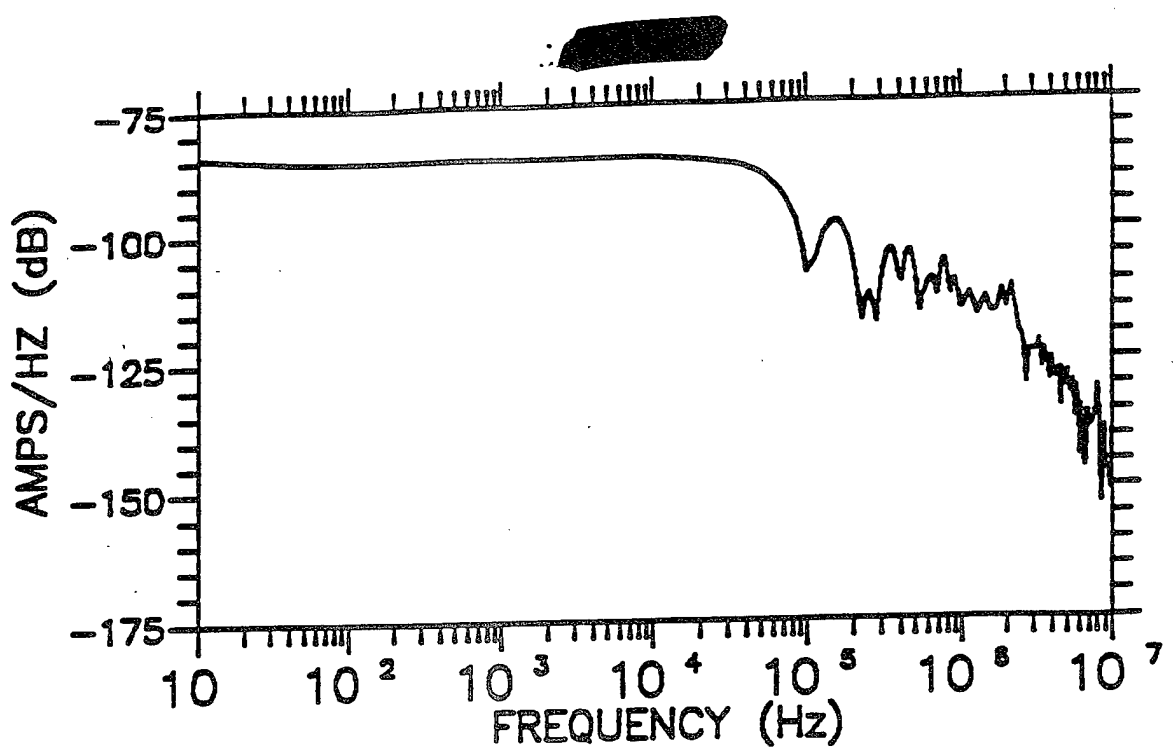


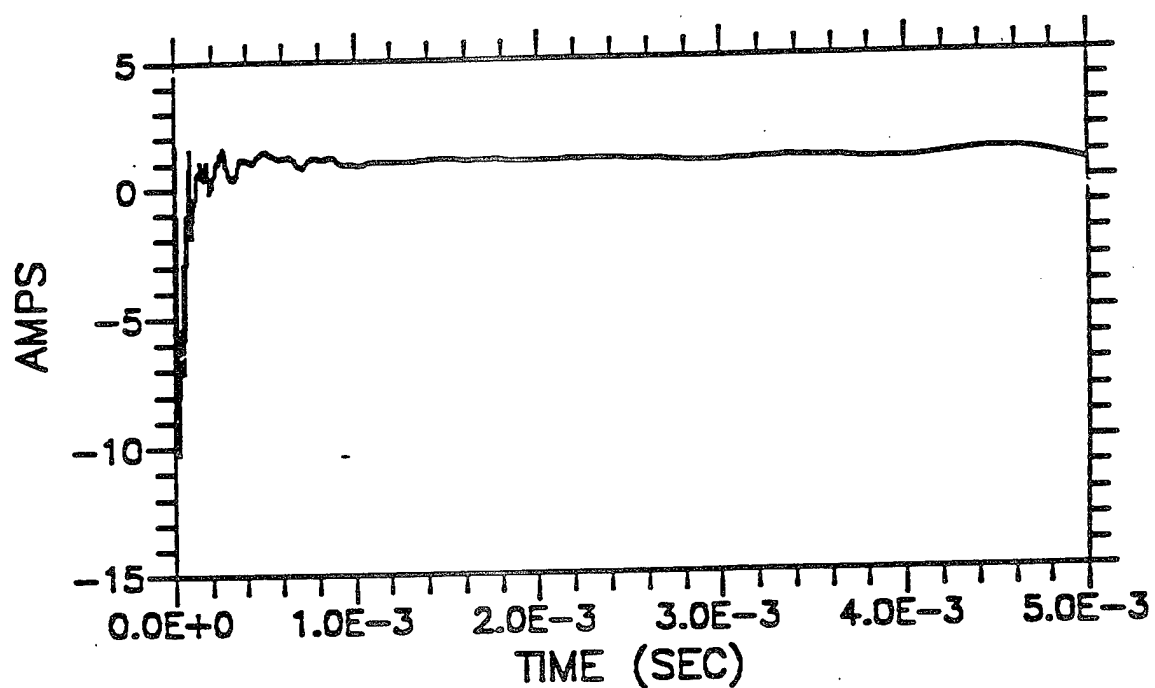
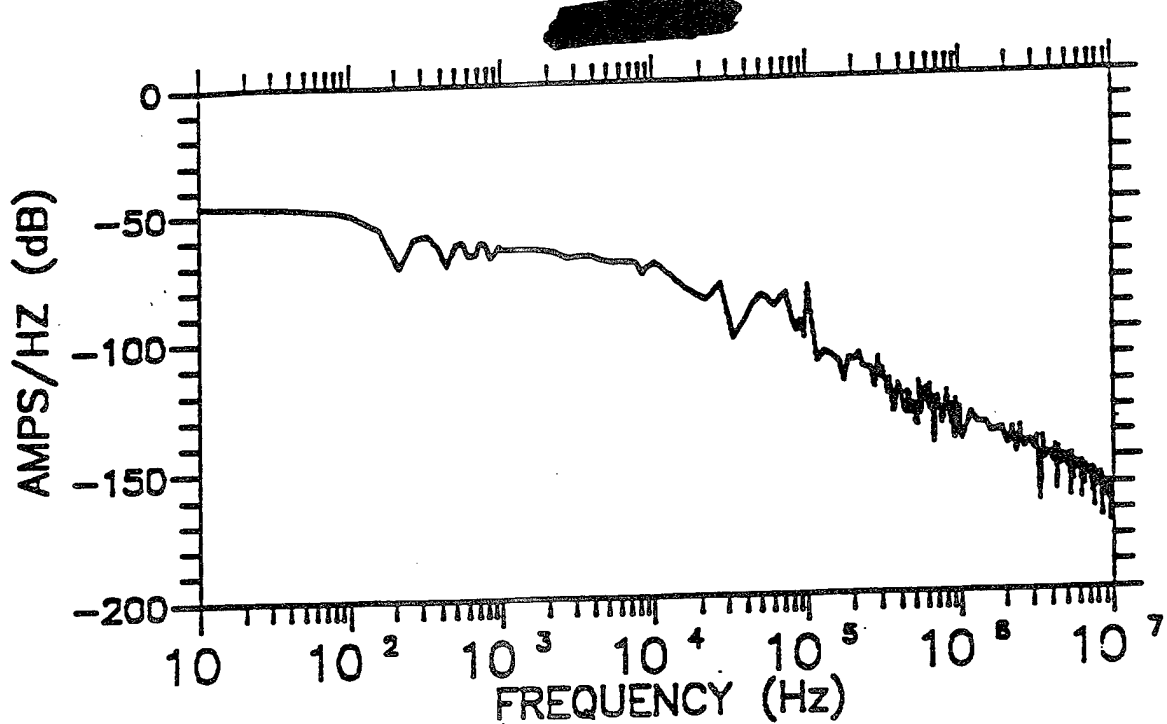


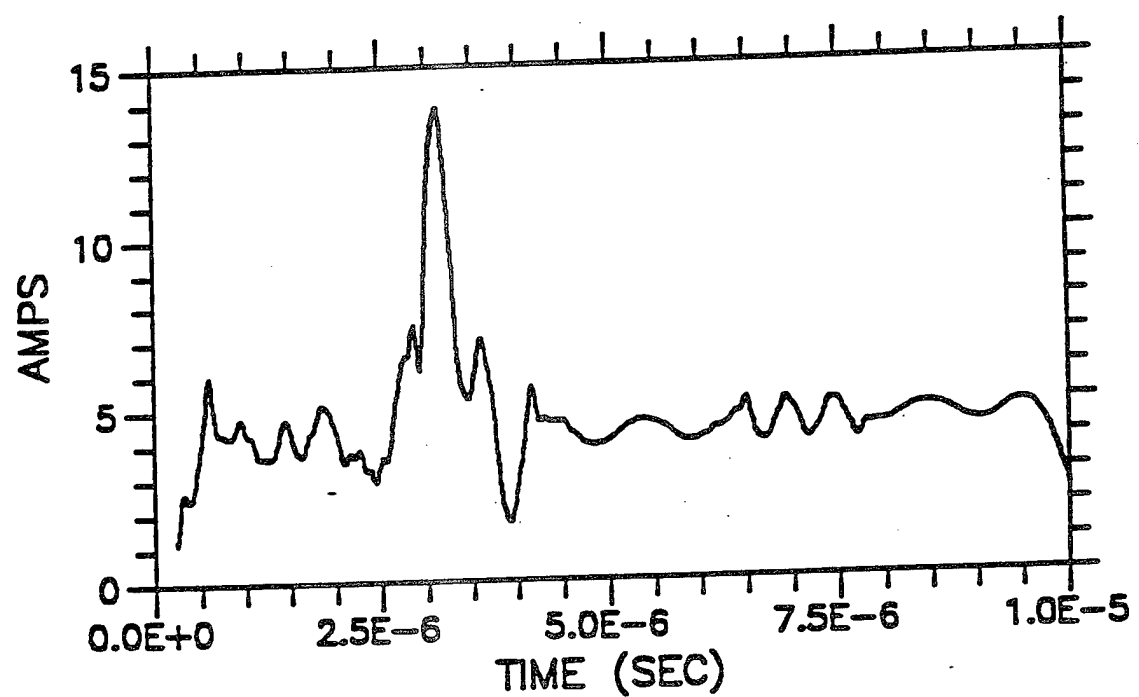
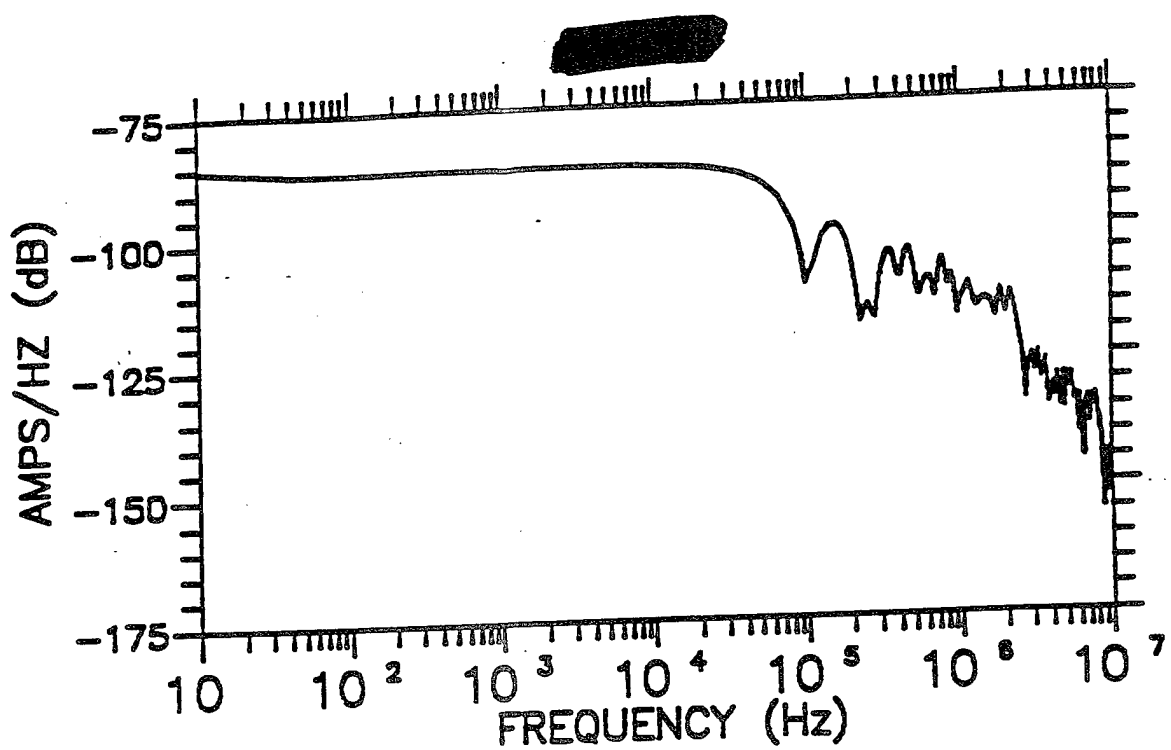


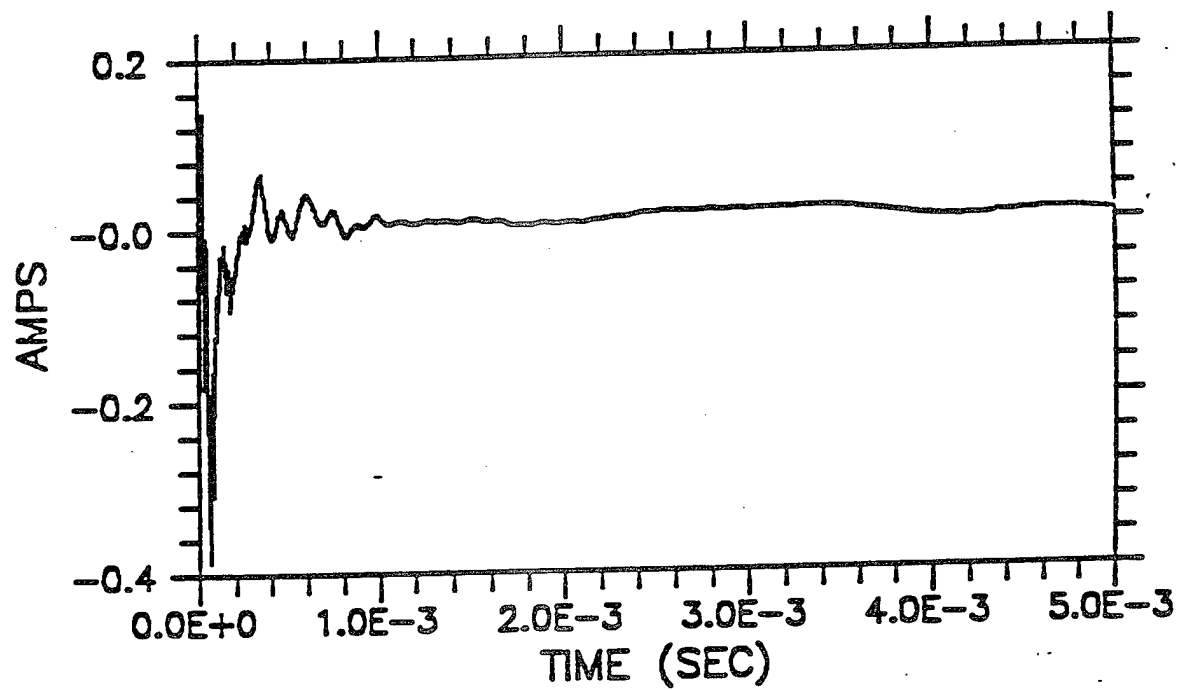
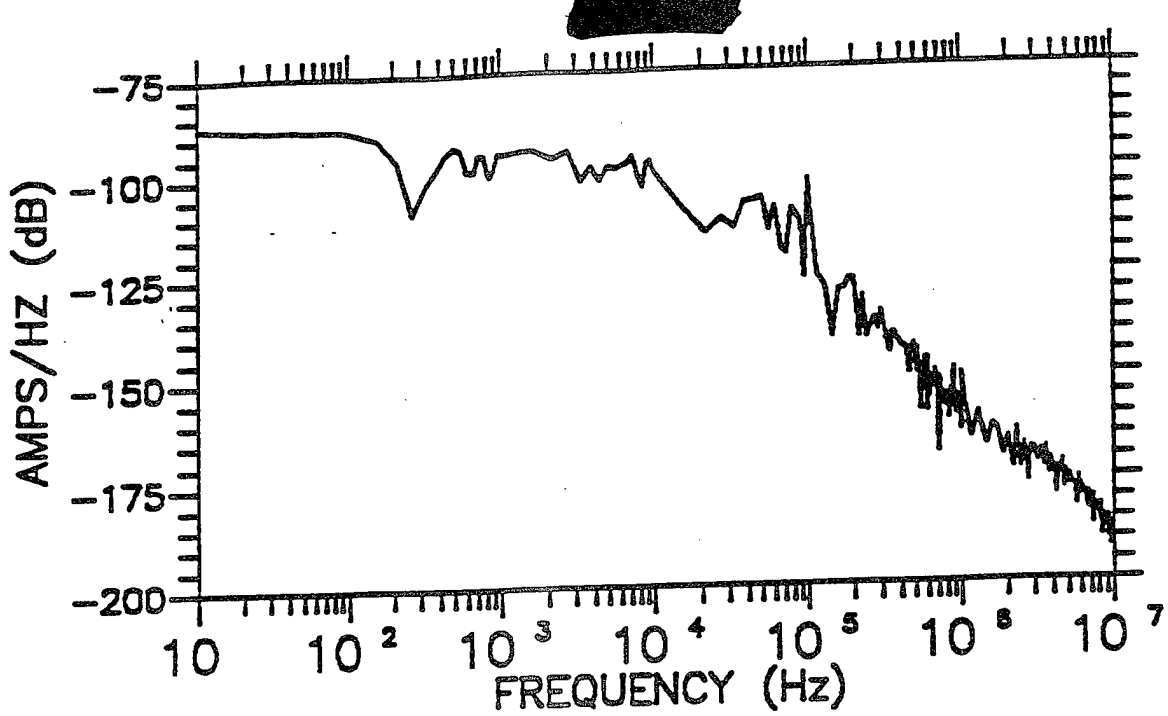


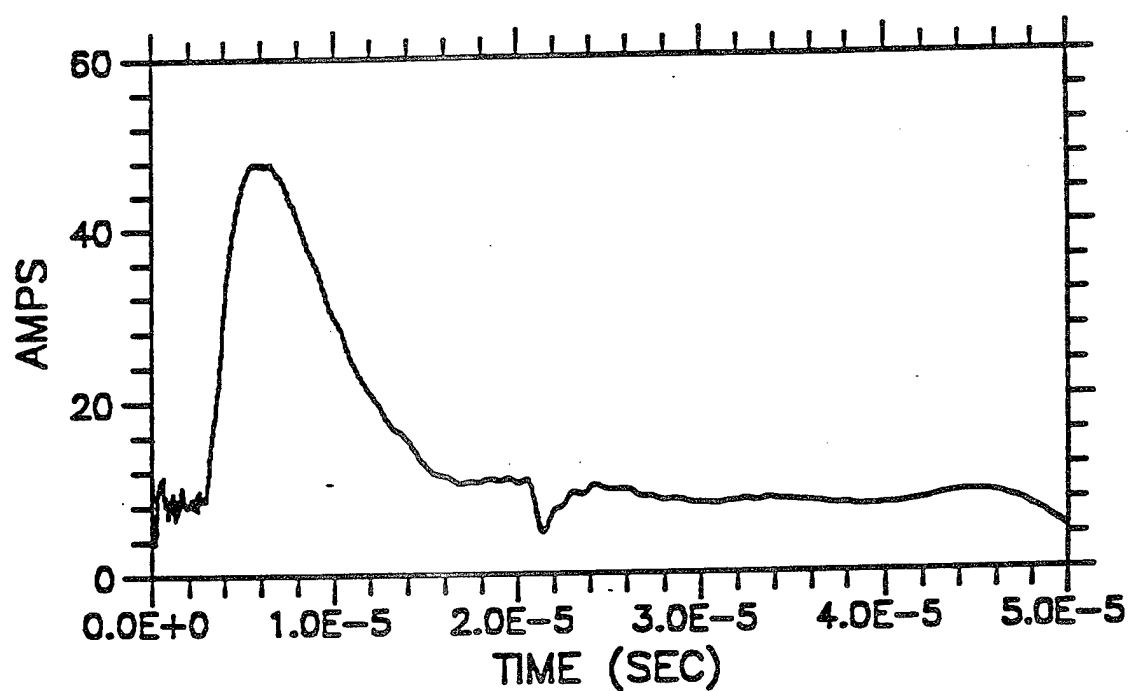
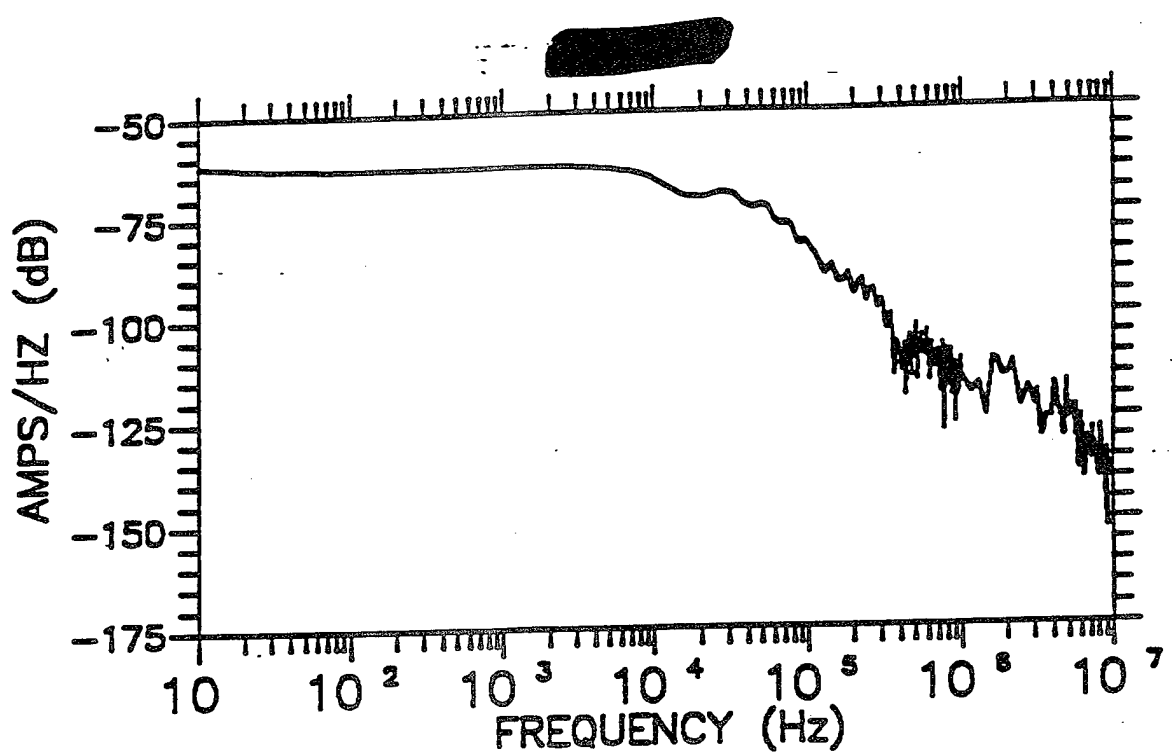


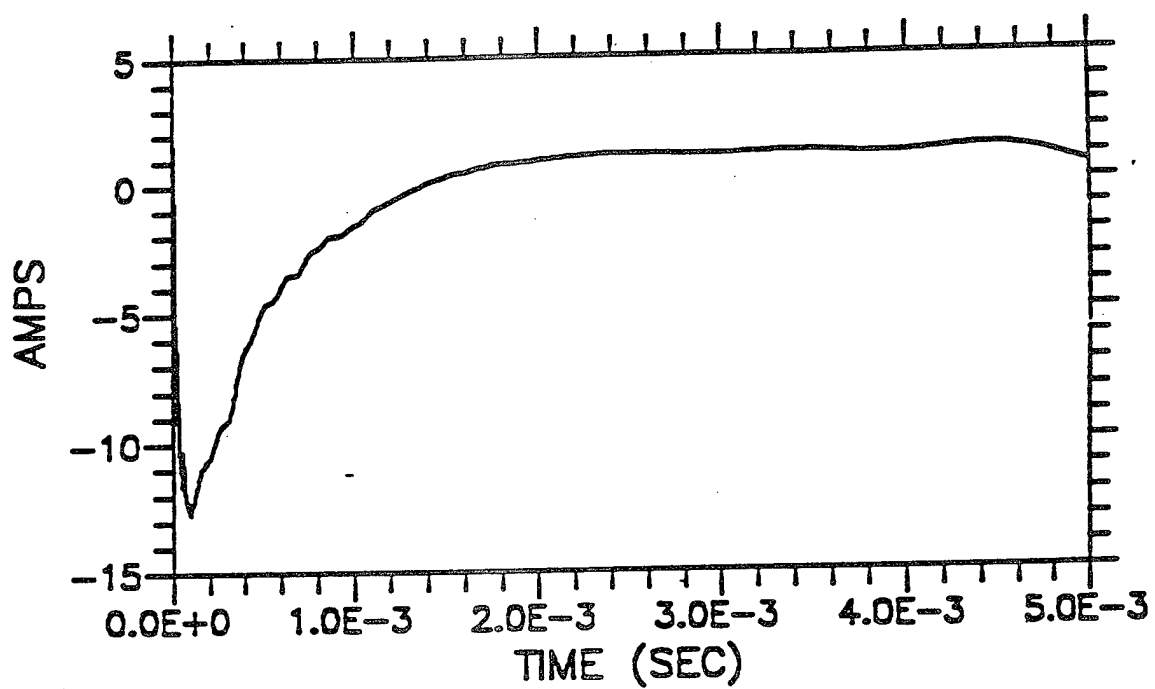
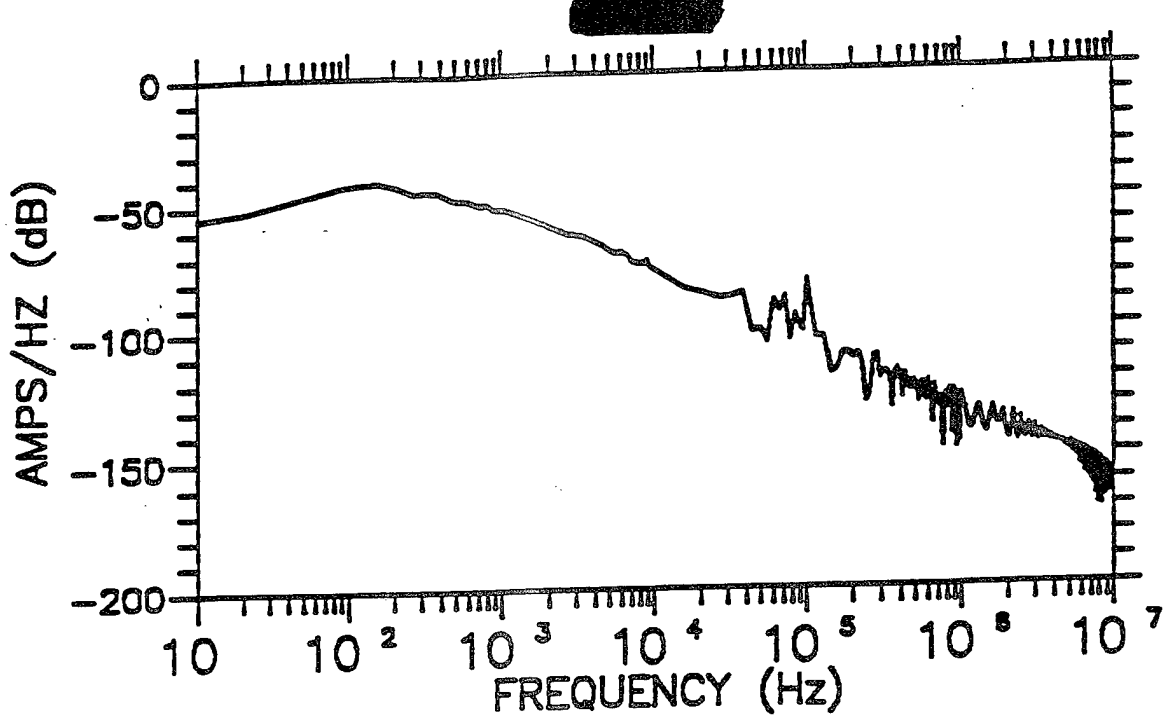


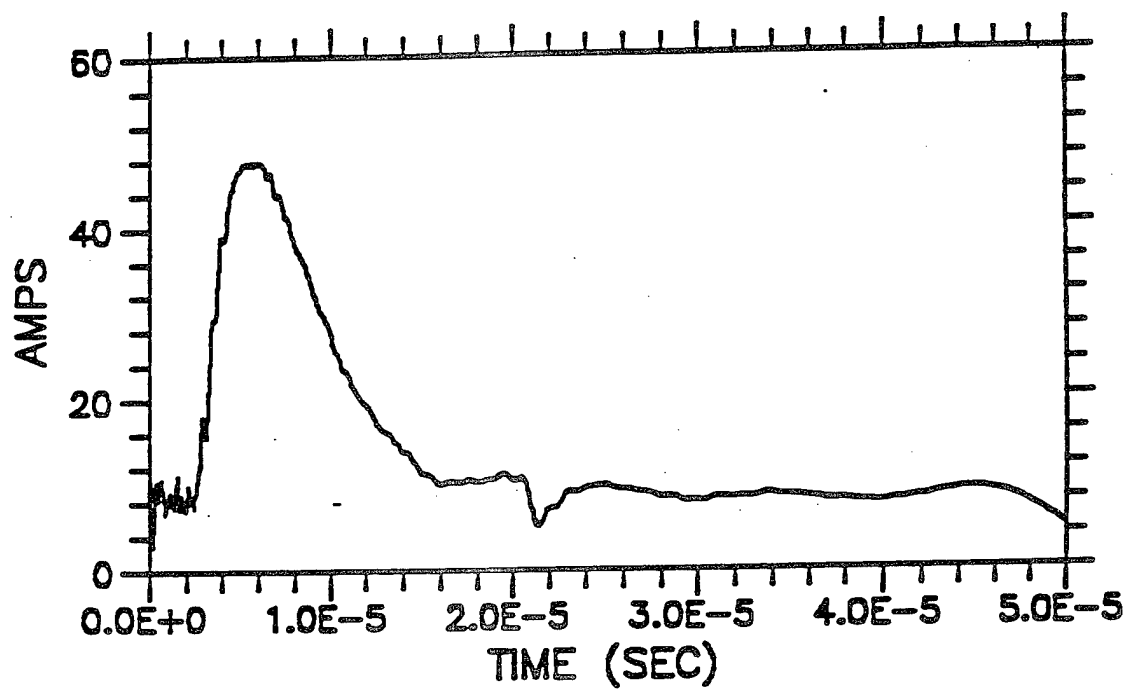
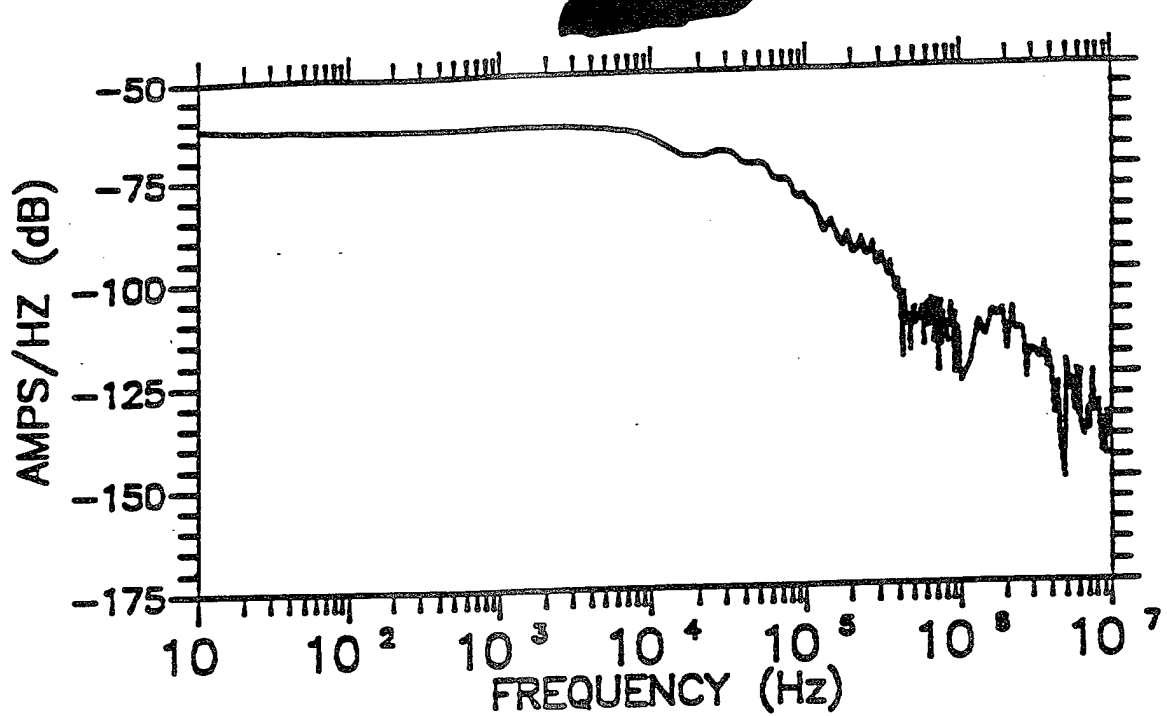


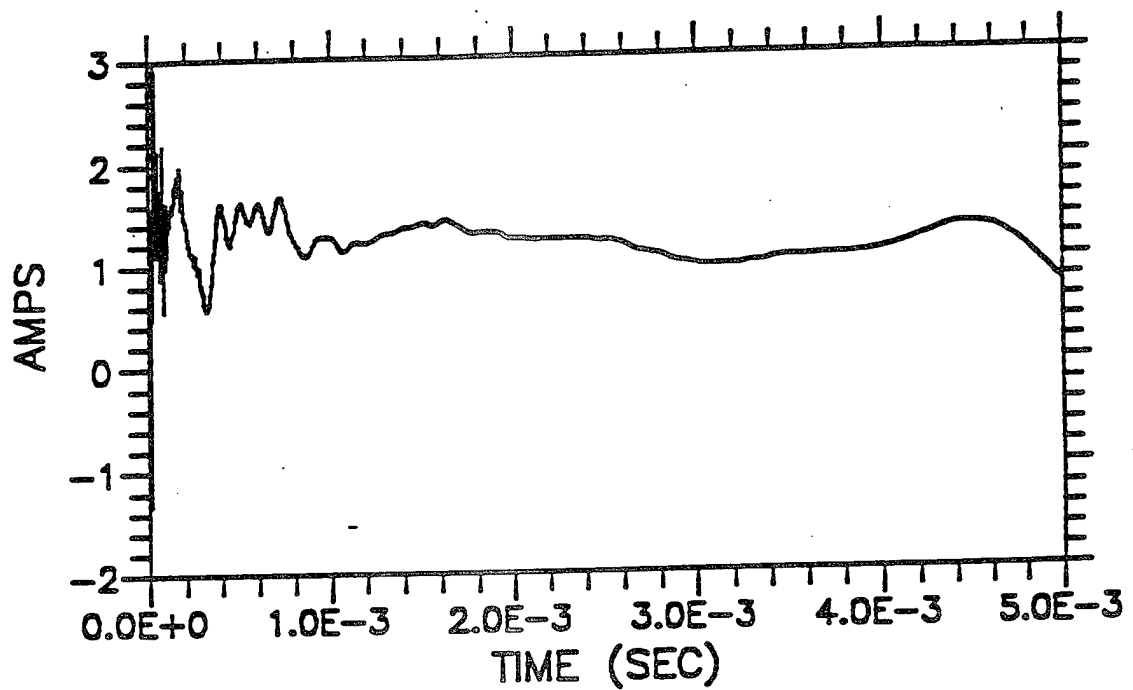
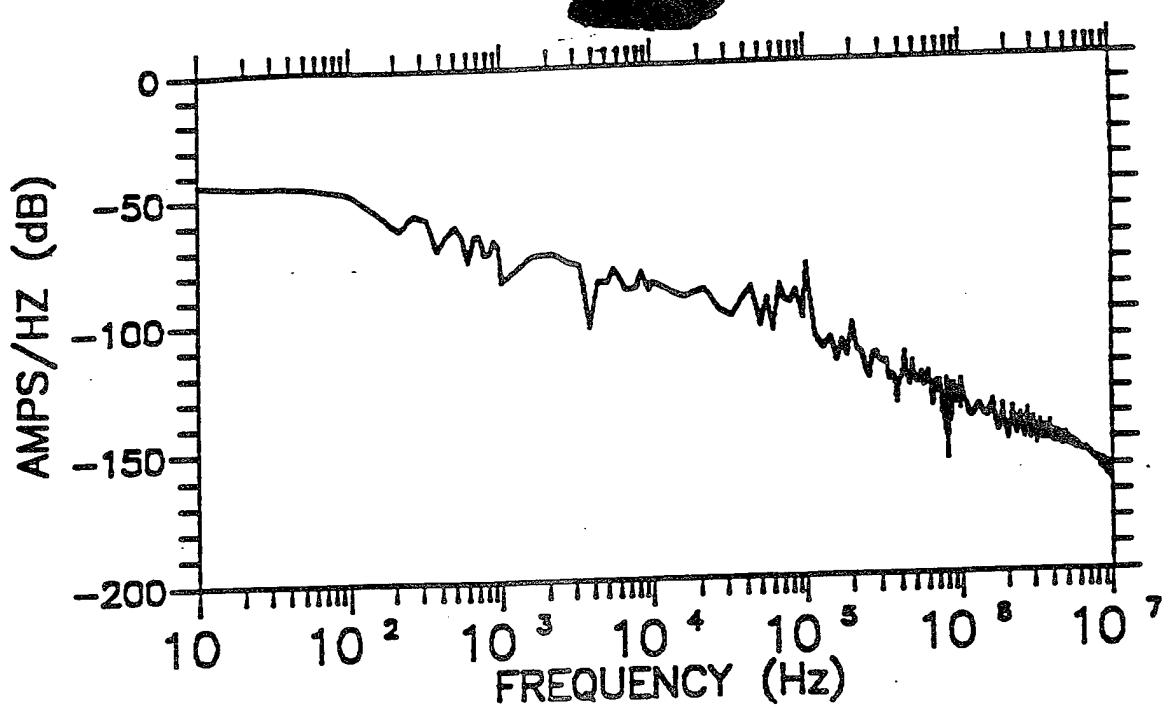


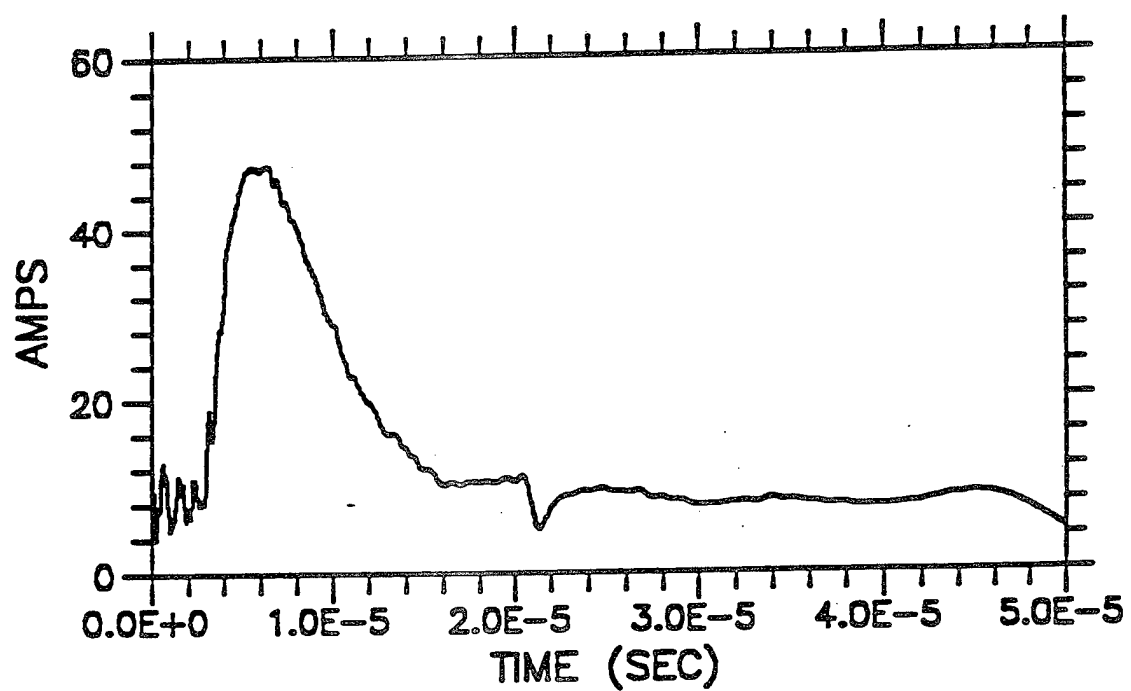
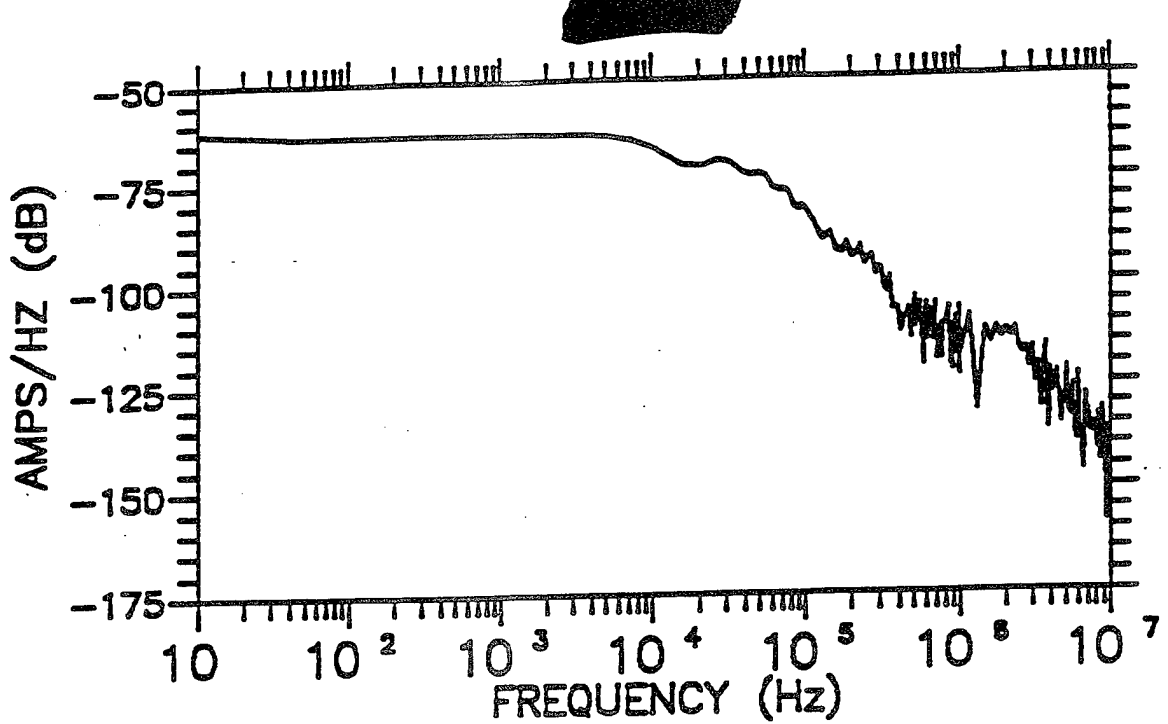


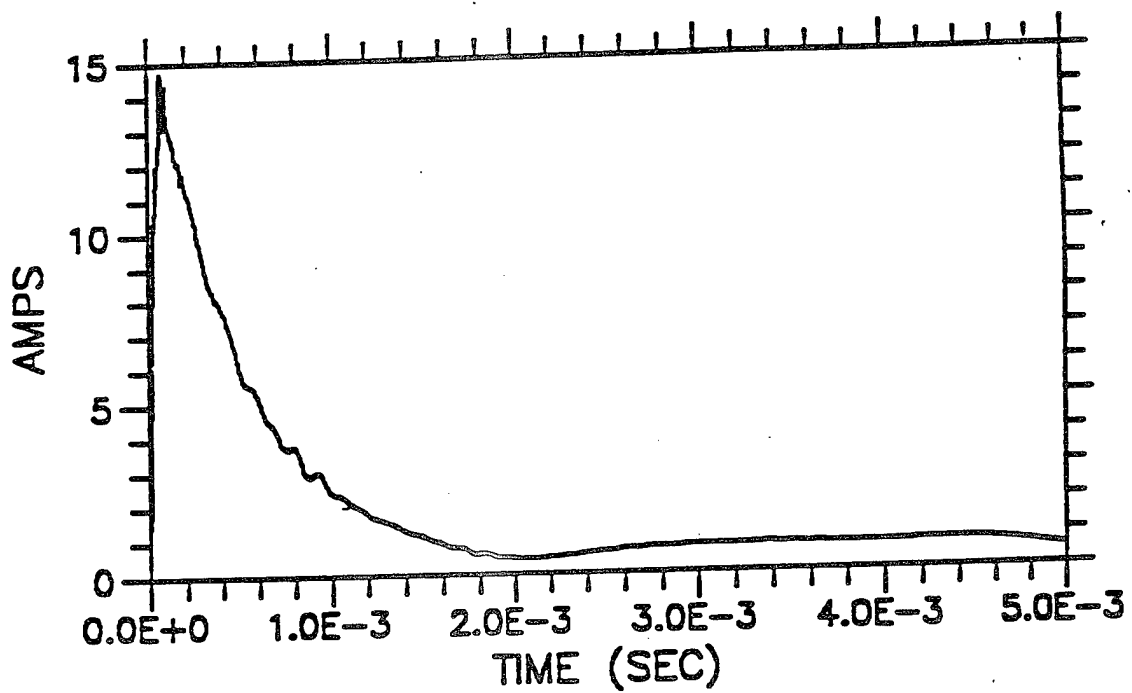
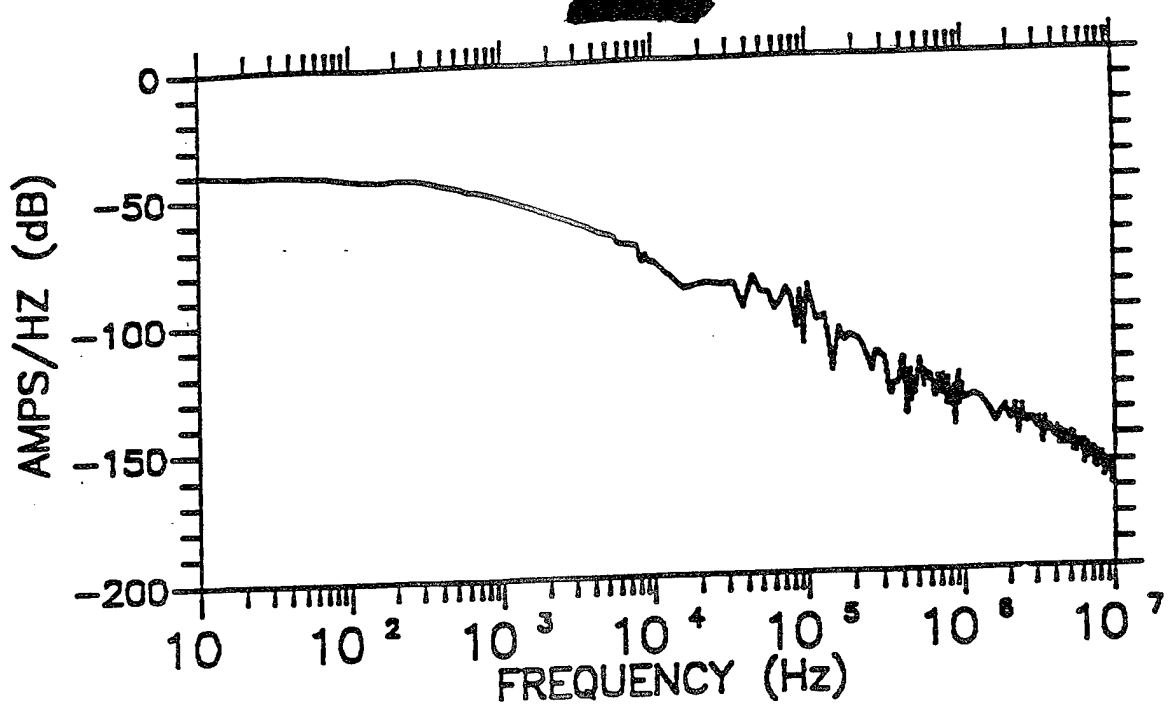


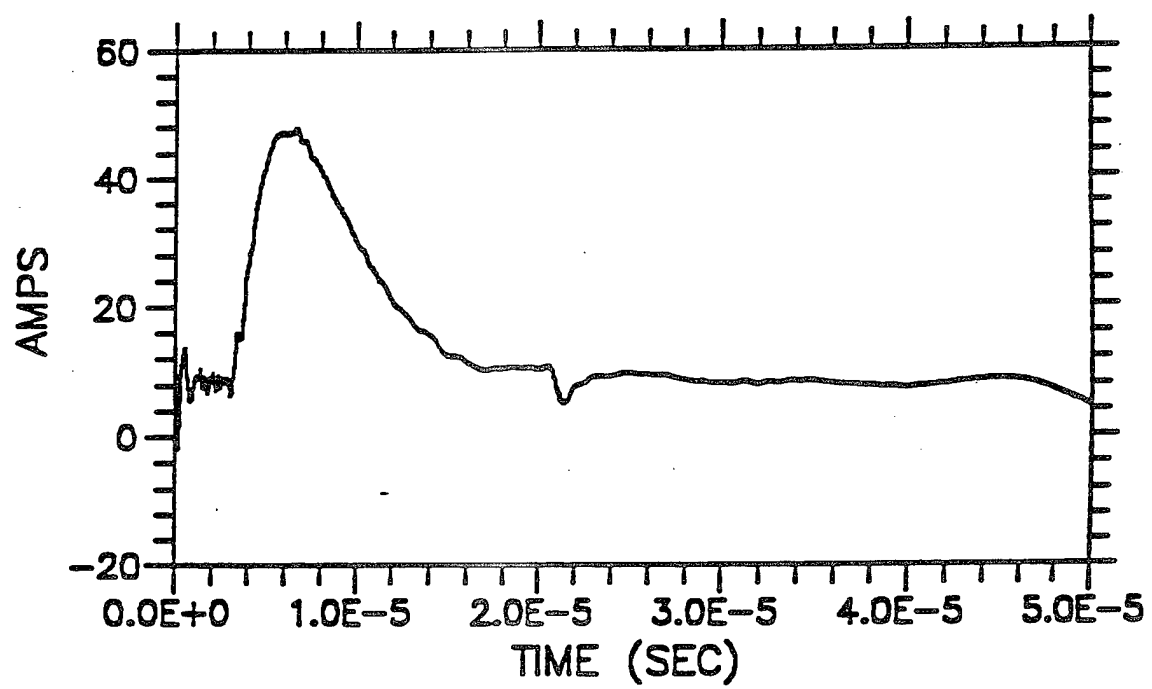
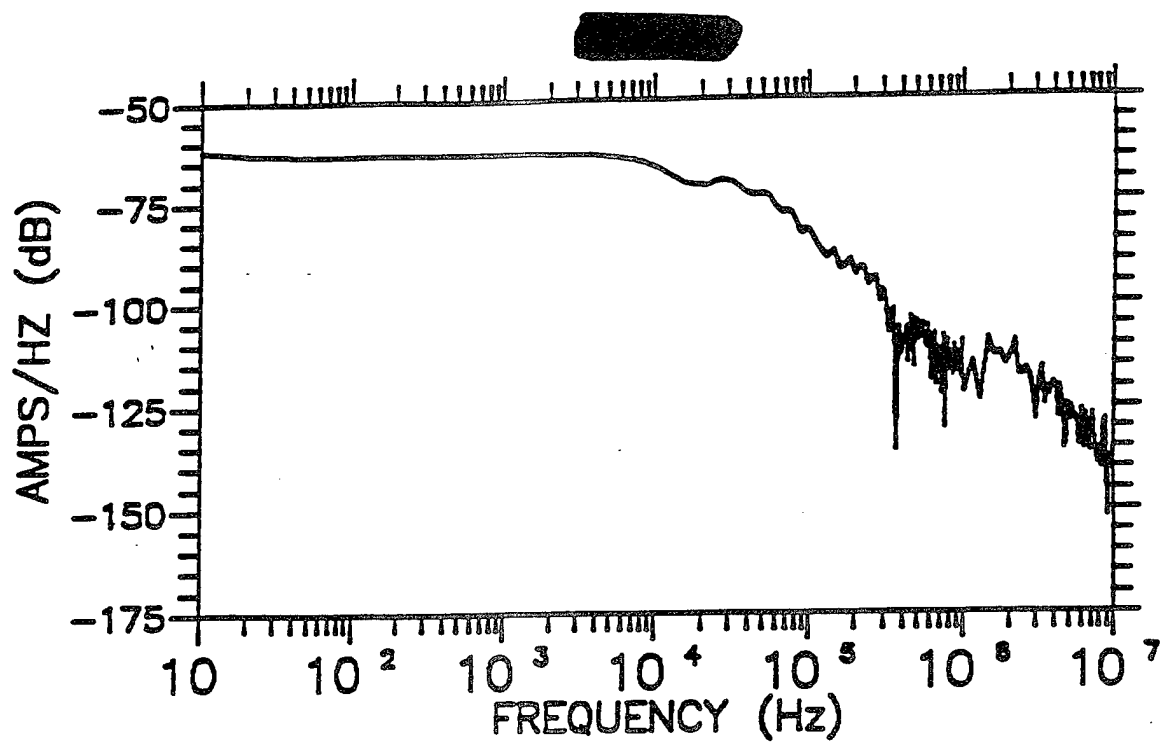


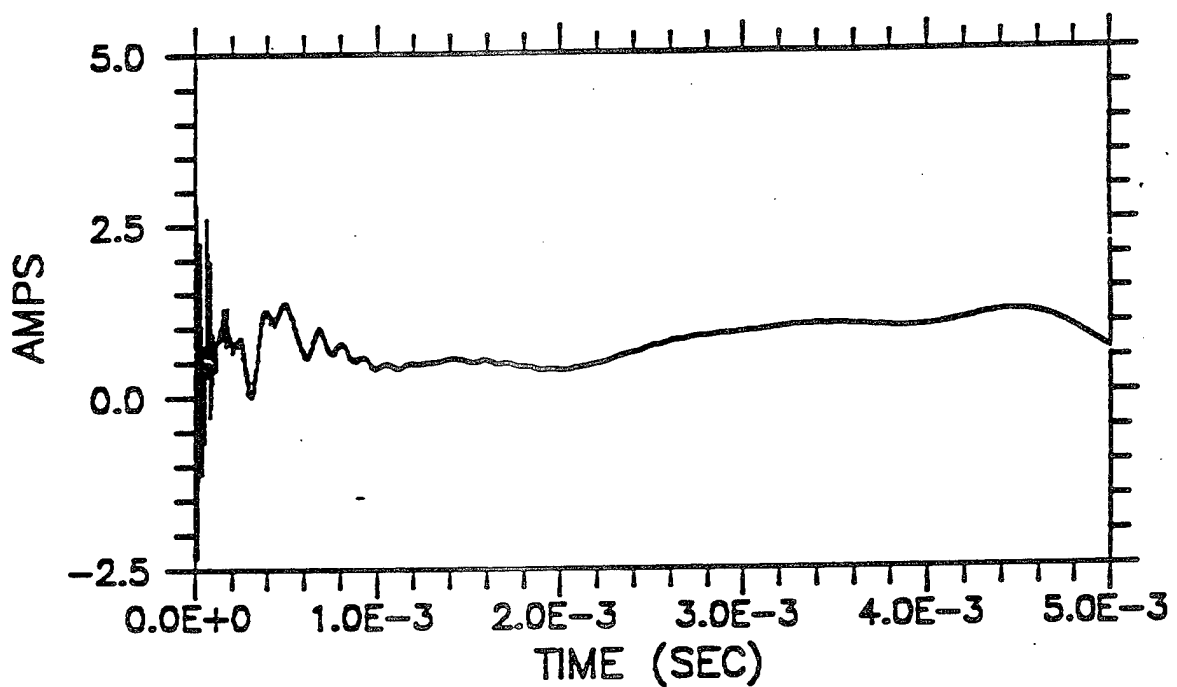
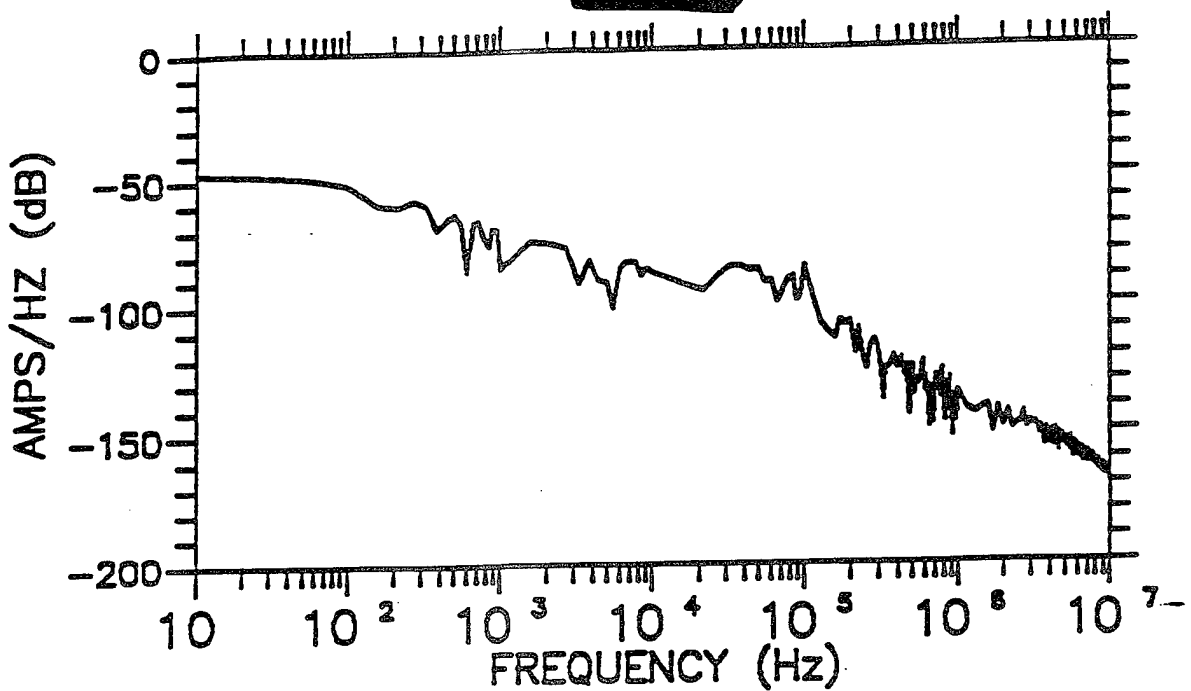












SECTION 4

HEMP COUPLING MEASUREMENTS TO [REDACTED] ANTENNAS

4.1 OBJECTIVES AND OVERVIEW OF DATA ACQUIRED.

[REDACTED] antennas [REDACTED] were selected for CW illumination to measure the field-to-antenna transfer functions. These frequency domain measurements were then extrapolated to the HEMP environments, and inverse Fourier transformed.

From the time domain transients, the waveform descriptors ([REDACTED]) were calculated.

Table 4-1 lists the acquired measurements (files).

[REDACTED] antennas were illuminated with a field polarized parallel to the principal radiating structure to simulate worst-case HEMP coupling. In addition, most were also illuminated with a cross-polarized field (i.e., the simulator field was perpendicular to the antenna radiating structure).

Hence, Table 4-1 indicates two measurements (L_c , L_{c0}) for each illumination.

4.2 [REDACTED] ANTENNAS TESTED.

Brief descriptions of each antenna and simulation configurations are provided in the following subsections.

Table 4-1. CW illumination measurements of [redacted] antennas.

No.	Antenna	File	Polar.	load (ohms)	$R_o(x,y,z)$	$R_i(x,y,z)$	$F(R_o)/F(R_i)$ file	Peak (A)	Inside CWMS volume	Peak Error (dB)
1	H011	worst case		0	$H_z(45,0,1)$	$E_y(133,-3,13)$	HR1	2880	[redacted]	[redacted]
	H012	worst case		50	$H_z(45,0,1)$	$E_y(133,-3,13)$	HR1	1320	[redacted]	yes
	H021	perp.		0	$H_z(45,0,1)$	$E_y(133,-3,13)$	HR1	539	[redacted]	yes
	H022	perp.		50	$H_z(45,0,1)$	$E_y(133,-3,13)$	HR1	304	[redacted]	yes
	H051	perp.		0	$H_z(22,2,1)$	$E_y(79,8,13)$	HR5	250	[redacted]	yes
	H052	perp.		50	$H_z(22,2,1)$	$E_y(79,8,13)$	HR5	125	[redacted]	yes
2										4

Table 4-1. CW illumination measurements of [REDACTED] antennas. (Continued)

No.	Antenna	File	Polar.	load (ohms)	$R_o(x,y,z)$	$R_i(x,y,z)$	$F(R_o)/F(R_i)$ file	Peak (A)	Inside CWMS volume	Peak Error (dB)
3	H061	perp.	0	$H_i(22,2,1)$	$E_i(79,8,13)$	HR5	372	[REDACTED] yes		
	H062	perp.	50	$H_i(22,2,1)$	$E_i(79,8,13)$	HR5	180	[REDACTED] yes	< 1	
	V091A	worst case	0	$H_i(54,0,1)$	$E_i(54,0,13)$	VR9C	47	[REDACTED] yes		
	V092A	worst case	50	$H_i(54,0,1)$	$E_i(54,0,13)$	VR9C	10	[REDACTED] yes	5	
4	H091	perp.	0	$H_i(41,-35,1)$	$E_i(41,-35,13)$	HR9	8	[REDACTED] no		
	H092	perp.	50	$H_i(41,-35,1)$	$E_i(41,-35,13)$	HR9	2	[REDACTED] no		

Table 4-1. CW illumination measurements of [REDACTED] antennas. (Continued)

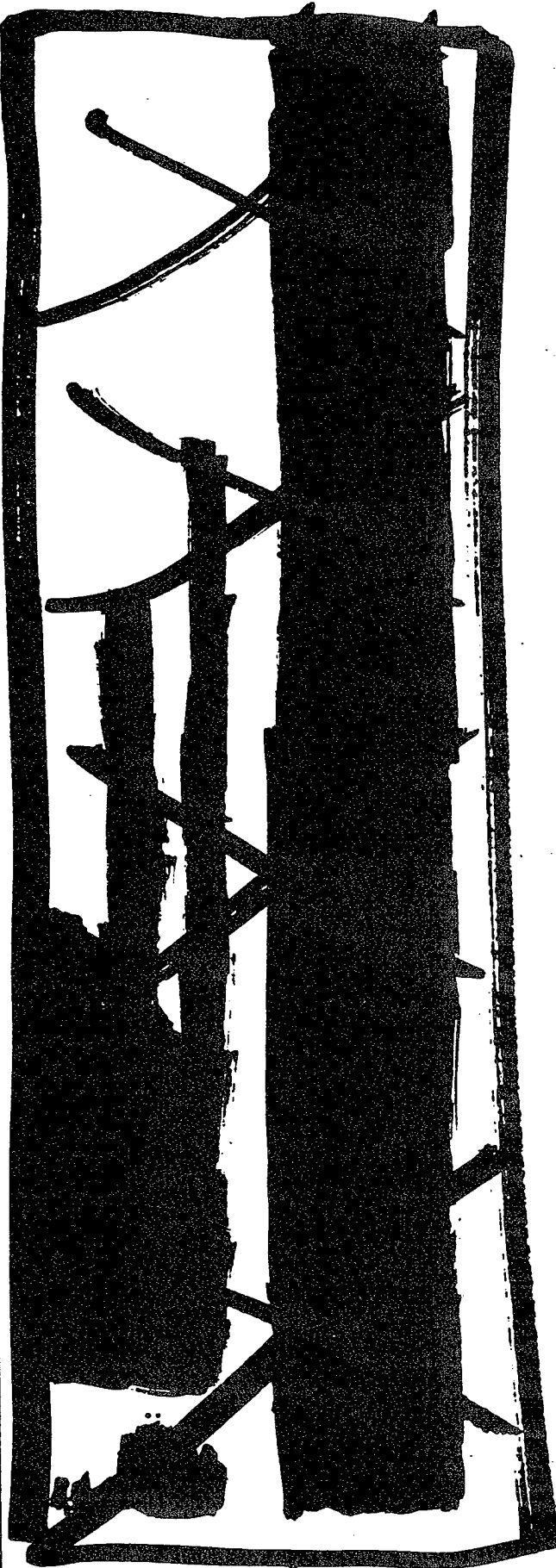
No.	Antenna	F _{file}	Polar.	load (ohms)	R _o (x,y,z)	R _i (x,y,z)	F(R _o)/F(R _i) file	F(R _o)/F(R _i)	Peak (A)	Inside CWMS volume	Peak Error (dB)
V101	worst case	0	H _y (54,0,1)	E _x (54,0,13)	VR9C	25	[REDACTED]	[REDACTED]	yes	[REDACTED]	[REDACTED]
V102	worst case	50	H _y (54,0,1)	E _x (54,0,13)	VR9C	12	[REDACTED]	[REDACTED]	yes	[REDACTED]	5
H101	perp.	0	H _x (41,-35,1)	E _y (41,-35,13)	HR9	11	[REDACTED]	[REDACTED]	no	[REDACTED]	[REDACTED]
H102	perp.	50	H _x (41,-35,1)	E _y (41,-35,13)	HR9	5	[REDACTED]	[REDACTED]	no	[REDACTED]	[REDACTED]
V111	worst case	0	H _y (54,0,1)	E _x (54,0,13)	VR9C	52	[REDACTED]	[REDACTED]	yes	[REDACTED]	[REDACTED]
V112	worst case	50	H _y (54,0,1)	E _x (54,0,13)	VR9C	20	[REDACTED]	[REDACTED]	yes	[REDACTED]	5
H111	perp.	0	H _x (41,-35,1)	E _y (41,-35,13)	HR9	39	[REDACTED]	[REDACTED]	no	[REDACTED]	[REDACTED]
H112	perp.	50	H _x (41,-35,1)	E _y (41,-35,13)	HR9	21	[REDACTED]	[REDACTED]	no	[REDACTED]	[REDACTED]

Table 4-1. CW illumination measurements of [REDACTED] antennas. (Continued)

No.	Antenna	File	Polar.	load (ohms)	$R_o(x,y,z)$	$R_i(x,y,z)$	$F(R_o)/F(R_i)$ file	Peak (A)	Inside CWMS volume	Peak Error (dB)
H031A	worst case	0			$E_r(43,66,13)$	live ref.	827	[REDACTED]	[REDACTED]	no
H032A	worst case	50			$E_r(43,86,13)$	live ref.	472	[REDACTED]	[REDACTED]	no
V031	perp.	0	$H_r(63,0,1)$		$E_r(79,0,13)$	VR3	191	[REDACTED]	[REDACTED]	yes
V032	perp.	50	$H_r(63,0,1)$		$E_r(79,0,13)$	VR3	156	[REDACTED]	[REDACTED]	yes
H041	worst case	0	$H_r(11,19,1)$		$E_r(28,-50,13)$	FLDCHK1	2320	[REDACTED]	[REDACTED]	no
H042	worst case	50	$H_r(11,19,1)$		$E_r(28,-50,13)$	FLDCHK1	1370	[REDACTED]	[REDACTED]	no
V041	perp.	0	$H_r(22,0,1)$		$E_r(57,0,13)$	VR4	711	[REDACTED]	[REDACTED]	yes
V042	perp.	50	$H_r(22,0,1)$		$E_r(57,0,13)$	VR4	405	[REDACTED]	[REDACTED]	yes
										2

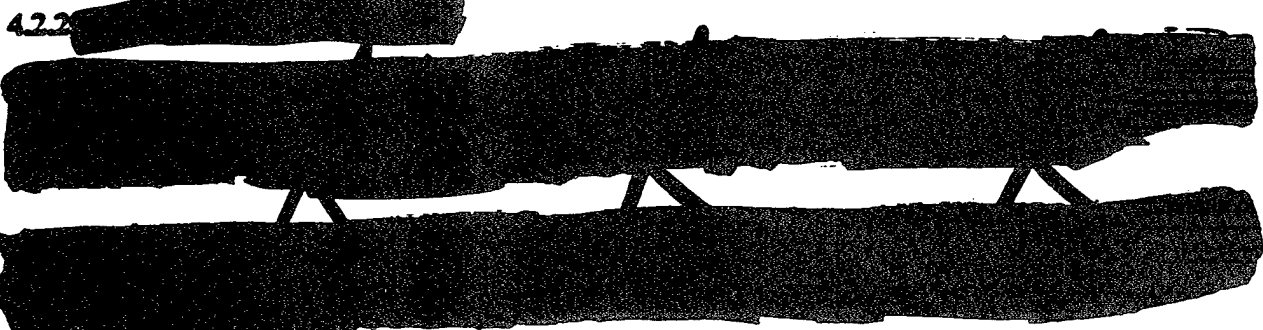
Table 4-1. CW illumination measurements of [redacted] antennas. (Continued)

No.	Antenna	File	Polar.	load (ohms)	$R_t(x,y,z)$	$R_t(x,y,z)$	$F(R_t)/F(R_s)$	Peak (A)	Inside CWMS volume	Peak Error (dB)
V071	[redacted]	worst case	0	$H_t(38,0,1)$	$E_t(191,0,13)$	VR7	402	[redacted]	yes	[redacted]
V072	[redacted]	worst case	50	$H_t(38,0,1)$	$E_t(191,0,13)$	VR7	196	[redacted]	yes	1

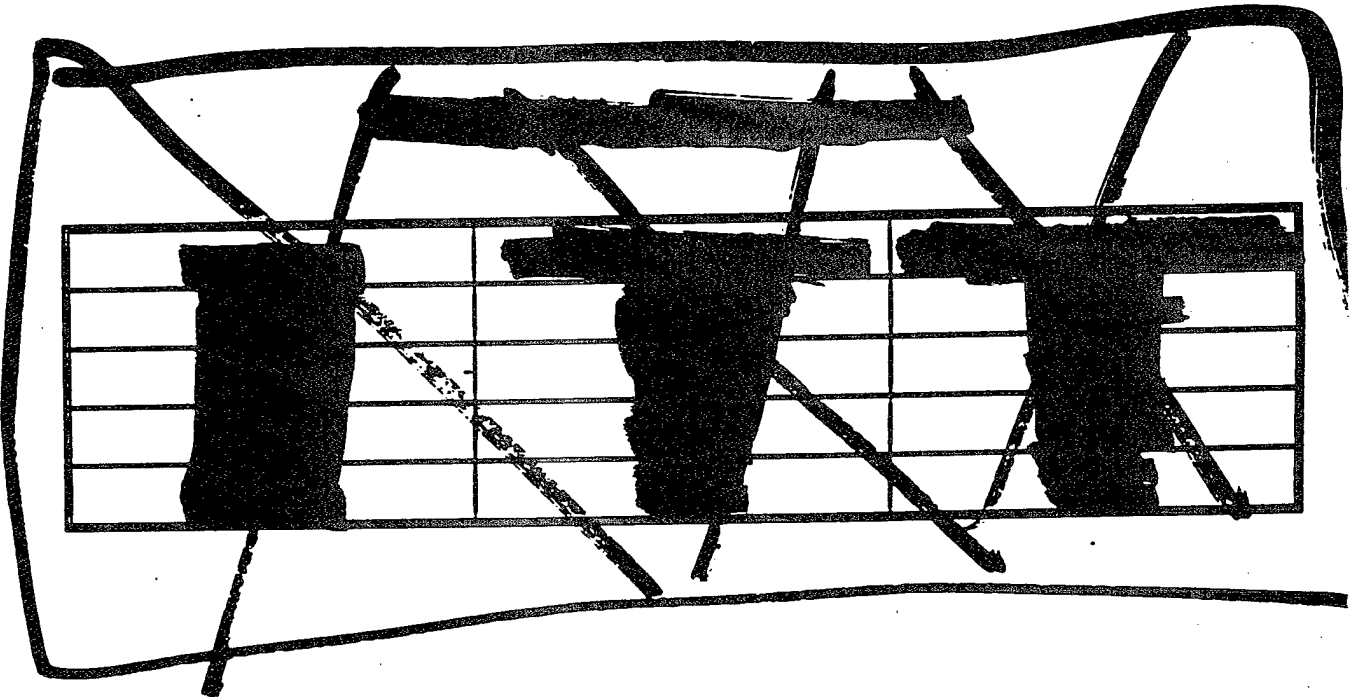
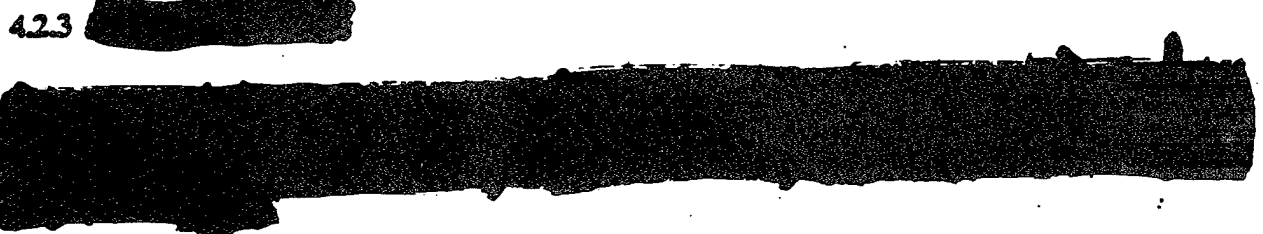


First, the center line [REDACTED] was aimed at the supporting tower for the CWMS drooping dipole antenna. This orientation is depicted as arrow 1 in Figure 4-2 and should provide the worst case threat (filenames H011 and H012). [REDACTED] is parallel to the CWMS drooping dipole depicted as arrow 2 in Figure 4-2 (filenames H021 and H022). [REDACTED] operating volume of the CWMS horizontally polarized simulator.

4.2.2



4.2.3



Pages 84-87
removed in their
entirety.

[REDACTED]

4.2.4 [REDACTED]

[REDACTED]

4.2.5 [REDACTED]

4.3 DESCRIPTION OF THE TESTS AND DATA PROCESSING.

4.3.1 Horizontally Polarized Illumination.

Test Setup: Figure 4-9 shows the CWMS simulator used to radiate horizontally polarized fields; i.e., the major electric field is parallel to the ground. The simulator uses an inverted-V dipole to radiate at discrete frequencies between 100 kHz to 102 MHz, and a logperiodic antenna from 102 MHz to 1 GHz.

Ideally, one would measure the transfer function I_{ANT}/E_y , where I_{ANT} is the current in the antenna line, and E_y is the field at the antenna location, but with the antenna removed (i.e., the undisturbed total field at the antenna location). If this transfer function could be measured, the HEMP induced current could simply be obtained by multiplying this transfer function by the E_y produced by HEMP at the same location.

In practice, the antenna cannot be "temporarily removed." To measure the undisturbed (i.e., not affected by the antenna scatter) simulation field, the field sensor is placed away from the antenna in an open area. In addition, due to test equipment constraints and the rough terrain, it was also necessary to utilize an intermediate field measurement closer to the simulator. These field measurements are referred to as "reference sensor" measurements below.

In sum, the measurement setup was as shown in Figure 4-9. Hence, the antenna current relative to the simulator field at R_1 is:

$$\frac{I_{ANT}}{E_y(R_1)}(\omega) = \left[\frac{I_{ANT}}{H_z(R_o)} \right] \cdot \left[\frac{H_z(R_o)}{E_y(R_1)} \right] \quad (A \cdot m/V) \quad (4-1)$$

where the quantities in the square brackets indicate measurements. The first measurement is the antenna current relative to the magnetic field at R_o , and the second is the electric field at R_1 ; i.e., closest to the antenna, relative to the magnetic field at R_o . Since the magnetic field cancels out (in theory and in practice), the antenna current relative to E_y at R_1 is obtained. The reference locations R_o and R_1 are identified in Table 4-1 for each measurement.

Processing: To calculate the antenna response due to a HEMP, the transfer function in Equation (4-1) is extrapolated; i.e., it is multiplied by the electric field strength which a HEMP would produce at R_1 . The denominator of the transfer function is the total (incident plus reflected off the ground) electric field at 13 m above ground. Since the extrapolation function must be consistent with the simulation, we need to calculate the total HEMP field at that location per Appendix A. Thus, the extrapolated current is

$$I_{ANT}^{HEMP}(\omega) = \frac{I_{ANT}}{E_y(R_1)} \cdot E_y^{inc,HEMP}(\omega) [1 + R_H e^{-\alpha z}] \quad (A/Hz) \quad (4-2)$$

where R_H and α are from Appendix B. The incident field $E_y^{inc,HEMP}$ is the unclassified HEMP waveform EMP-1 defined by Reference 10:

$$E_{EMP-1}^{inc}(t) = 6.425E4 (e^{-at} - e^{-bt}) \quad (V/m) \quad (4-3)$$

$$a = 3.00E7 \text{ sec}^{-1}, b = 4.76E8 \text{ sec}^{-1}$$

The result is the frequency spectrum of the antenna current due to a HEMP, and the current transient is obtained by taking the Fourier inverse transform:

$$i_{ANT}^{HEMP}(t) = \frac{1}{\pi} \int_{-\omega_0}^{\omega_0} I_{ANT}^{HEMP}(\omega) e^{j\omega t} d\omega \quad (4-4)$$

With two exceptions,¹ the antenna currents measured with the horizontal illumination field were processed accordingly. The results are contained in Appendix C. In addition, the ambient noise was measured at several antennas. Comparison plots of CWMS signal measured vs. ambient noise are included in Appendix D.

4.3.2 Vertically Polarized Illumination.

Test Setup: Figure 4-10 shows the CWMS simulator used to radiate vertically polarized fields; i.e., the major electric field is perpendicular to the ground. The simulator uses a monopole fed on the ground to radiate at frequencies between 100 kHz to 102 MHz, and a vertical logperiodic on top of the monopole at frequencies up to 1 GHz. Hence, the radiation source for the low frequency simulation is near the ground, while the radiation source above 102 MHz is about 21 m above the ground (the logperiodic antenna is mounted on top of the monopole structure). The consequences of this inconsistency are discussed below.

For the reasons discussed in the previous section, two reference (field) sensors were employed. The antenna current relative to the vertical electric field at R_1 is:

$$\frac{I_{ANT}}{E_z(R_1)}(\omega) = \left[\frac{I_{ANT}}{H_y(R_o)} \right] \cdot \left[\frac{H_y(R_o)}{E_z(R_1)} \right] \quad (A \cdot m/V) \quad (4-5)$$

where the quantities in the square brackets indicate measurements. The first measurement is the antenna current relative to the magnetic field at R_o , and the second is the electric field at R_1 ; i.e., closest to the antenna, relative to the magnetic field at R_o . Since the magnetic field cancels out, the antenna current relative to E_z at R_1 is obtained. The reference locations R_o and R_1 are identified in Table 4-1 for each measurement.

¹The only exceptions are files H031A and H032A, where the antenna currents were directly measured relative to the horizontal electric field at R_1 . This is indicated in Table 4-1 by the comment "live ref."

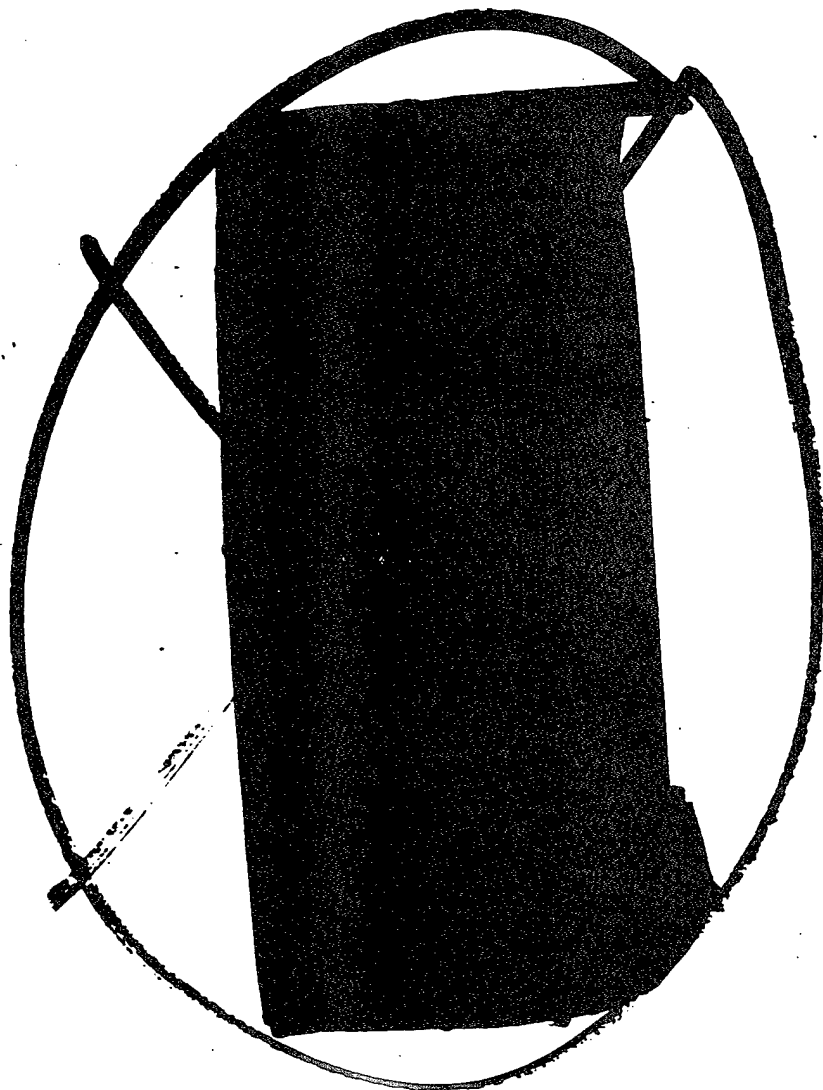


Figure 4-10.

Processing: To calculate the antenna response due to a HEMP, the transfer function in Equation (4-5) is extrapolated; i.e., it is multiplied by the electric field strength which a HEMP would produce at R_s . As before, the extrapolation function must be consistent with the reference field (i.e., the denominator of Equation (4-5)). Since the simulator has two different source locations, we must consider two cases:

100 kHz to 102 MHz: The radiating element is a monopole above a lossy ground. If the ground were a good conductor, the simulator would be electromagnetically equivalent (by image theory) to a dipole in free space; i.e., the radiated fields would be purely incident fields. Since the ground is a moderate conductor, the fields are incident fields, modified by a correction term to account for the finite earth conductivity. For the present purposes, the correction term is neglected; and, hence, the extrapolation is:

$$I_{\text{ANT}}^{\text{HEMP}}(\omega) = \frac{I_{\text{ANT}}}{E_z(R_1)} \cdot E_z^{\text{inc., HEMP}}(\omega) \quad (\text{A/Hz}) \quad (4-6)$$

As before, the unclassified waveform EMP-1 is used for $E_z^{\text{inc., HEMP}}$.

102 MHz to 1 GHz: The radiating element is a logperiodic antenna, roughly 21 m above ground. It produces a total field (incident plus reflected off the ground) at the reference sensor at R_1 . Accordingly, the extrapolation function (from Appendix A) is:

$$E_z^{\text{inc., HEMP}}(\omega) [1 + R_V e^{-j\phi}] \approx E_z^{\text{inc., HEMP}} \left(\frac{V/m}{\text{Hz}} \right) \quad (4-7)$$

The approximation follows from Appendix B which shows that R_V is much smaller than unity; hence, the extrapolation function in Equation (4-6) can be also be used at high frequencies.

The resulting frequency spectra for the HEMP induced antenna currents, and the inverse Fourier transforms are presented in Appendix C.

4.4 HEMP INDUCED ANTENNA CURRENTS.

All measurements were processed as described in Section 4-2, and are contained in Appendix C. The results are summarized in Table 4-1 of Section 4-1.

The file name indicates whether the horizontal CWMS simulator was used (prefix "H"), or the vertical simulator (prefix "V"). The column entitled "Polar" describes whether the simulator fields were parallel to the principal antenna radiating structure ("WORST CASE"), or perpendicular ("PERP"). The next column identifies the load on the antenna coaxial cable; i.e., whether the current was measured into 50 ohms or into a short circuit.

The waveform descriptors peak current

The column entitled "Inside CWMS Volume" indicates whether the test object (antenna) was outside the simulation volume.

The last column accounts for the fact that the reference location R_1 was not at each test object as discussed in Section 4-2, but closer to the simulator. Since the simulation field strength decreases as 1/distance (cf. References 9, 11), the error is $20 \log(d/R_1)$, where d is the distance from the simulator to the antenna, and R_1 is the distance from the simulator to the reference location R_1 .

4.4.1 Representative Results for Each Antenna.

Table 4-1 shows that worst case polarization indeed produces the largest currents in the antennas. The currents induced in a 50 ohm test load and into a short circuit are overlaid in the following figures (Figures 4-11 to 4-19) for the worst case polarization of the incident field, except in the two cases indicated. Each figure displays the spectra and the time domain transients.

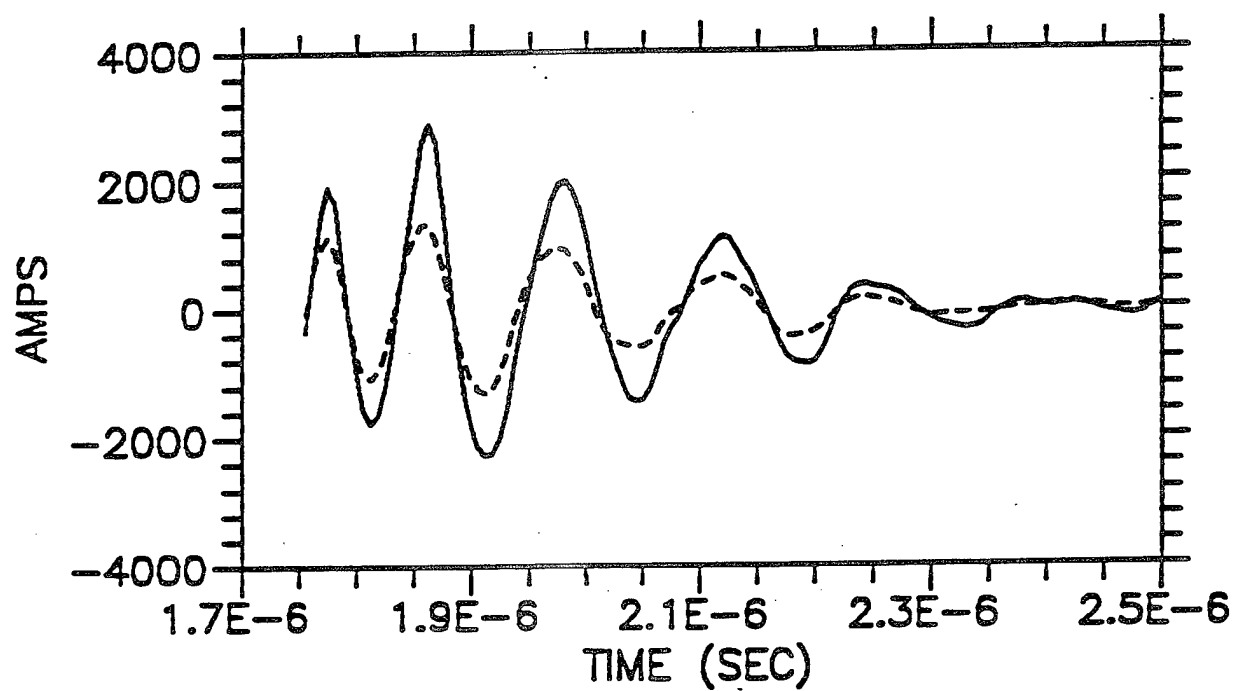
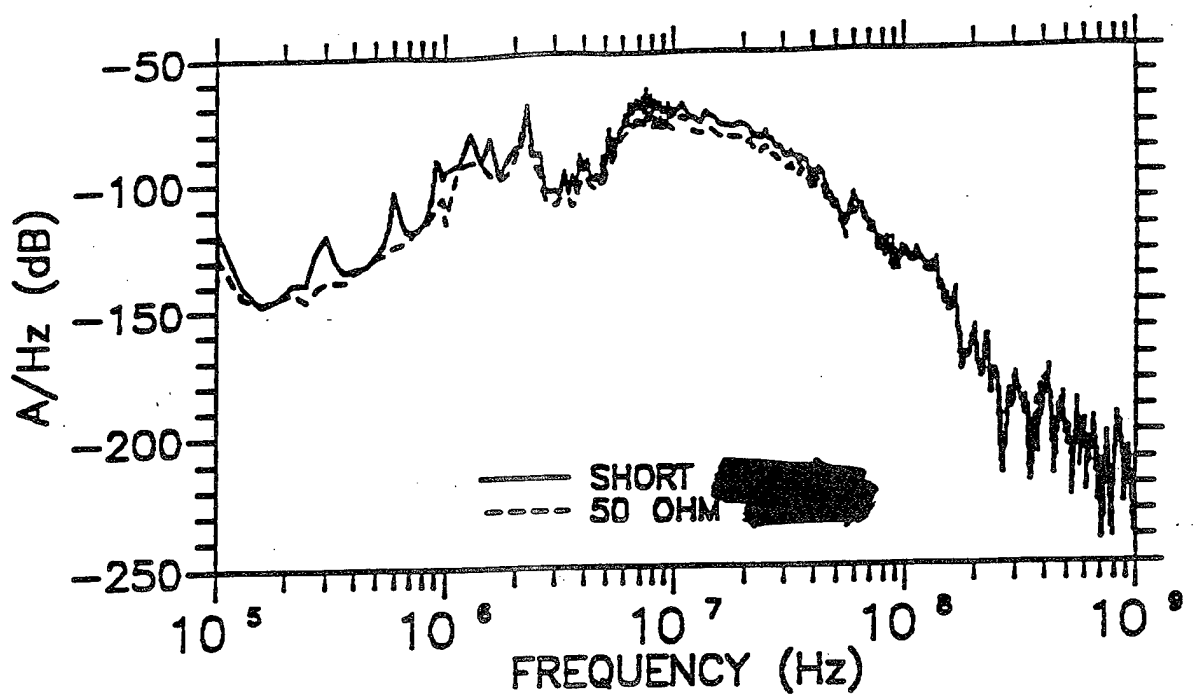
Note that the short-circuit and 50 ohm current waveforms are quite similar; i.e., the short-circuit current is about twice the current into 50 ohms. The reason for this is discussed in the next section.

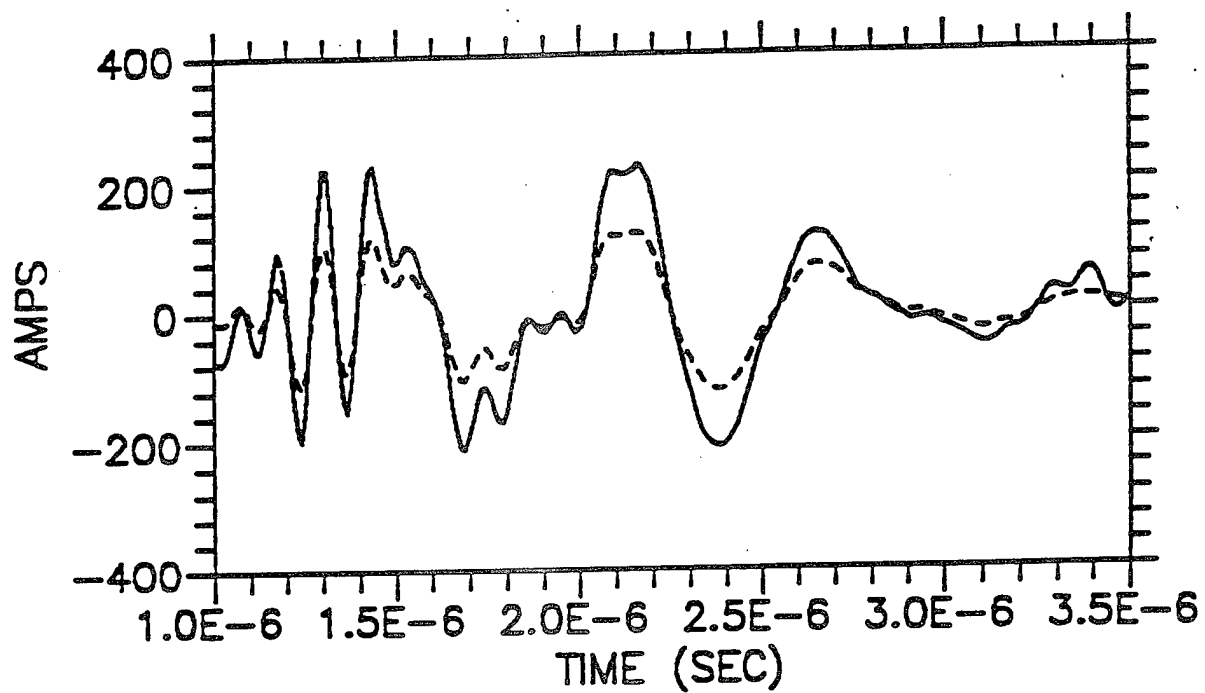
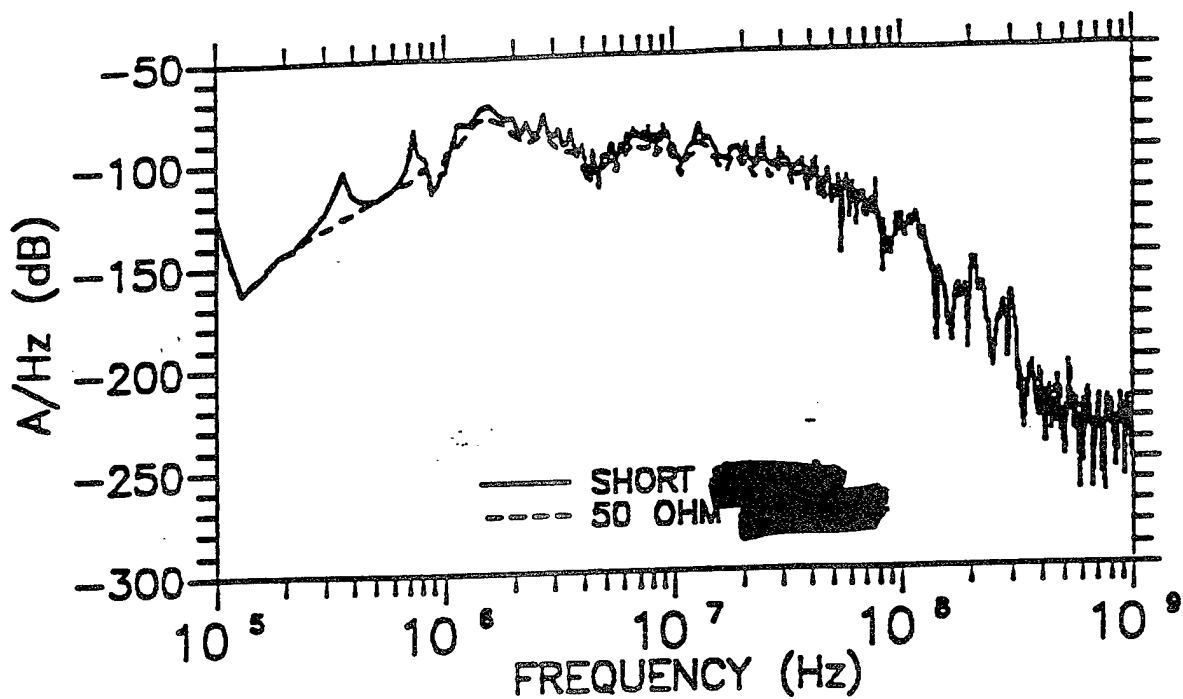
4.4.2 Antenna Impedance.

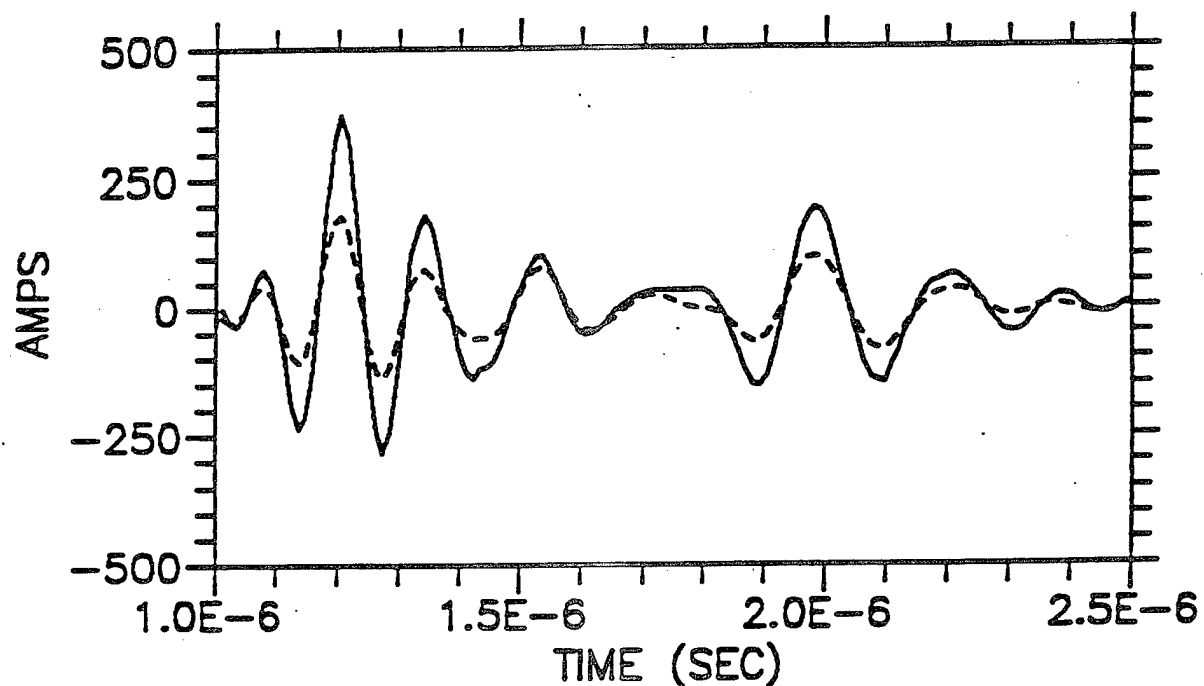
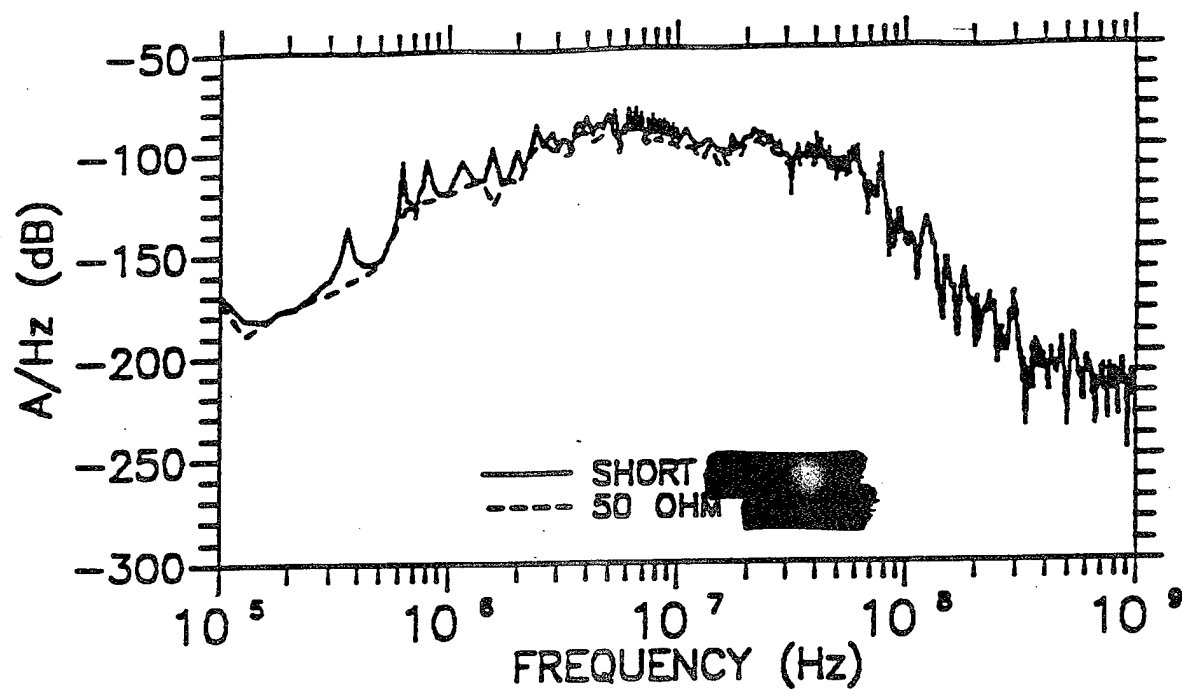
Figure 4-20 shows the electrically important elements of the coupling path from the voltage generated at the antenna terminals to the test load, and the equivalent circuit for this path. This circuit represents the HEMP stress seen by the radio equipment; hence, it is the ideal injection test simulator.

The only unknown in this circuit is the input or source impedance Z_{in} , which can be calculated by

$$Z_{in} = 50 \frac{I_{50}}{I_{sc} - I_{50}} \quad (\Omega) \quad (4-8)$$







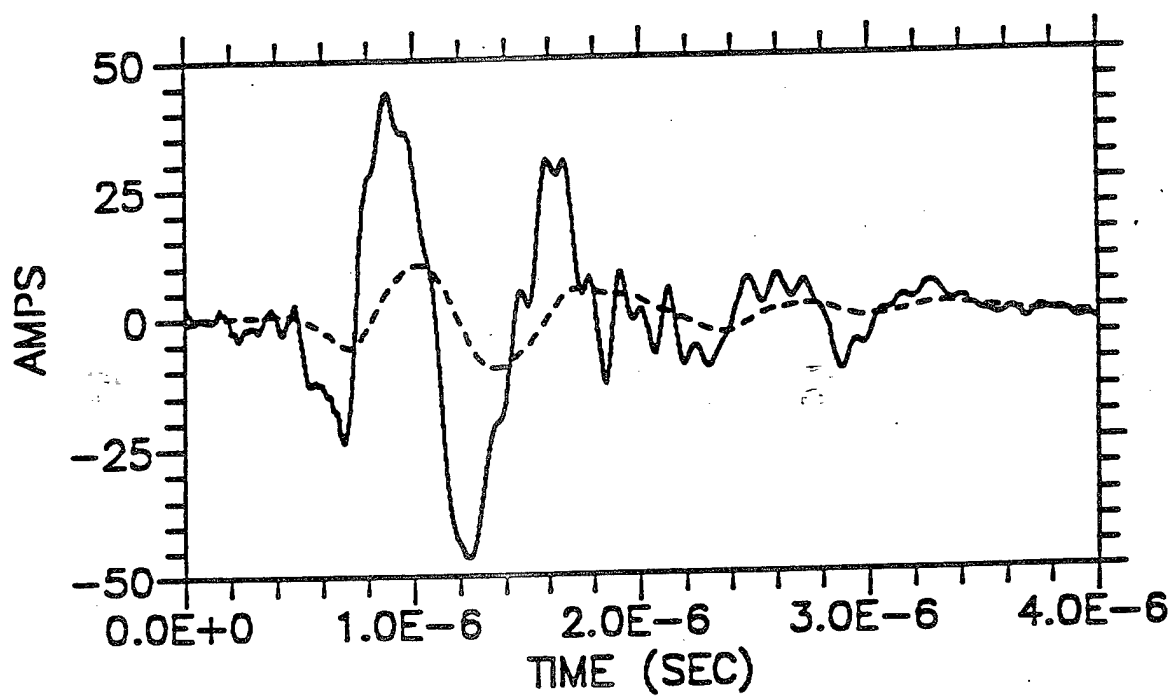
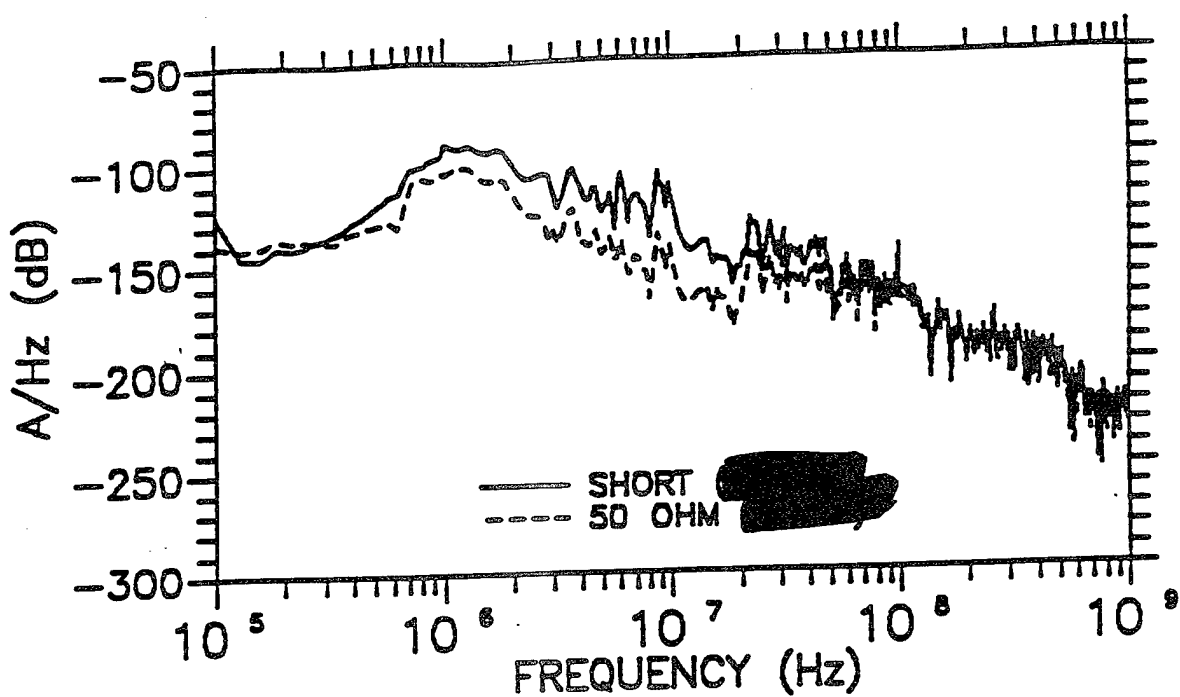
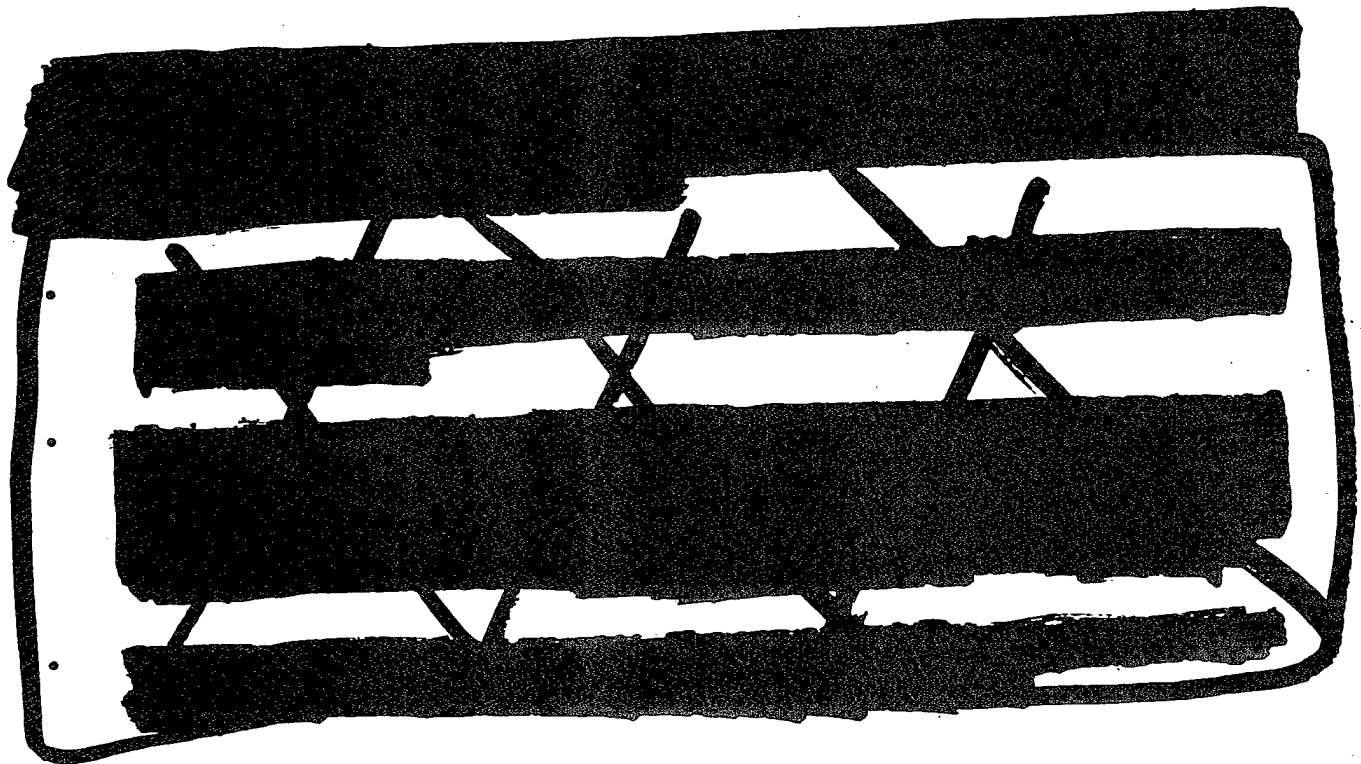
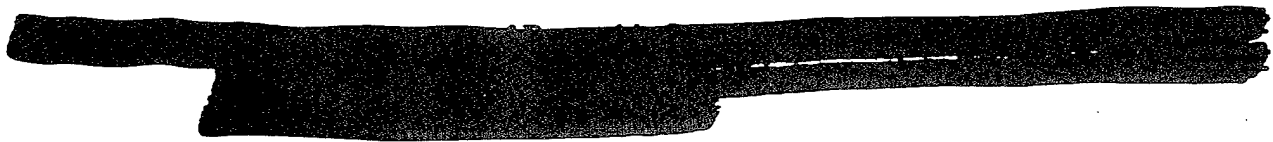
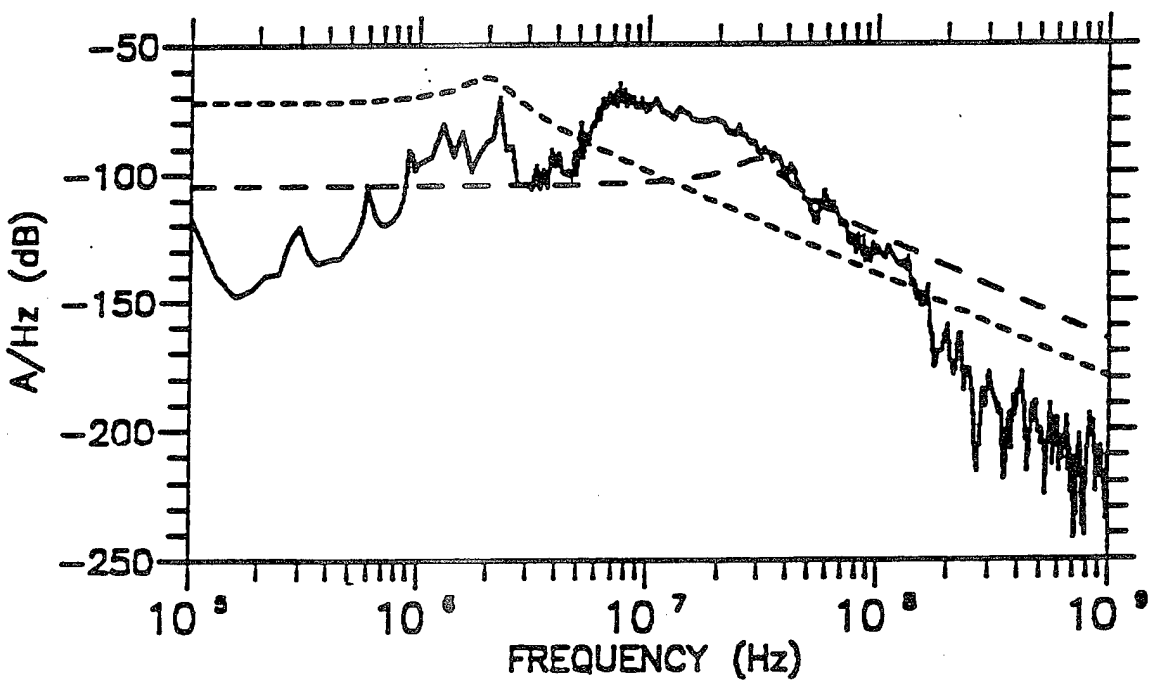
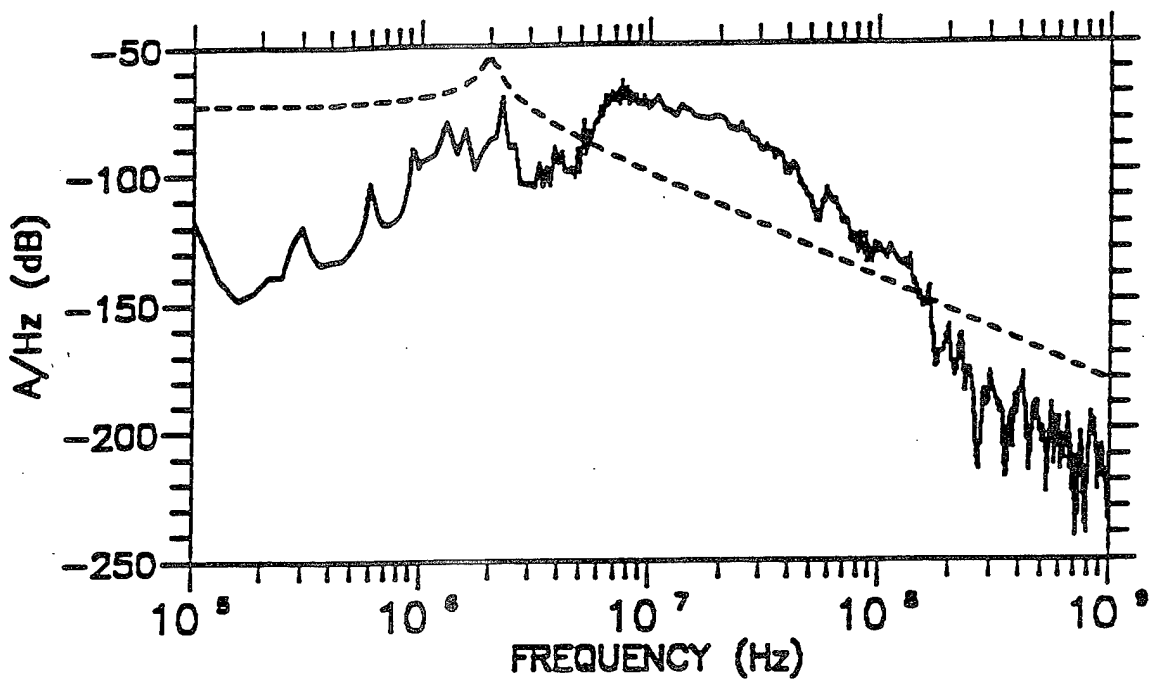


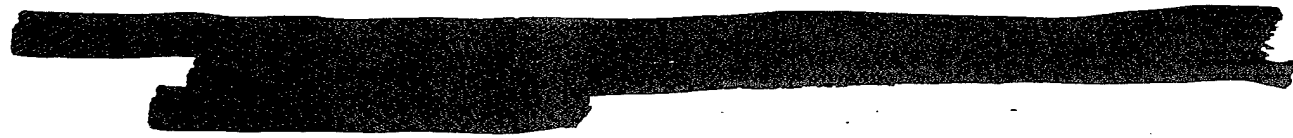
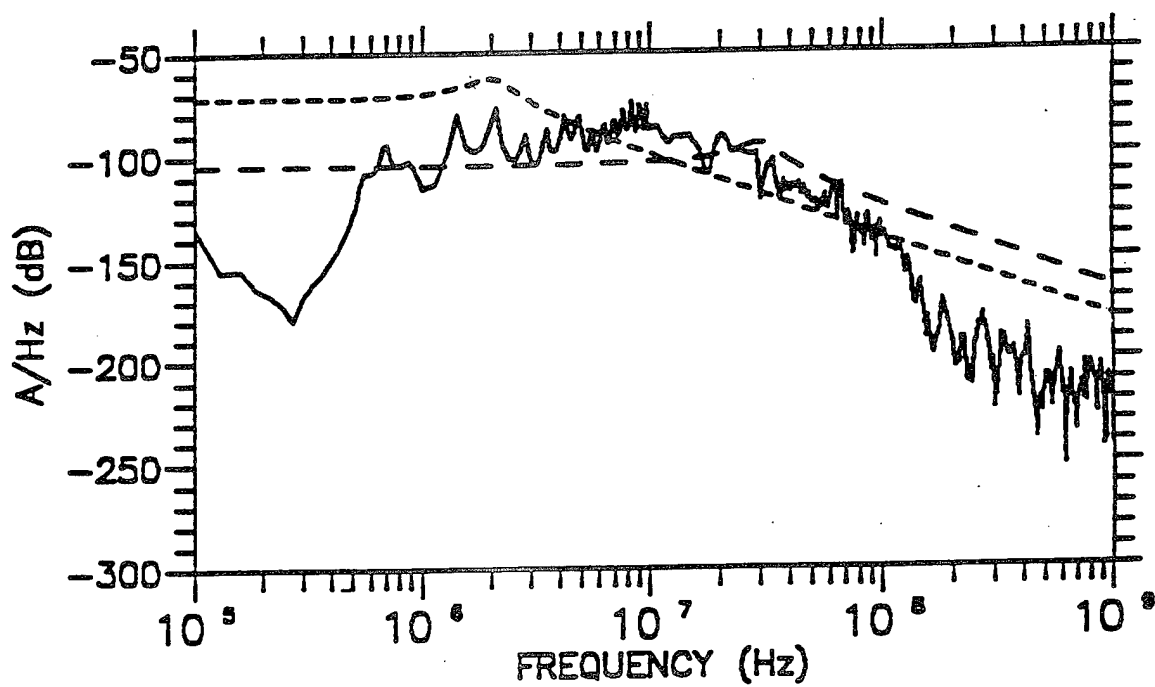
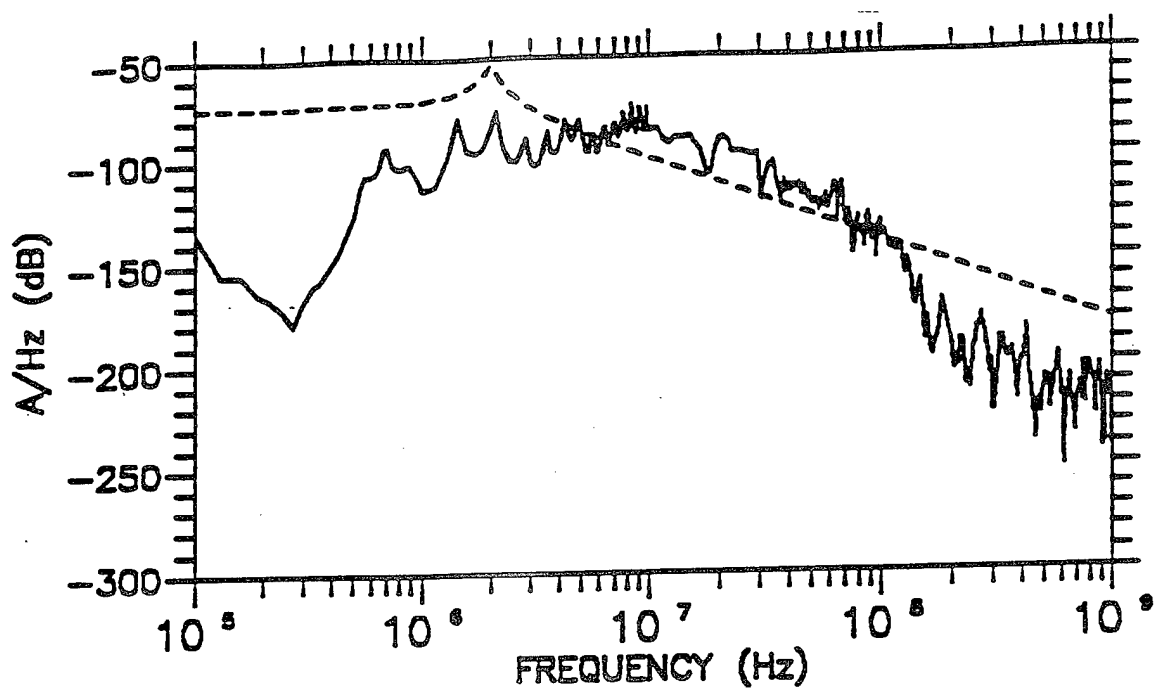
Table 4-3.

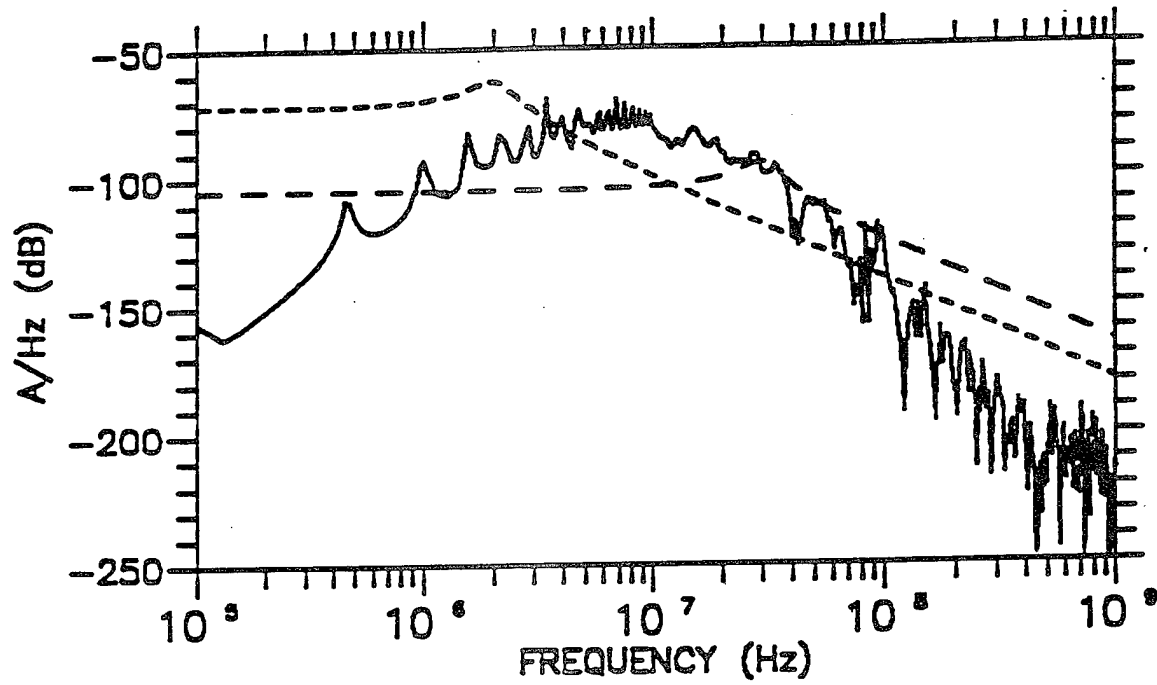
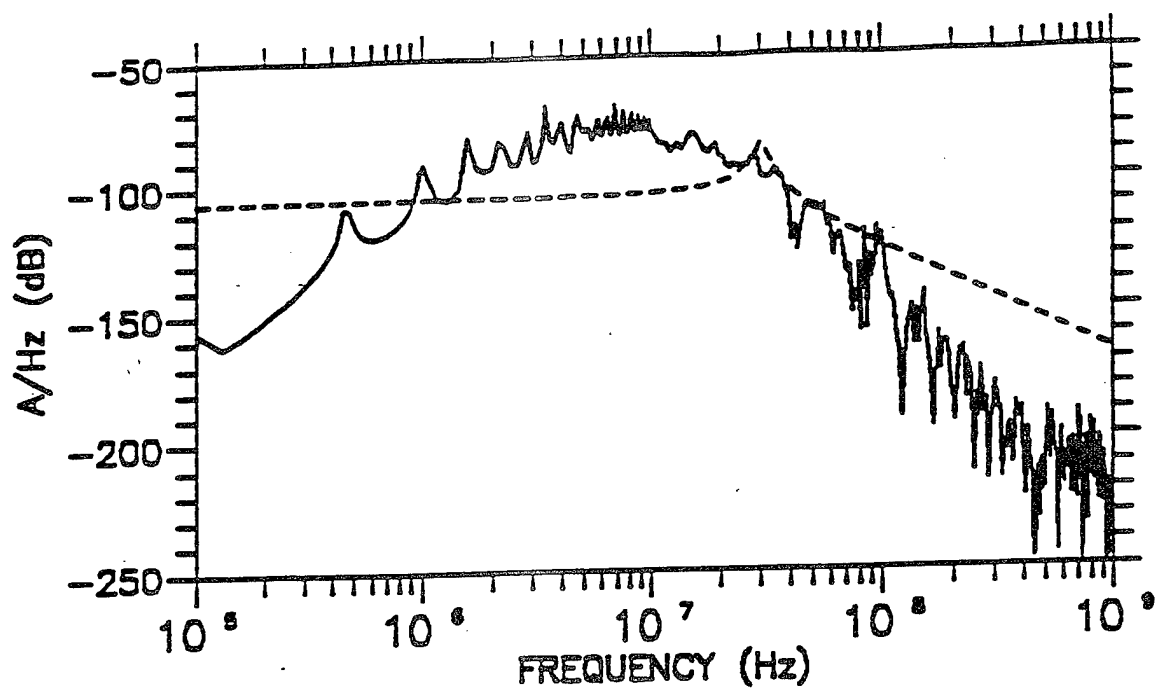
A 10x10 grid of black ink blots on a white background. The blots are irregular shapes with varying degrees of speckling. A thick vertical black bar is positioned along the left edge of the grid. Two diagonal black lines are drawn across the grid: one from the top-left corner to the bottom-right corner, and another from the bottom-left corner to the top-right corner.

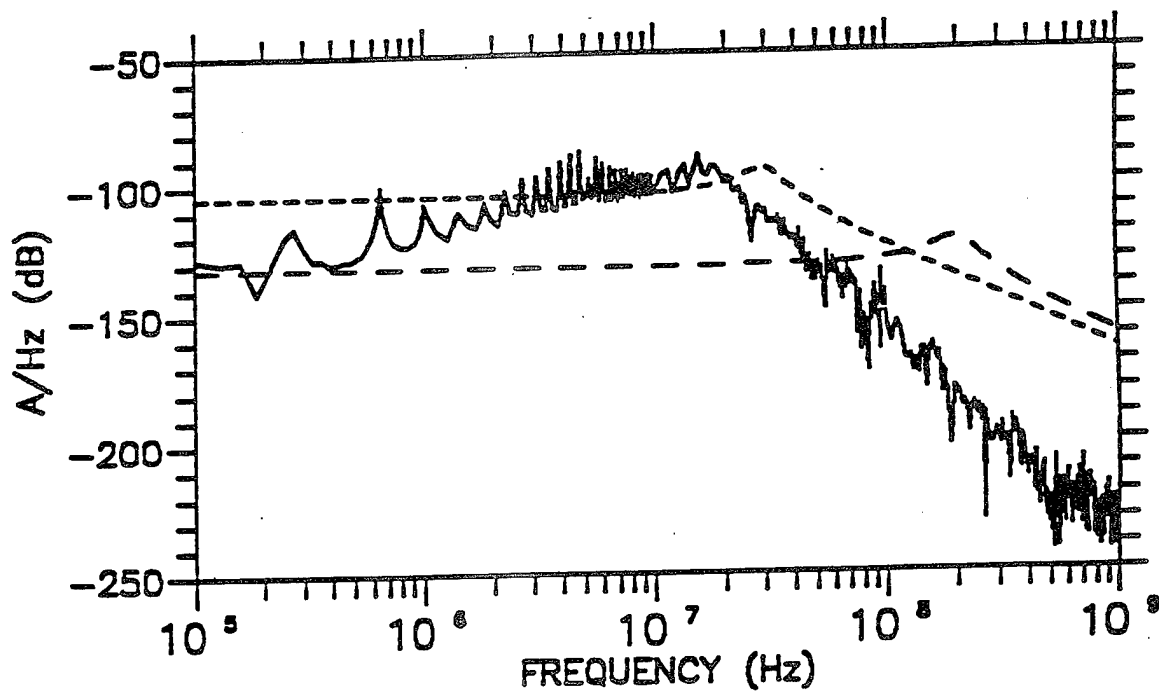
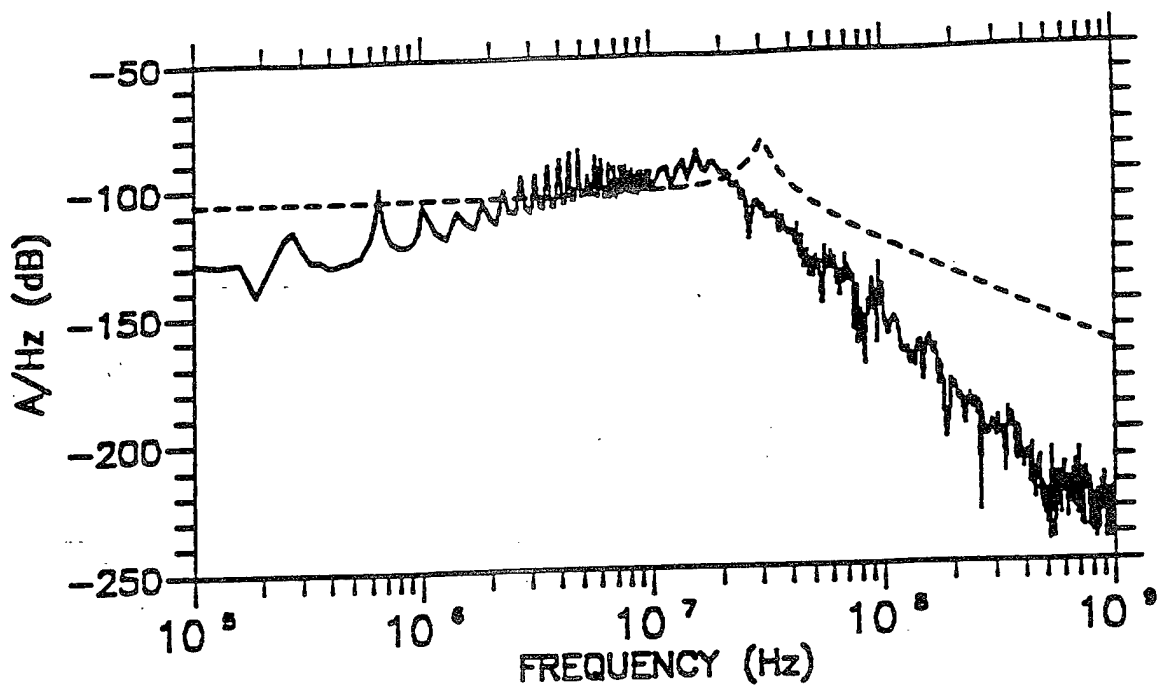
compare the extrapolated short-circuit currents with the two test requirements. The test coverage provided by the standard appears deficient. The revision suggested by Reference 7 improves the coverage.

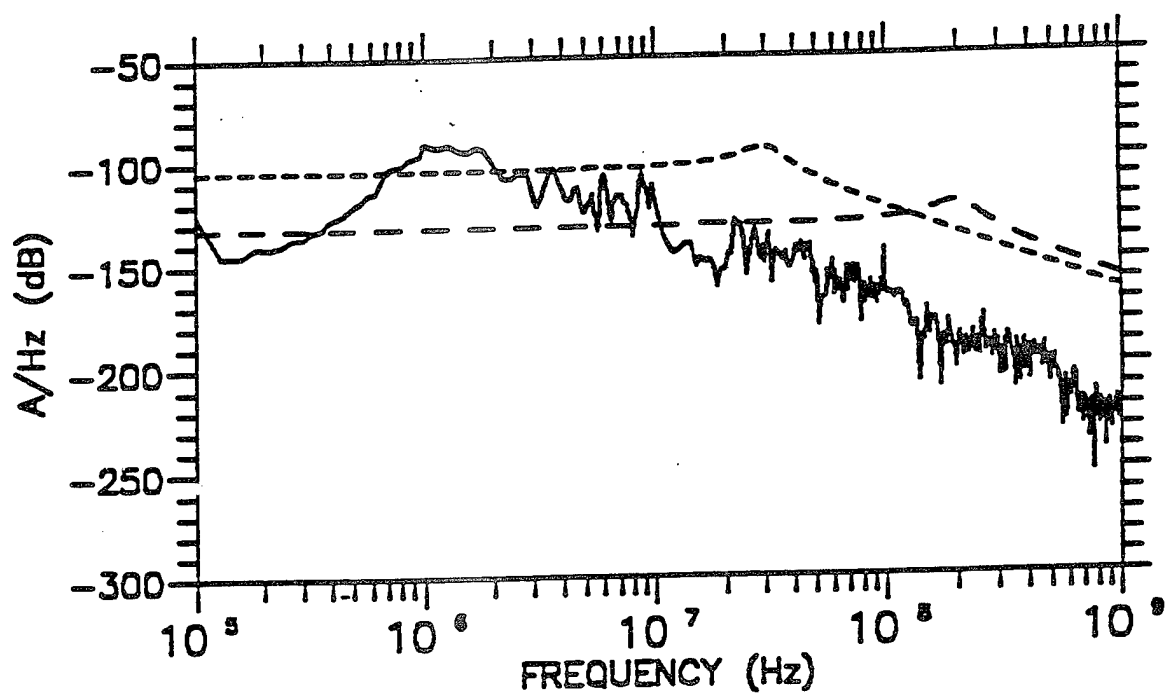
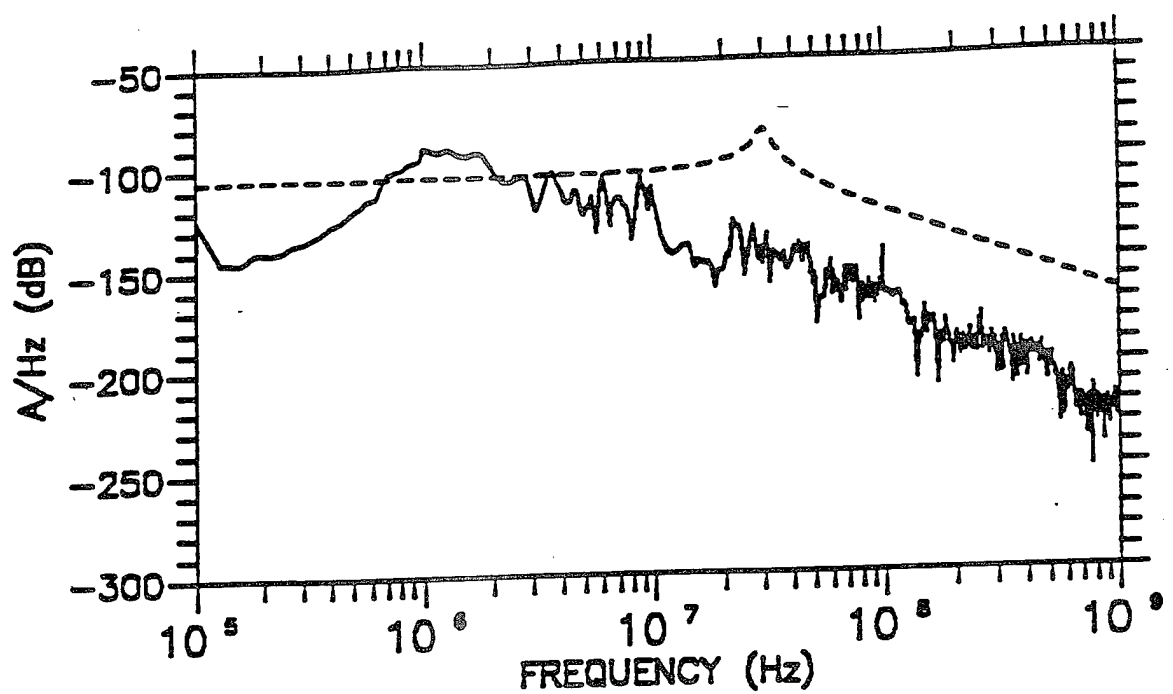


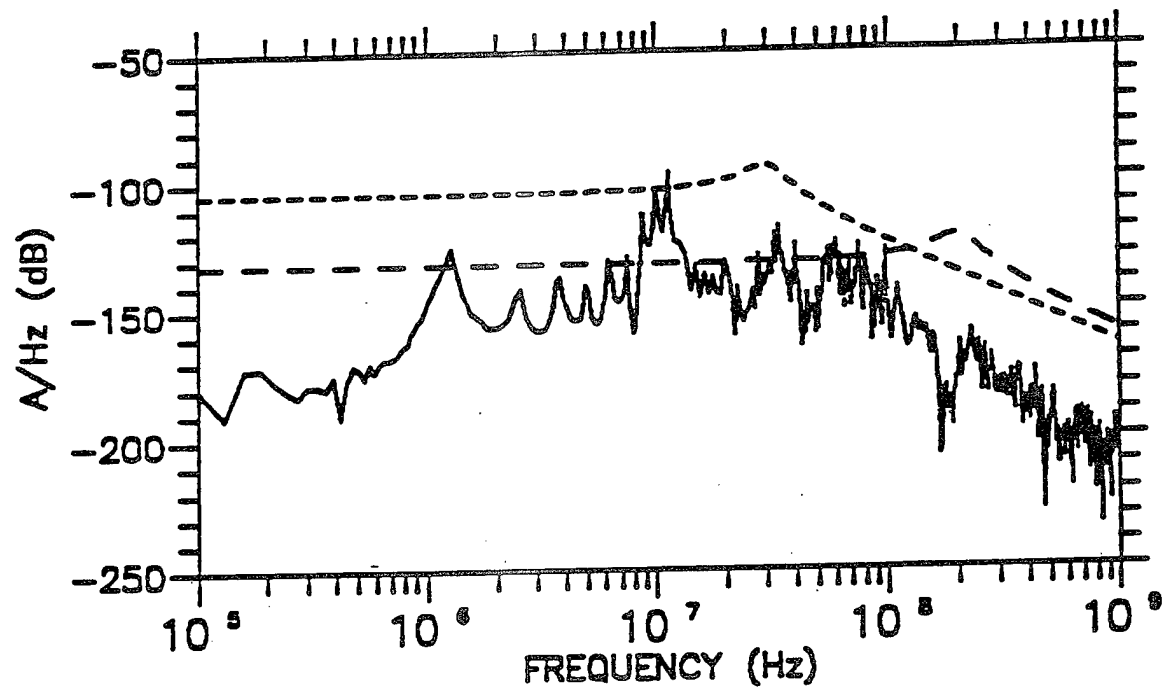
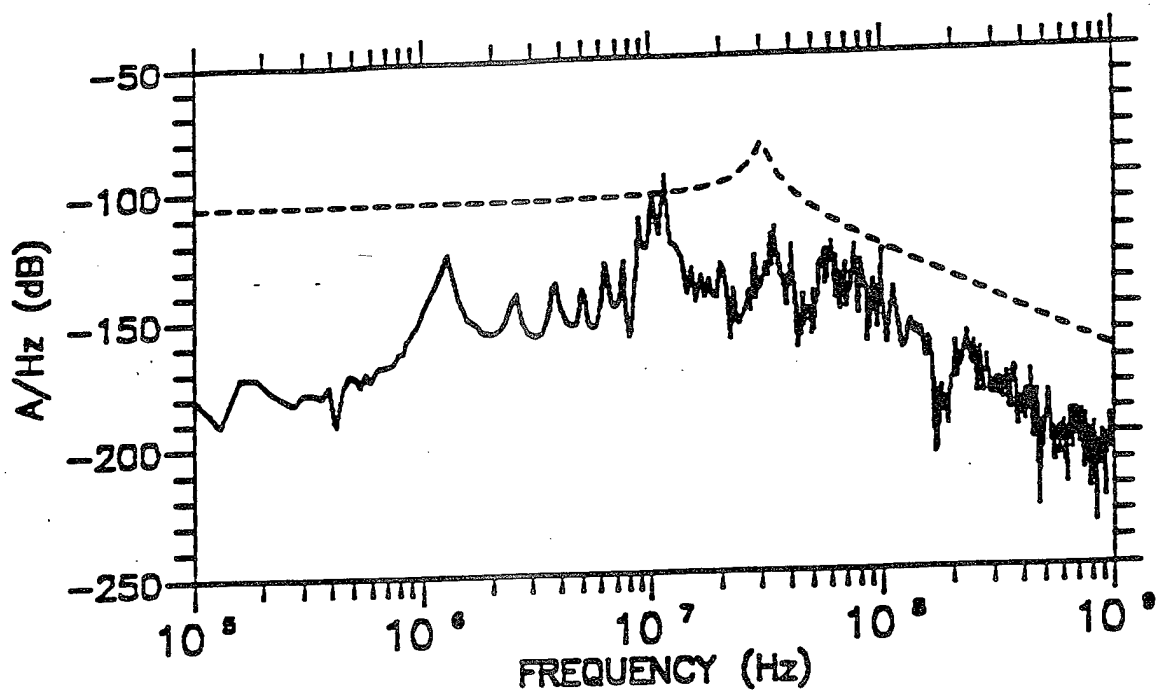


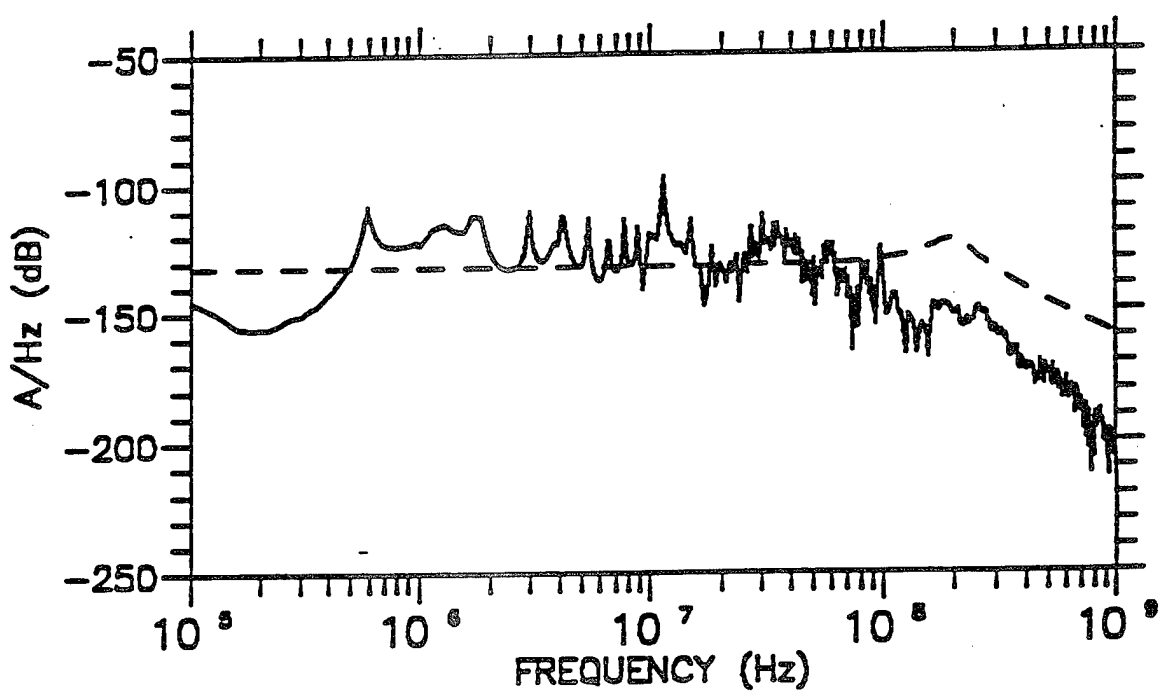
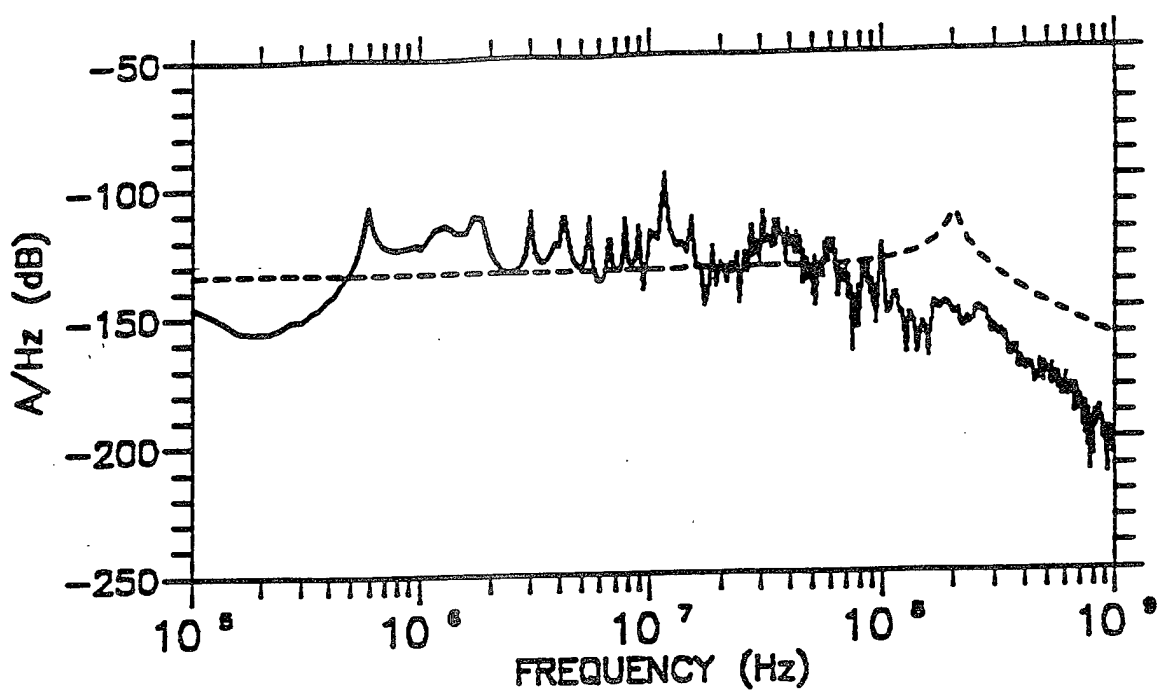








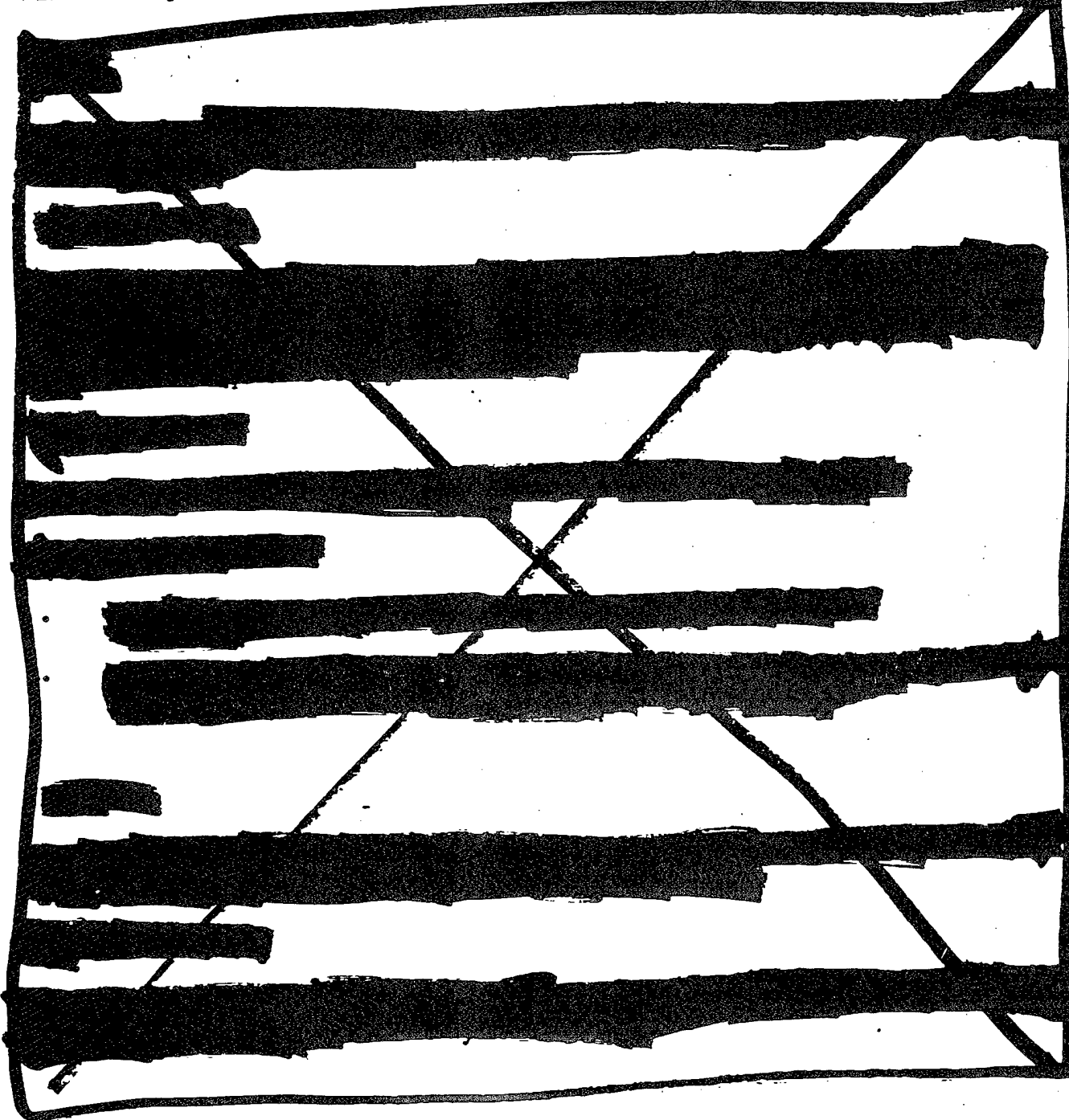


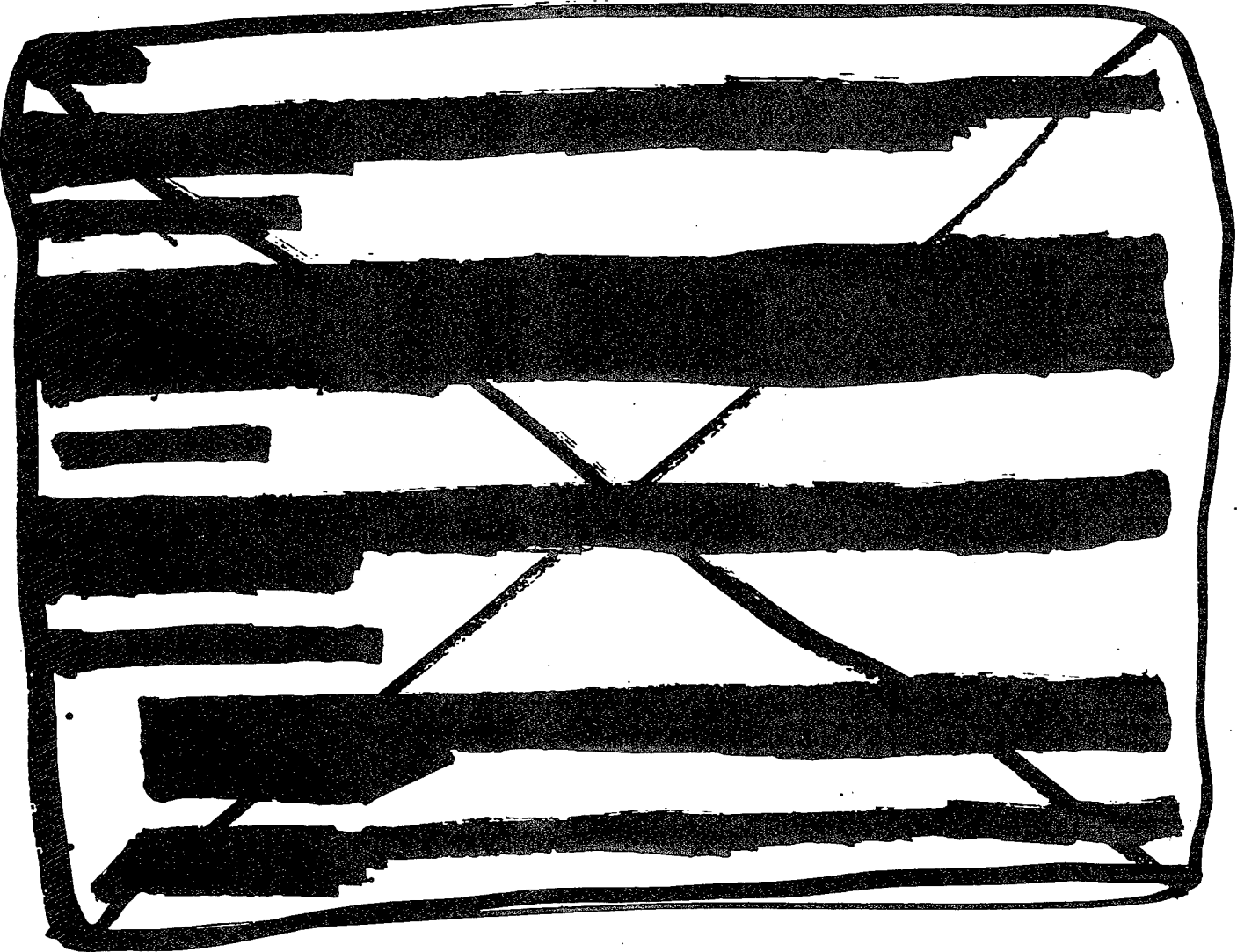


SECTION 5

CONCLUSIONS AND RECOMMENDATIONS

The test met all objectives. The test results provide complete answers to all issues addressed. [REDACTED] Each issue is discussed separately below.





ISSUE:

What test waveforms adequately simulate HEMP stresses on test radio equipment connected to antennas?

OBSERVATIONS:

HEMP coupled stresses to antennas can be adequately simulated with damped sinusoids as suggested by MIL-STD-188-125.

The revision to the standard in Reference 7 provides better test coverage because it uses two damped sinusoids for each antenna.

The transients stressing the radio equipment can be represented by an equivalent Thevenin circuit with source impedance of 50 to 100 ohms. Observed quality factors (Q) are lower than the Q = 10 required by MIL-STD-188-125.

CONCLUSIONS:

Neither MIL-STD-188-125 nor previously suggested revisions account for the effects of a tower.

RECOMMENDATIONS:

- Adopt the suggested revision in Reference 7, but add the requirement that the radio equipment must also be tested with a damped sinusoid at 2 MHz with 500 A [redacted]

SECTION 6

REFERENCES

1. "Military Standard, High-Altitude Electromagnetic Pulse Protection for Ground-Based C4I Facilities Performing Critical, Time-Urgent Missions," MIL-STD-188-125, 26 June 1990.
2. T. Zwolinski, "Test Director's Report for the [REDACTED] HEMP Simulation Test," MRC/COS-R-1309, July 1992.
3. D. Schafer, "E3 Pulser and Data Line Coupler/Isolator Acceptance Test," MRC/ABQ-R-1494, March 1992.
4. G. Estepp and D. Schafer, "Operation and Maintenance Manual" (for E3 Pulser), MRC/ABQ-R-1446, January 1992.
5. H. Fowles and D. Schafer, "Long Pulse Current Injection Experiments on an Operating GBC4I Facility Mockup," MRC/ABQ-R-1524, August 1992.
6. B. Harlacher, "Characterization of the E2 Pulse Generator," MRC/COS-M-95-7, 3 January 1992.
7. J. Lubell, "Changes to Appendix B" (of MIL-STD-188-125), Memorandum to W. Scott, Maj. R. Launstein, J. Zych, 13 March 1992.
8. R. Shoup, "Field Mapping Test of the DNA CW Antenna System," DNA-TR-84-168, 7 September 1983.
9. W. Bereuter and R. Racca, "Processing of CWMS Field Map Measurements," MRC/COS-N-131, 9 November 1987.
10. Classification Guide for "Advanced Fixed GBC4I Testing Program," 1 July 1989.
11. R. Racca and S. Dunivin, "DNA CW Antenna Field Map Test," MRC/COS-R-1082, 5 October 1990.
12. R. Racca, W. Bereuter, and S. Dunivin, "DNA CW Antenna Test," MRC/COS-N-179, 29 January 1991.

THIS PAGE INTENTIONALLY LEFT BLANK

APPENDIX A

[REDACTED]

[REDACTED]

1.0 BACKGROUND

Section 3 describes the simulated HEMP testing.

Pulser qualification testing indicates that the E2 pulser delivers a double exponential short-circuit current with peak amplitudes up to 500 A, rise times less than 1 μ s, and durations (FWHM) of about 5 ms (Reference 6).

The purpose of this appendix is to describe the circuit models used to estimate the responses.

2.0 CIRCUIT MODELS

The schematic in Fig. 1(a) can be reduced to an equivalent circuit shown in Fig. 1(c) using standard circuit equivalences. The first reduction reflects the 2 ohm load resistance.

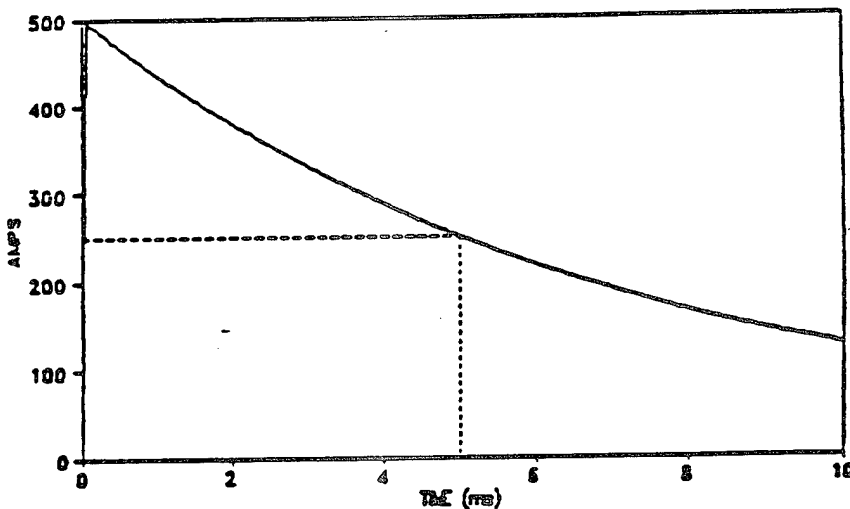
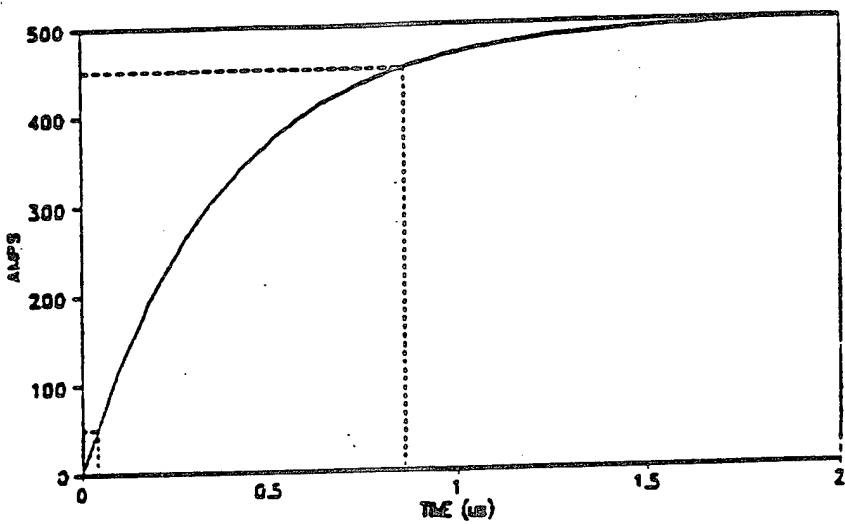
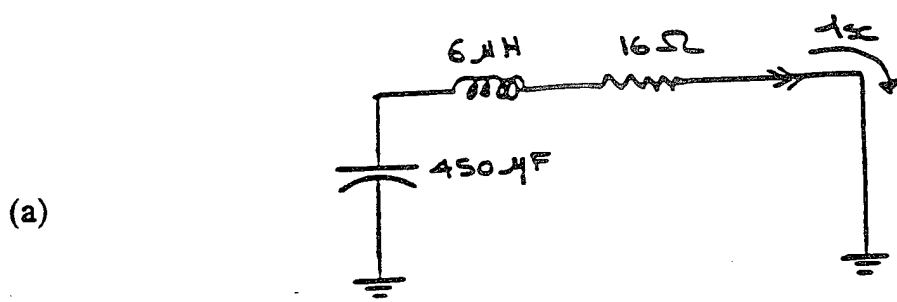


Figure 2. Circuits and responses for the E2 pulser: (a) circuit model, (b) early-time response, and (c) late-time response.

A-5

Pages A-6 through A-9
are removed in their
entirety.

THIS PAGE INTENTIONALLY LEFT BLANK

APPENDIX B

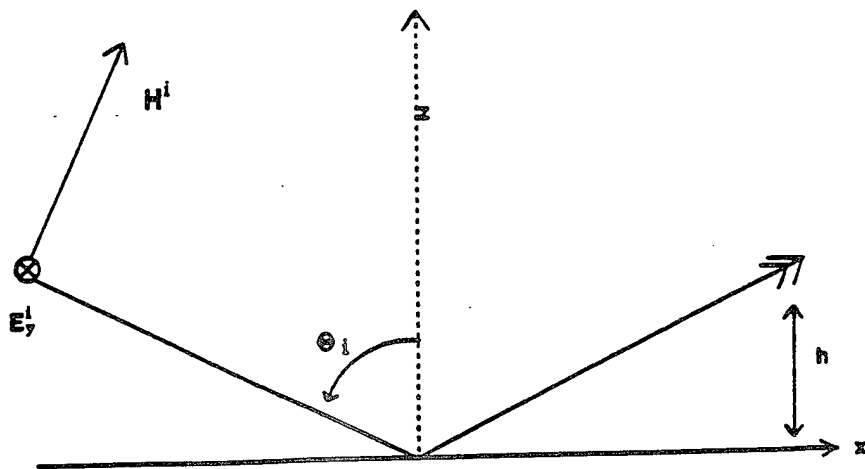
CALCULATION OF TOTAL FIELDS

This Appendix contains the equations to calculate the total (incident plus ground reflected) fields at a height h above the ground. The equations are for a horizontally polarized plane wave (incident electric field is parallel to the ground), and for a vertically polarized plane wave (incident magnetic field is parallel to the ground). The plane waves are incident along a propagation direction which is in the xy plane and forms an angle θ_i with the z -axis.

The angles of incidence are between 68° and 83° , depending on the antenna distance to the CWMS simulator and the height of the antenna tested. The earth parameters E_i, σ were estimated by matching the calculated field transfer functions to the measured transfer functions. The estimated values are $\epsilon_r = 5$, and $\sigma = .01$ to 1 mho/m.

The approximations for small x are provided for convenience. They are valid at frequencies where the ground is a good conductor.

HORIZONTAL POLARIZATION



$$R_H = \frac{\cos\theta_i - [\epsilon_r(1+\chi) - \sin^2\theta_i]^{1/2}}{\cos\theta_i + [\epsilon_r(1+\chi) - \sin^2\theta_i]^{1/2}} = -1+2\cos\theta_i \sqrt{\frac{j\omega\epsilon_0}{\sigma}}$$

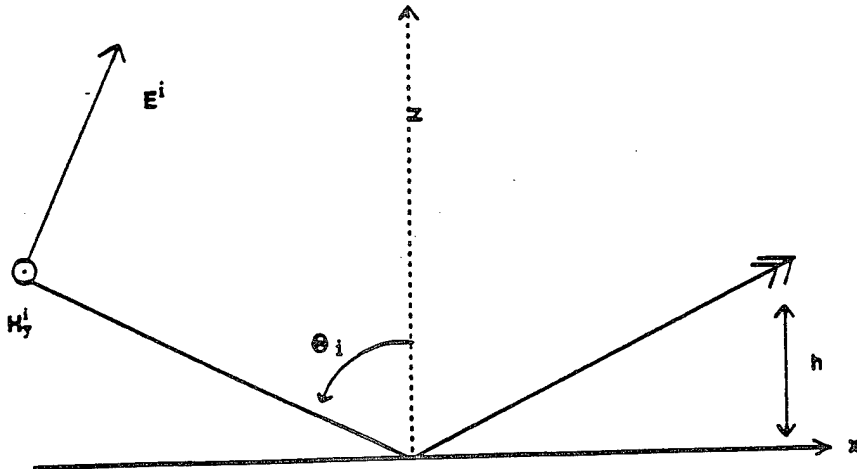
$$E_y^{TOT} = E_o(1+R_H e^{-j\alpha}) = 2E_o \cos\theta_i \sqrt{\frac{j\omega\epsilon_0}{\sigma}}$$

$$H_x^{TOT} = \frac{E_o}{\eta_0} \cos\theta_i (1-R_H e^{-j\alpha}) = \frac{E_o}{\eta_0} 2 \cos\theta_i \left(1 - \cos\theta_i \sqrt{\frac{j\omega\epsilon_0}{\sigma}} \right)$$

$$H_z^{TOT} = \frac{E_o}{\eta_0} \sin\theta_i (1+R_H e^{-j\alpha}) = \frac{E_o}{\eta_0} 2 \sin\theta_i \cos\theta_i \sqrt{\frac{j\omega\epsilon_0}{\sigma}}$$

$$\alpha = 2k_o h \cos\theta_i; \quad \chi = \sigma/j\omega\epsilon, \text{ approx. valid for } |\chi| >> 1$$

VERTICAL POLARIZATION



$$R_v = \frac{\epsilon_r(1+\chi) \cos\theta_i - [\epsilon_r(1+\chi) - \sin^2 \theta_i]^{1/2}}{\epsilon_r(1+\chi) \cos\theta_i + [\epsilon_r(1+\chi) - \sin^2 \theta_i]^{1/2}} = 1 - \frac{2}{\cos\theta_i} \sqrt{\frac{j\omega\epsilon_0}{\sigma}}$$

$$E_x^{TOT} = E_o \cos\theta_i (1 - R_v e^{-j\alpha}) = E_o 2 \sqrt{\frac{j\omega\epsilon_0}{\sigma}}$$

$$E_z^{TOT} = E_o \sin\theta_i (1 + R_v e^{-j\alpha}) = E_o 2 \sin\theta_i \left(1 - \frac{1}{\cos\theta_i} \sqrt{\frac{j\omega\epsilon_0}{\sigma}} \right)$$

$$H_y^{TOT} = \frac{E_o}{\eta_o} (1 + R_v e^{-j\alpha}) = \frac{E_o}{\eta_o} 2 \left(1 - \frac{1}{\cos\theta_i} \sqrt{\frac{j\omega\epsilon_0}{\sigma}} \right)$$

$$\alpha = 2k_o h \cos\theta_i; \quad \chi = \sigma/j\omega\epsilon, \quad \text{approx. valid for } |\chi| > > 1$$

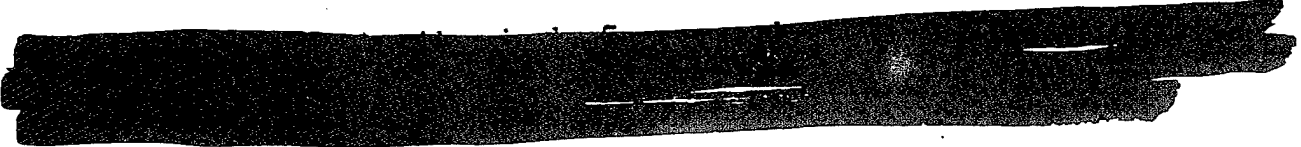
THIS PAGE INTENTIONALLY LEFT BLANK

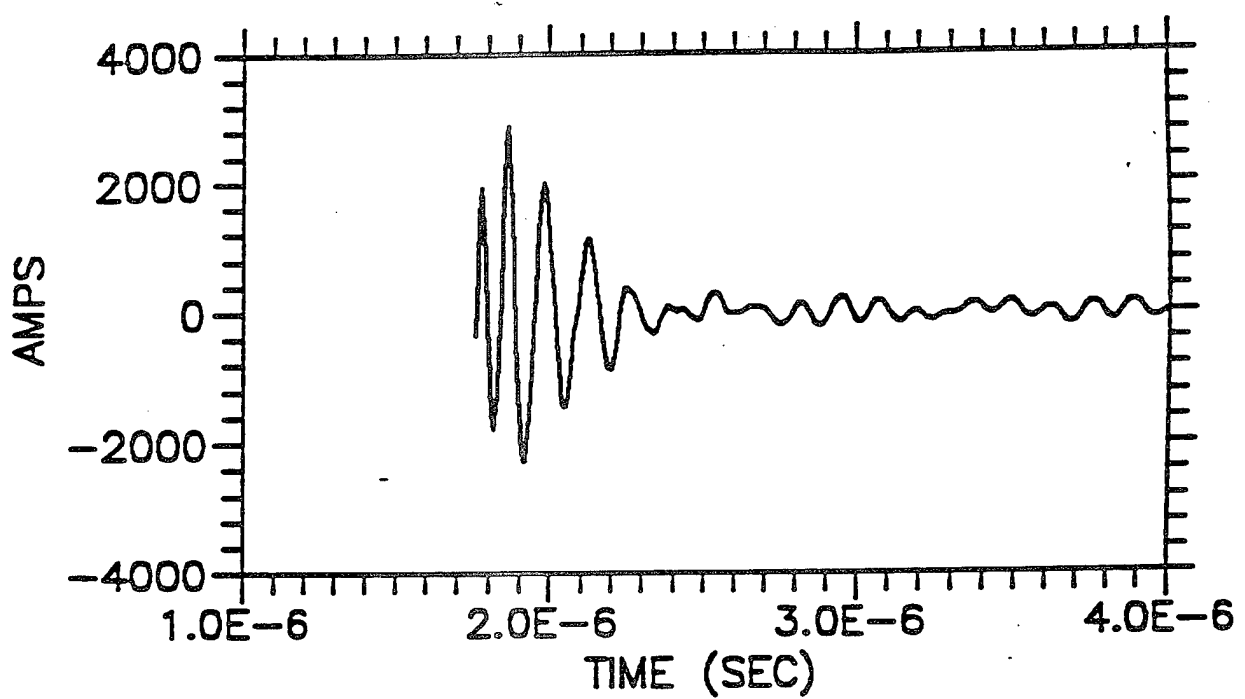
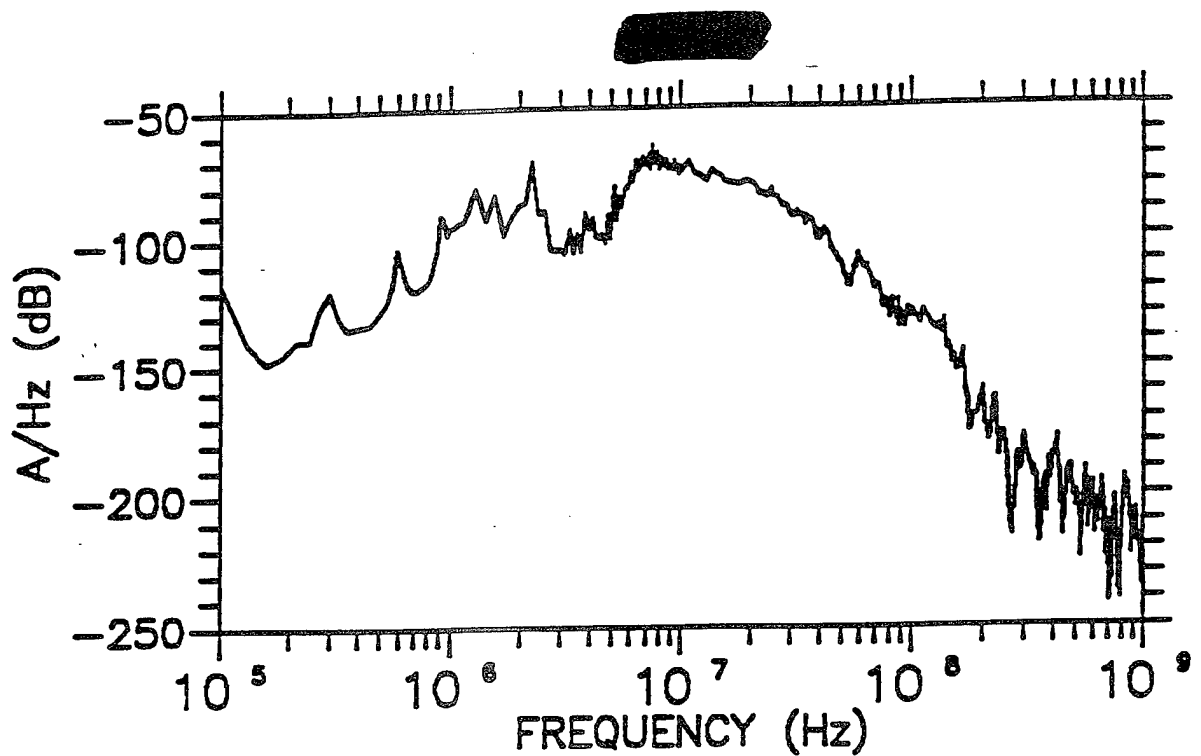
APPENDIX C

ANTENNA CURRENTS

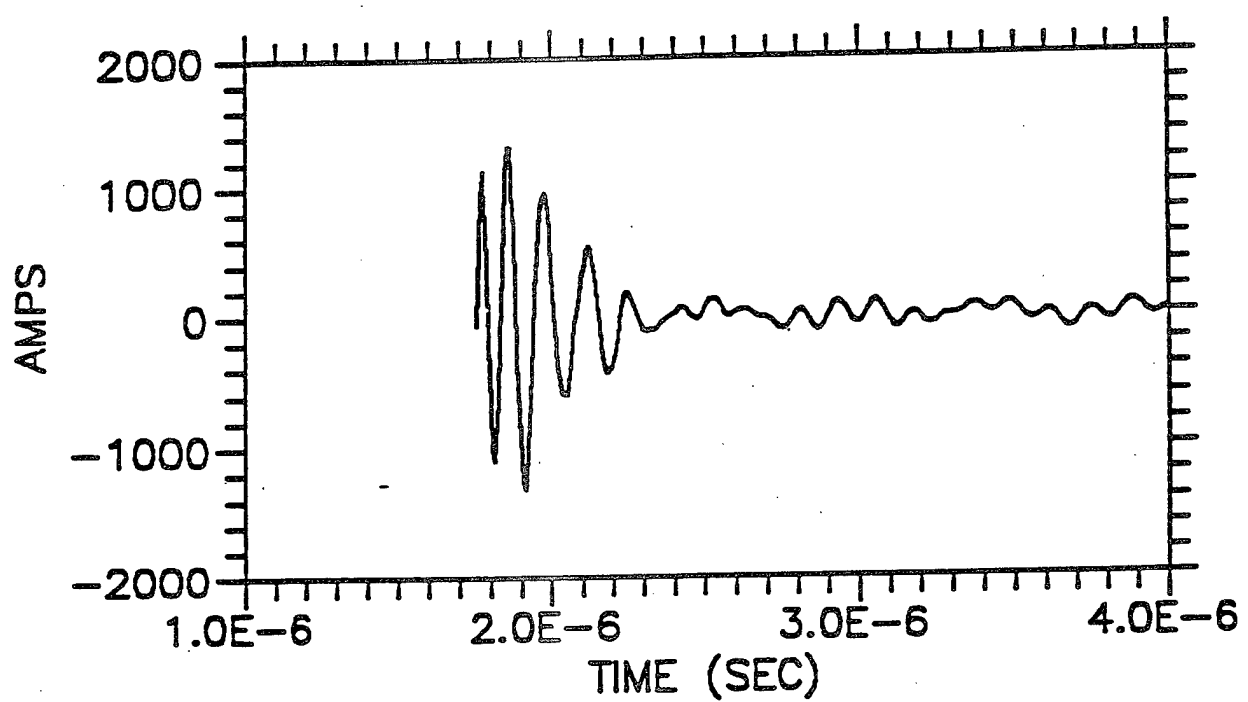
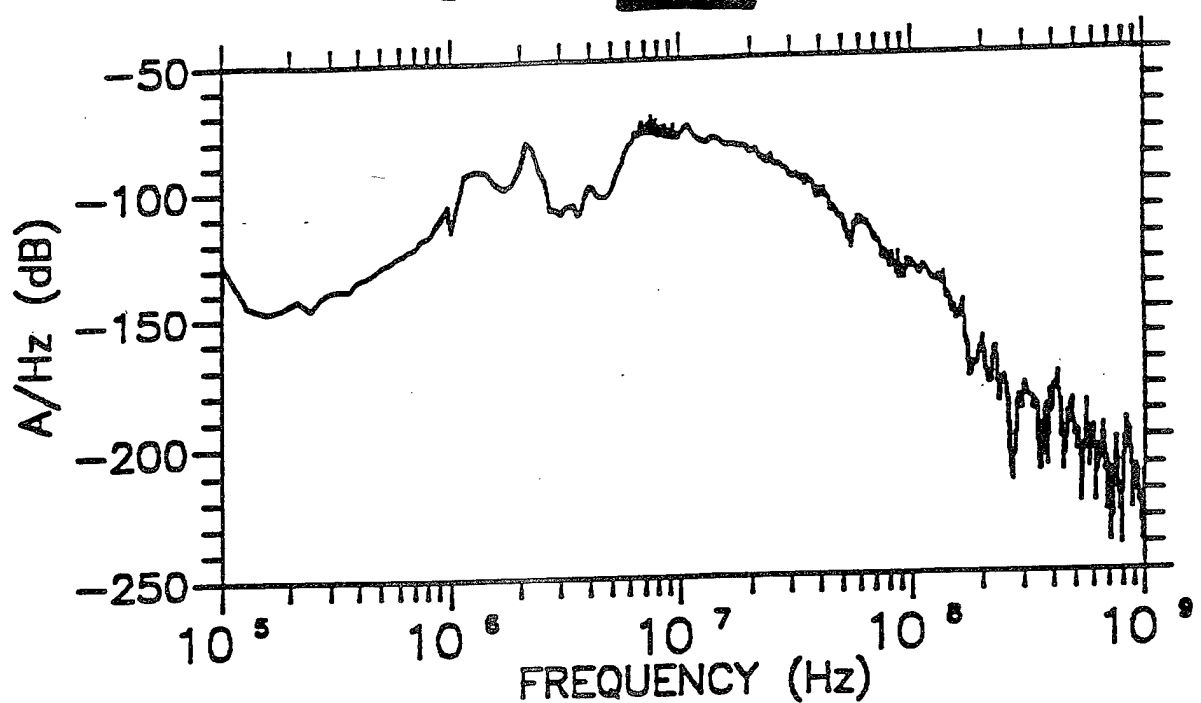
This appendix contains plots of the antenna currents measured [REDACTED] and extrapolated to HEMP environments. Measurements with prefix "H" were extrapolated to the total electric field (cf. Section 4.3.1), and measurements with prefix "V" were extrapolated to the incident electric field (cf. Section 4.3.2).

For each measurement, the frequency domain amplitude spectrum is plotted in $\text{dB} = 20 \log |I(\omega)|$. On the same page, the inverse Fourier transform is shown.

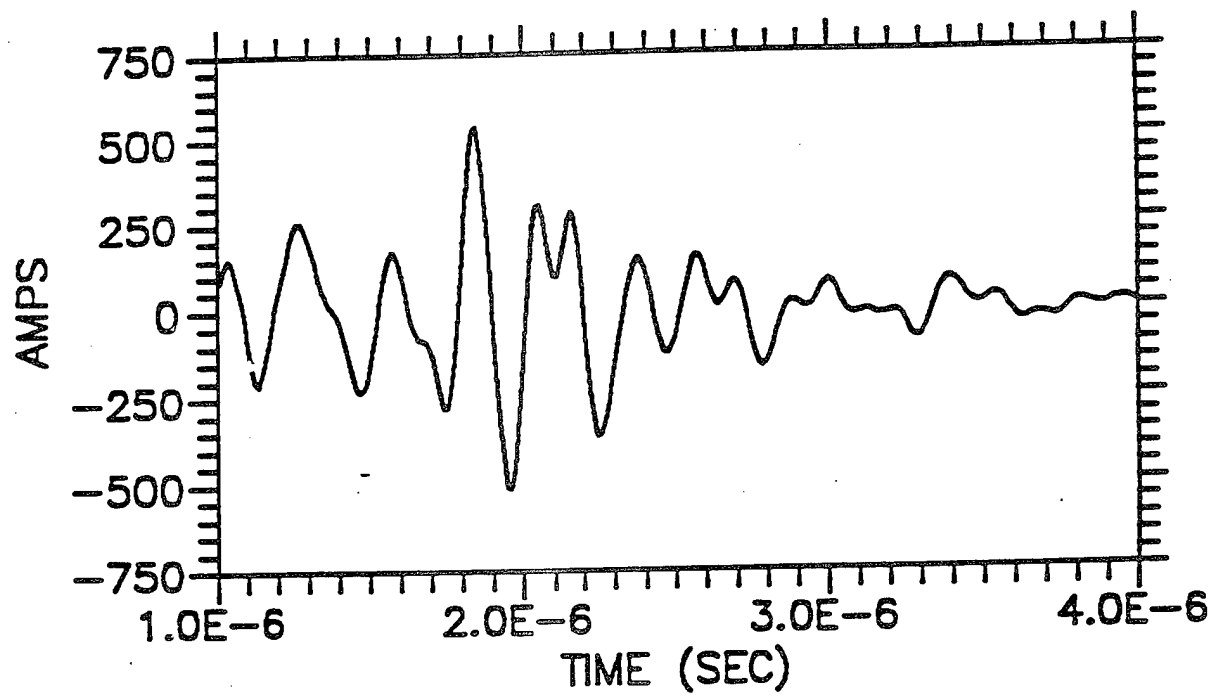
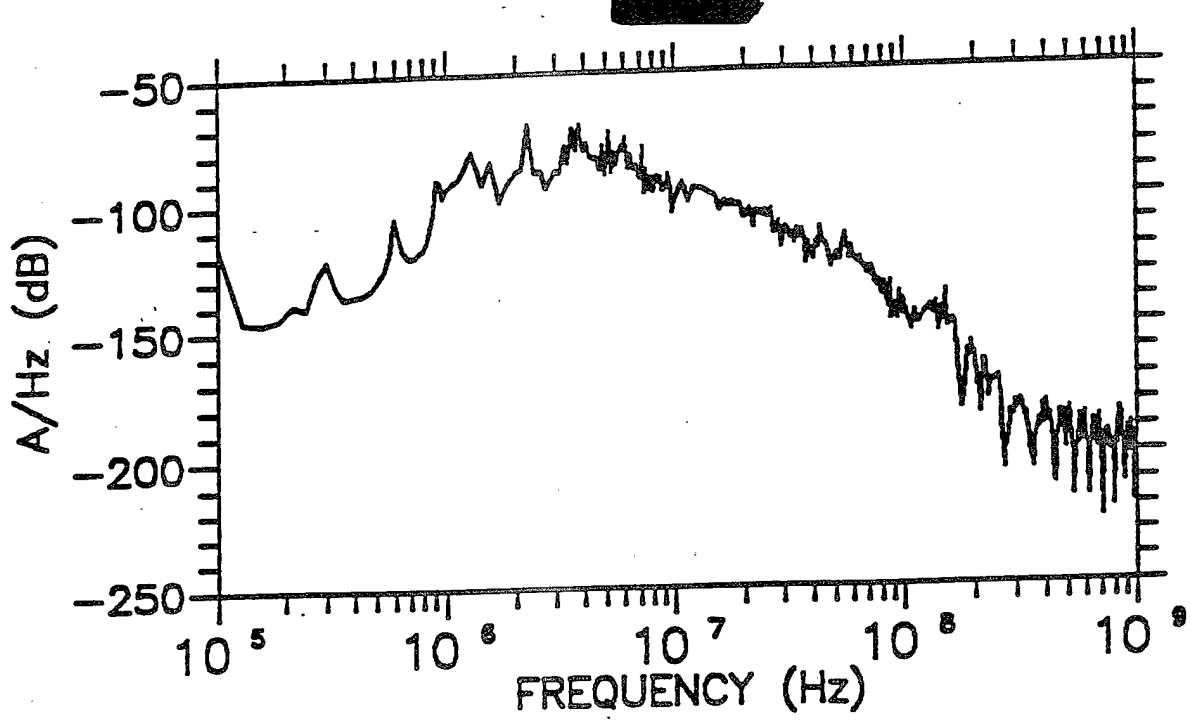




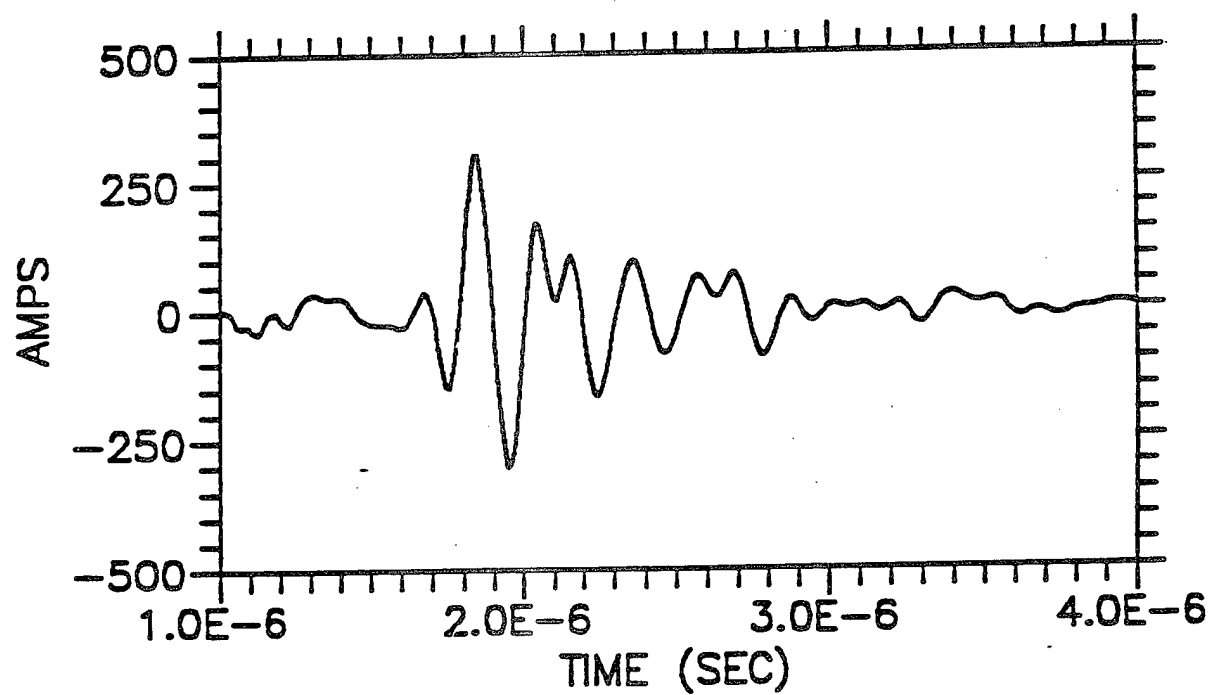
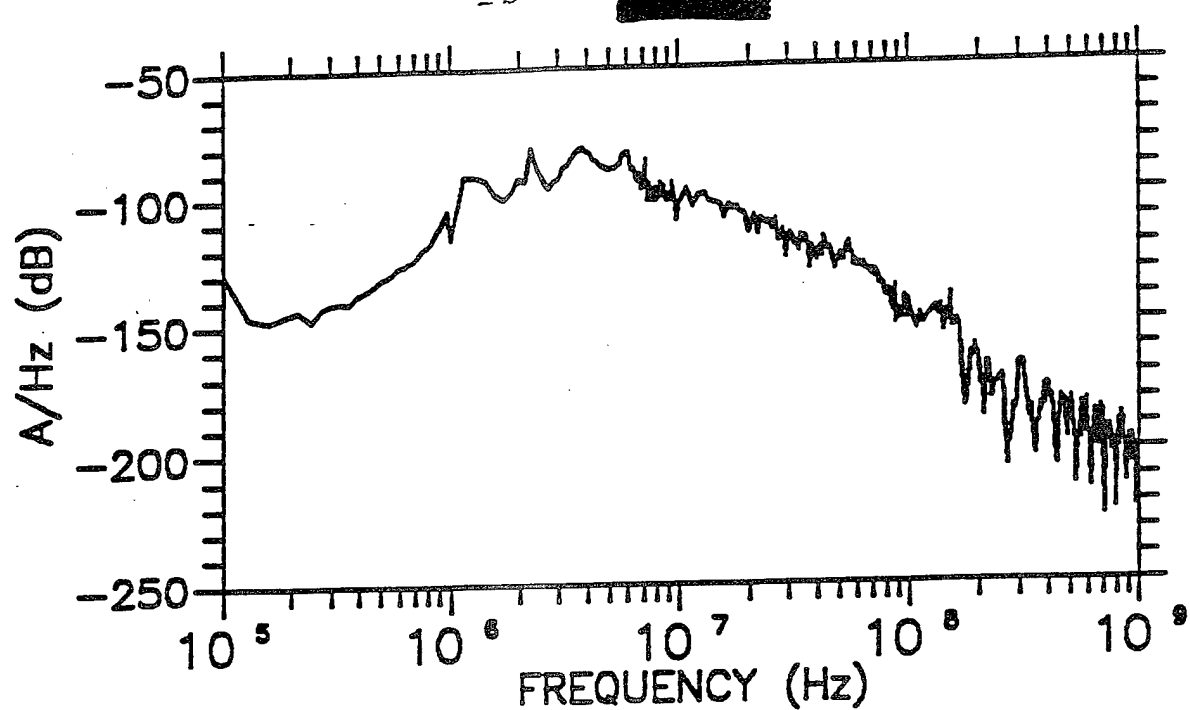
C-2

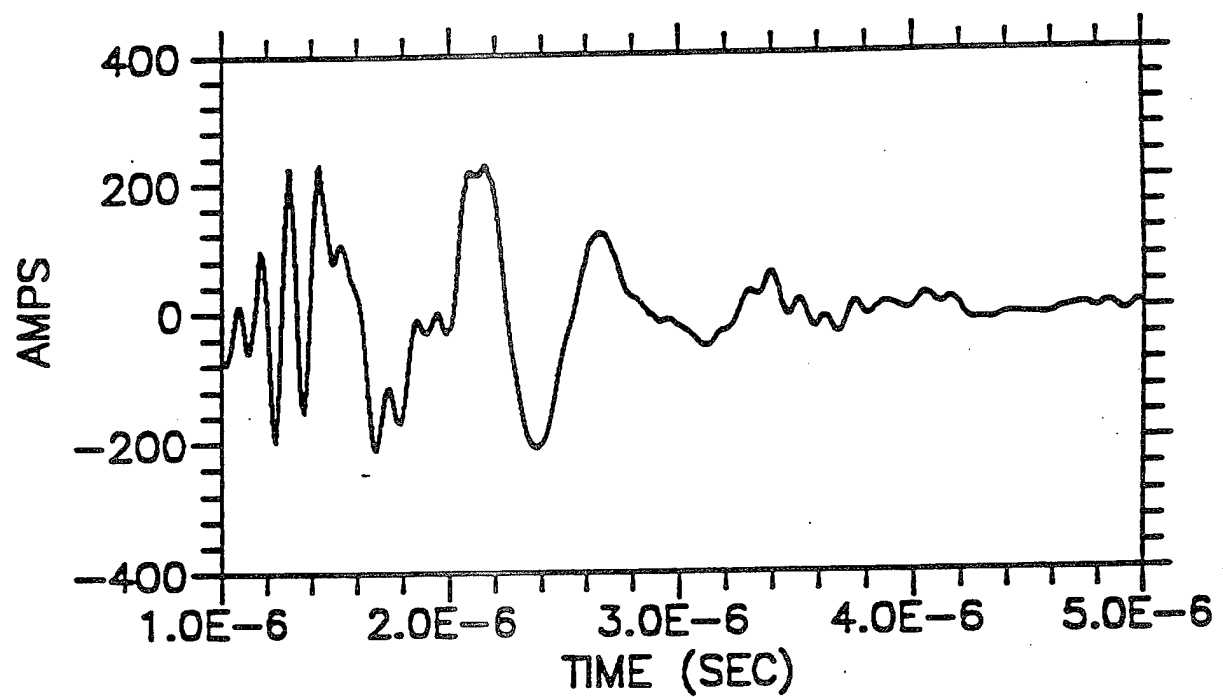
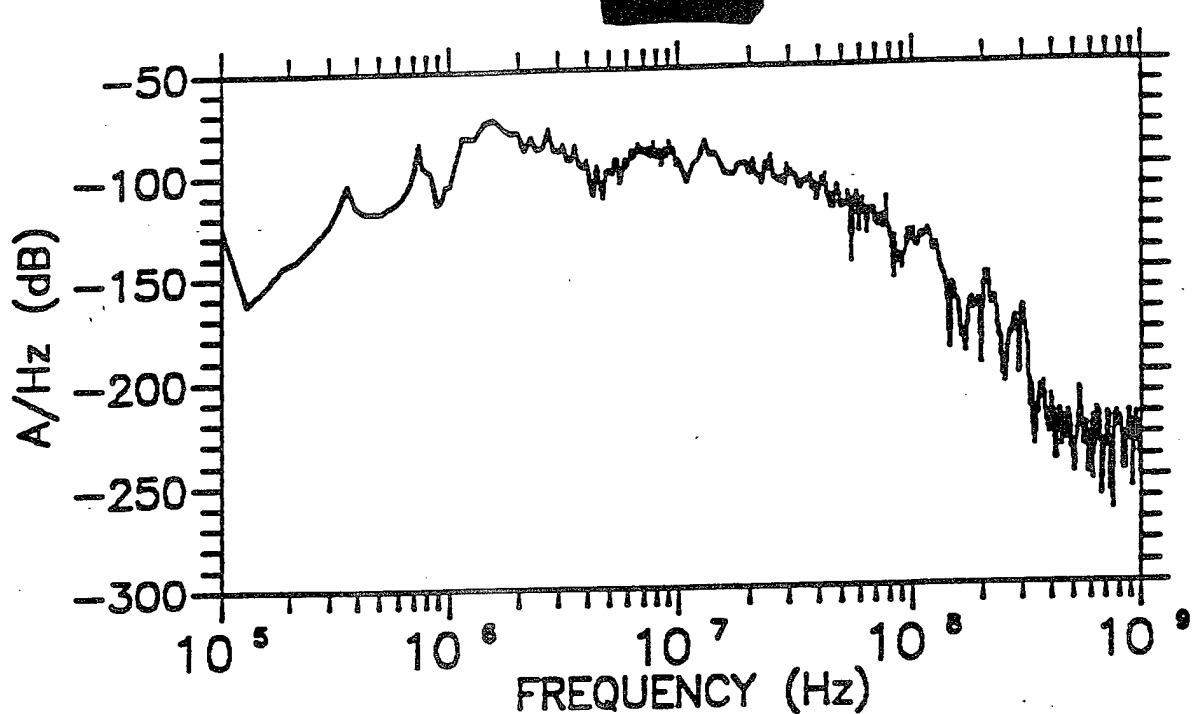


C-3

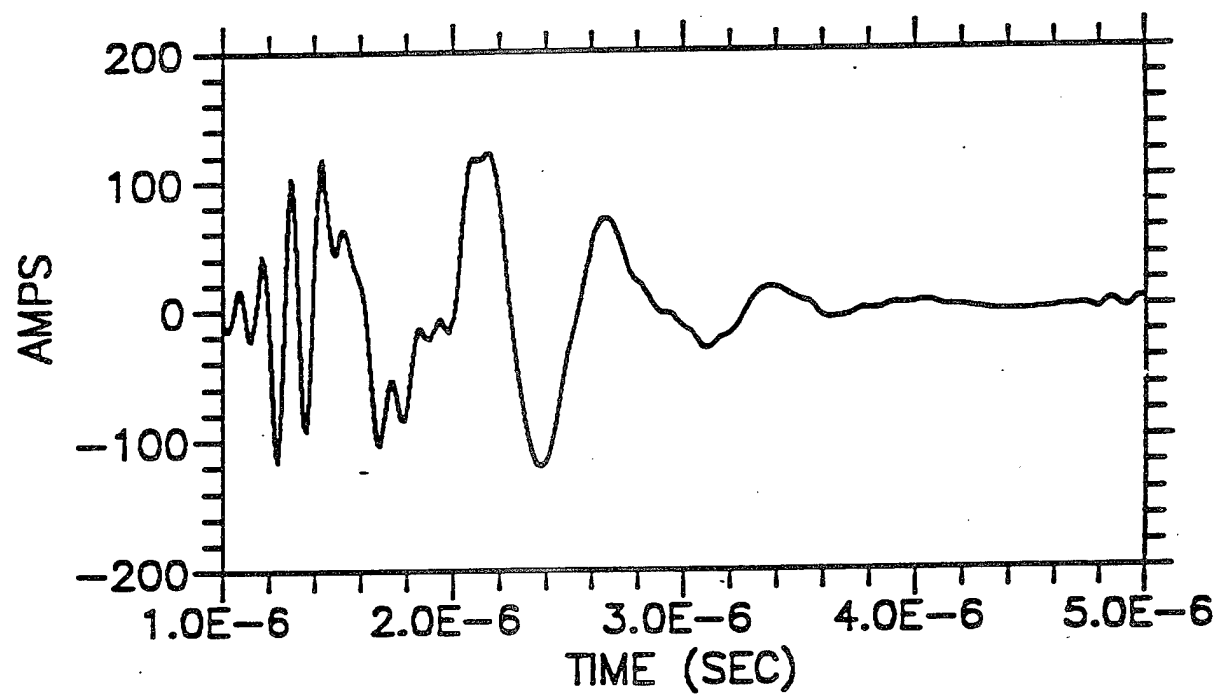
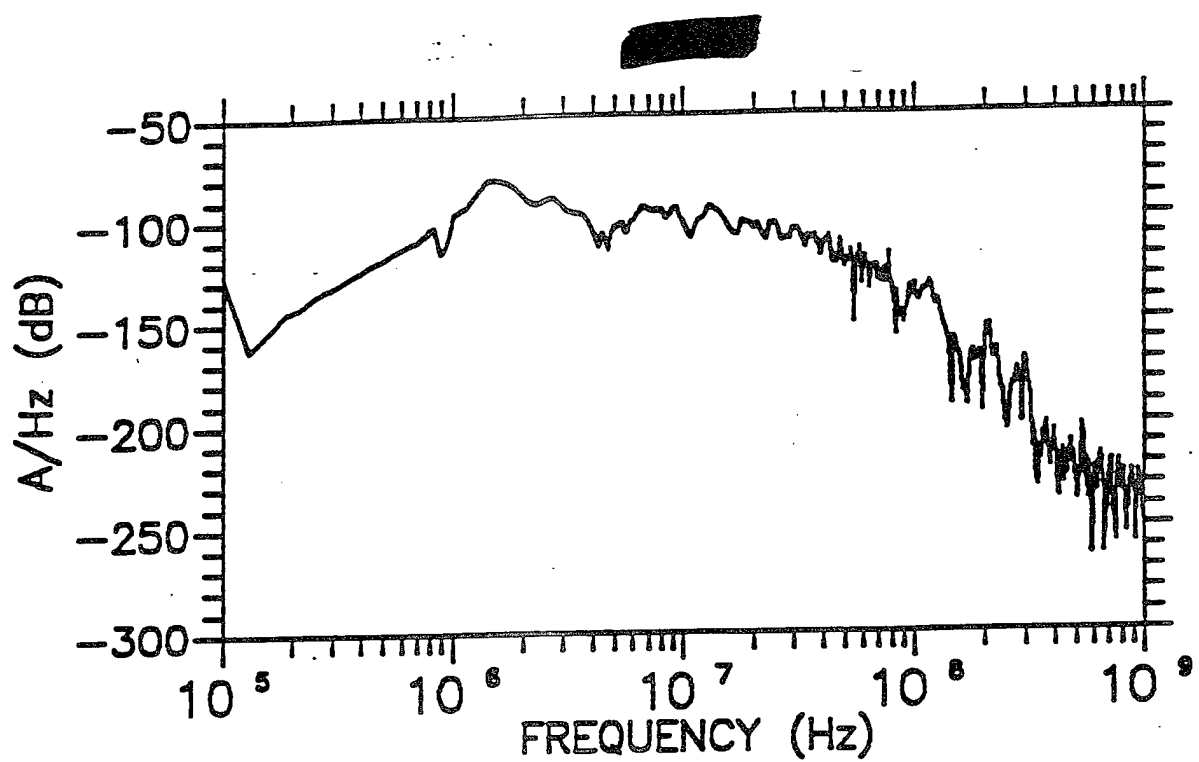


C4

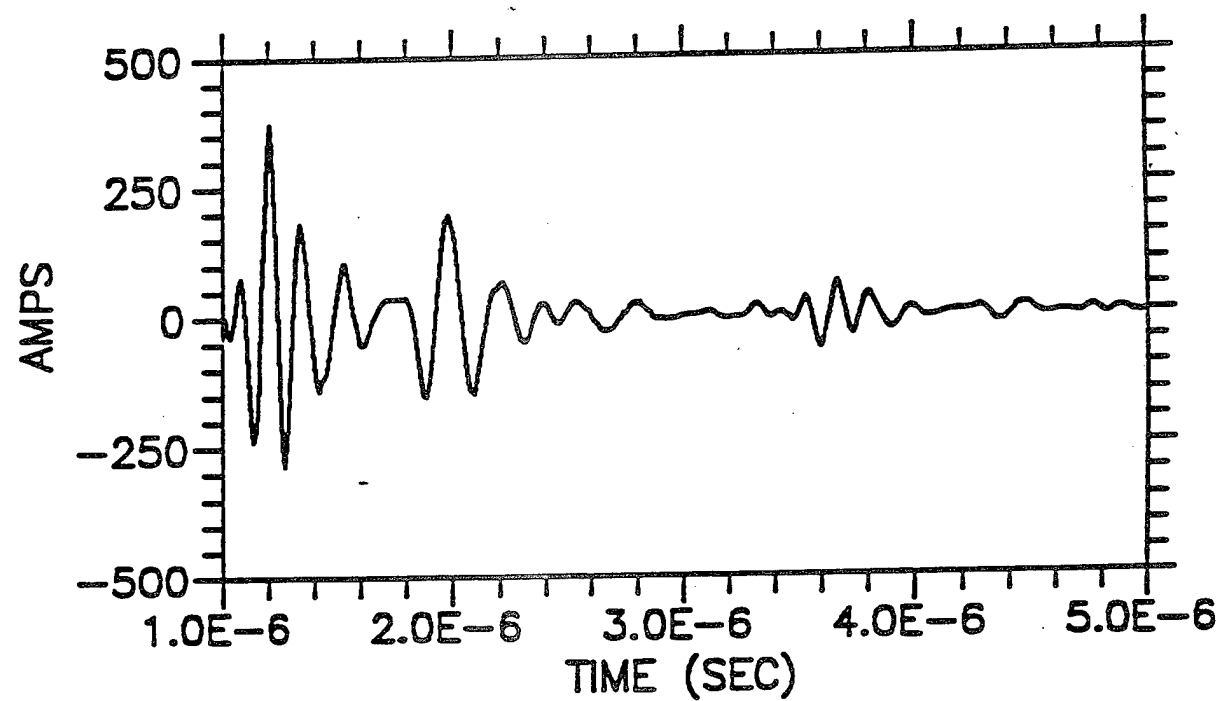
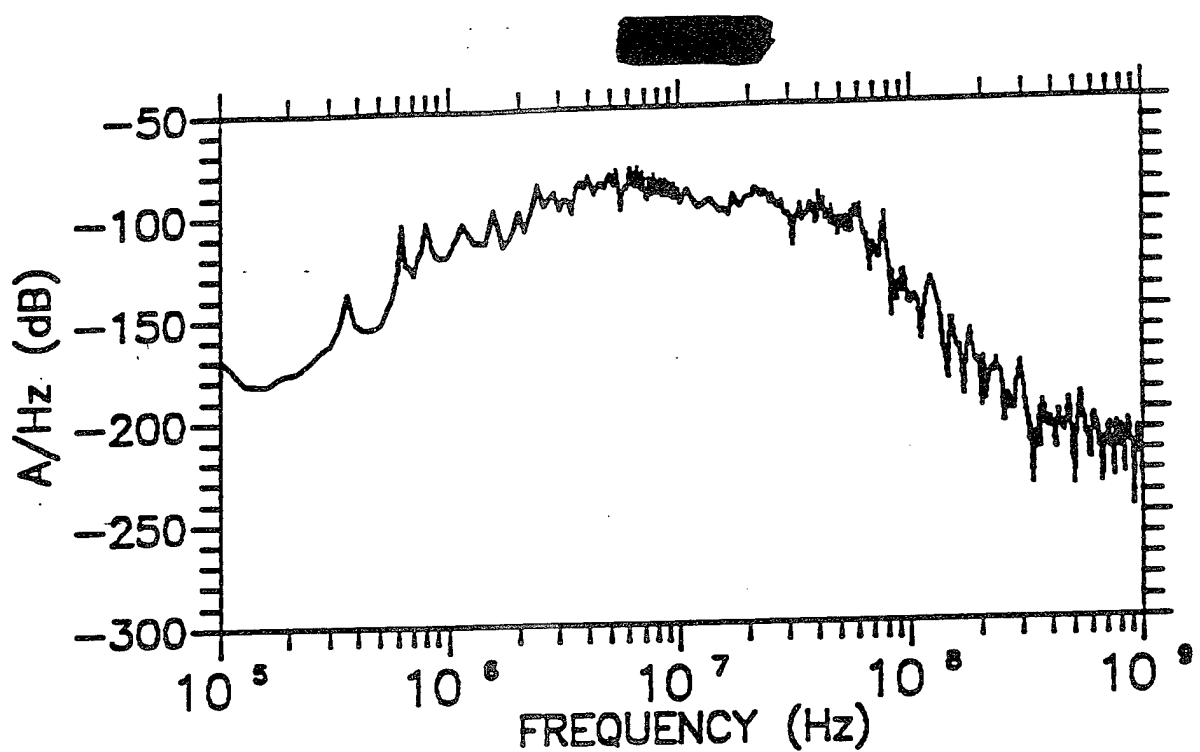


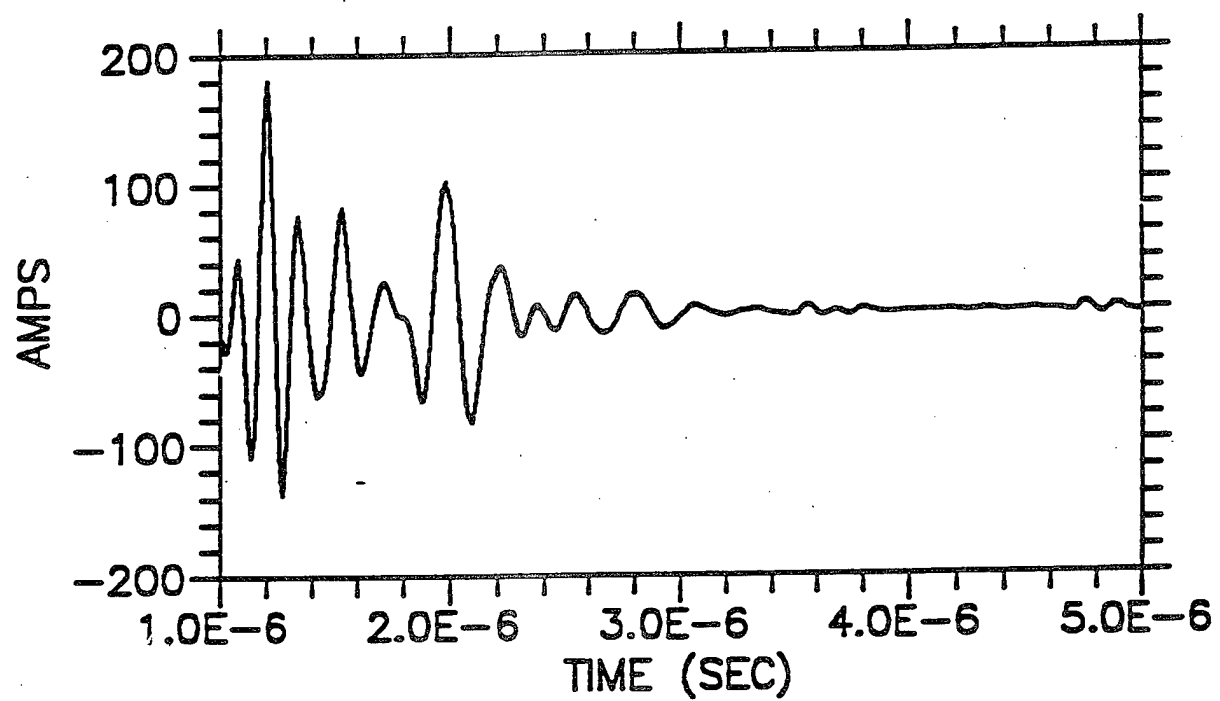
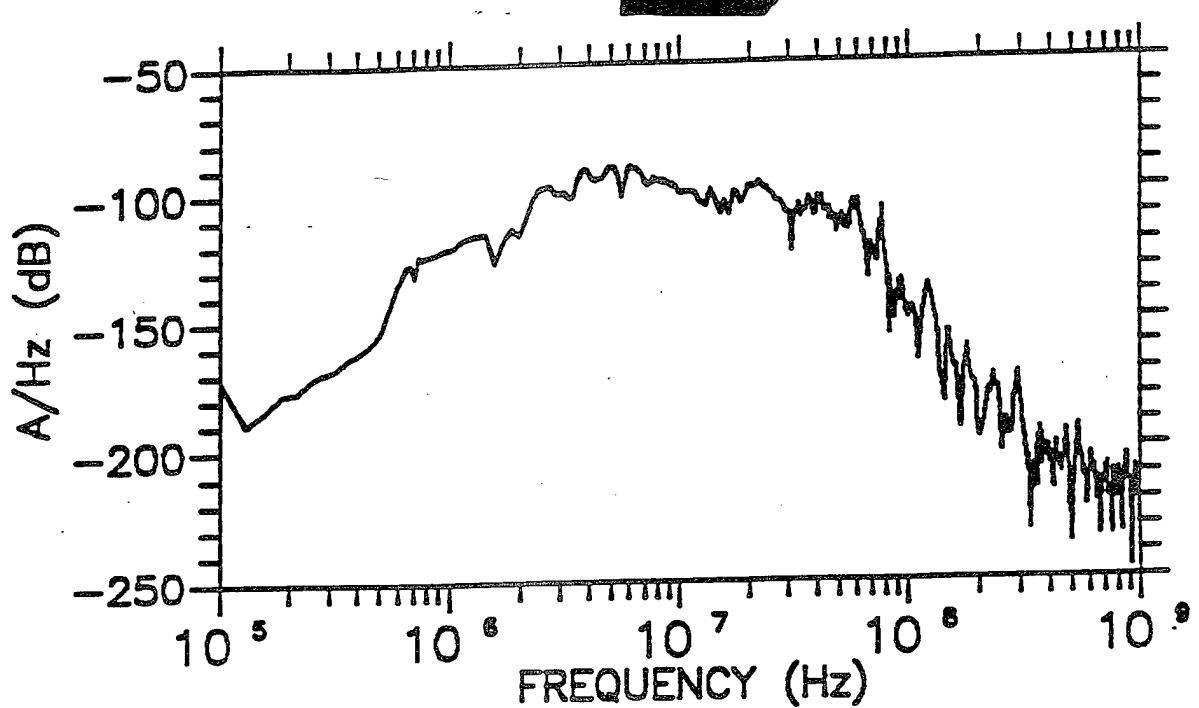


C-6

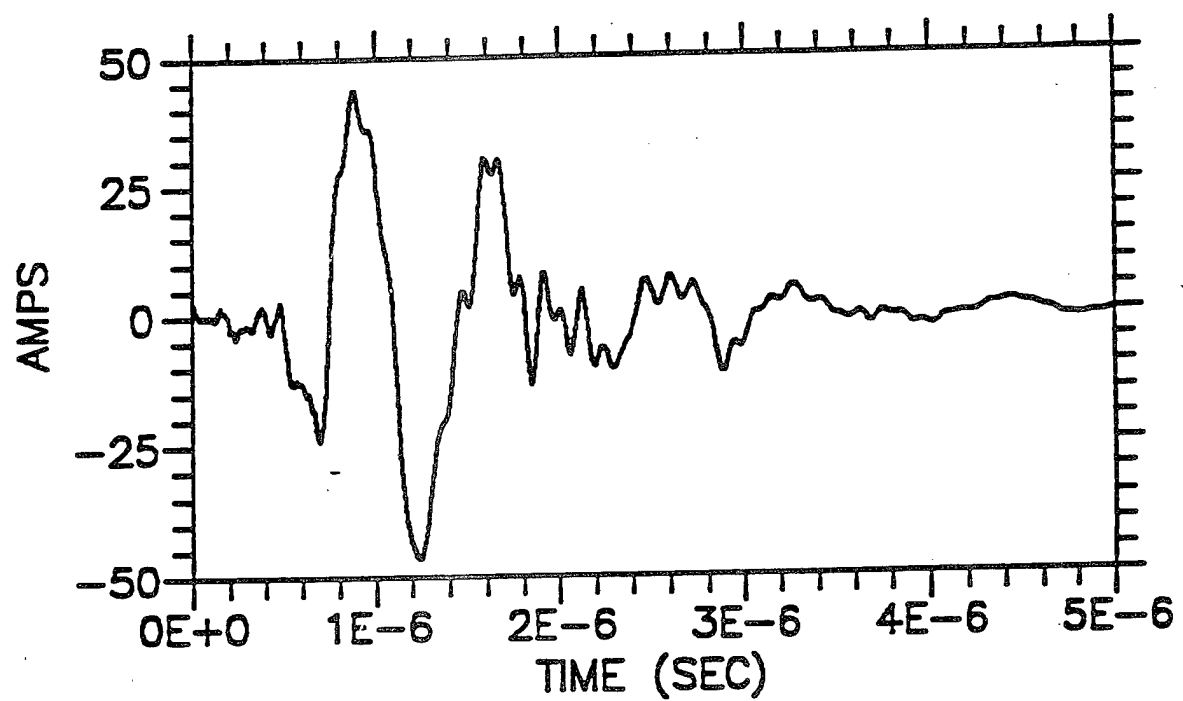
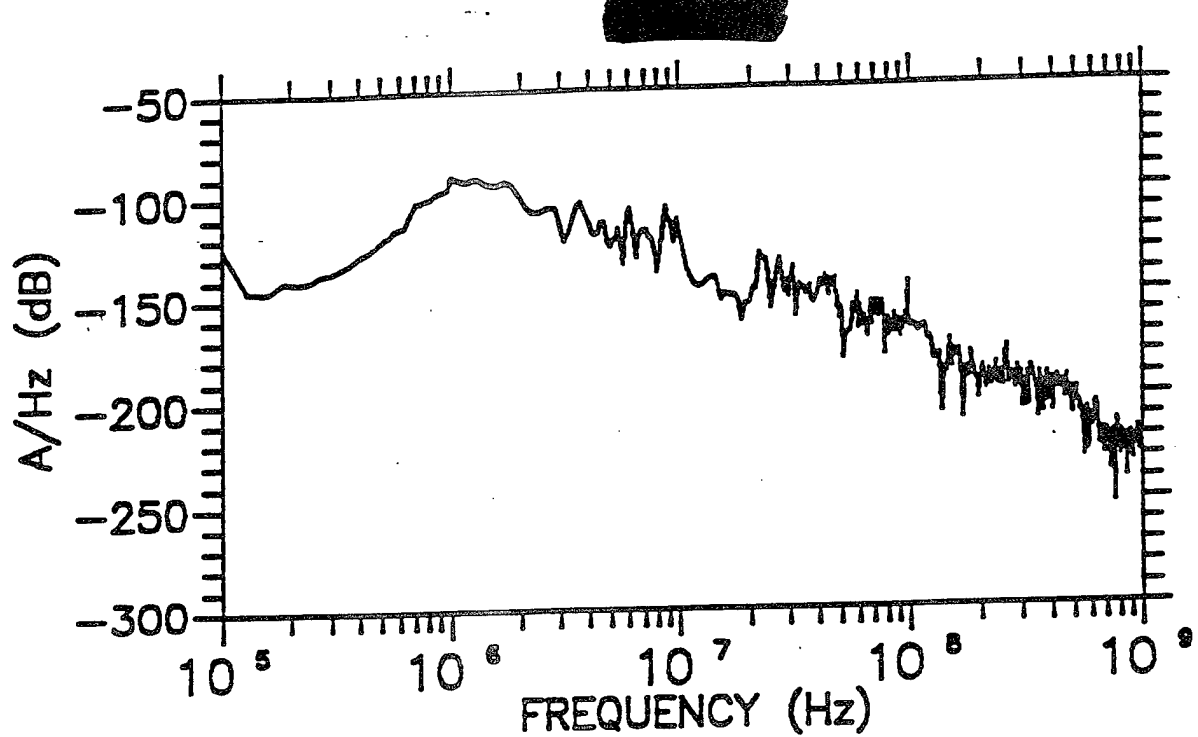


C-7

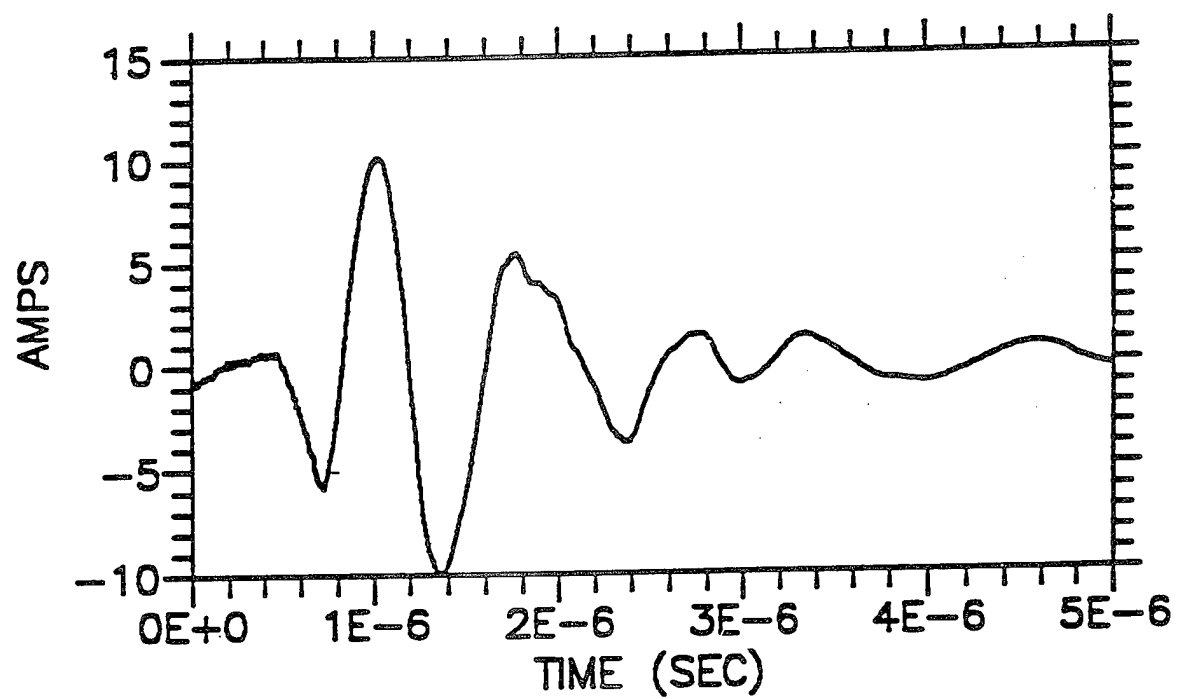
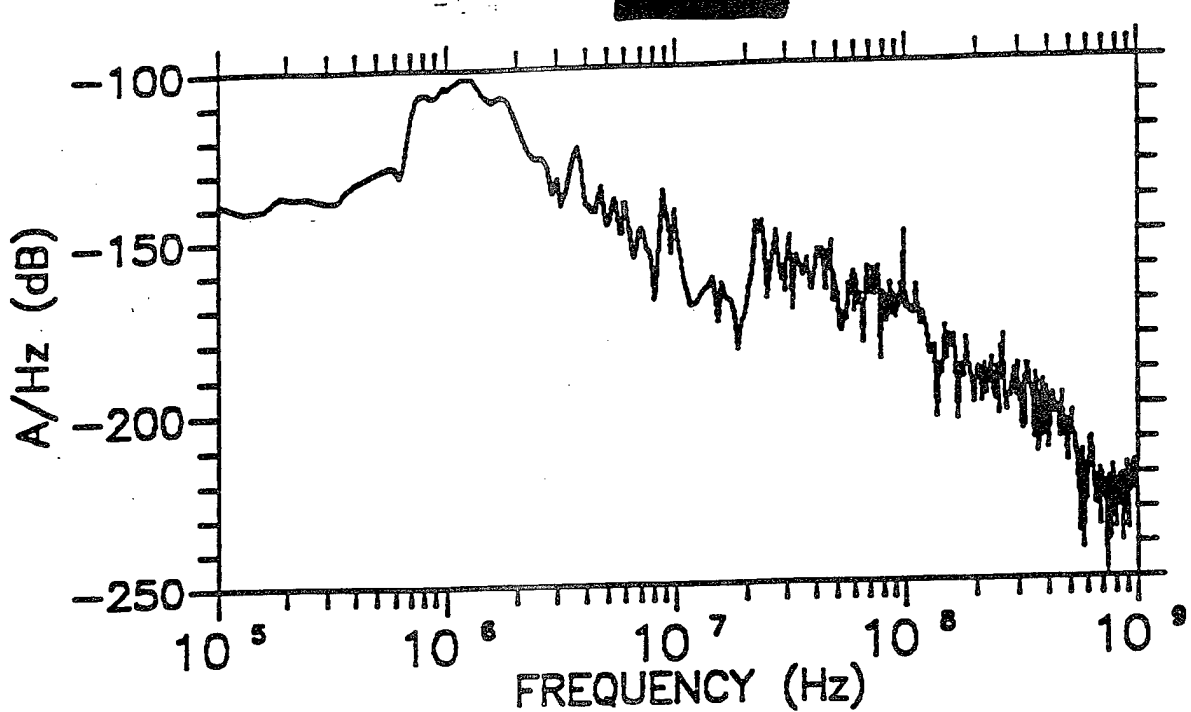




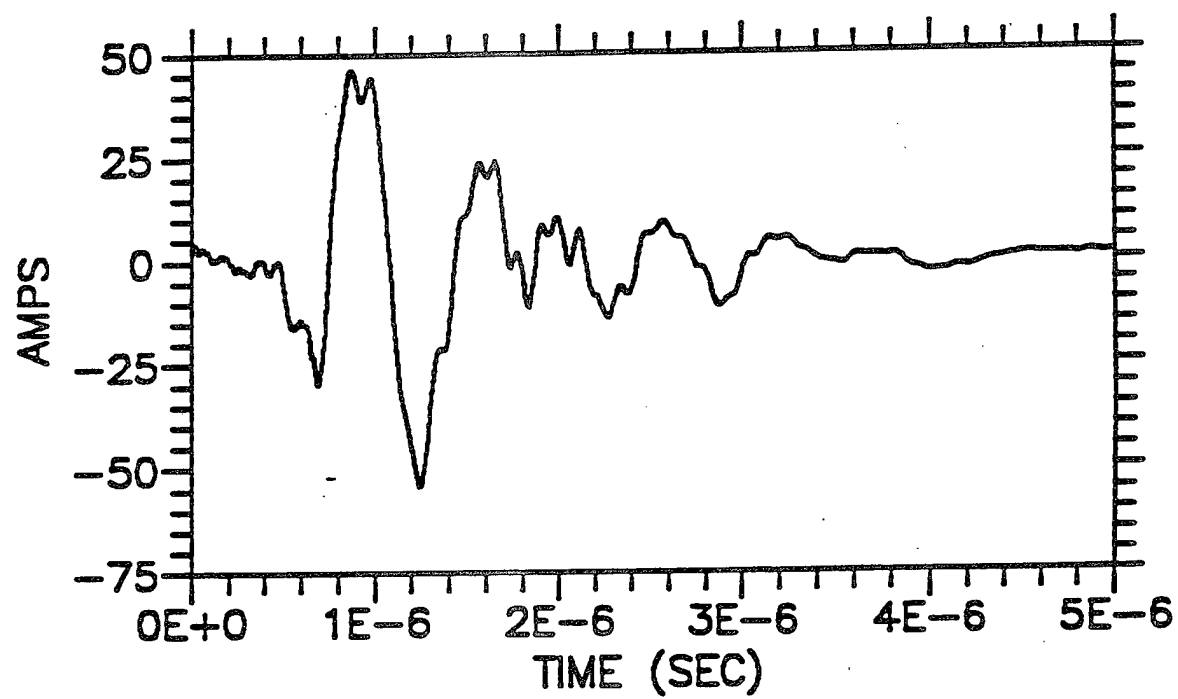
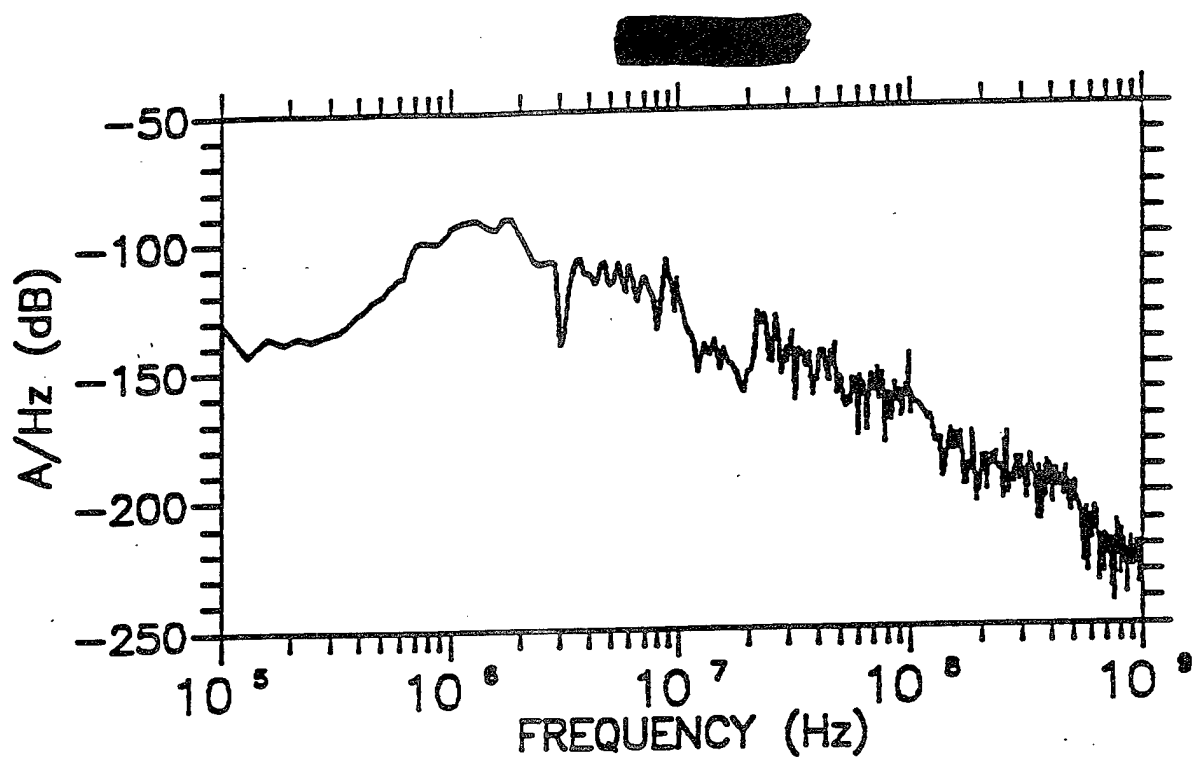
C-9



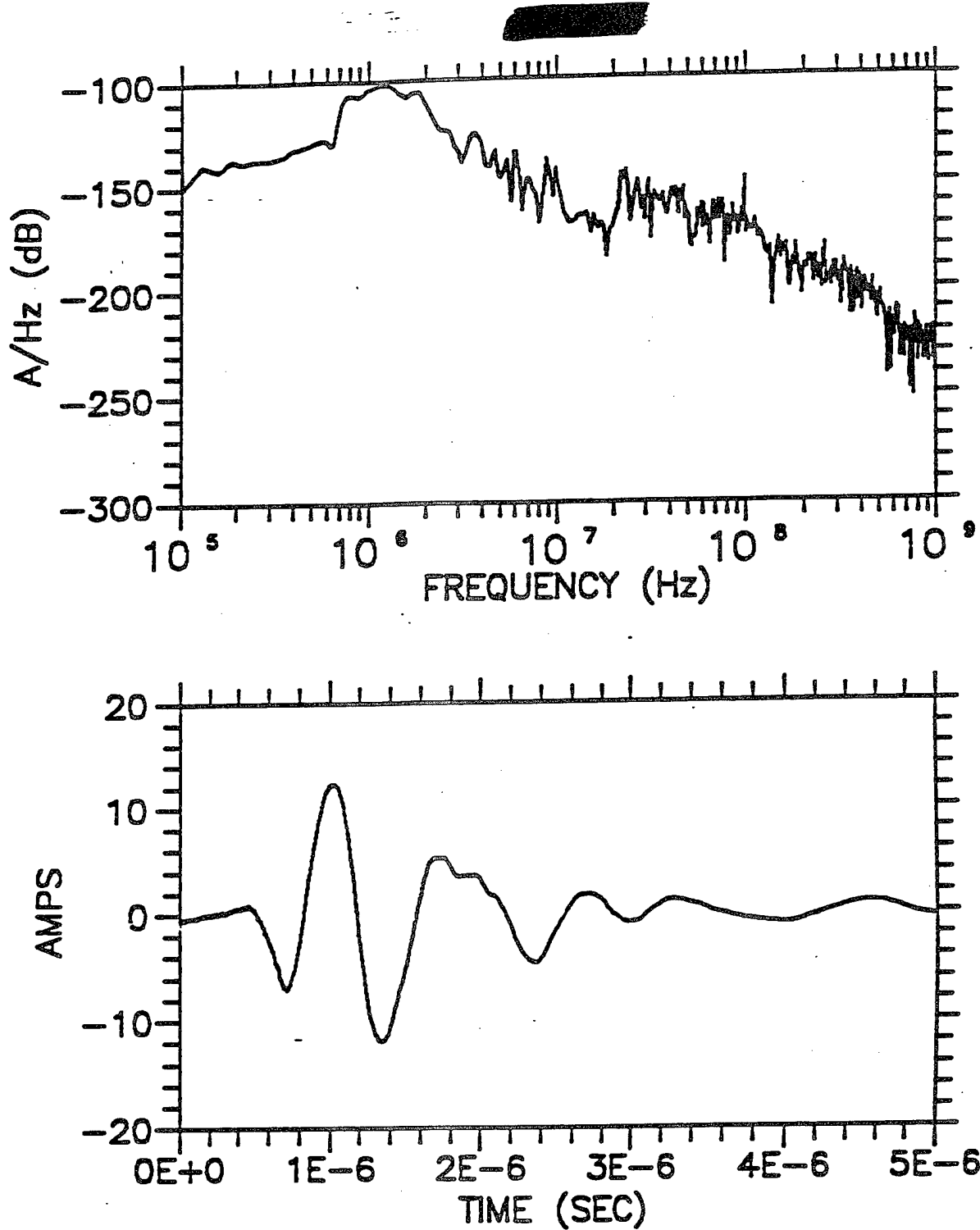
C-10



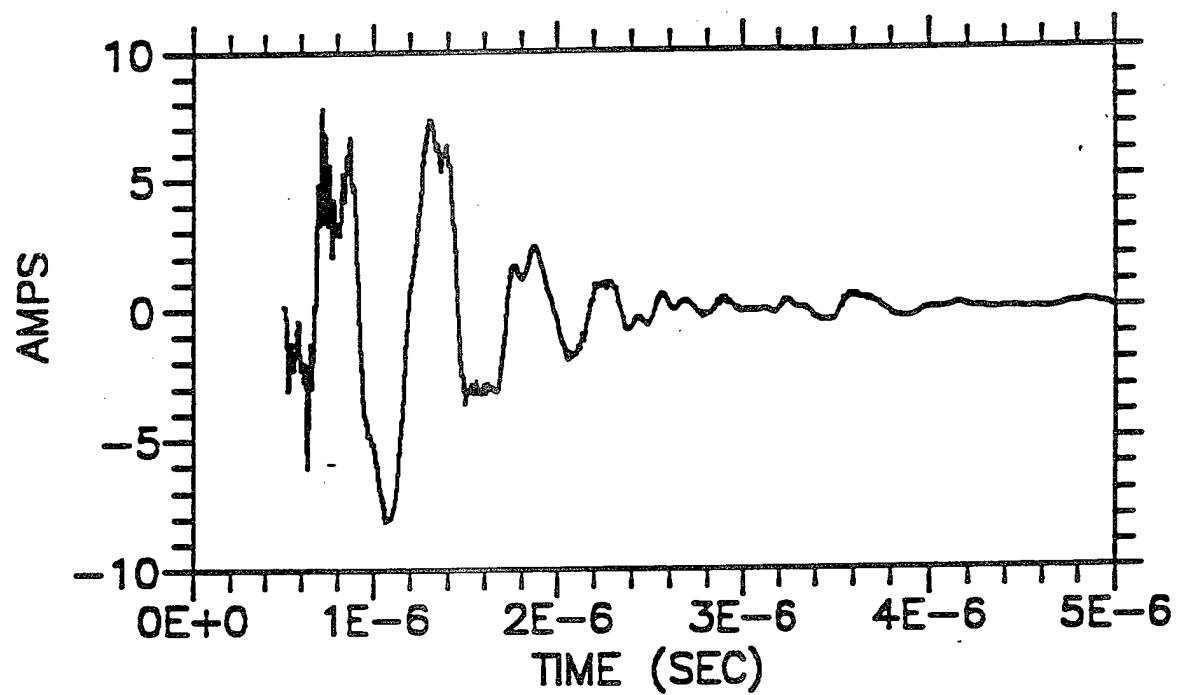
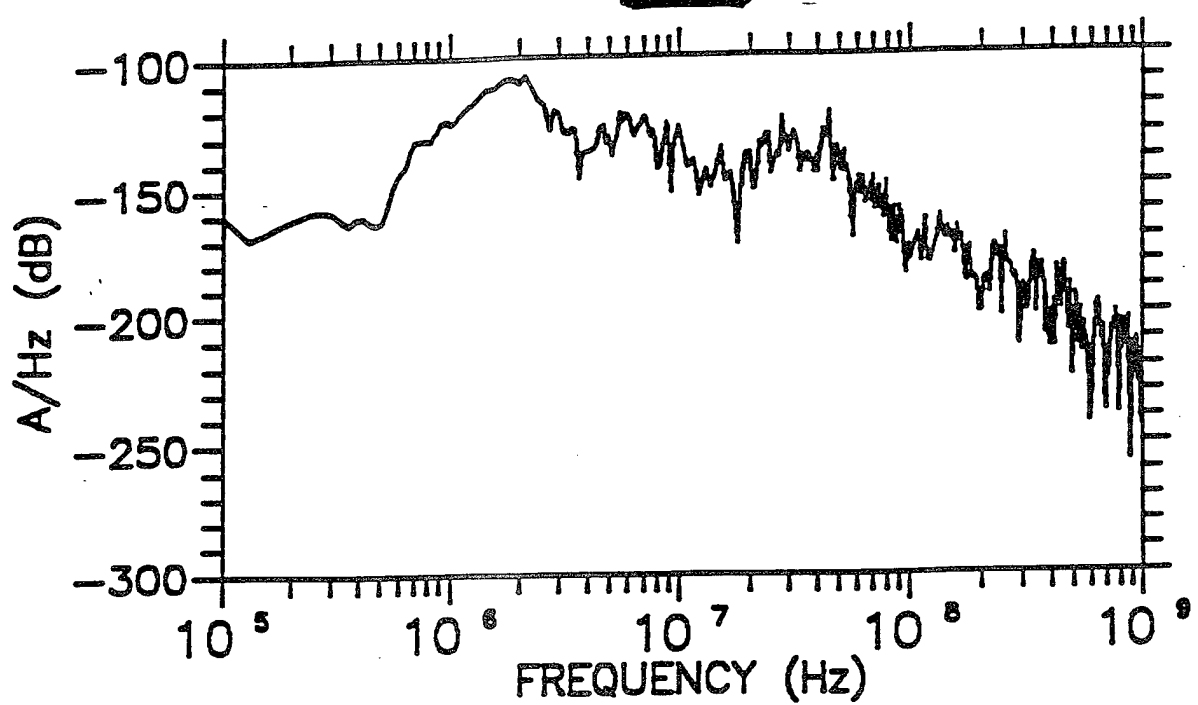
C-11



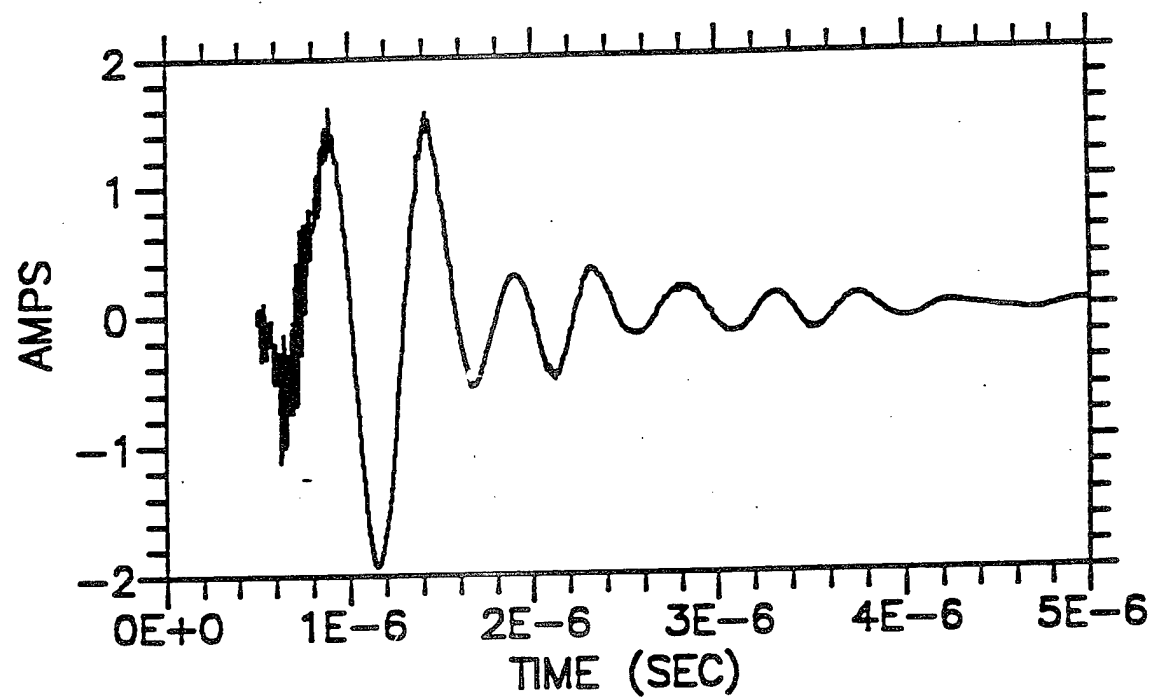
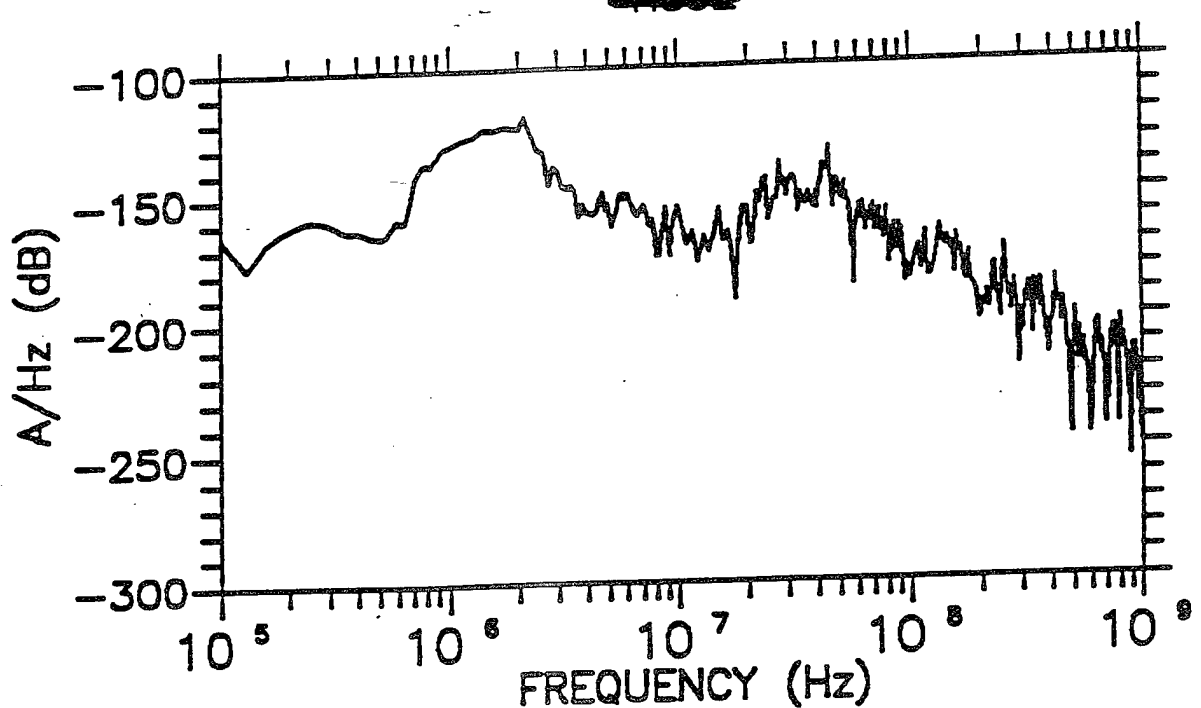
C-12



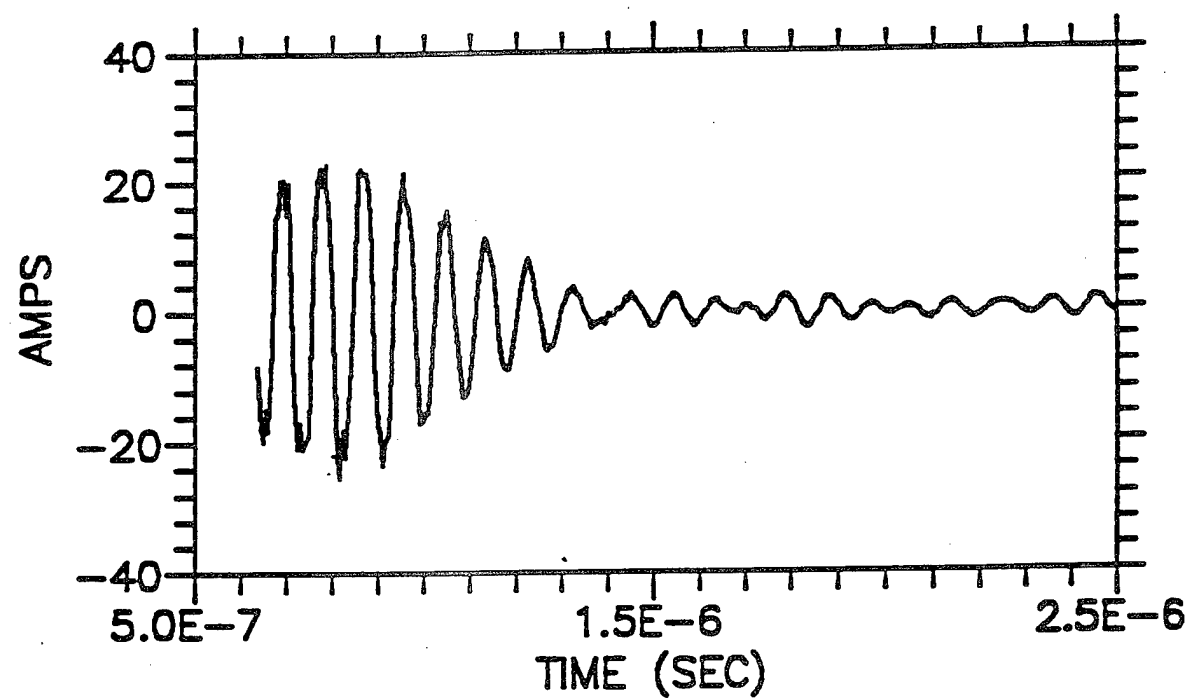
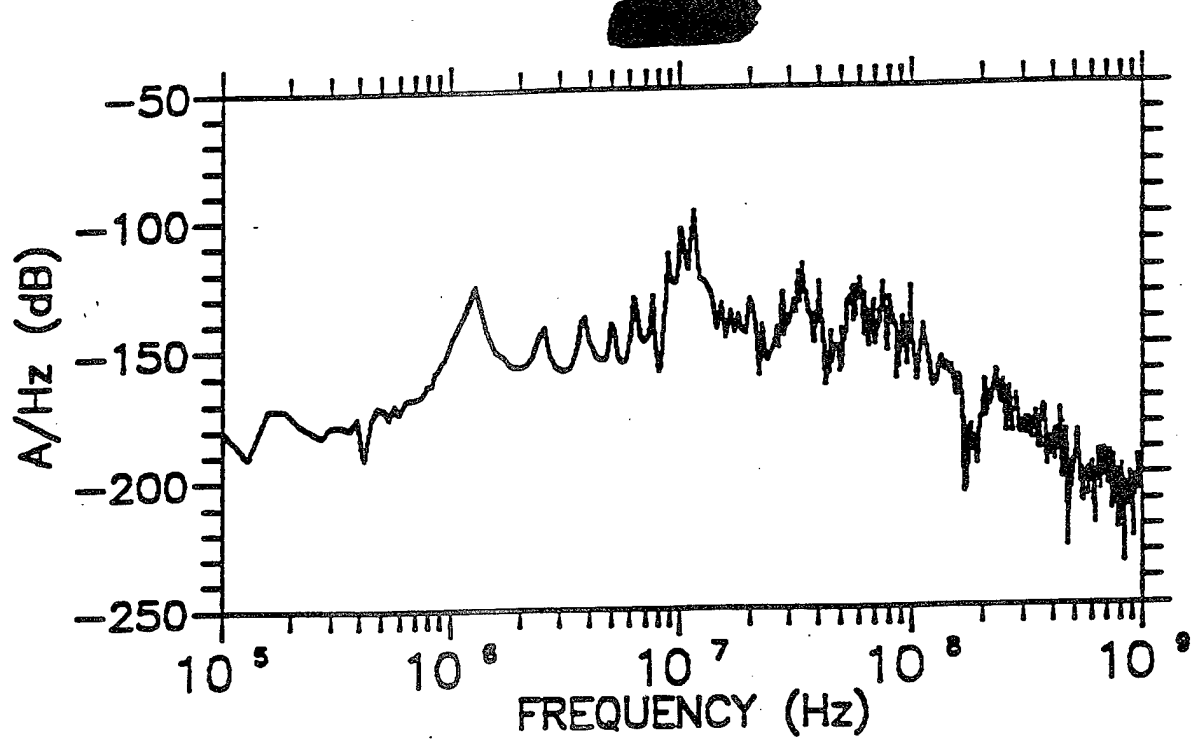
C-13

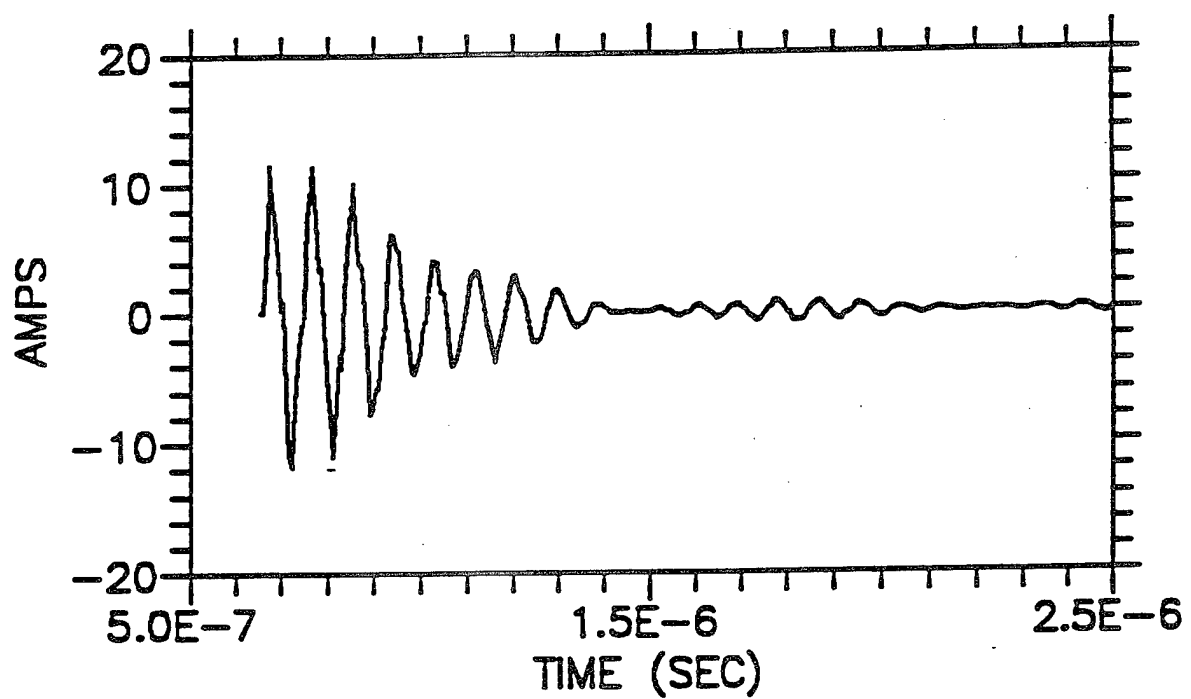
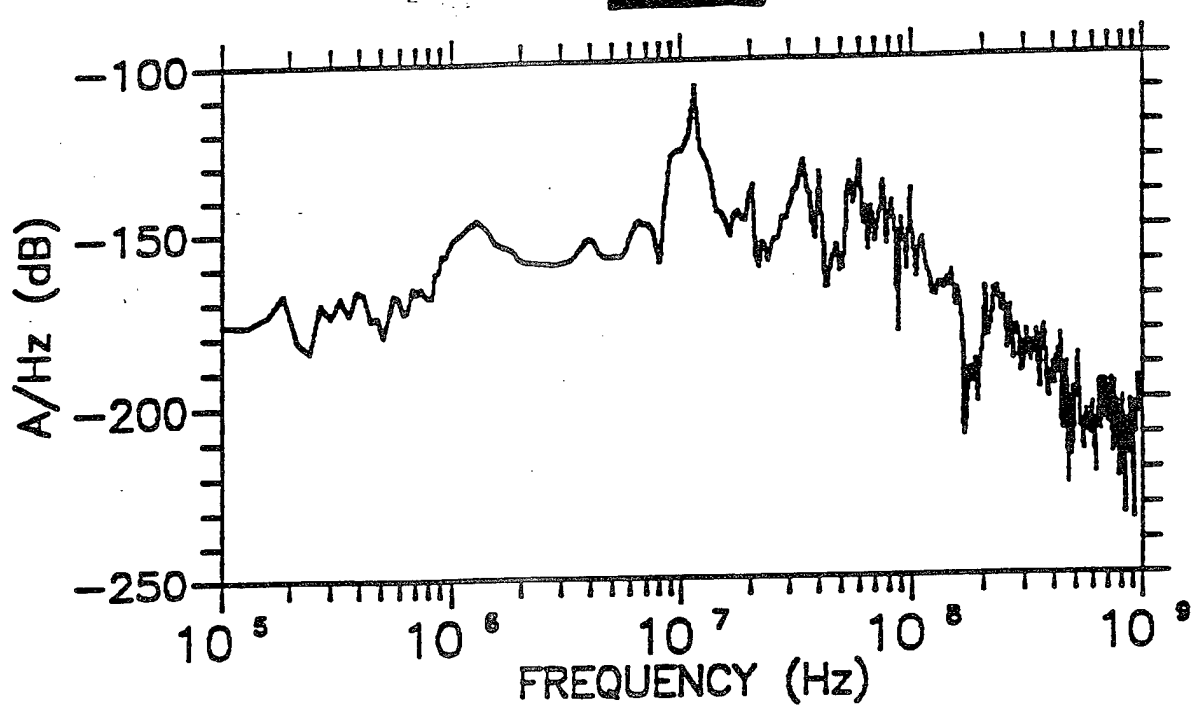


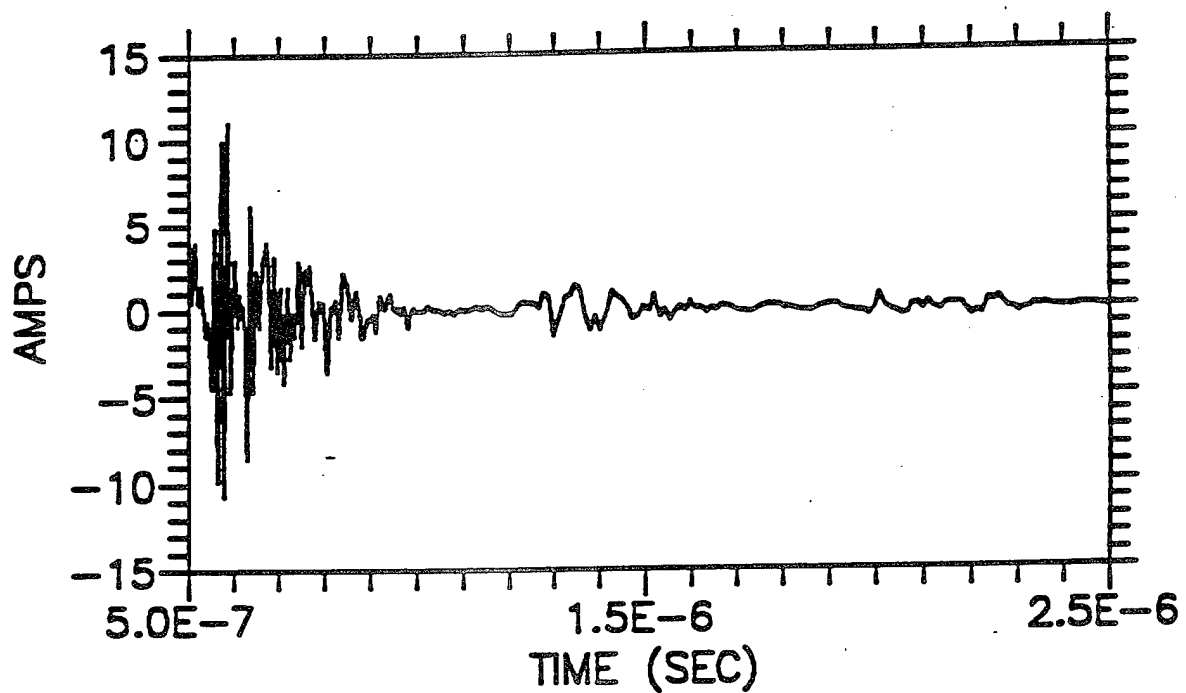
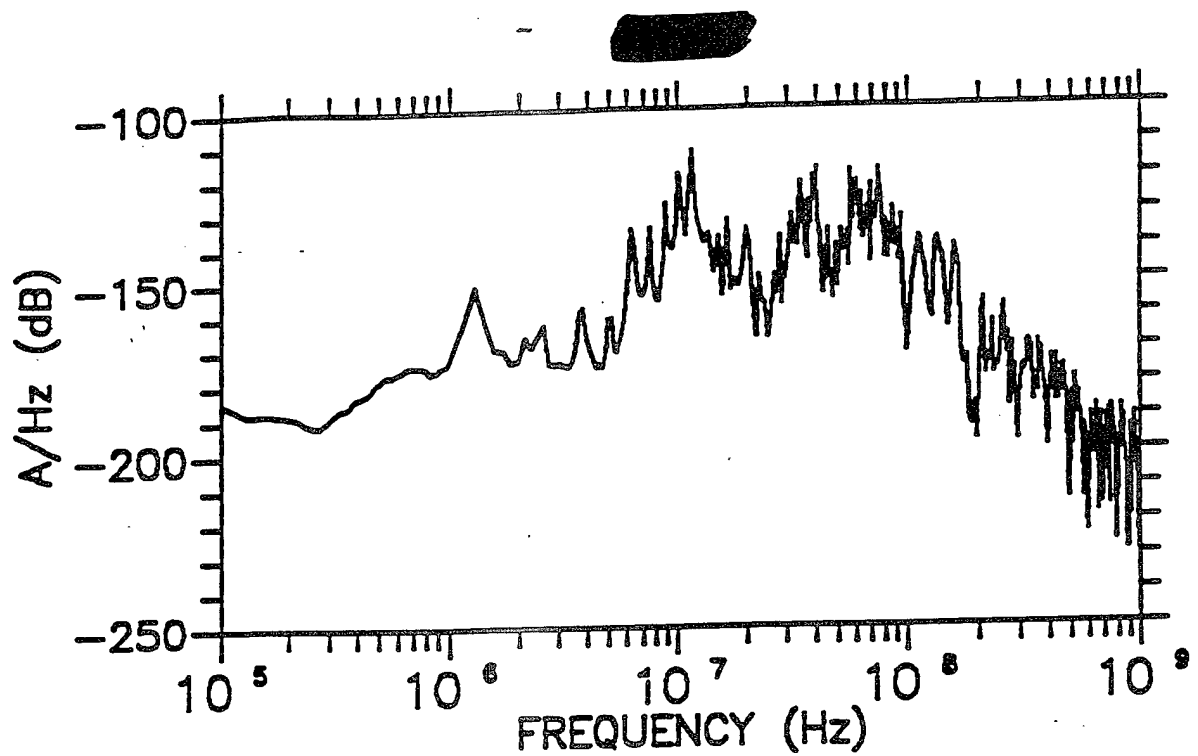
C-14

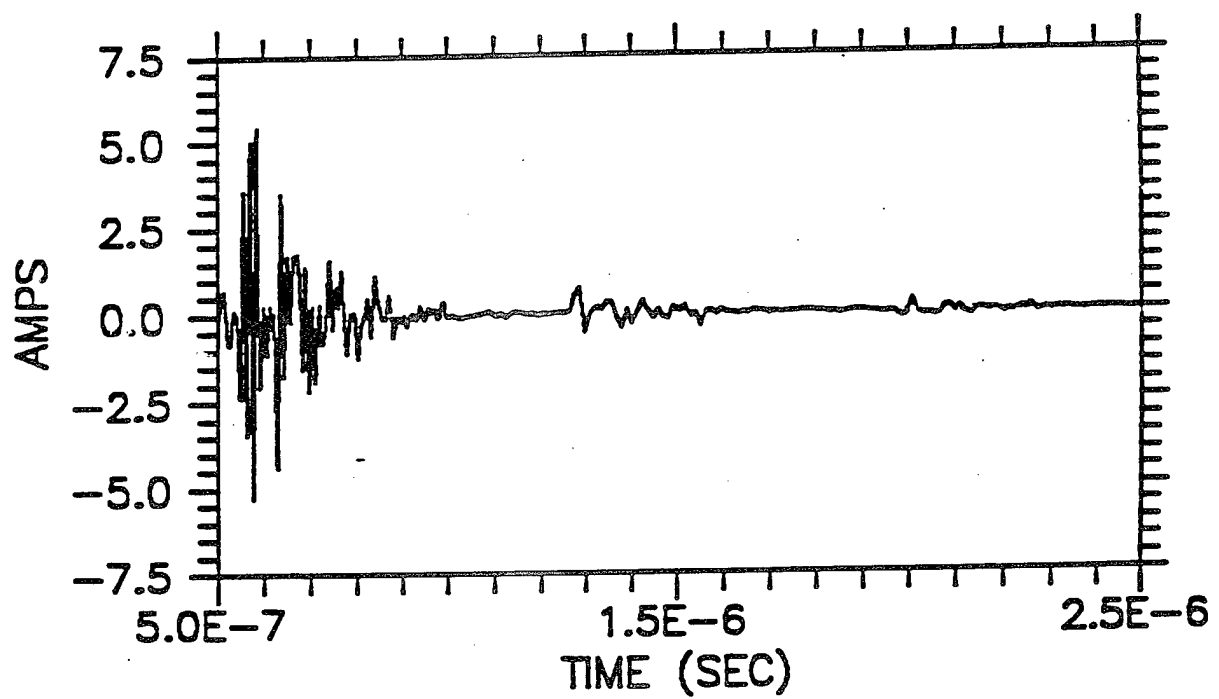
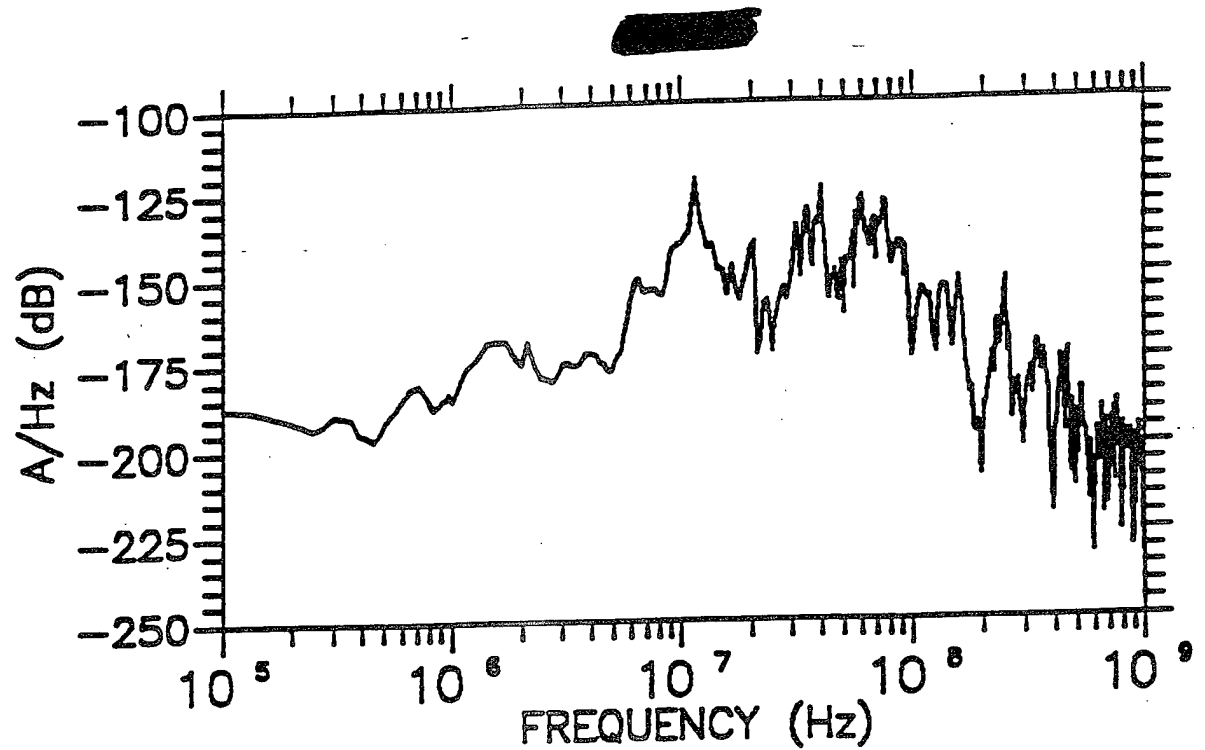


C-15

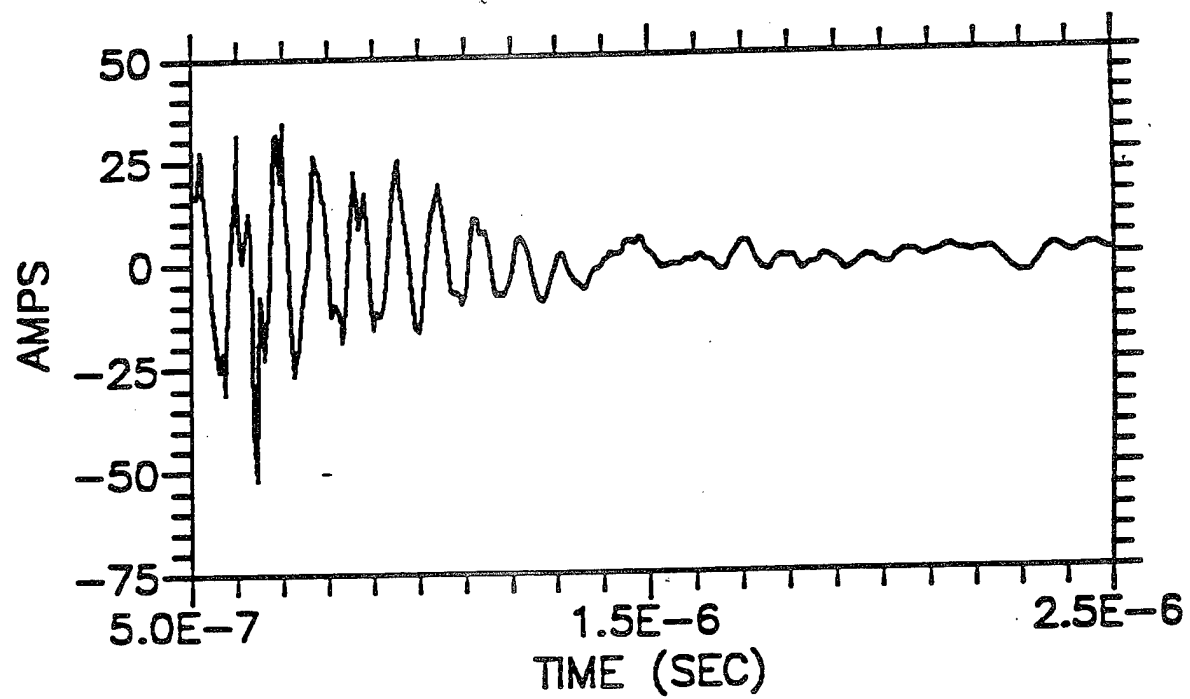
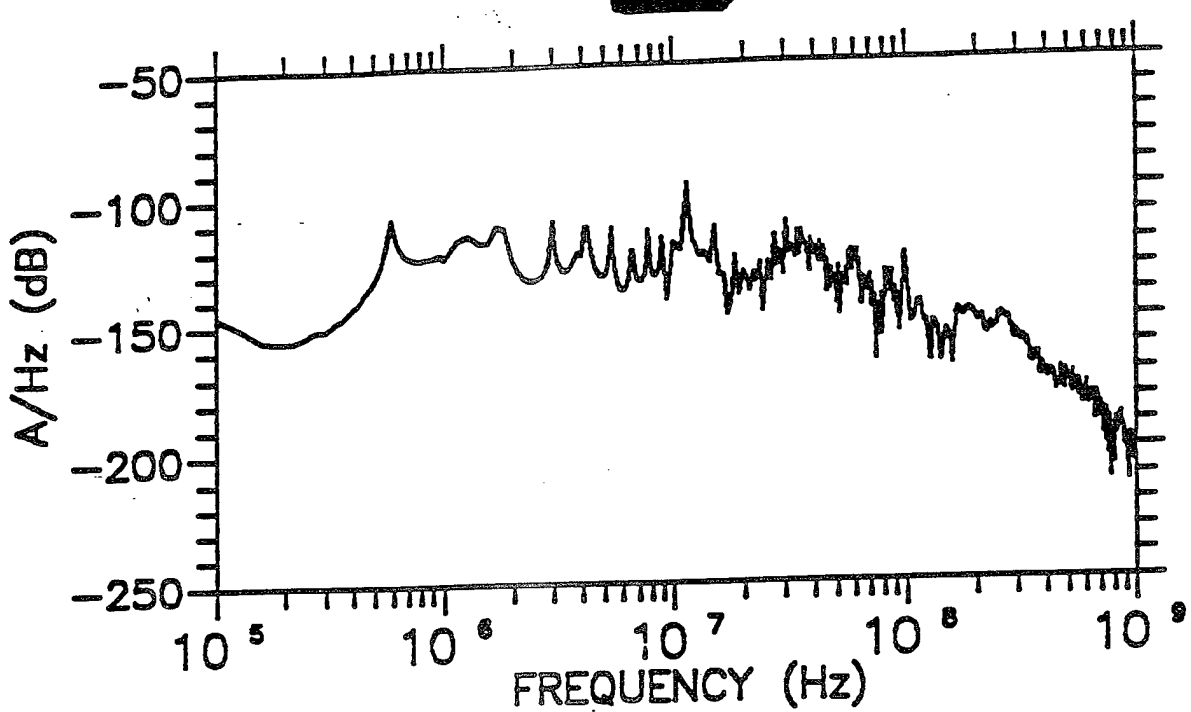


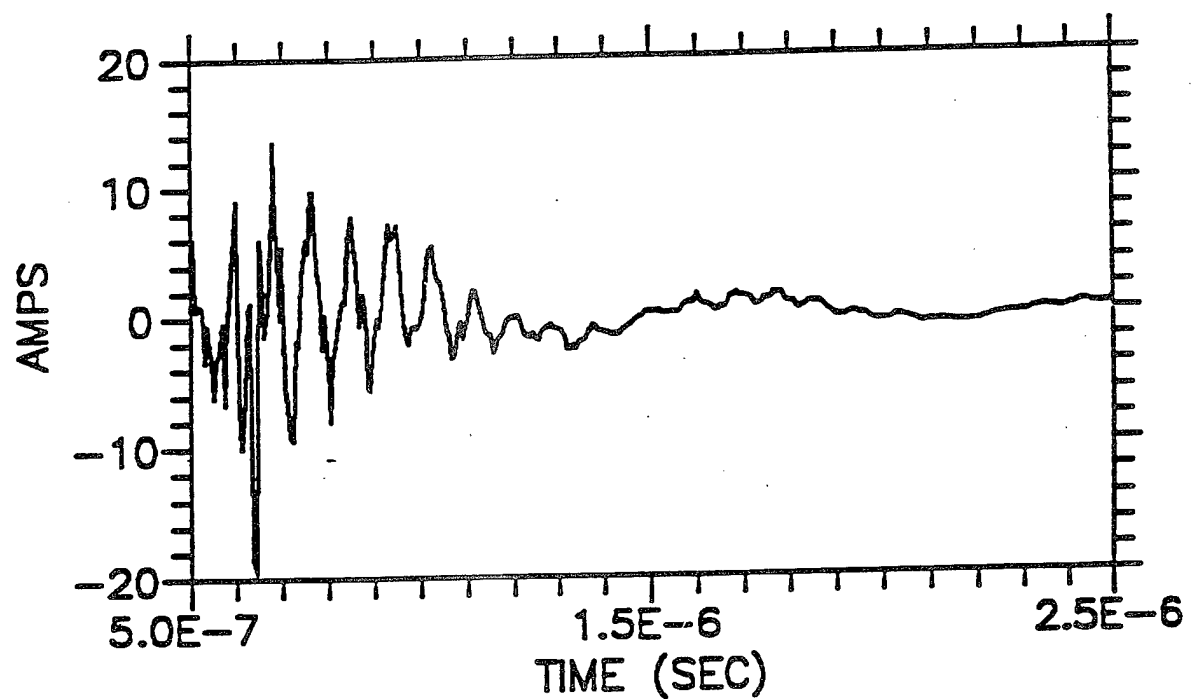
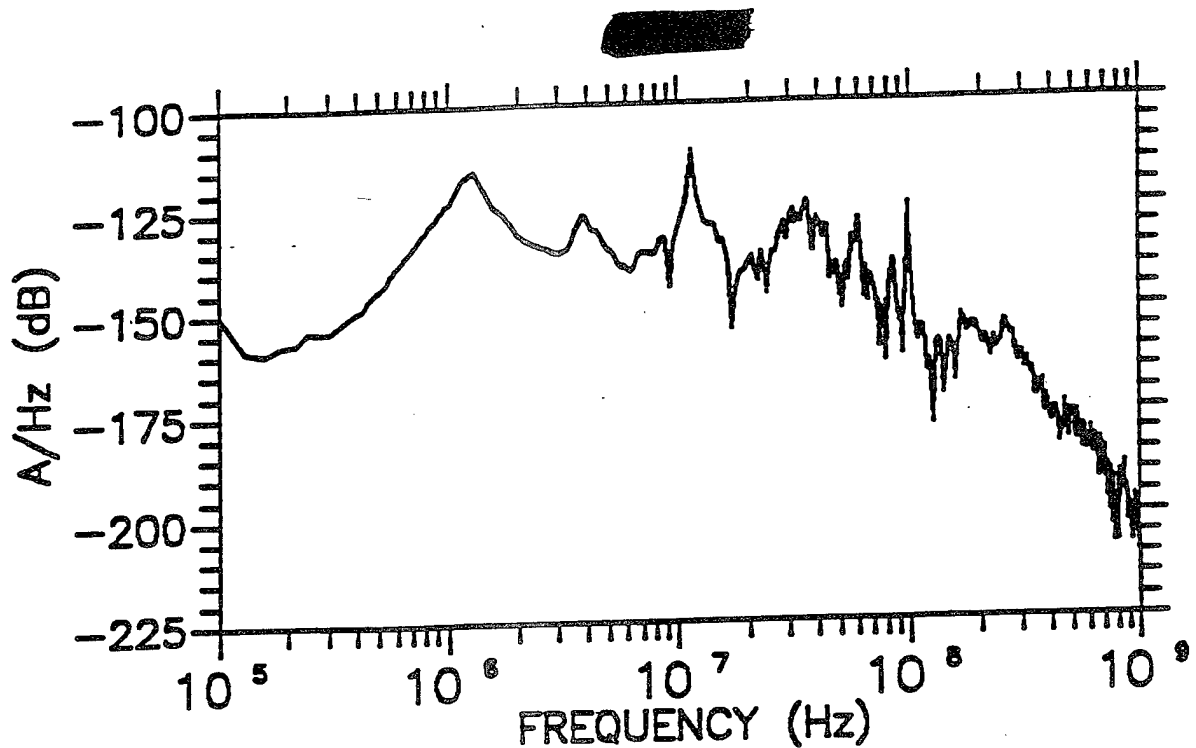


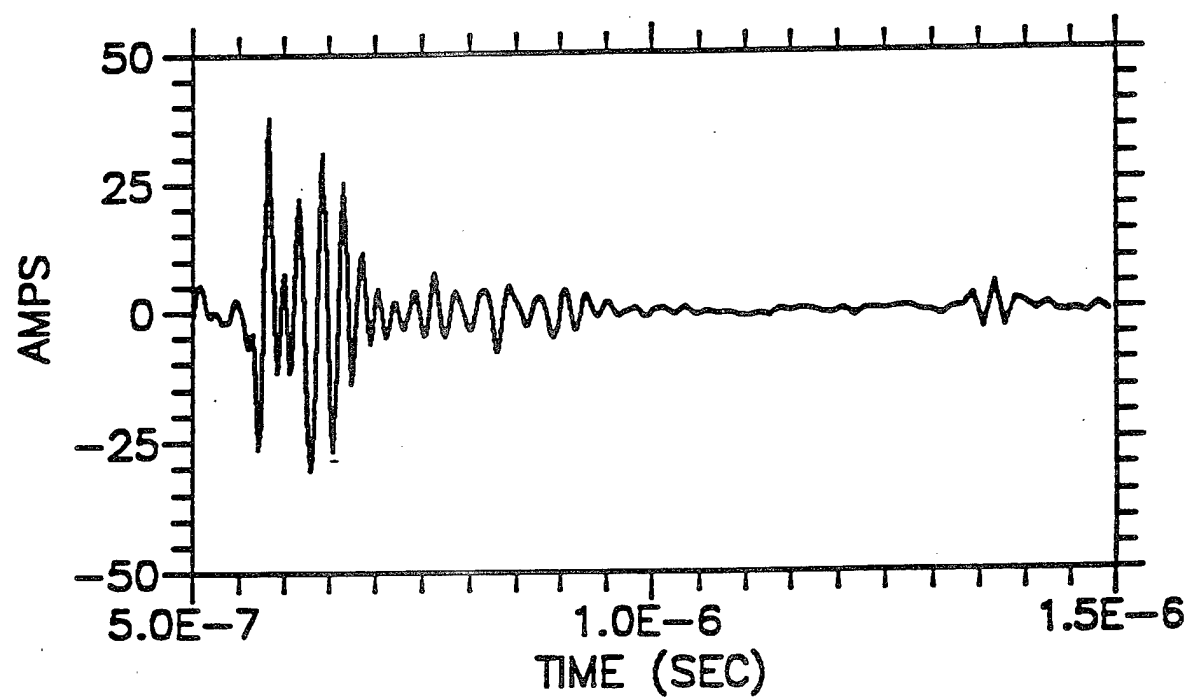
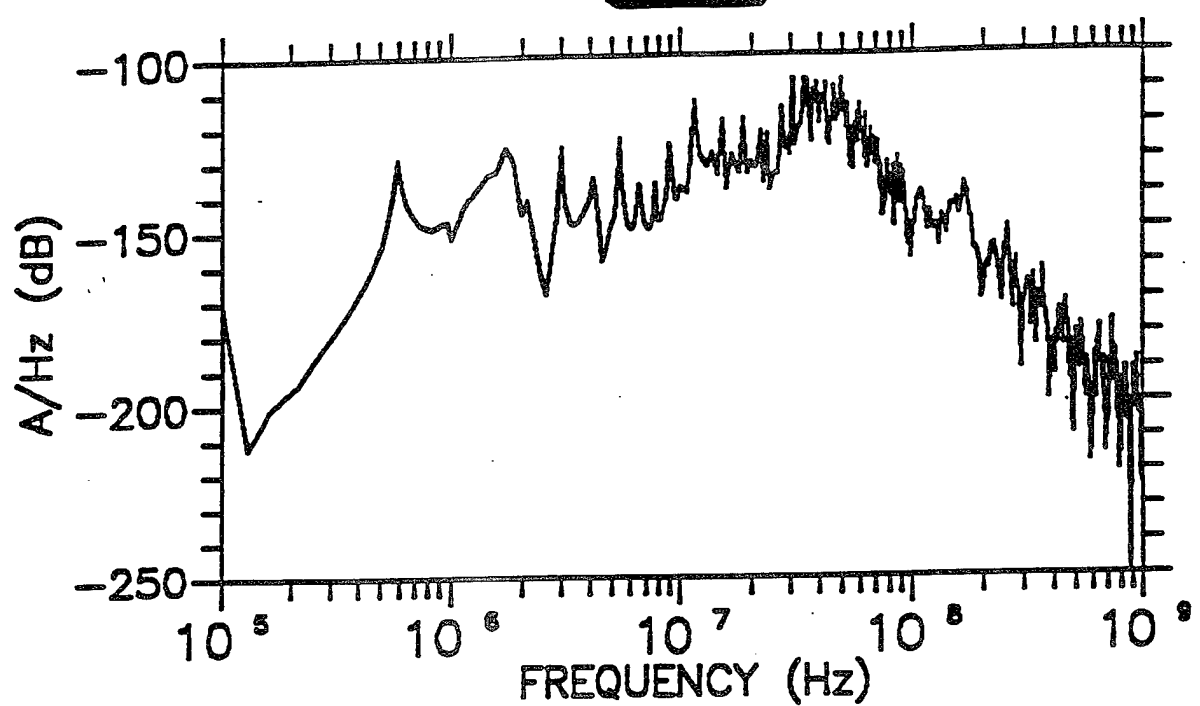




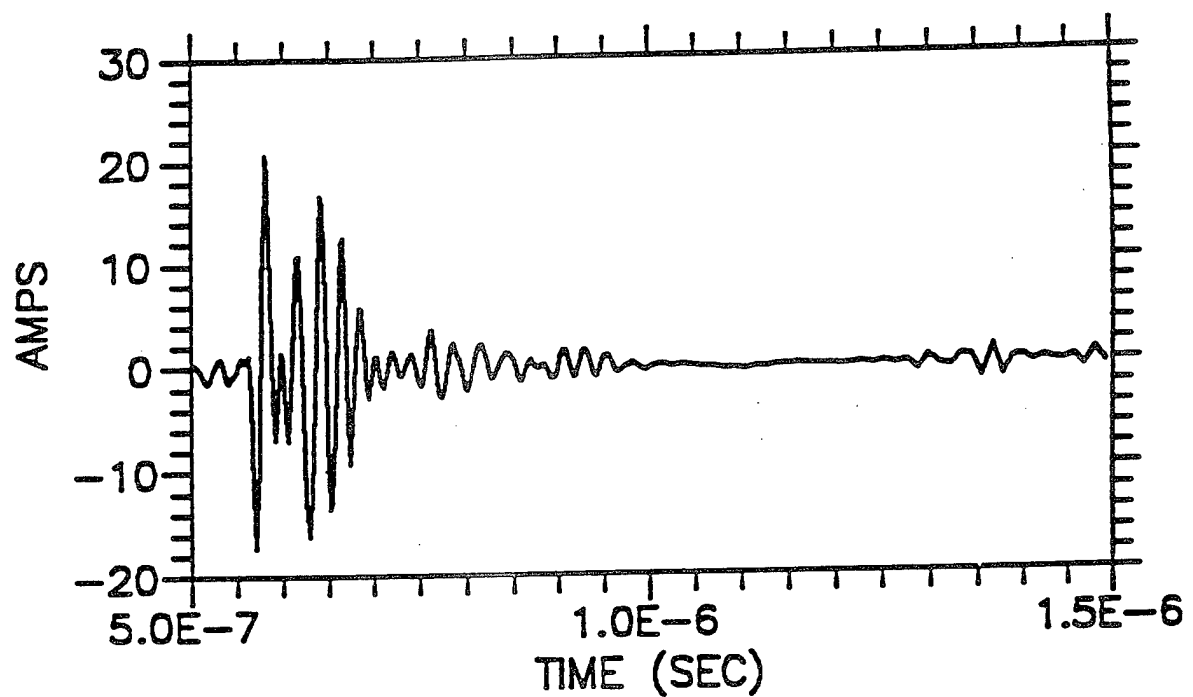
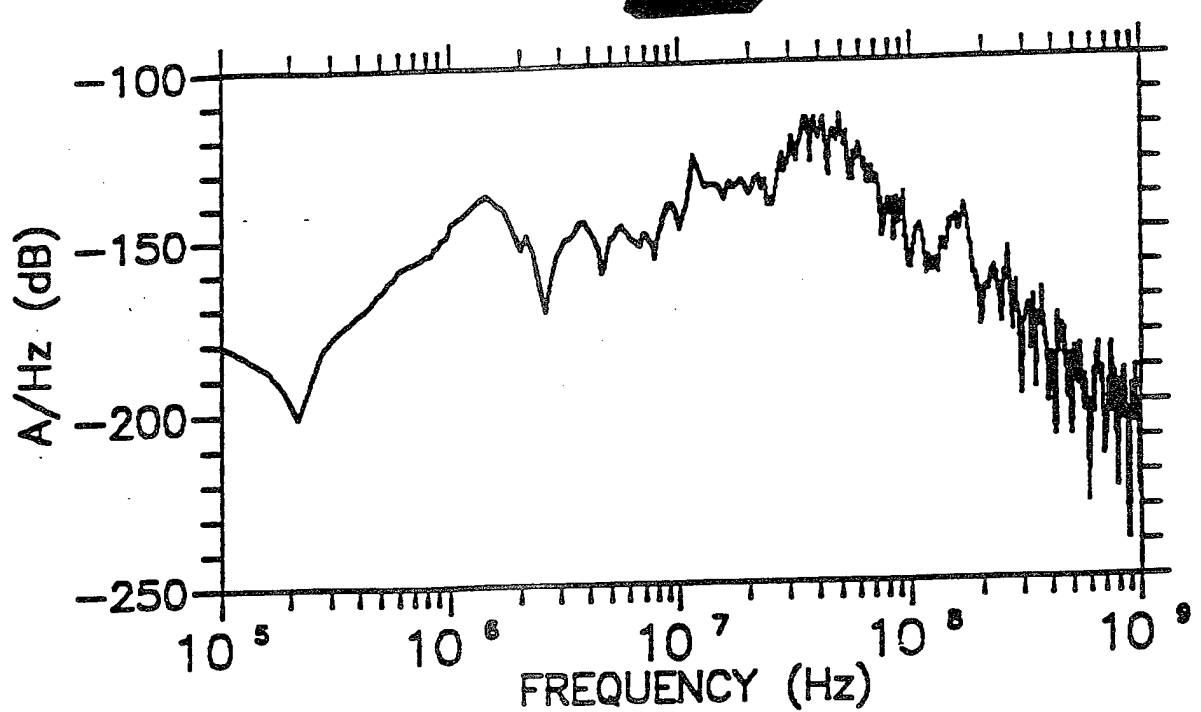
C-19

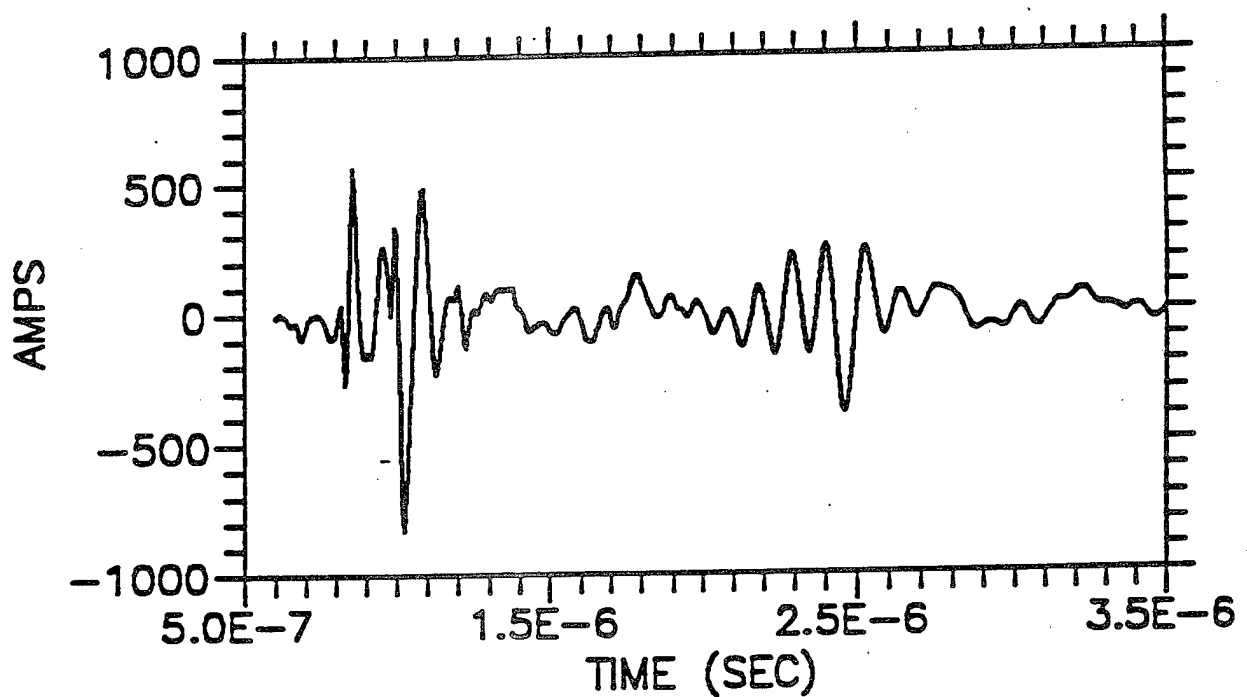
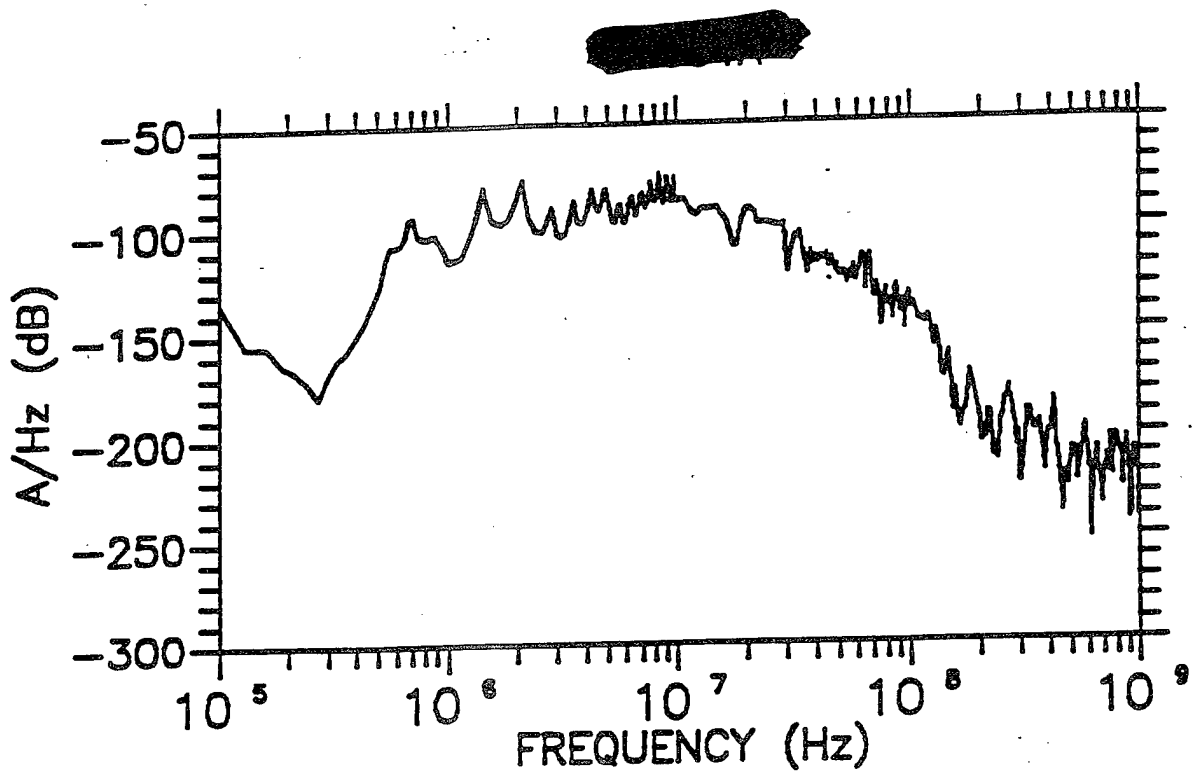


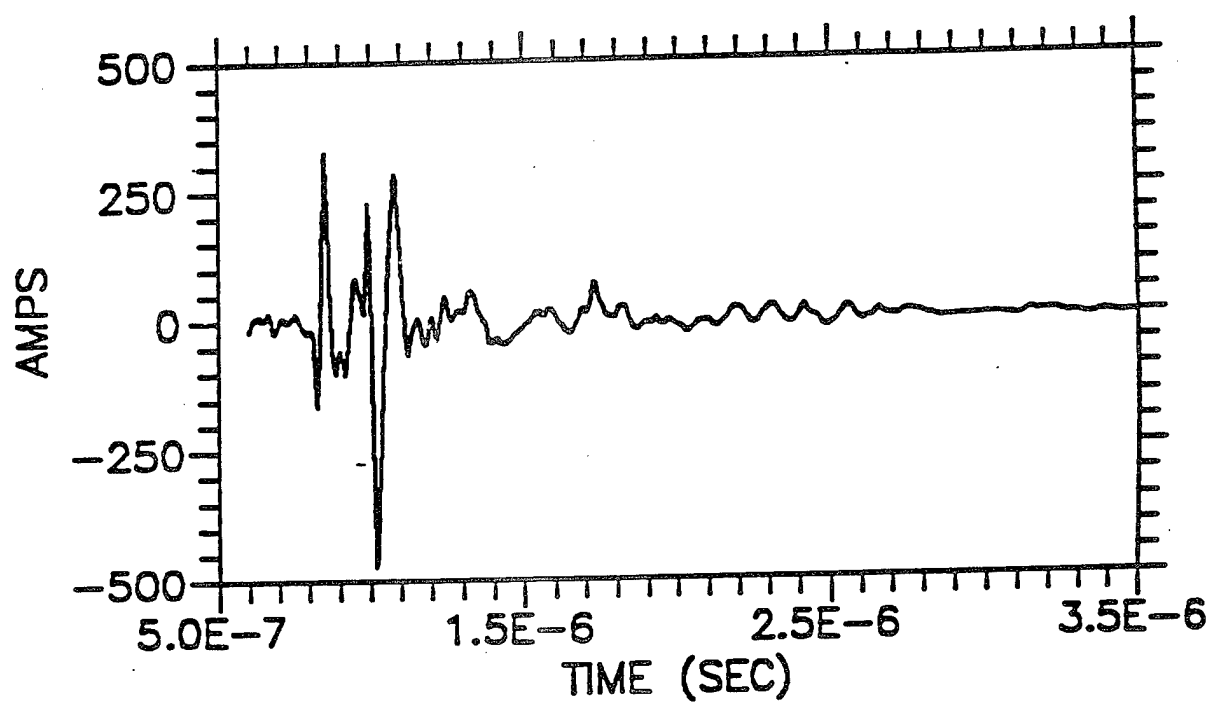
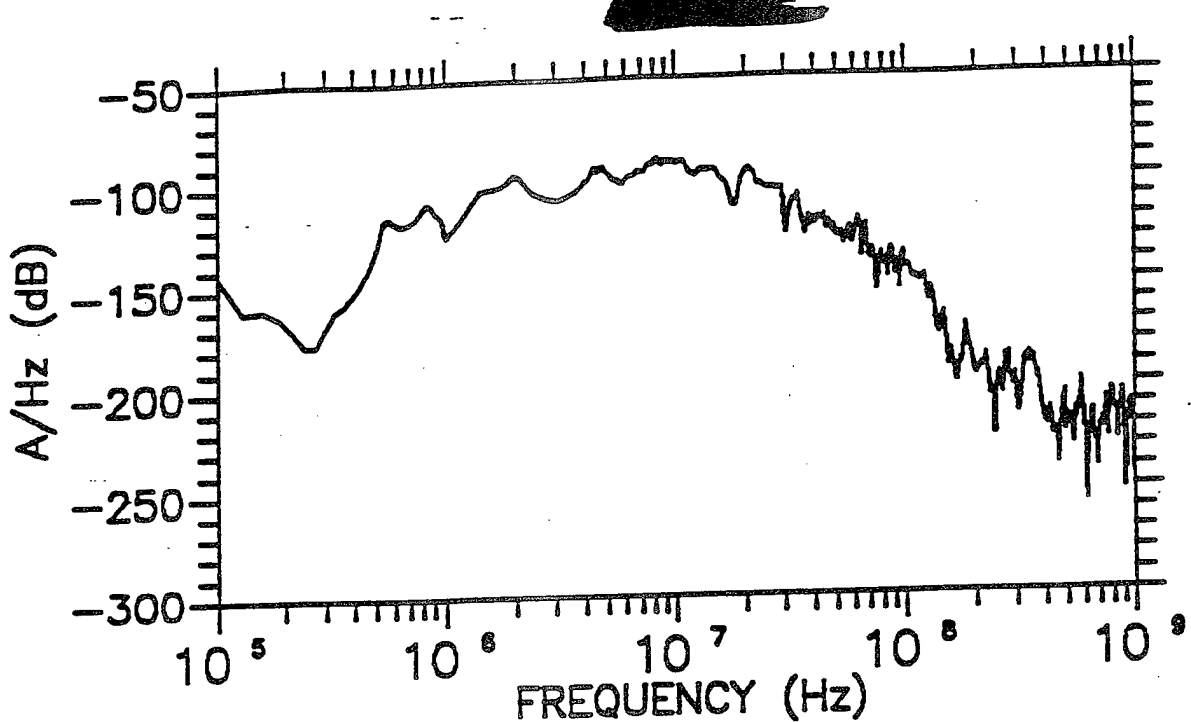




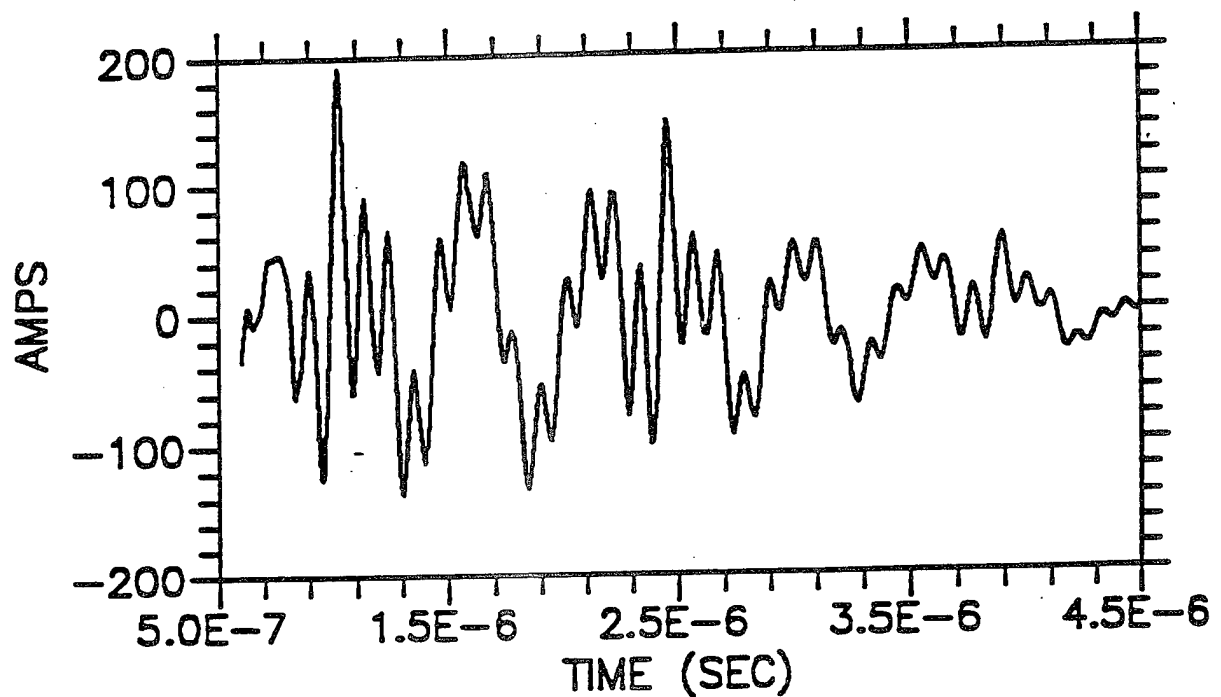
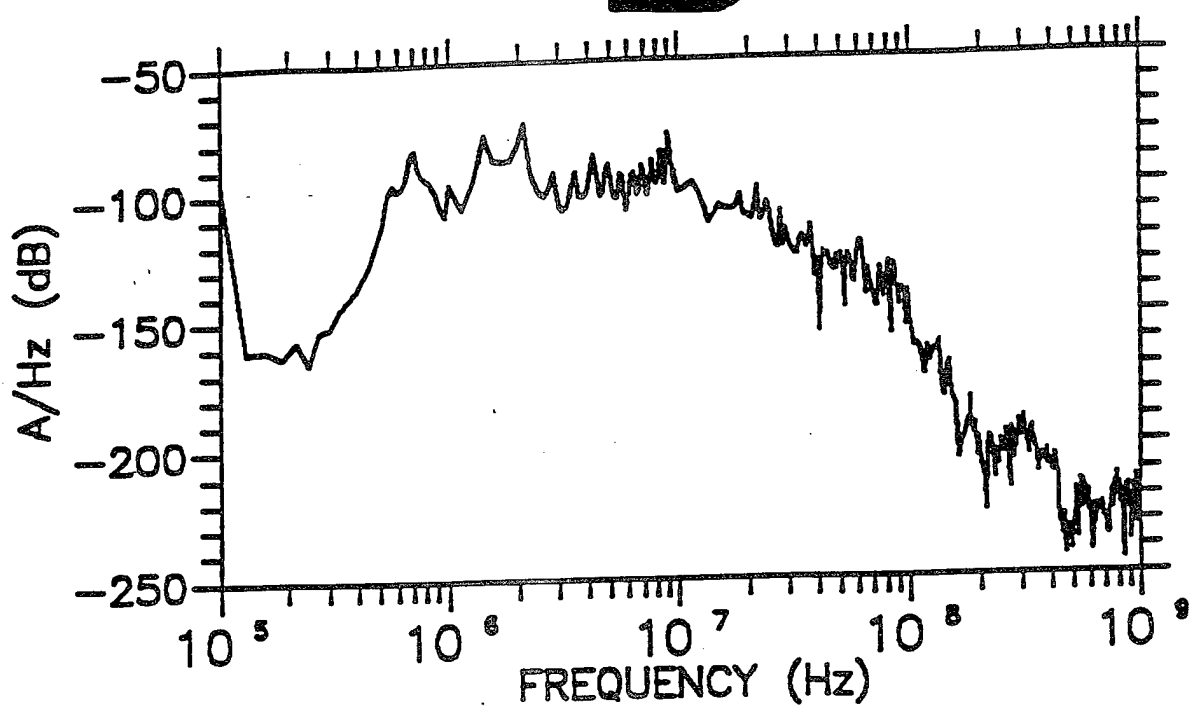
C-22

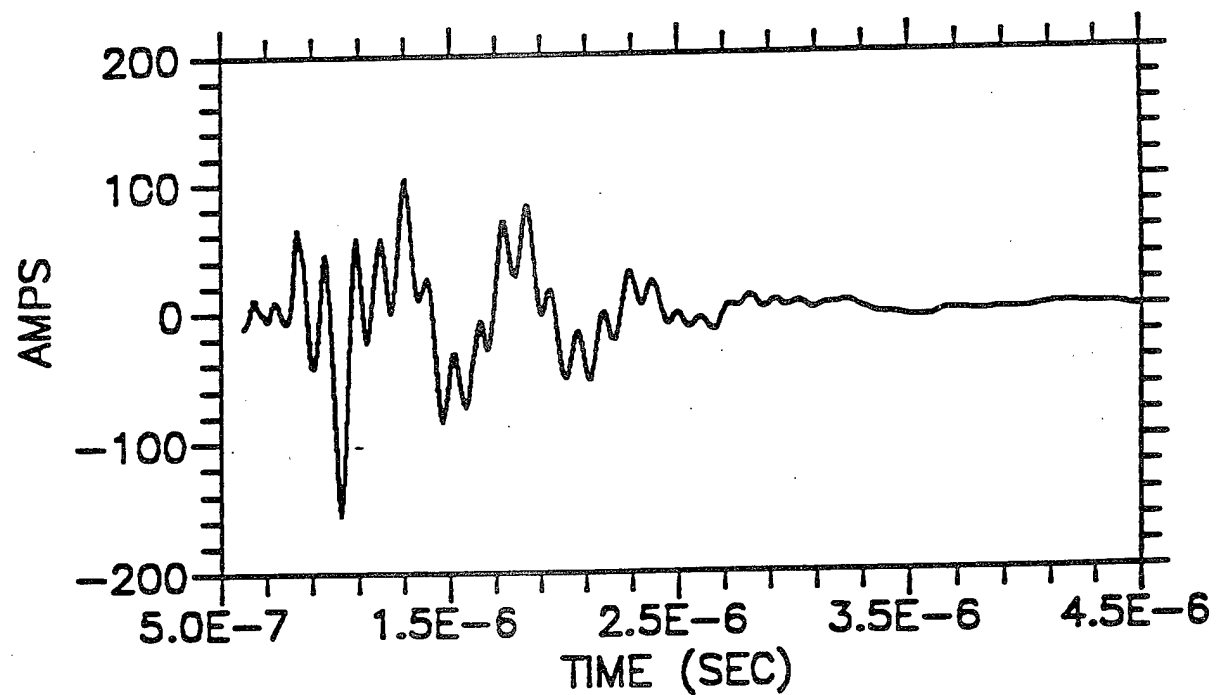
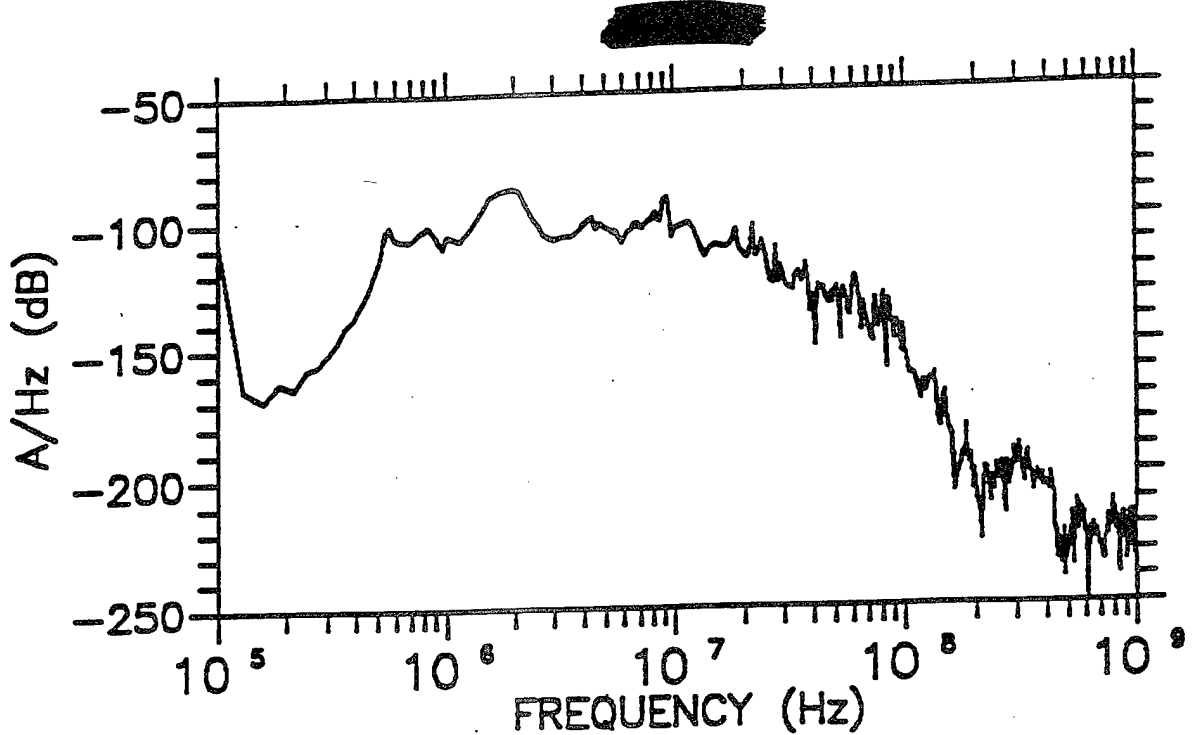


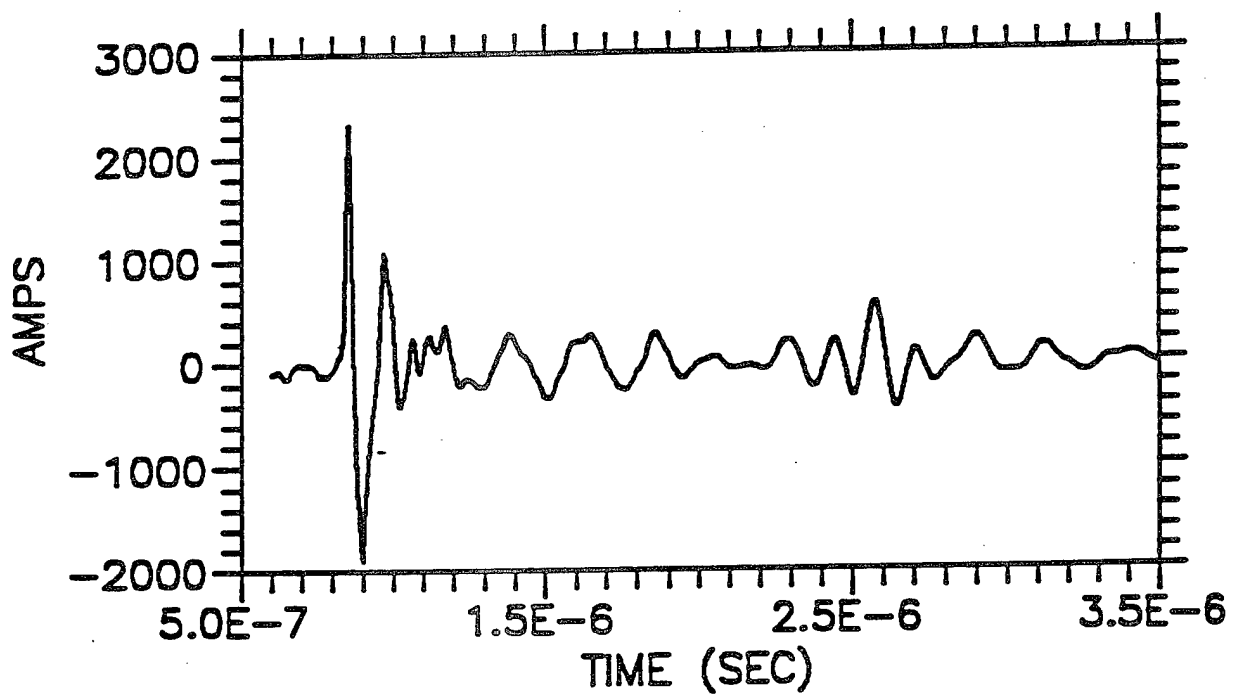
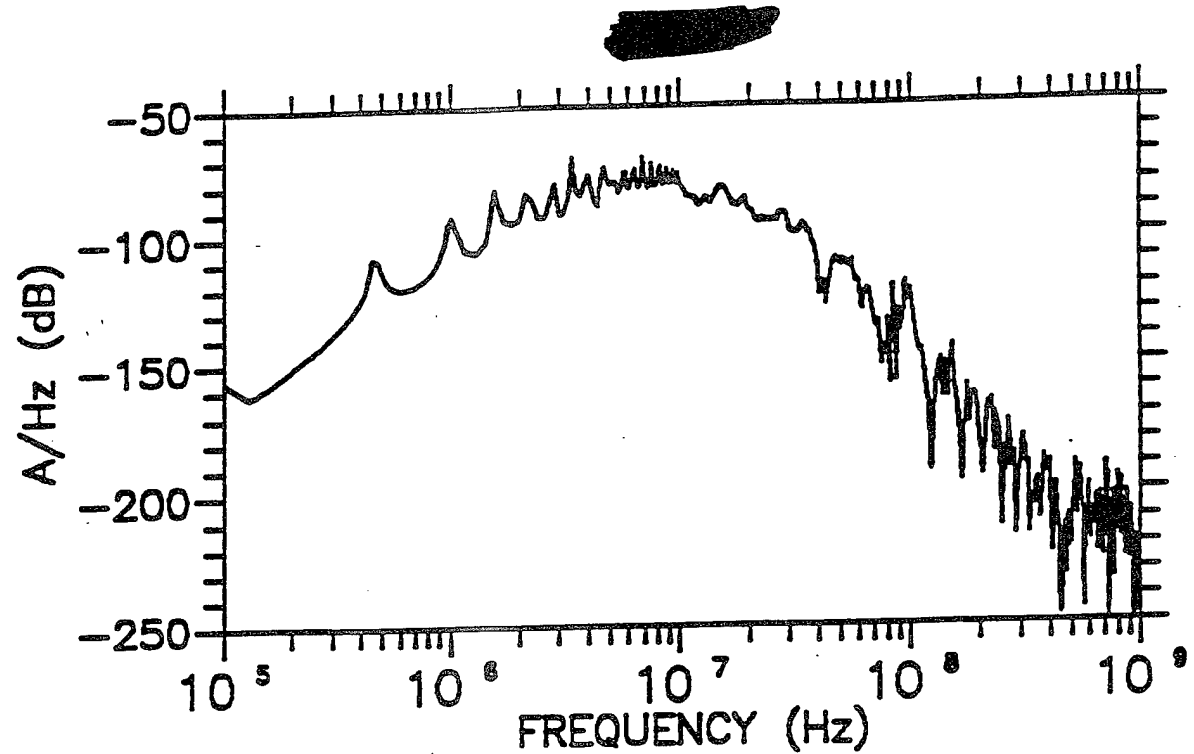


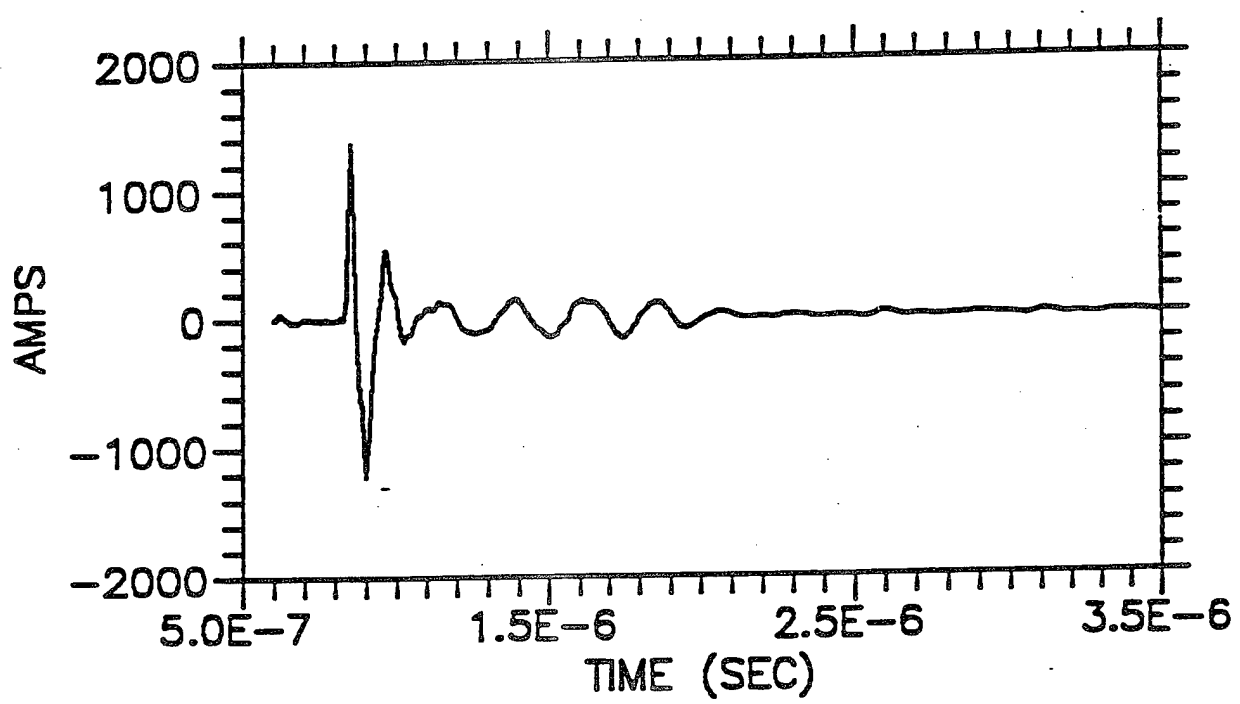
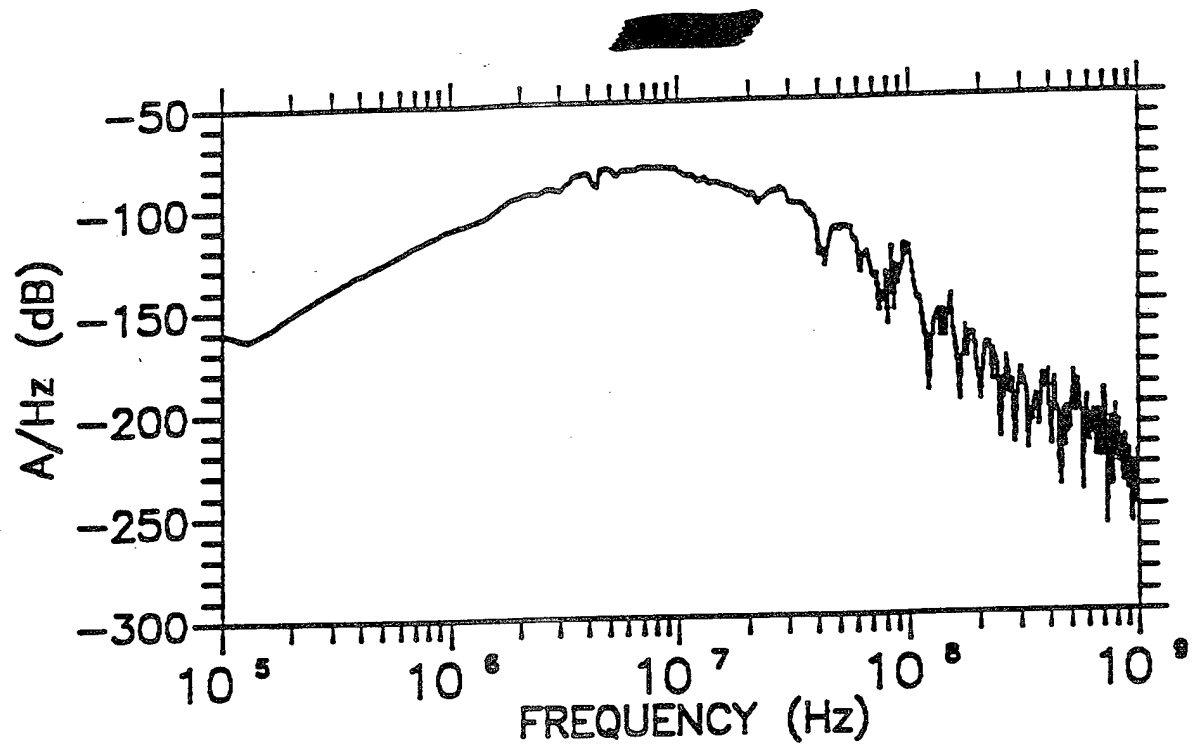


C-25

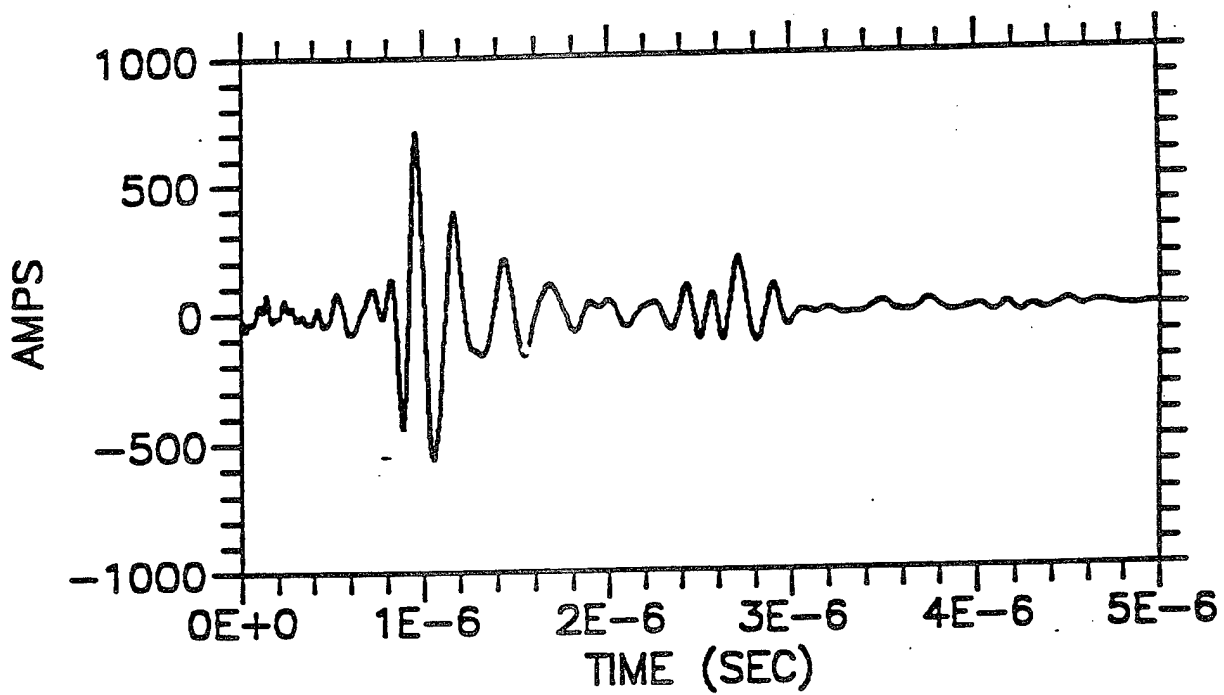
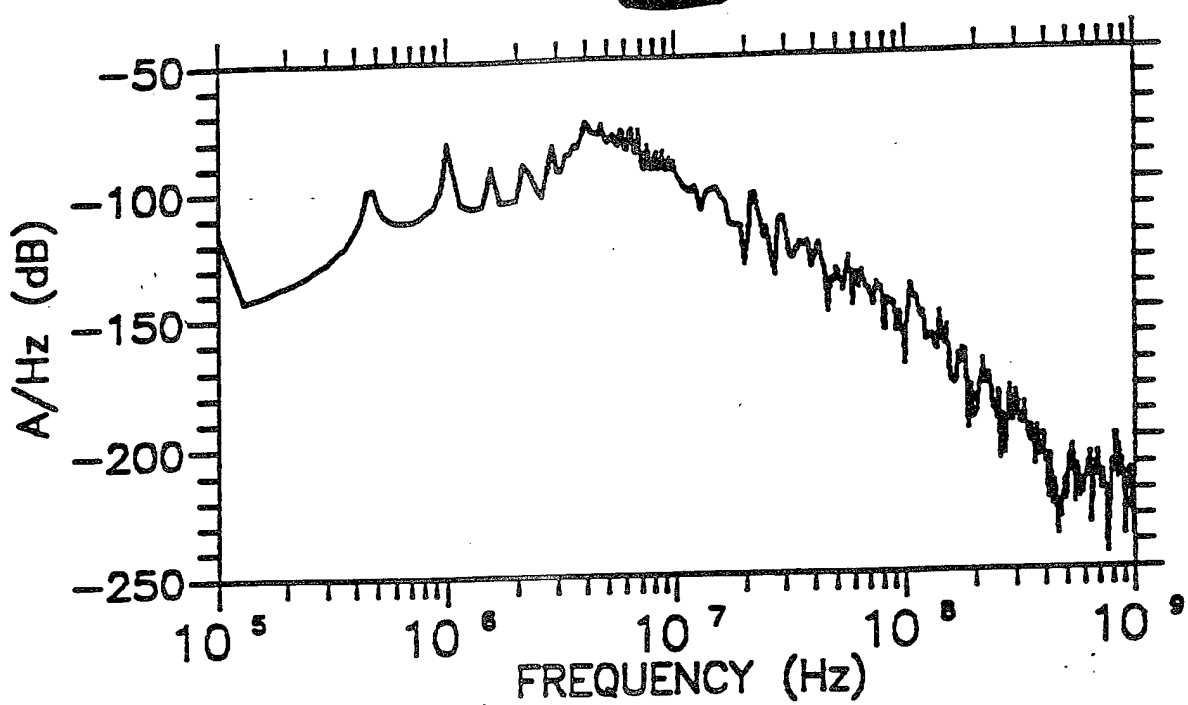


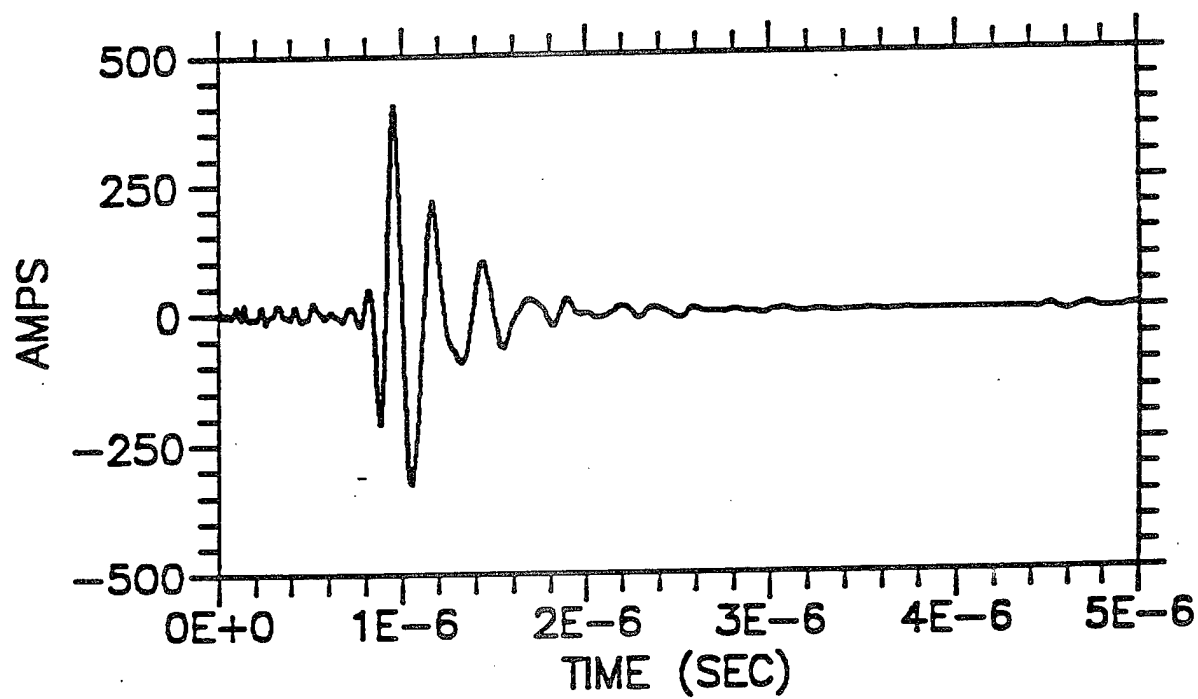
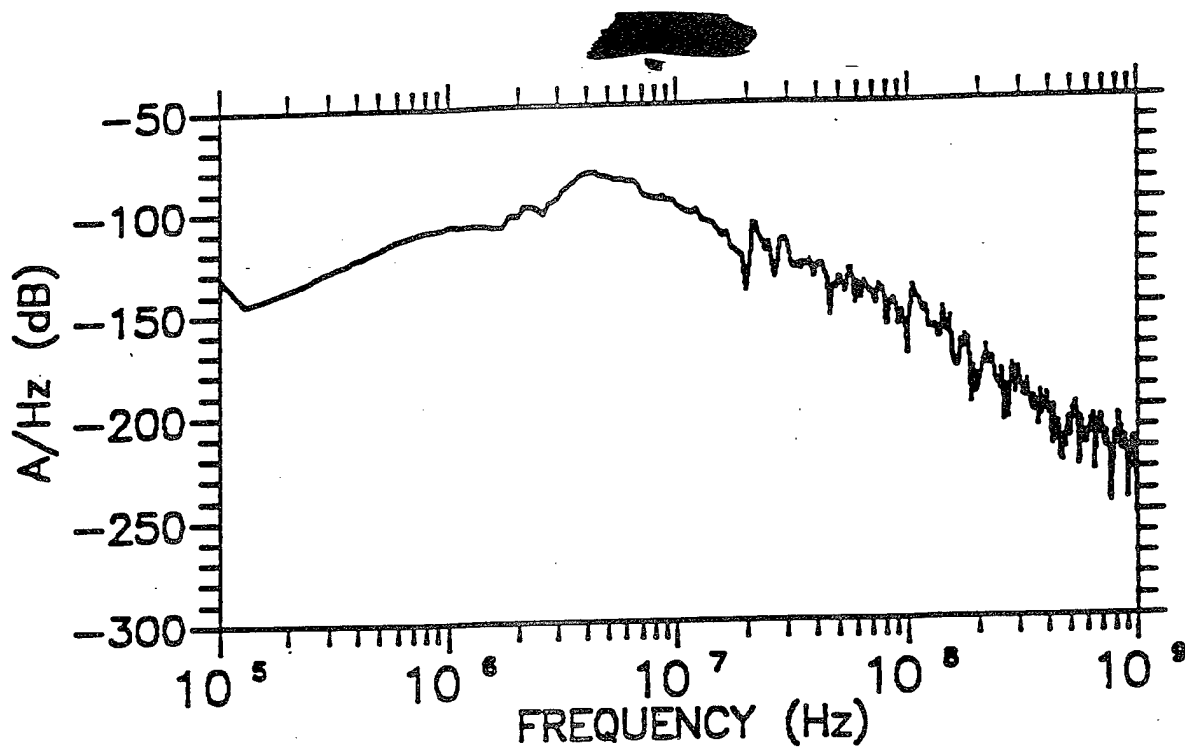


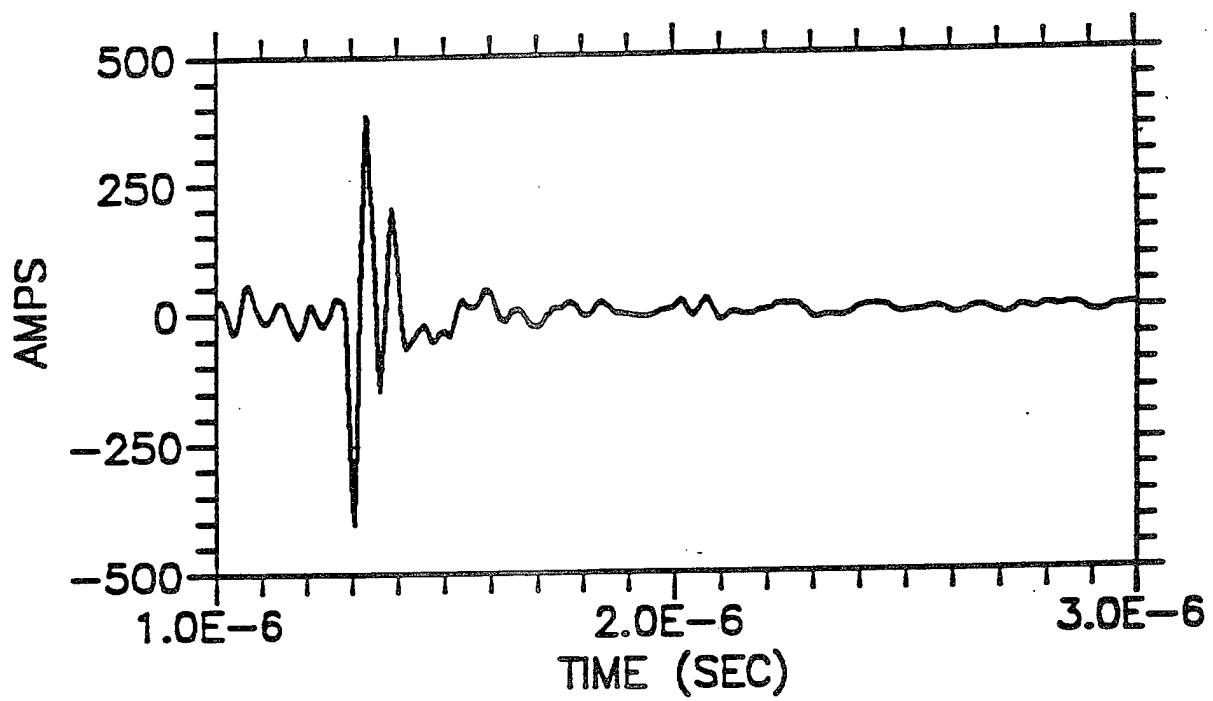
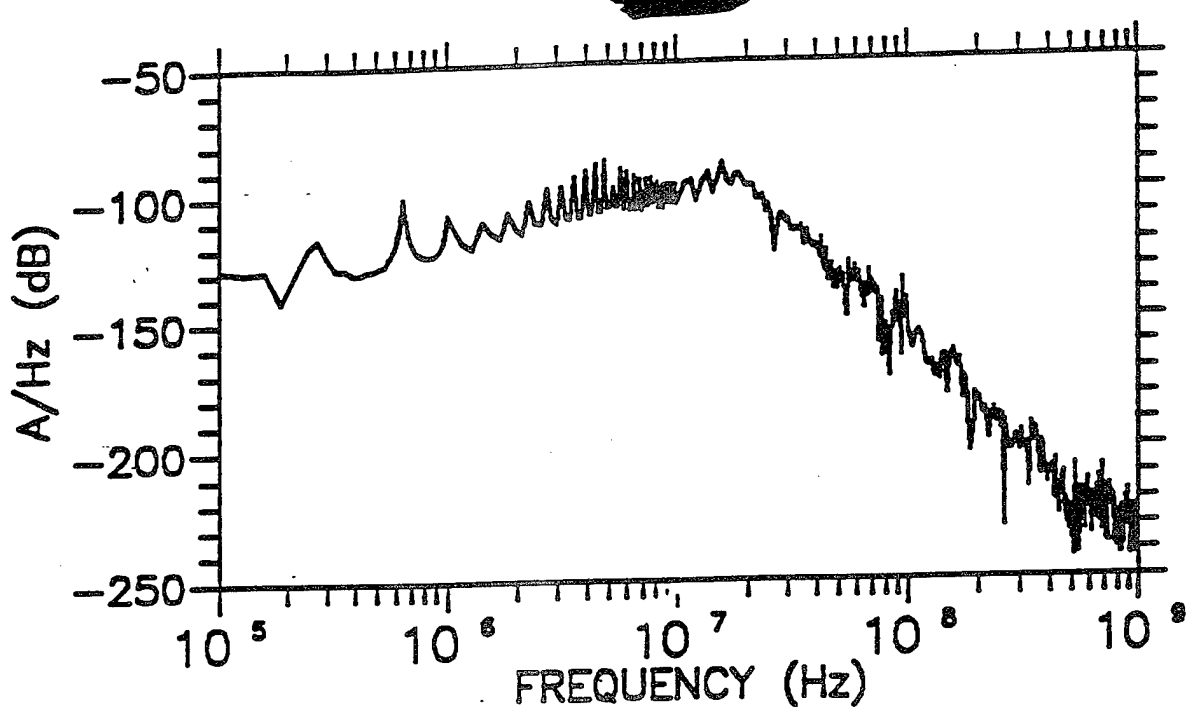




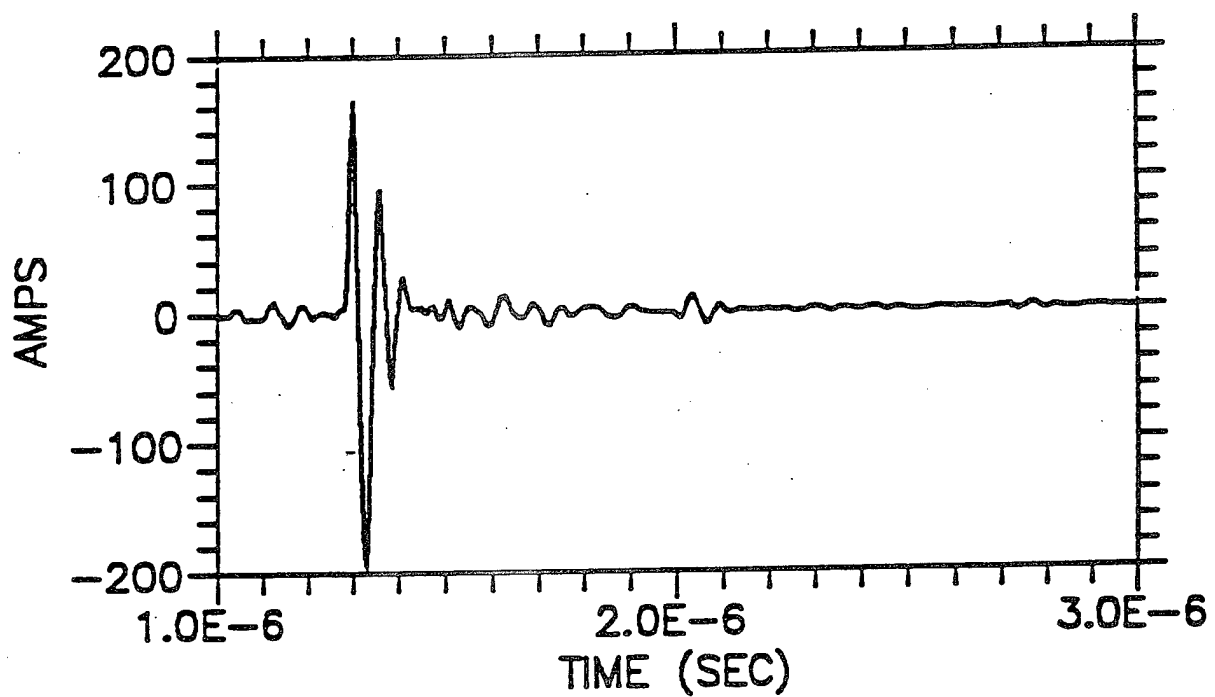
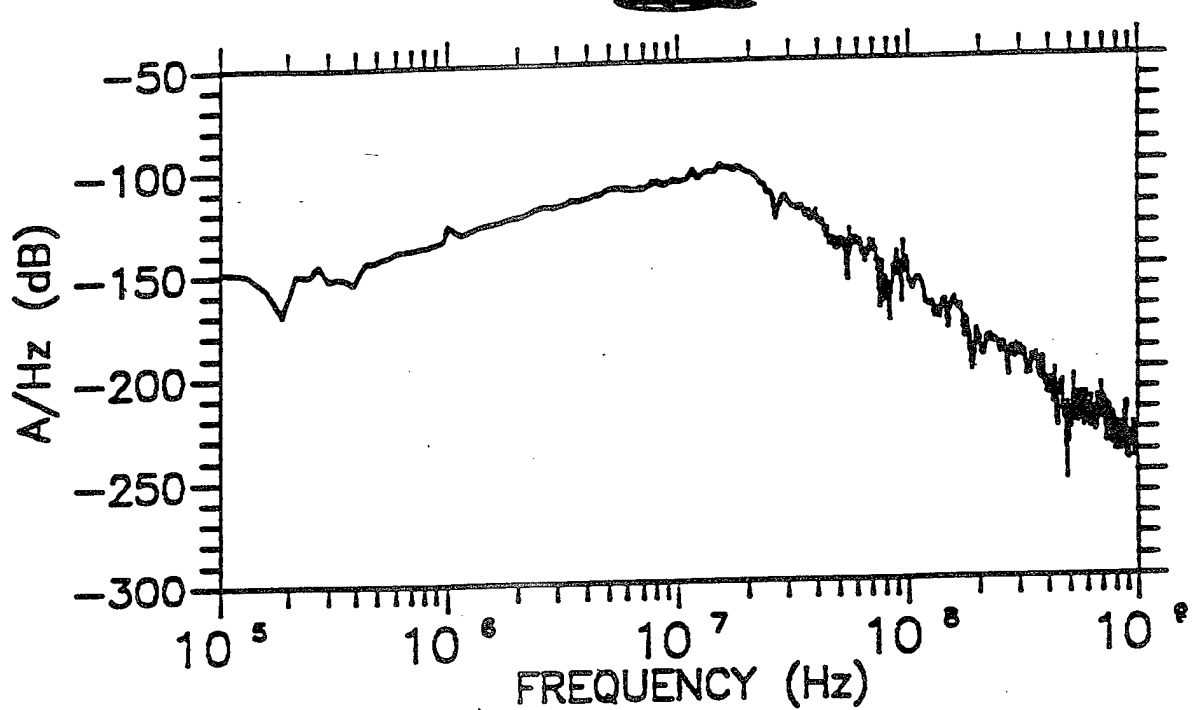
C-29







C-32



THIS PAGE INTENTIONALLY LEFT BLANK

APPENDIX D

**SIGNAL TO NOISE PLOTS FOR THE
CW ILLUMINATION MEASUREMENTS OF THE [REDACTED] ANTENNAS**

The upper trace shows the signal; the lower trace shows the corresponding ambient noise.
The difference is the signal-to-noise ratio in dB.

Signal to Noise Report

4: 44 PM TUE.. 16 JUNE. 1992

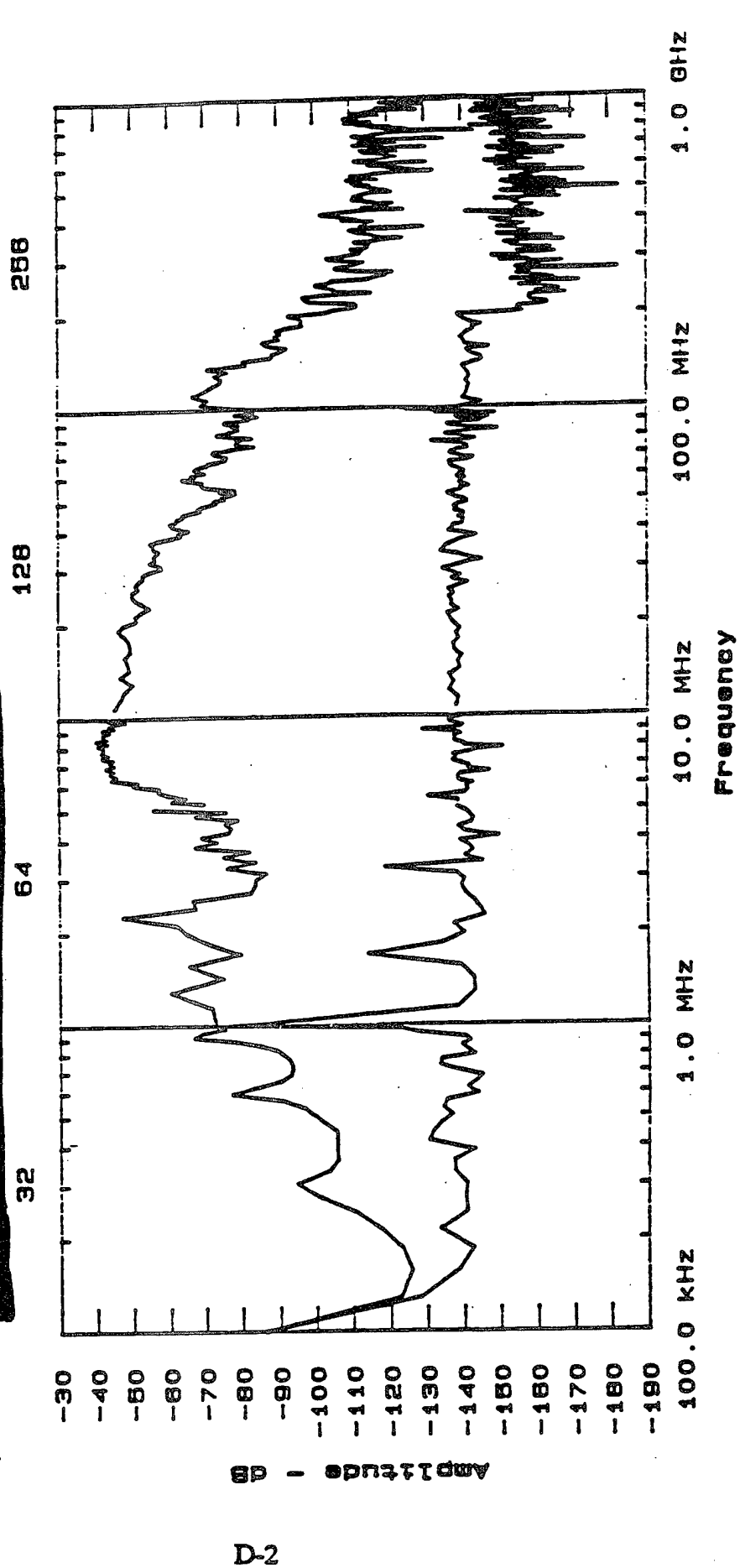
Test Point	HO11	Inst Link
Test Type	Wide Area	Noise Set
Facility	THE HOUSE	Sig Atten
Test Time	08-16-92 16: 29	Bandwidth
Sig Probe	IC39	Source Amp 1

Freq: Min 100.00 kHz Max 1000.0 MHz

Amp 1: Min -182.51 dB Max -40.48 dB

Source Amp 1 0.0 dB 10 Hz -12.0 dB

Description [REDACTED]



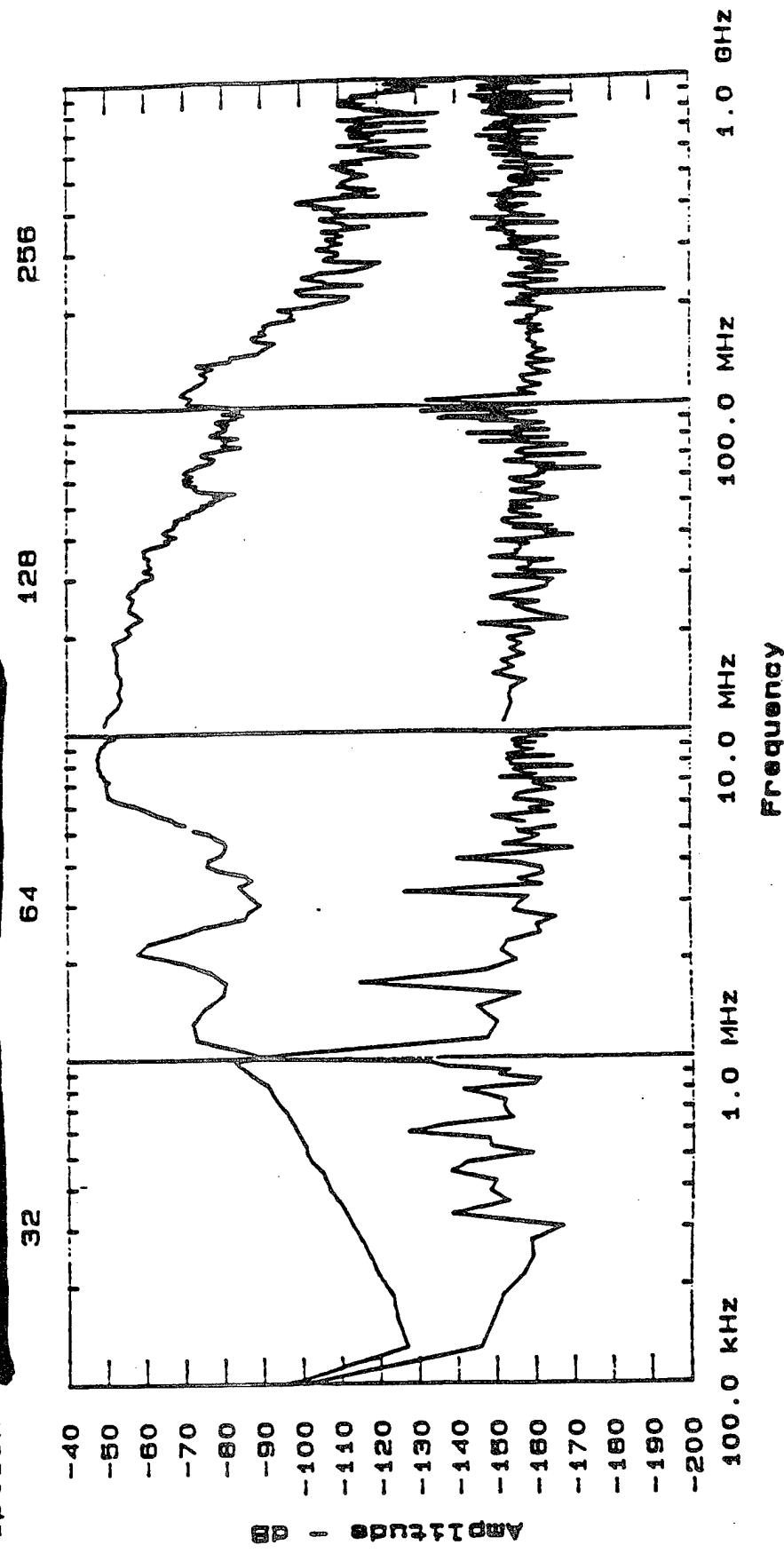
Signal to Noise Report

4: 46 PM TUE.. 16 JUNE. 1992

Test Point	HO12	Freq:	Min	100.00 kHz	Inst Link
Test Type	Wide Area	Max	1000.0 MHz	Noise Set	
Facility	THE HOUSE	Amp1:	Min	-193.66 dB	Sig Atten
Test Time	06-16-92 16: 30	Max	Max	-47.73 dB	BandWidth
Sig Probe	IC39				Source Amp1

Description [REDACTED]

D-3

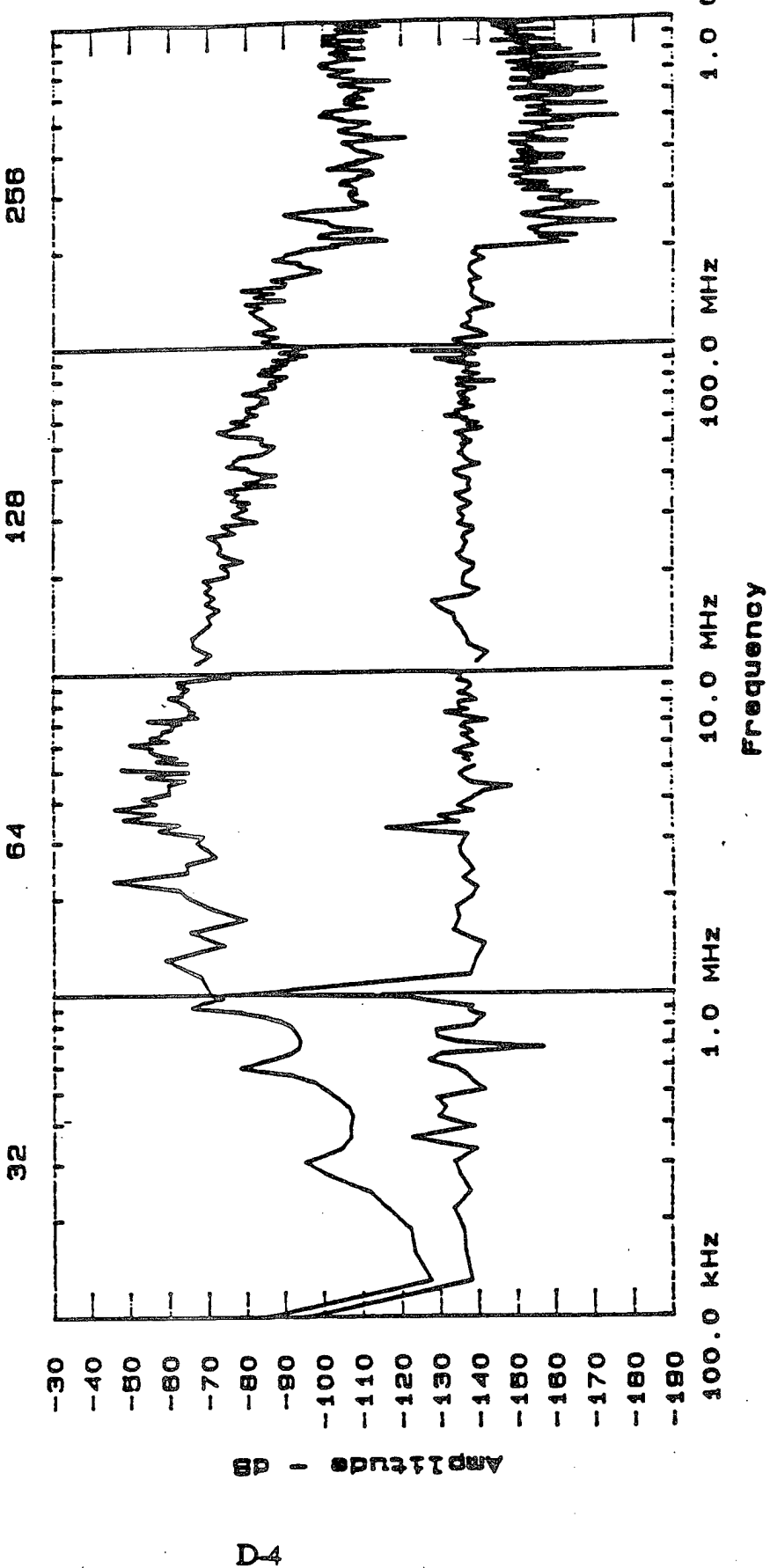


Signal to Noise Report

4:49 PM TUE.. 16 JUNE. 1992

Test Point	HO21	Freq:	Min 100.00 kHz	Inst Link	A
Test Type	Wide Area	Max	1000.0 MHz	Noise Set	HO21
Facility	THE HOUSE	Min	-175.73 dB	Sig Atten	0.0 dB
Test Time	06-16-92 16:31	Max	-45.94 dB	Bandwidth	40 Hz
Sig Probe	IC39			Source Amp1	-12.0 dB

Description [REDACTED]



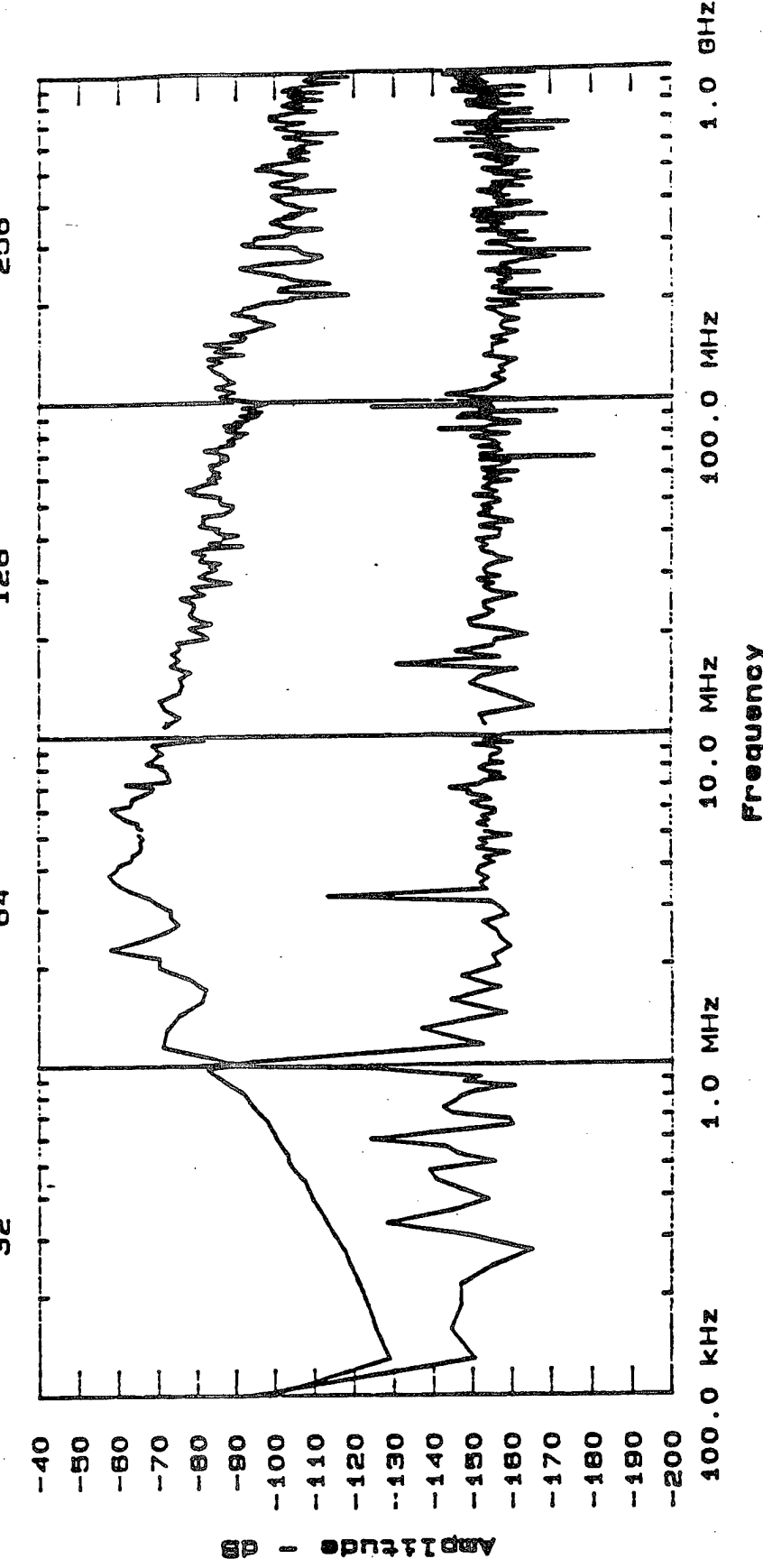
Signal to Noise Report

4: 52 PM TUE.. 16 JUNE. 1992

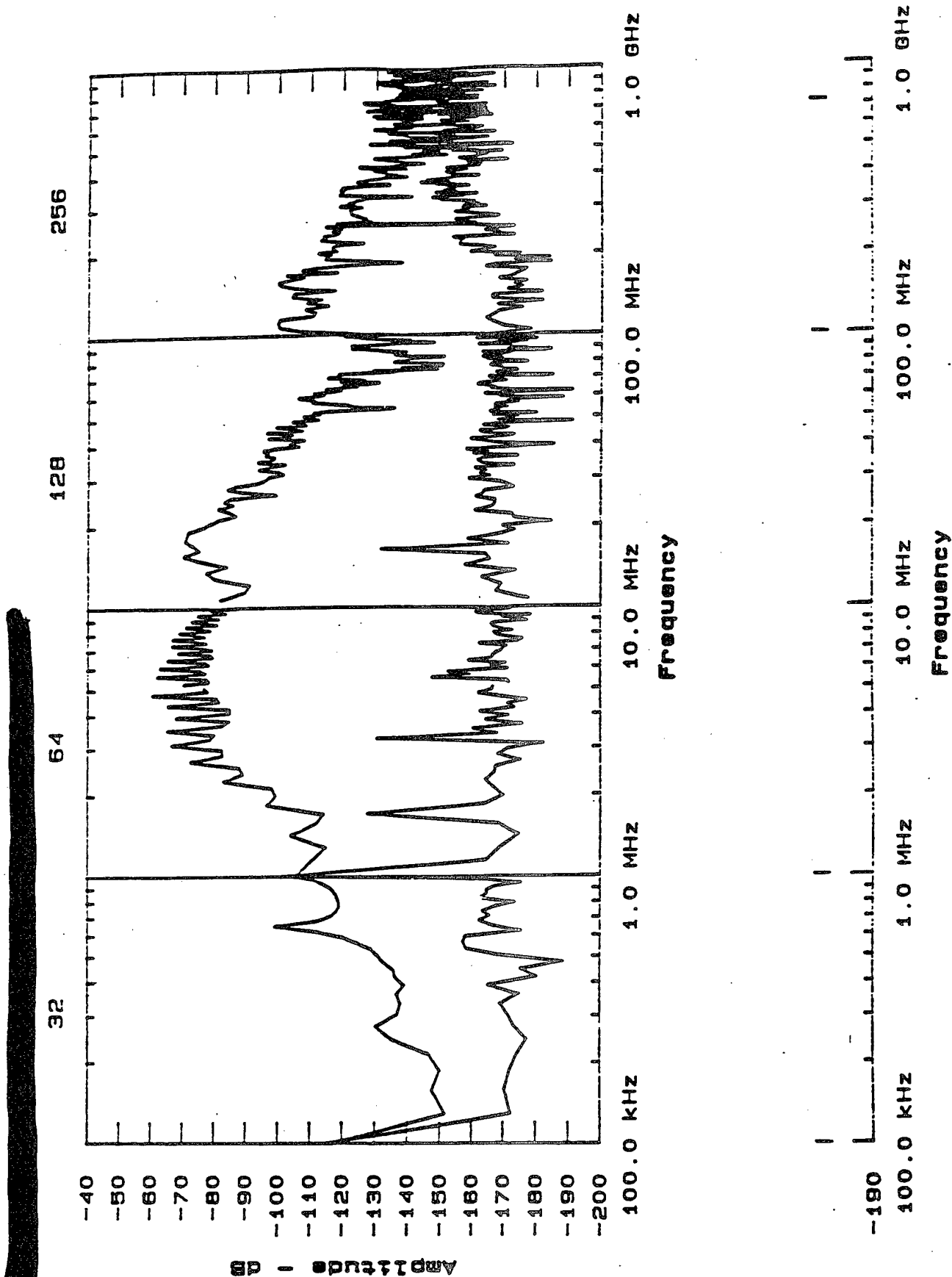
Test Point HO22
Test Type Wide Area
Facility THE HOUSE
Test Time 06-16-92 16: 32
Sig Probe IC39

Freq: Min 100.00 kHz Max 1000.0 MHz
Ampl: Min -182.66 dB Max -57.90 dB
Inst Link Noise Set 0.0 dB
S1g Atten 10 Hz
Bandwidth 10 Hz
Source Amp1 -12.0 dBm

Description D-5



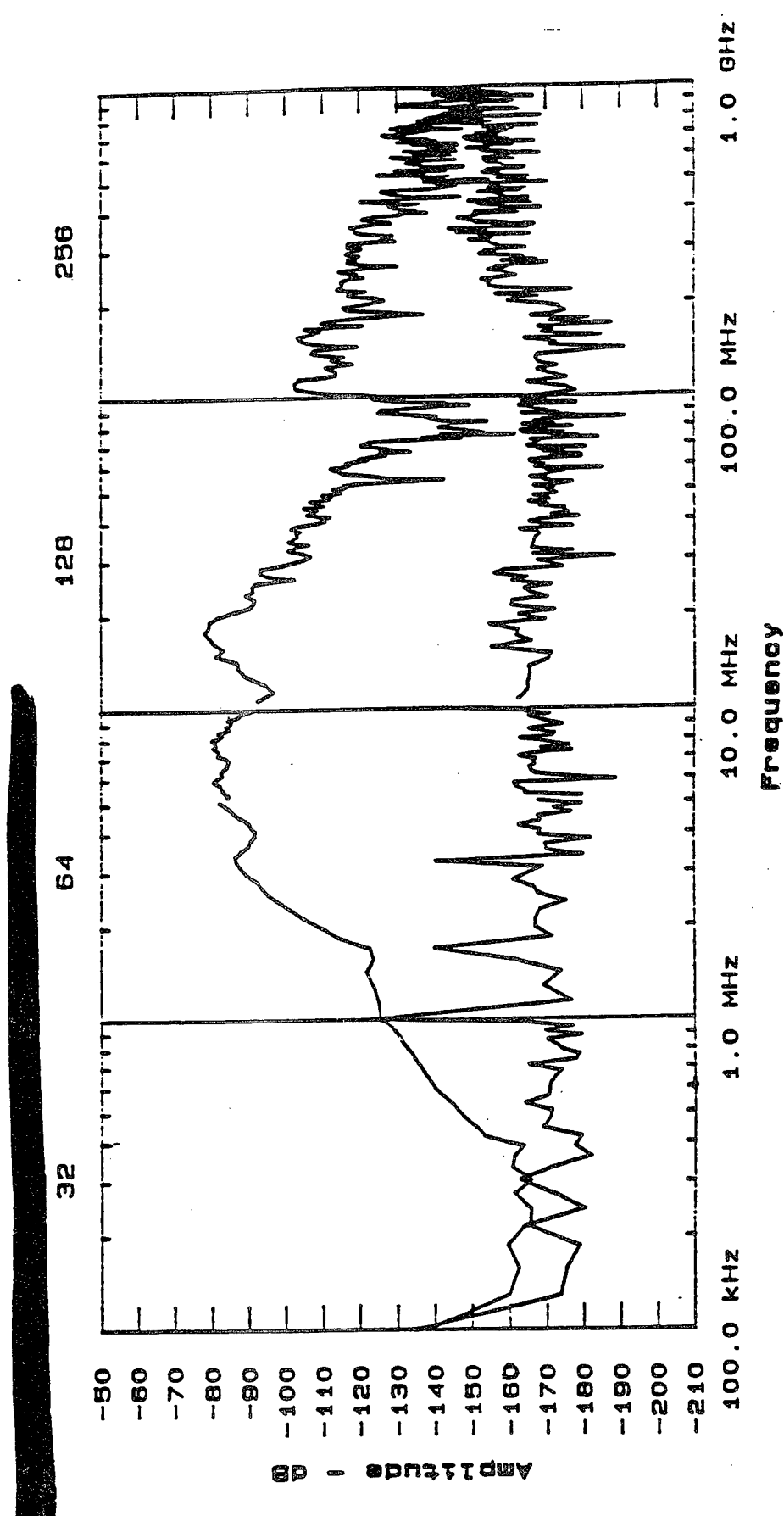
SOURCE AMP1 -12.0 dBm



Signal to Noise Report

12: 40 PM MON.. 8 JUNE. 1992

Test Point	v072	Freq:	Min 100.00 kHz	Inst Link
Test Type	Wide Area	Max 1000.0 MHz	Noise Set	
Facility	THE HOUSE	Amp1: Min -191.26 dB	Sig Atten 0.0 dB	
Test Time	06-08-92 12: 37	Max -78.17 dB	Bandwidth 10 Hz	
SIG Probe	IC39		Source Amp1 -12.0 dB	

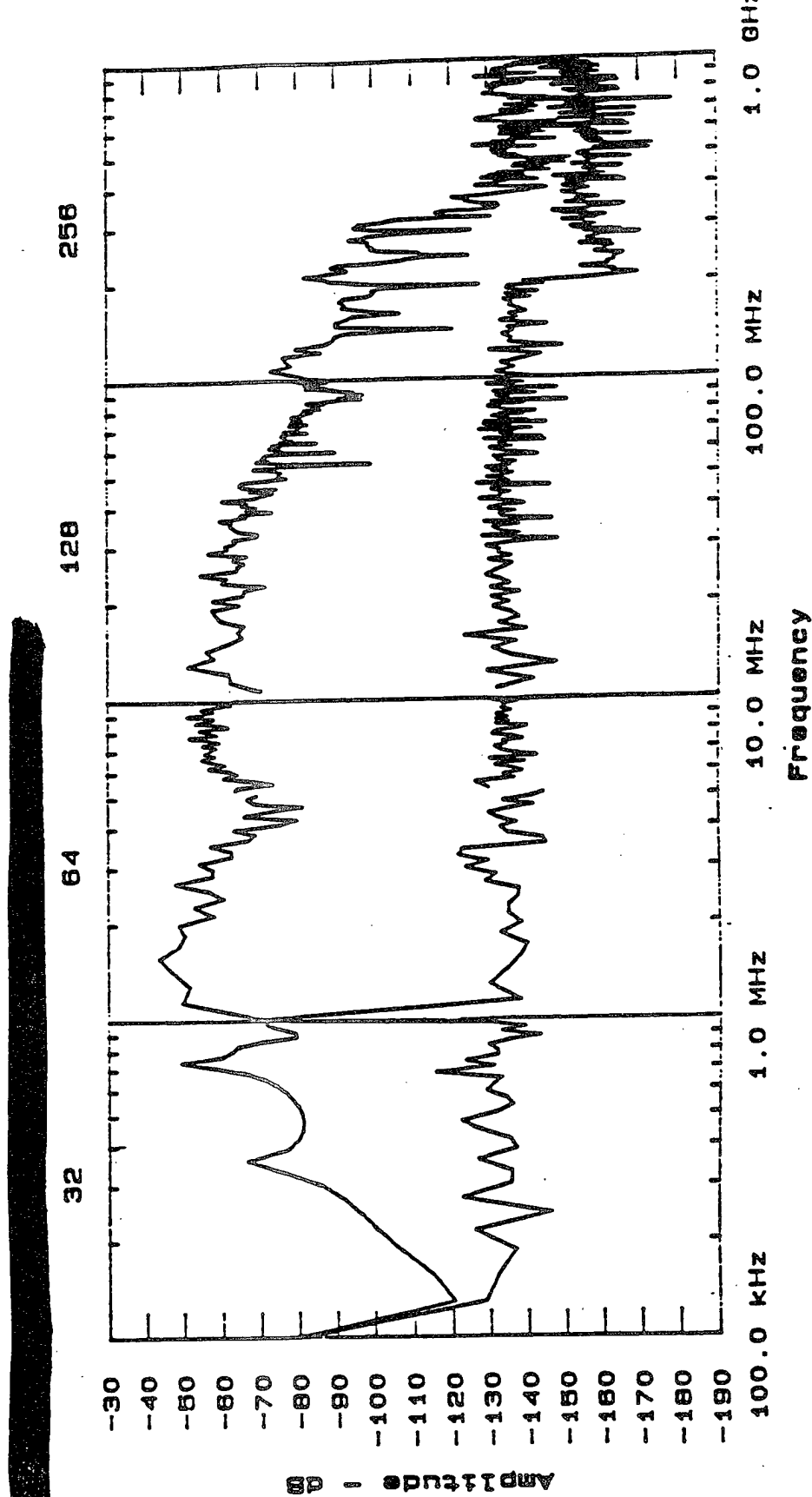


D-7

Signal to Noise Report

4: 27 PM TUE.. 16 JUNE. 1992

Test Point	HOB1	Freq:	Min 100.00 kHz	Inst Link	A
Test Type	Wide Area	Max	1000.0 MHz	Noise Set	HOB1
Facility	THE HOUSE	Amp1:	Min -178.54 dB	SIG Atten	0.0 dB
Test Time	06-16-92 16: 07	Max	-43.52 dB	Bandwidth	10 Hz
SIG Probe	IC39			Source Amp1	-12.0 dBm

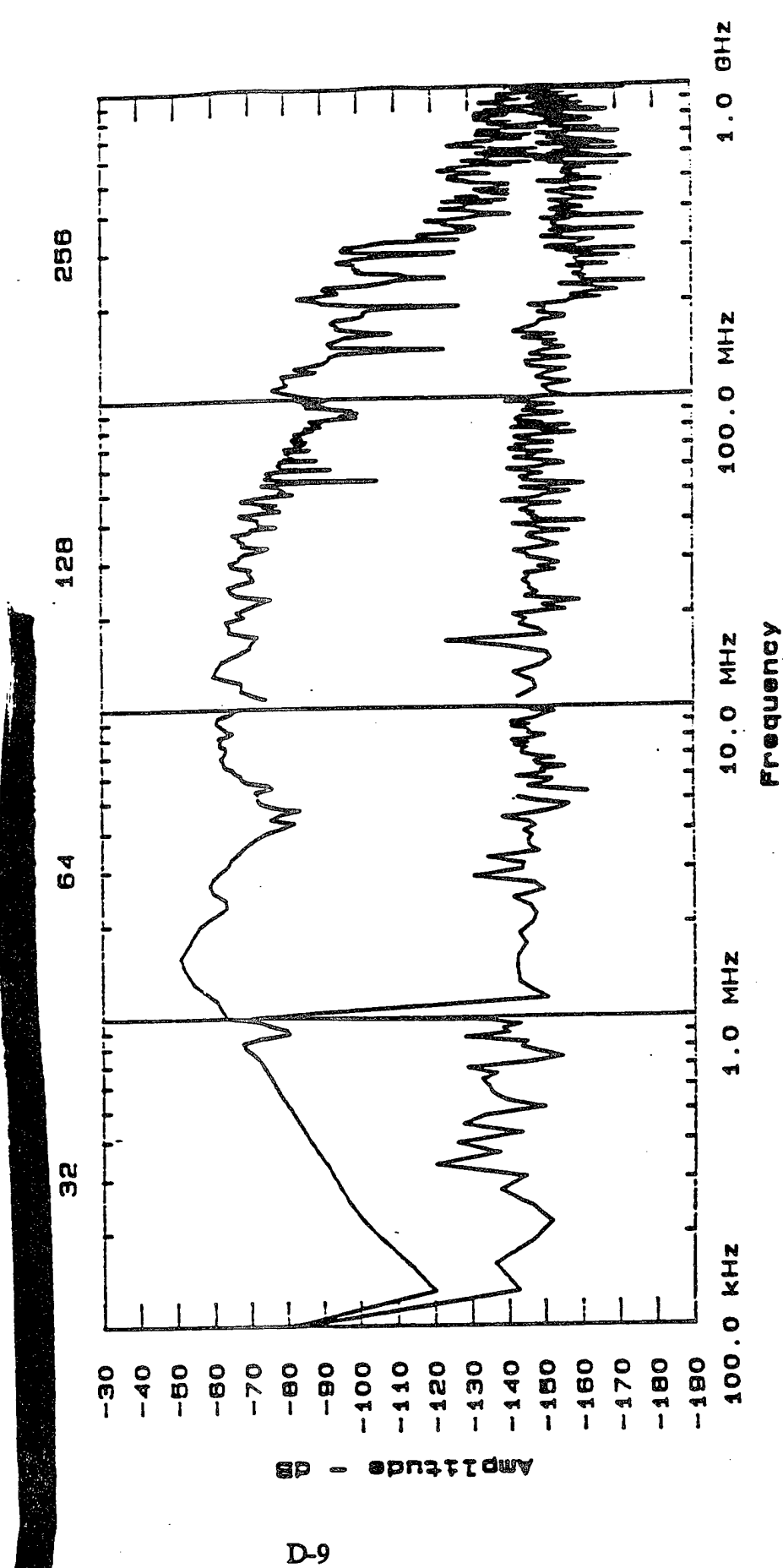


D-8

Signal to Noise Report

4: 30 PM TUE.. 16 JUNE. 1992

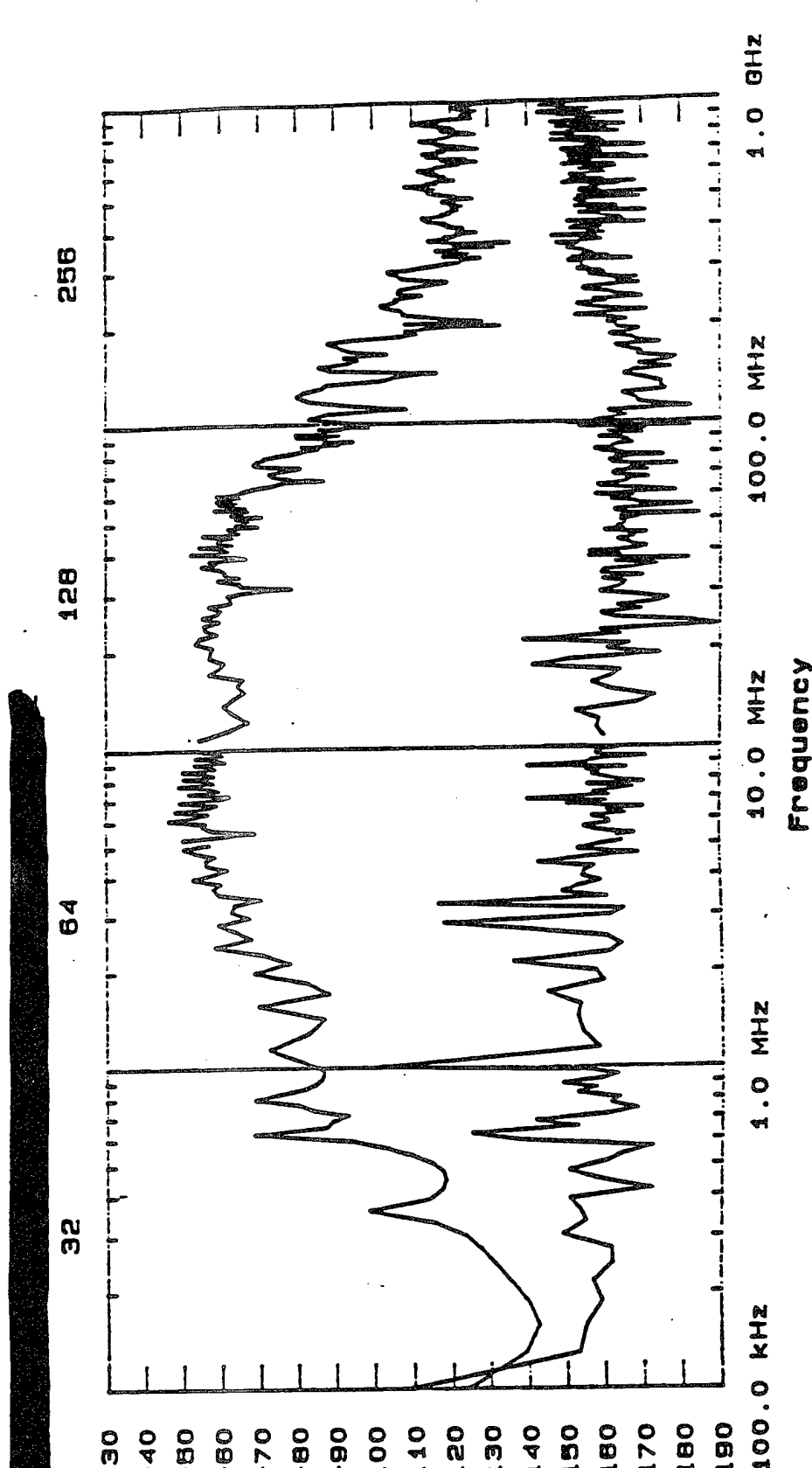
Test Point	HO82	Freq:	Min 100.00 kHz	Inst Link
Test Type	Wide Area	Max	1000.0 MHz	Noise Set
Facility	THE HOUSE	Amp1:	Min -177.49 dB	Sig Atten 0.0 dB
Test Time	06-16-92 16: 08	Max	-81.14 dB	BandWidth 10 Hz
SIG Probe	IC39			Source Amp1 -42.0 dB



Signal to Noise Report

4: 33 PM TUE.. 18 JUNE. 1992

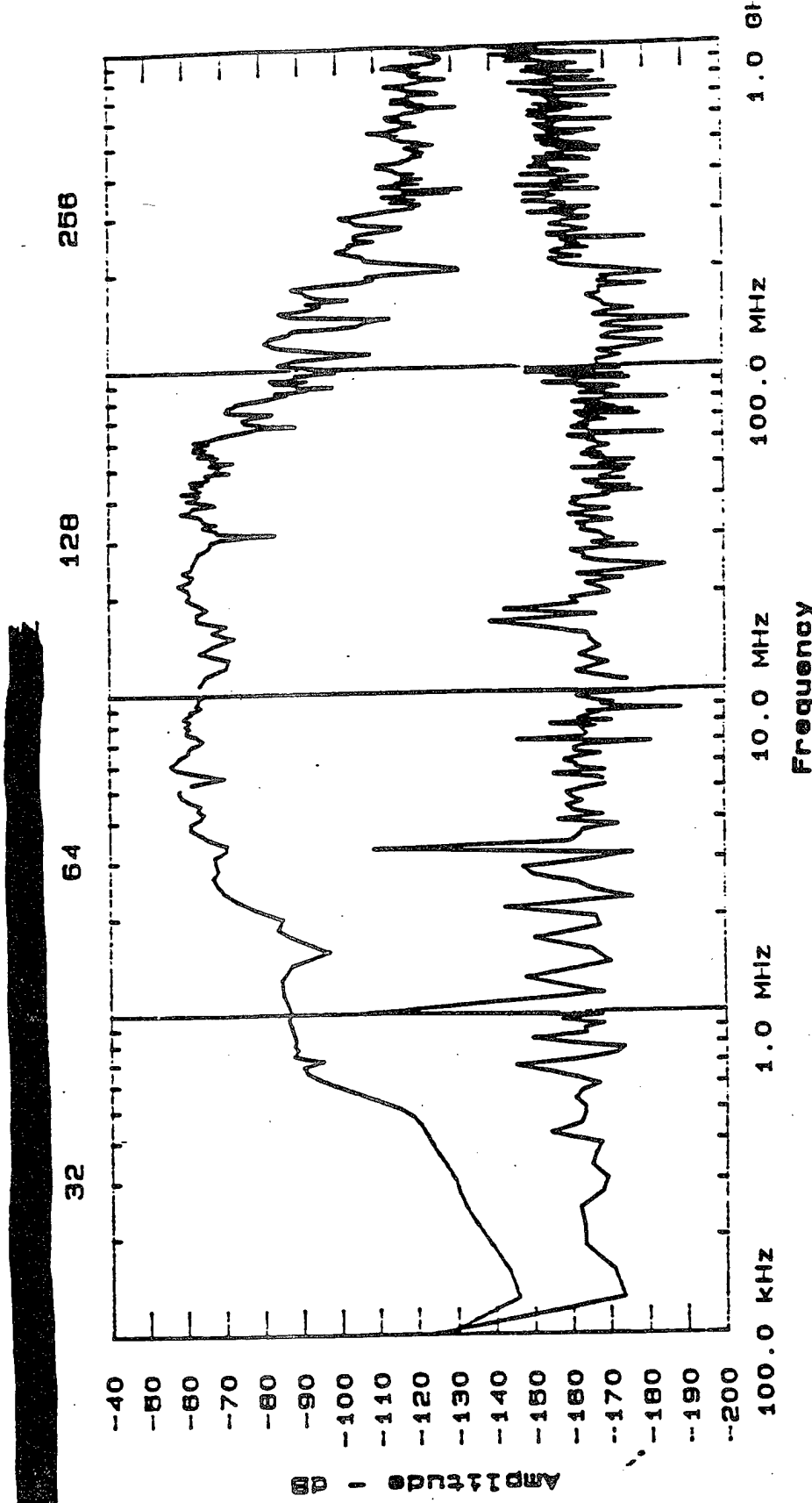
Test Point	H081	Inst Link
Test Type	Wide Area	Noise Set
Facility	THE HOUSE	Sig Atten
Test Time	08-18-92 16: 19	Bandwidth
Sig Probe	IC39	Source Amp 1



Signal to Noise Report

4: 35 PM TUE.. 16 JUNE. 1992

Test Point H062 Freq: Min 100.00 kHz
Test Type Wide Area Max 1000.0 MHz
Facility THE HOUSE Amp1: Min -191.72 dB
Test Time 08-16-92 16: 20 Max -56.47 dB
SIG Probe IC39 Source Amp1 -12.0 dB



D-11

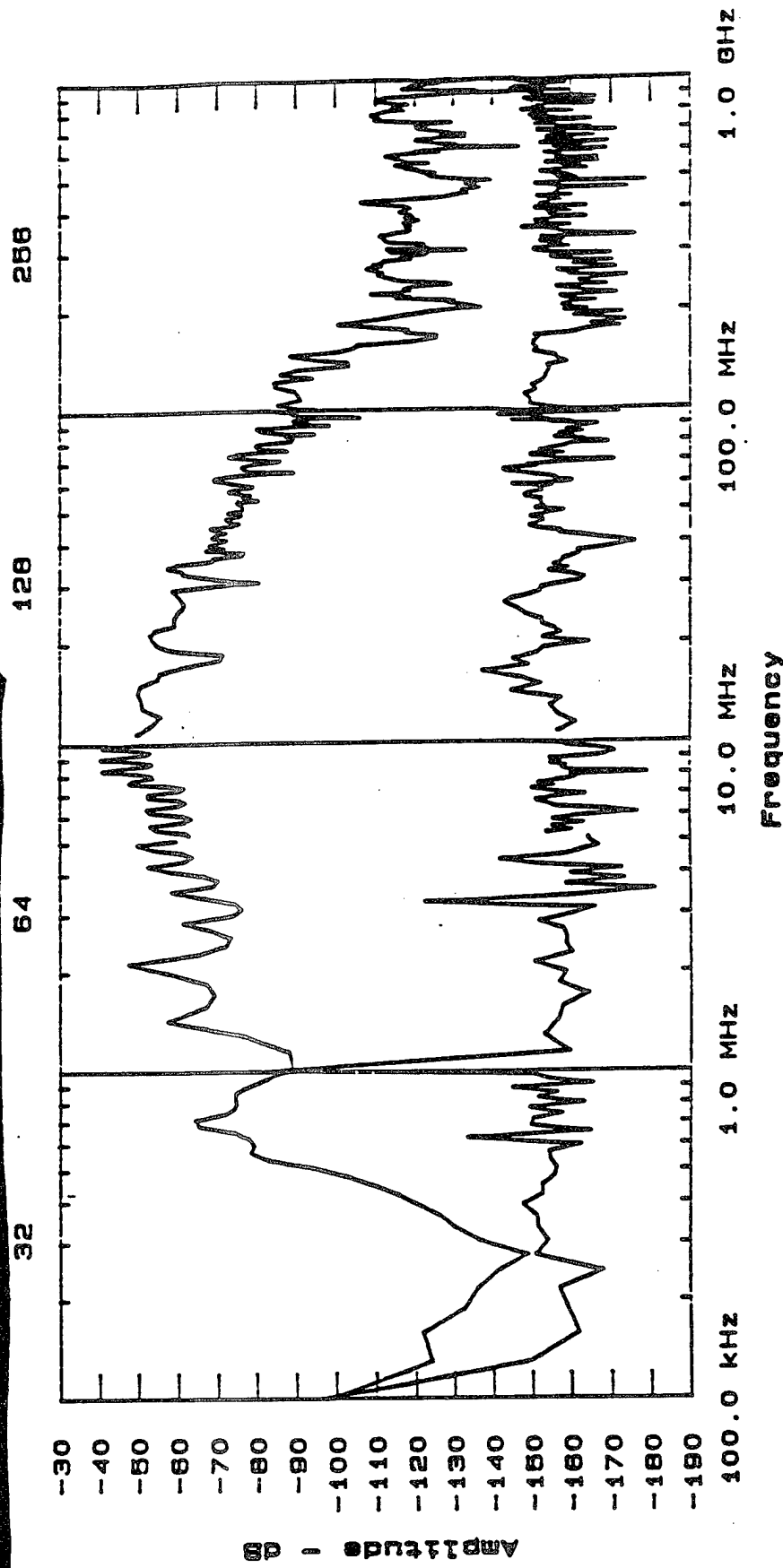
Signal to Noise Report

1:02 PM TUE.. 16 JUNE. 1992

Test Point H034A
Test Type Wide Area
Facility THE HOUSE
Test Time 06-16-92 13: 00
Sig Probe IC39

Freq: Min 100.00 kHz
Max 1000.0 MHz
Amp 1: Min -181.00 dB
Max -40.44 dB
Inst Link Noise Set
S1g Atten 0.0 dB
Bandwidth 10 Hz
Source Amp 1 -12.0 dBm

[REDACTED]

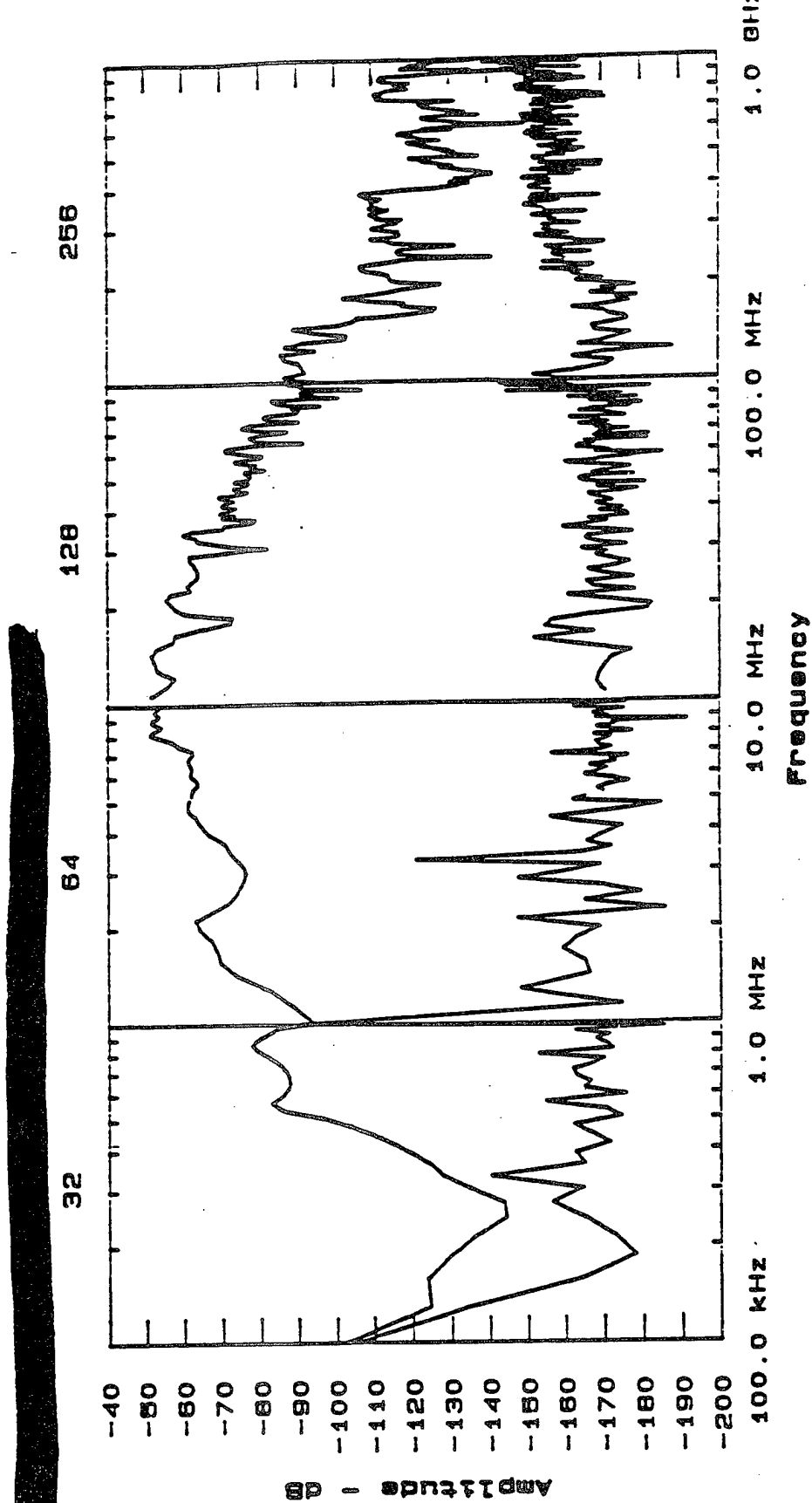


D-12

Signal to Noise Report

1: 04 PM TUE.. 16 JUNE. 1992

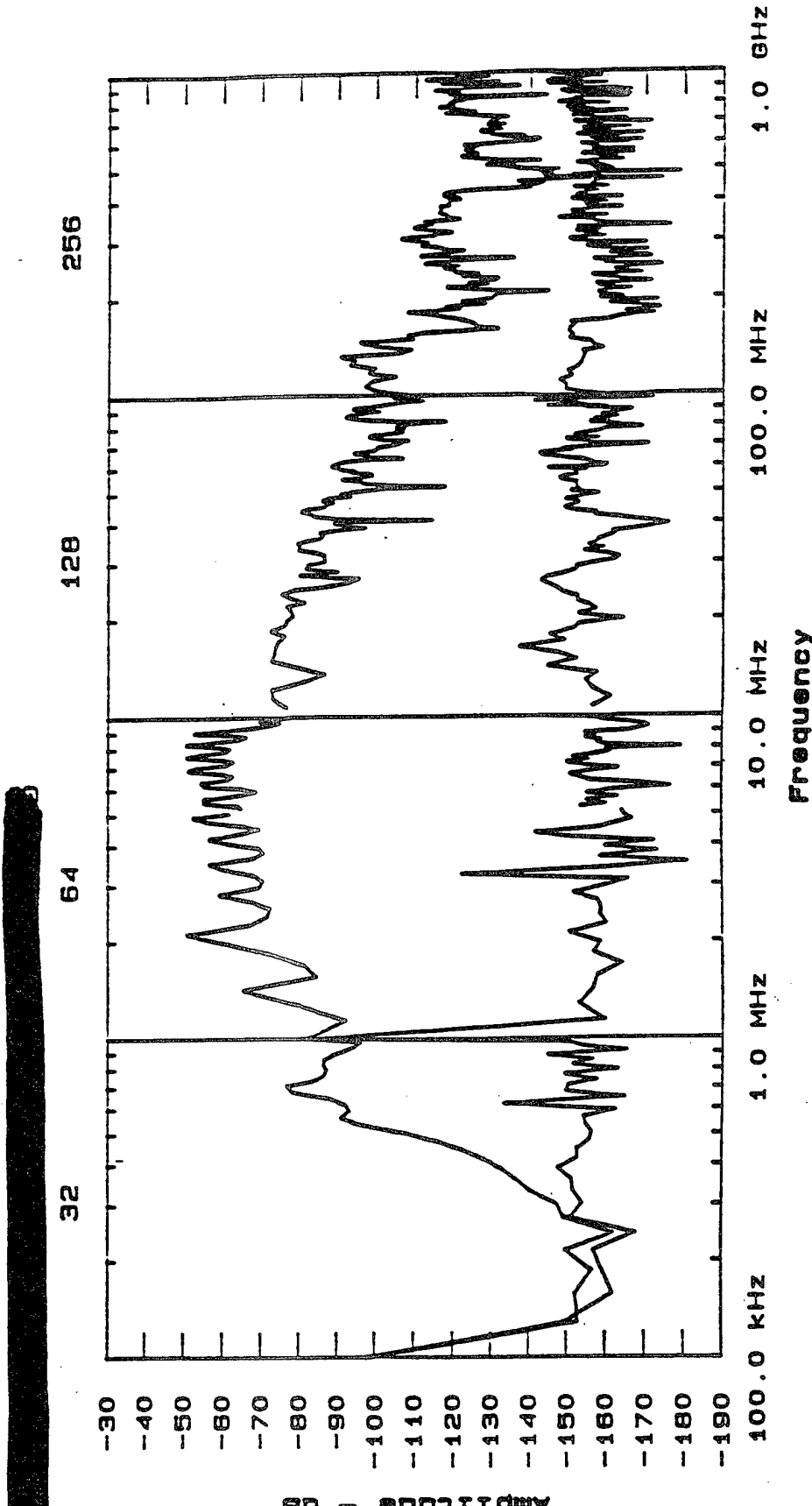
Test Point H032A Freq: Min 100.00 kHz Inst Link
Test Type Wide Area Max 1000.0 MHz Noise Set
Facility THE HOUSE Amp1: Min -191.73 dB 0.0 dB
Test Time 06-16-92 13: 01 Max -51.70 dB 10 Hz
SIG Probe IC39 Source Amp1 -12.0 dB



Signal to Noise Report

3: 21 PM THU.. 4 JUNE. 1992

Test Point	VO34	Freq:	Min	100.00 kHz	Inst Link	A
Test Type	Wide Area	Max	Max	4000.0 MHz	Noise Set	VO34
Facility	THE HOUSE	Amp1:	Min	-181.00 dB	Sig Atten	0.0 dB
Test Time	06-04-92 15: 20	Max	Max	-50.76 dB	Bandwidth	1.0 Hz
Sig Probe	IC39				Source Amp1	-12.0 dBm

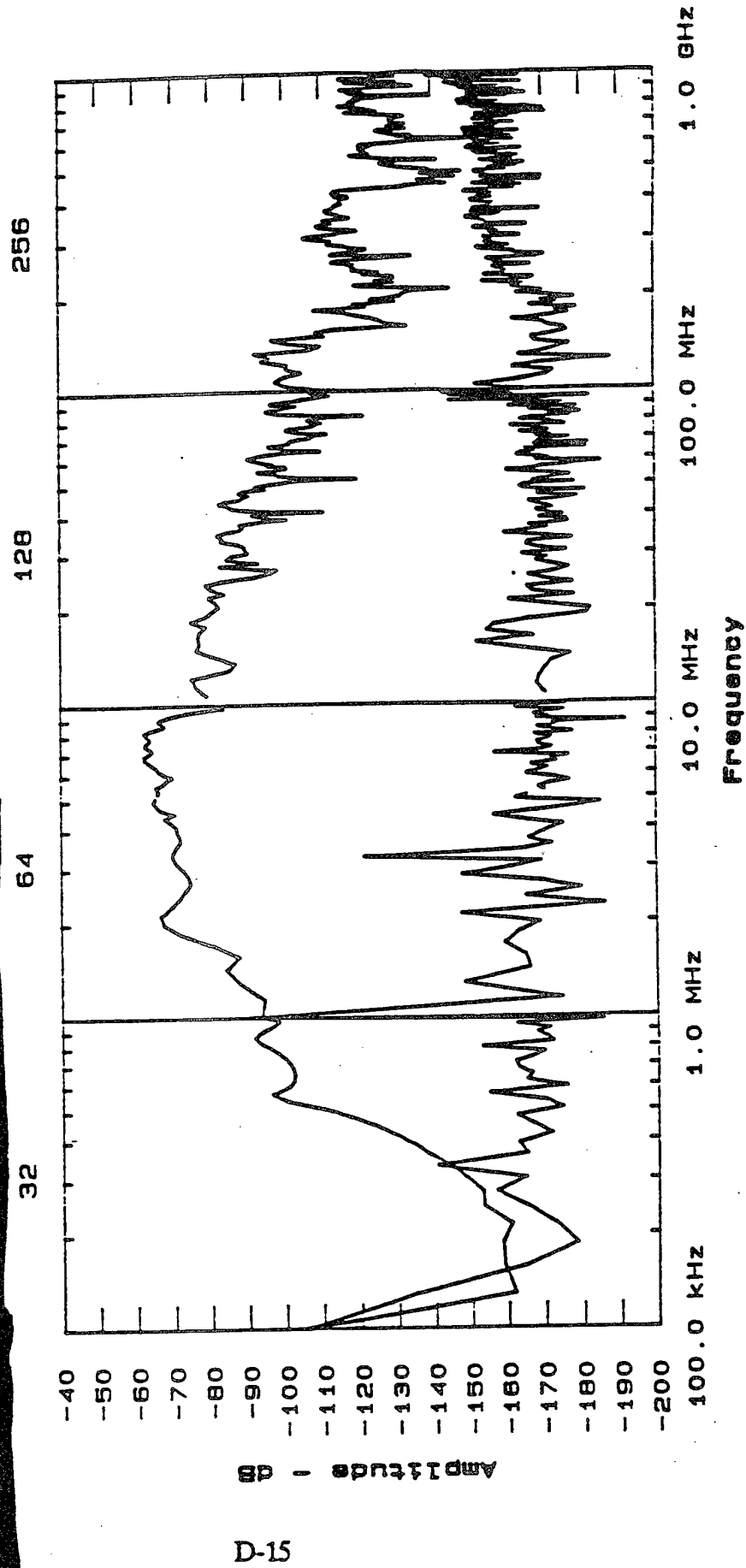


Sri Lanka to Nissei Report

3:24 PM THU.: 4 JUNE, 1992

Test Point	VO32
Test Type	Wide Area
Facility	THE HOUSE
Test Time	06-04-92 15: 21
S18 Probe	IC39

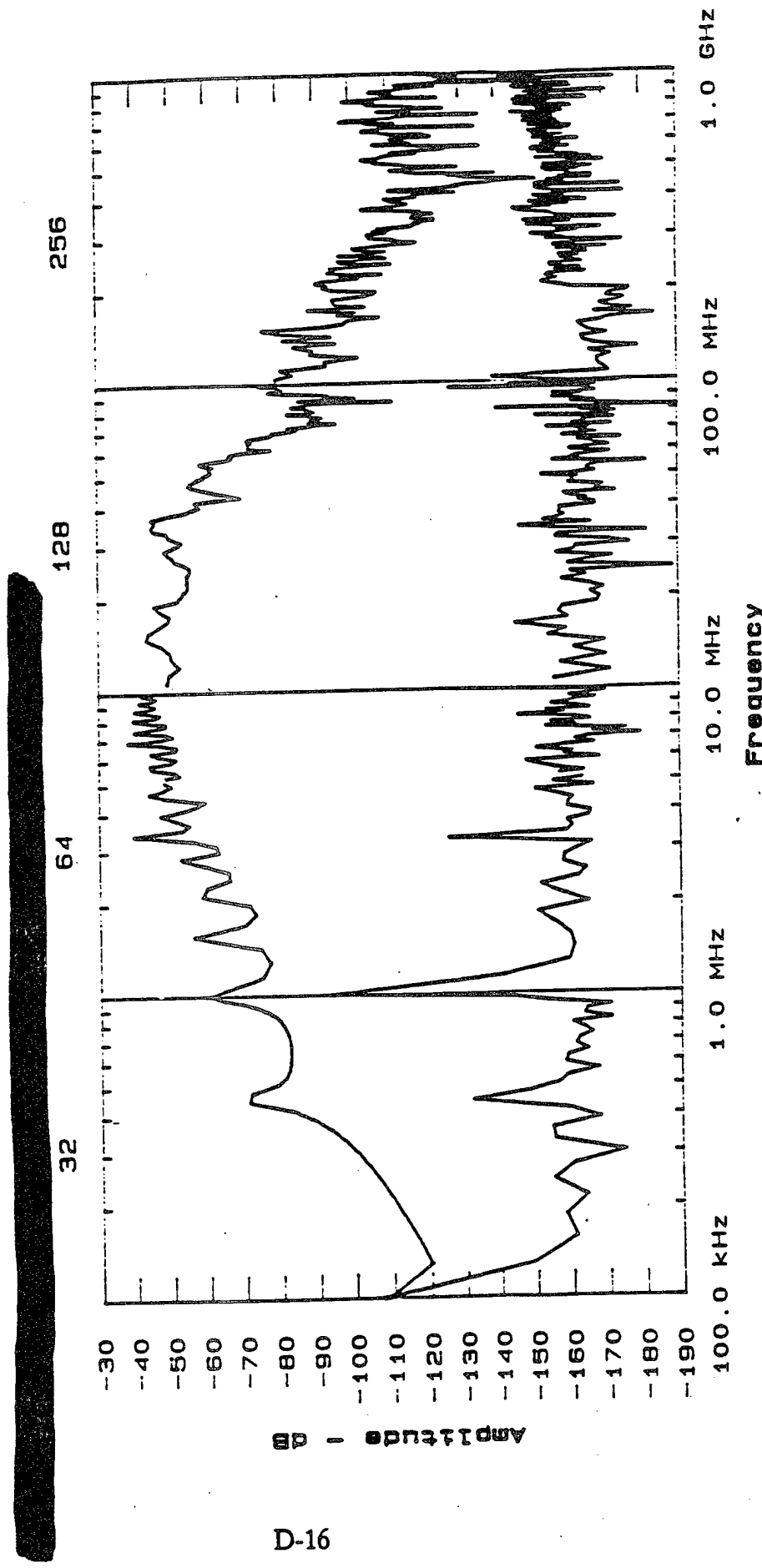
	A	v032	dB
Inst Link			
Noise Set		0.0	
Sig Atten		10 Hz	
Bandwidth			
Source Amp 1		-12.0	dBm



Signal to Noise Report

4: 11 PM TUE .. 9 JUNE. 1992

Test Point	HO44	Freq:	Min	100.00 kHz
Test Type	Wide Area	Max	1000.0 MHz	
Facility	THE HOUSE	Amp1:	Min -191.32 dB	
Test Time	06-09-92 16: 09	Max	-38.28 dB	
Sig Probe	IC39			
				Source Amp1 -12.0 dBm



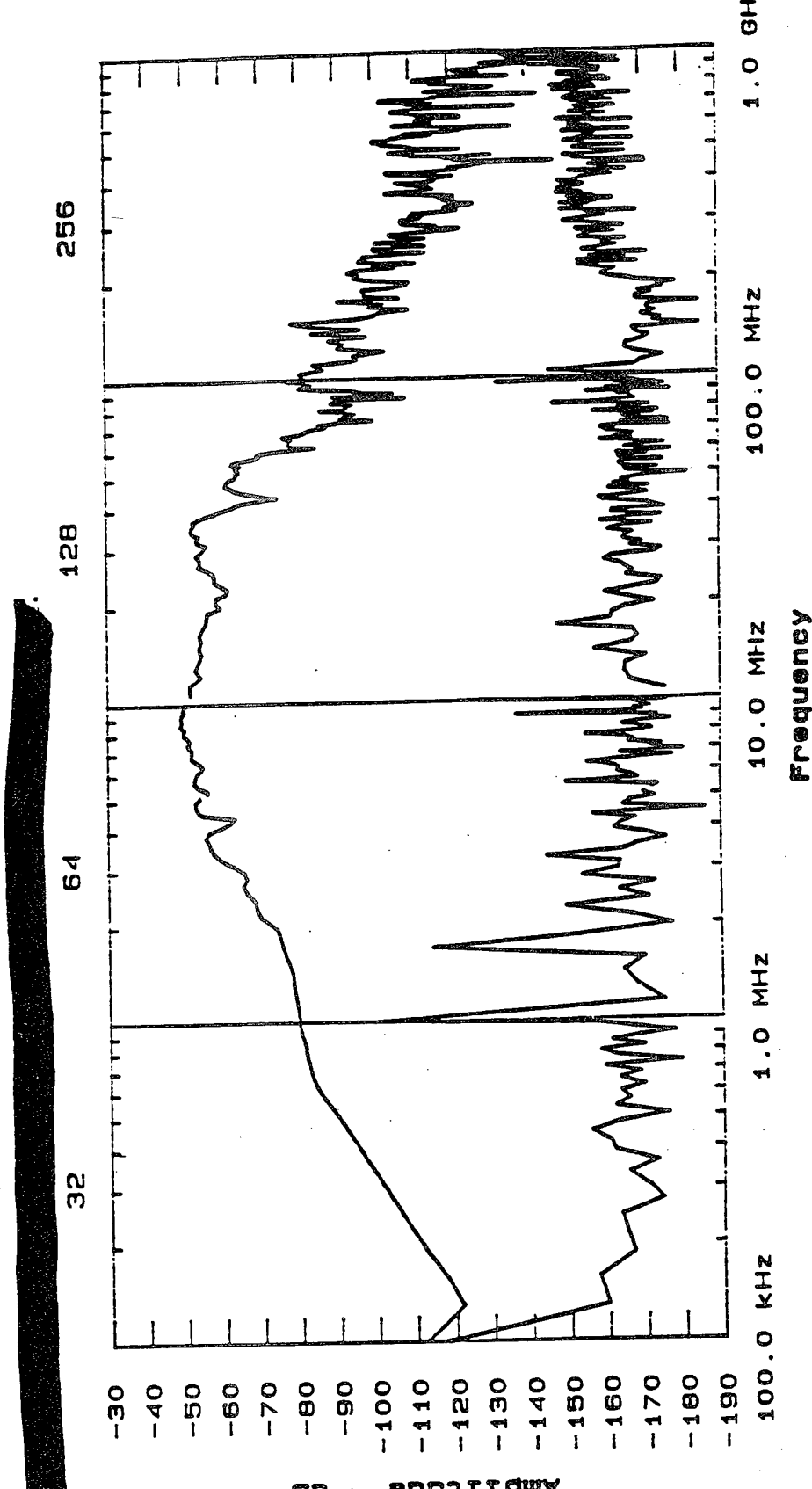
D-16

Signal to Noise Report

4: 14 PM TUE.. 9 JUNE. 1992

Test Point H042
Test Type Wide Area
Facility THE HOUSE
Test Time 06-09-92 16: 10
Sig Probe IC39

A
Inst Link V042
Noise Set 0.0 dB
Sig Atten 10 Hz
Bandwidth 10.0 dB
Source Amp 1 -12.0 dB



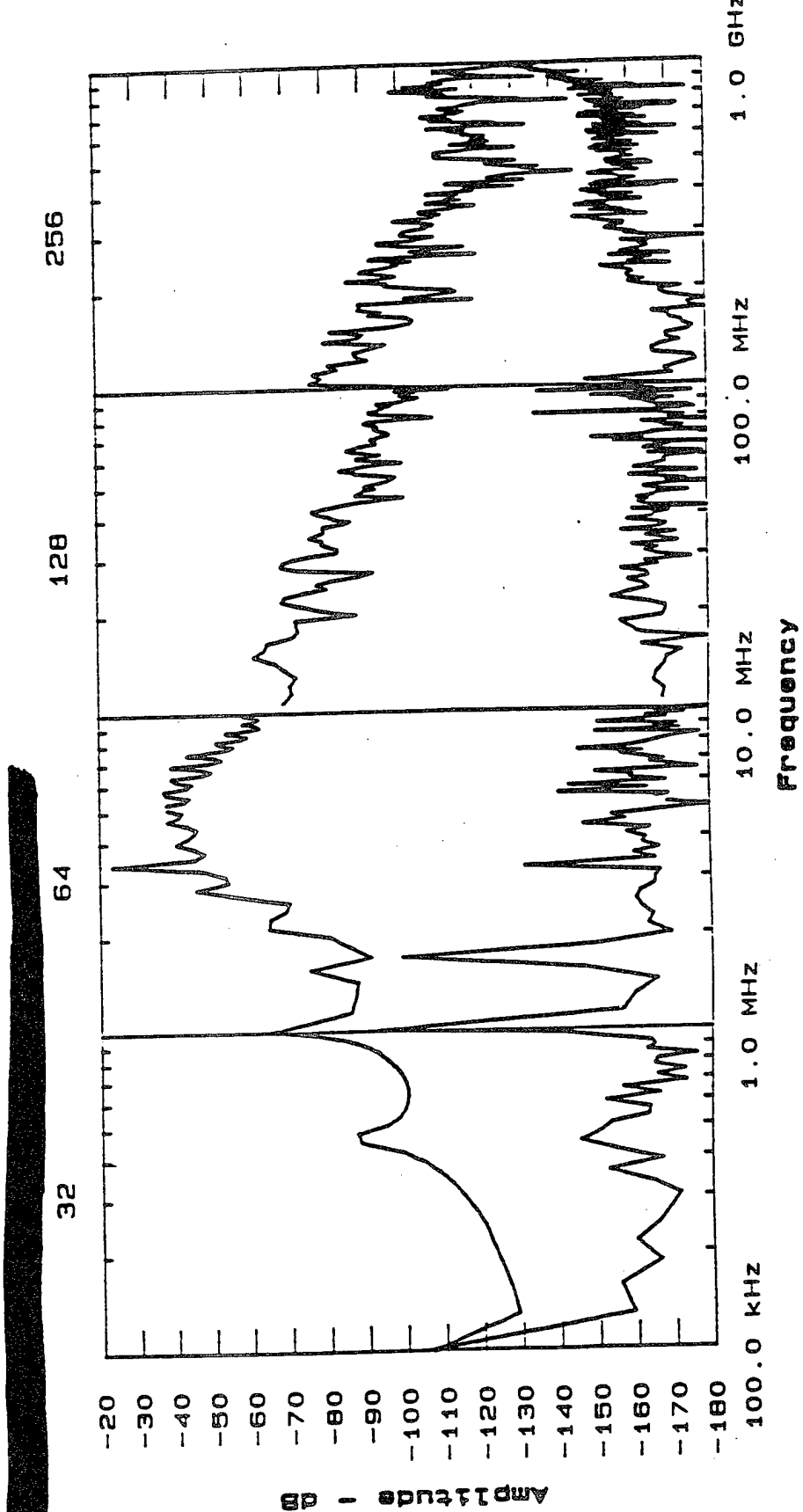
D-17

Signal to Noise Report

12: 12 PM THU., 4 JUNE. 1992

Test Point V041
 Test Type Wide Area
 Facility THE HOUSE
 Test Time 06-04-92 12: 10
 Sig Probe IC39

V041	Freq:	Min	100.00 kHz	Inst Link	A
Wide Area		Max	1000.0 MHz	Noise Set	V041
THE HOUSE	Ampl:	Min	-184.52 dB	Sig Atten	0.0 dB
06-04-92 12: 10		Max	-23.48 dB	Bandwidth	10 Hz
IC39				Source Amp1	-12.0 dBm

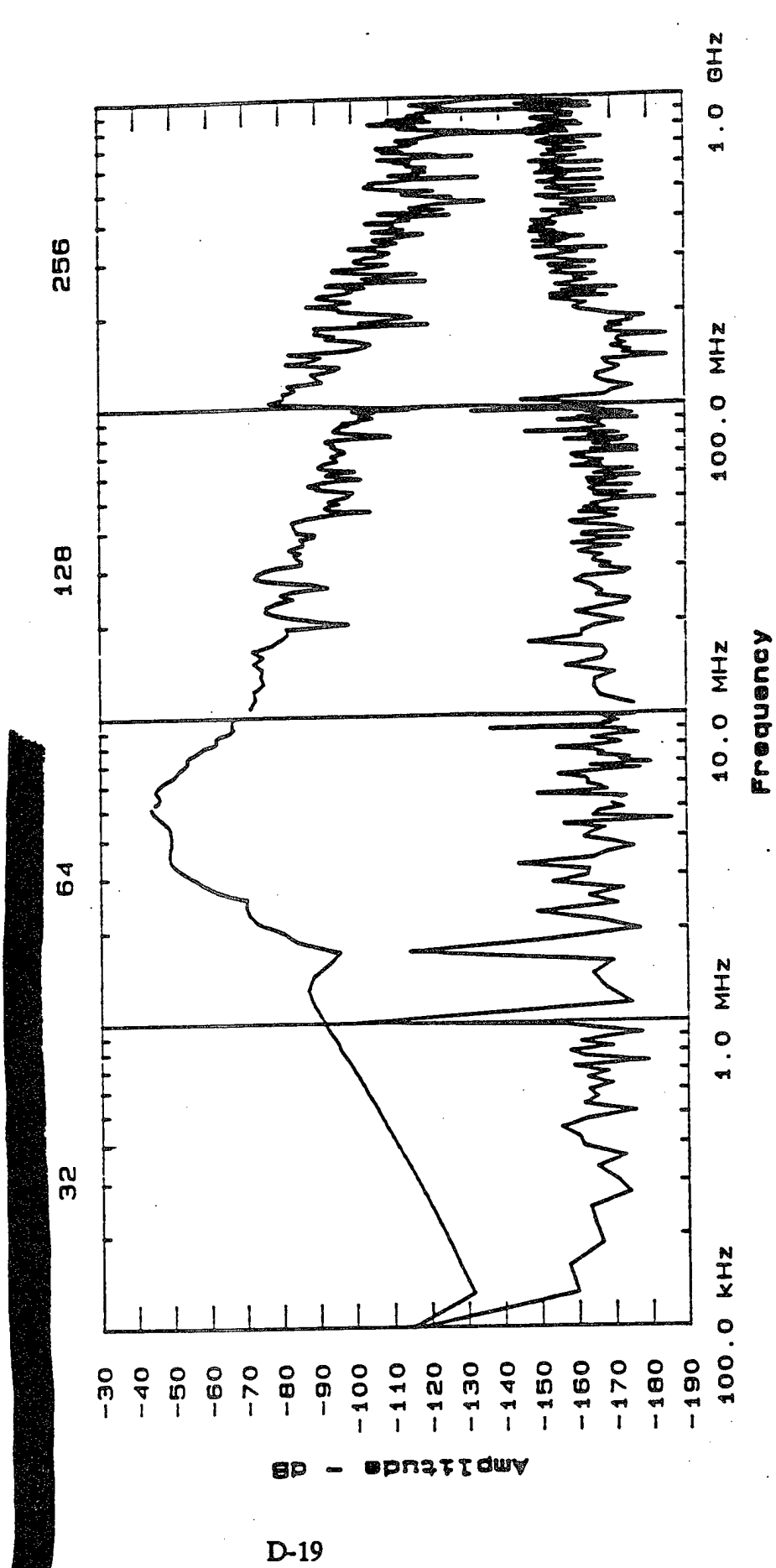


D-18

Signal to Noise Report

12: 15 PM THU.. 4 JUNE. 1992

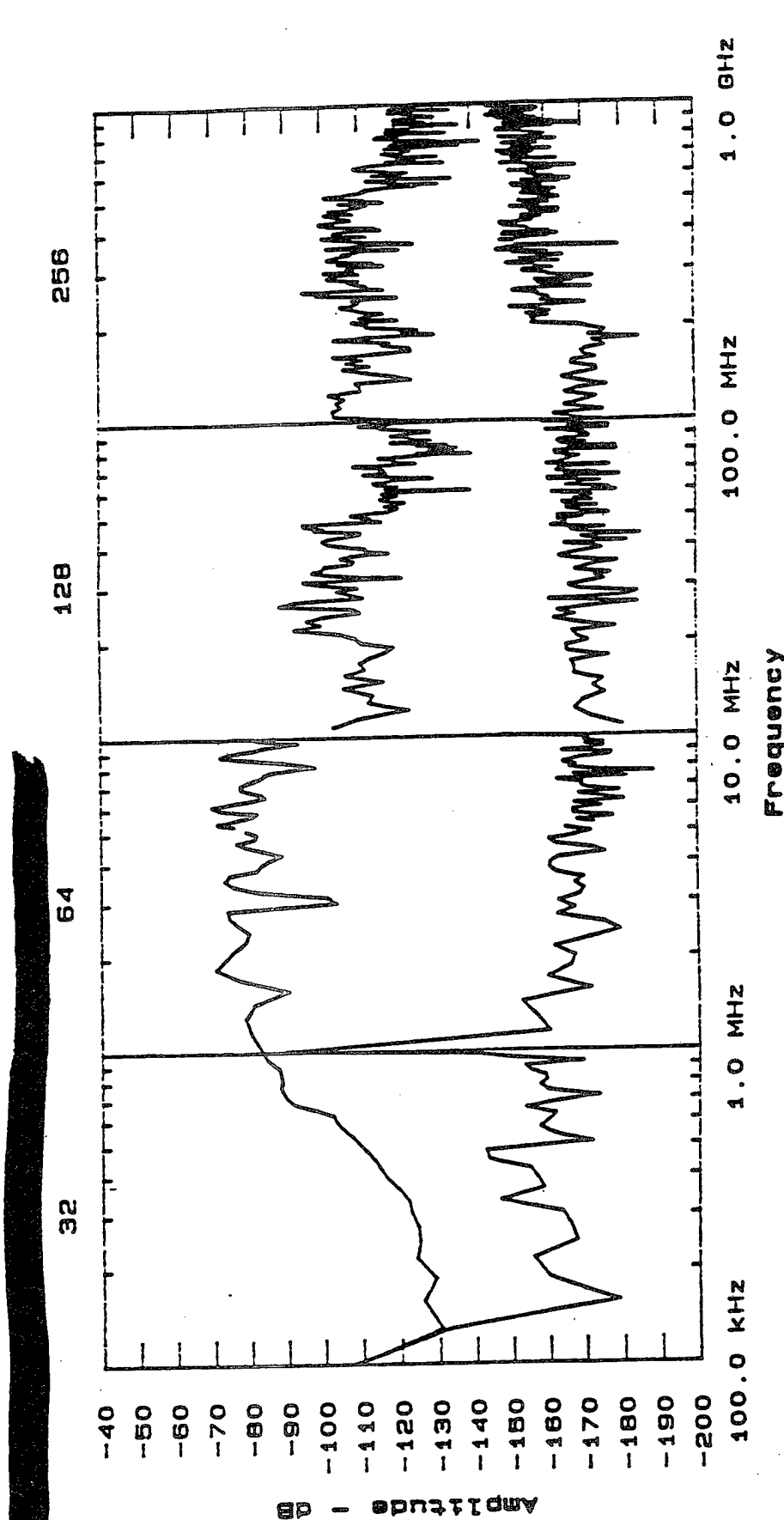
Test Point	VO42	Wide Area	Inst Link
Test Type			Noise Set
Facility	THE HOUSE	SIG Atten	0.0 dB
Test Time	06-04-92 12: 14	Bandwidth	10 Hz
SIG Probe	IC39	Source Amp1	-12.0 dB



Signal to Noise Report

4: 04 PM WED.. 3 JUNE. 1992

Test Point VO81B Freq: Min 100.00 kHz Inst Link
Test Type Wide Area Max 1000.0 MHz Noise Set 0.0 dB
Facility THE HOUSE Amp1: Min -188.62 dB Sig Atten 10 Hz
Test Time 08-03-92 16:03 Bandwidth 10 Hz
Sig Probe IC39 Source Amp1 -12.0 dBm

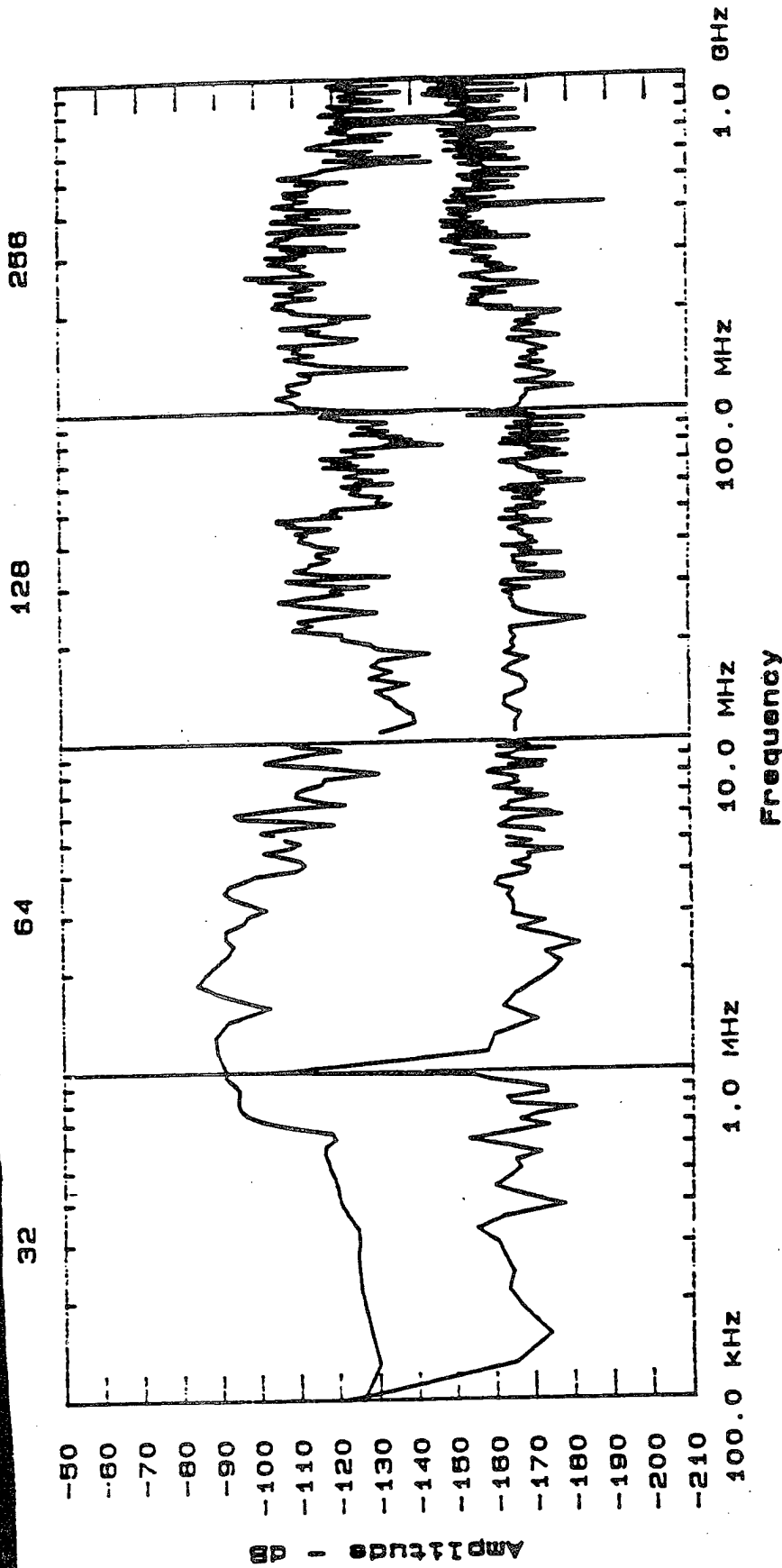


Signal to Noise Report

4: 07 PM WED., 3 JUNE, 1992

Test Point V092B
Test Type Wide Area
Facility THE HOUSE
Test Time 06-03-92 16: 03
Sig Probe IC39

Freq: Min 100.00 kHz
Max 1000.0 MHz
Amp1: Min -189.63 dB
Max -84.13 dB
Inst Link V092
Noise Set 0.0 dB
Sig Atten 10 Hz
Bandwidth 12.0 dBm
Source Amp1

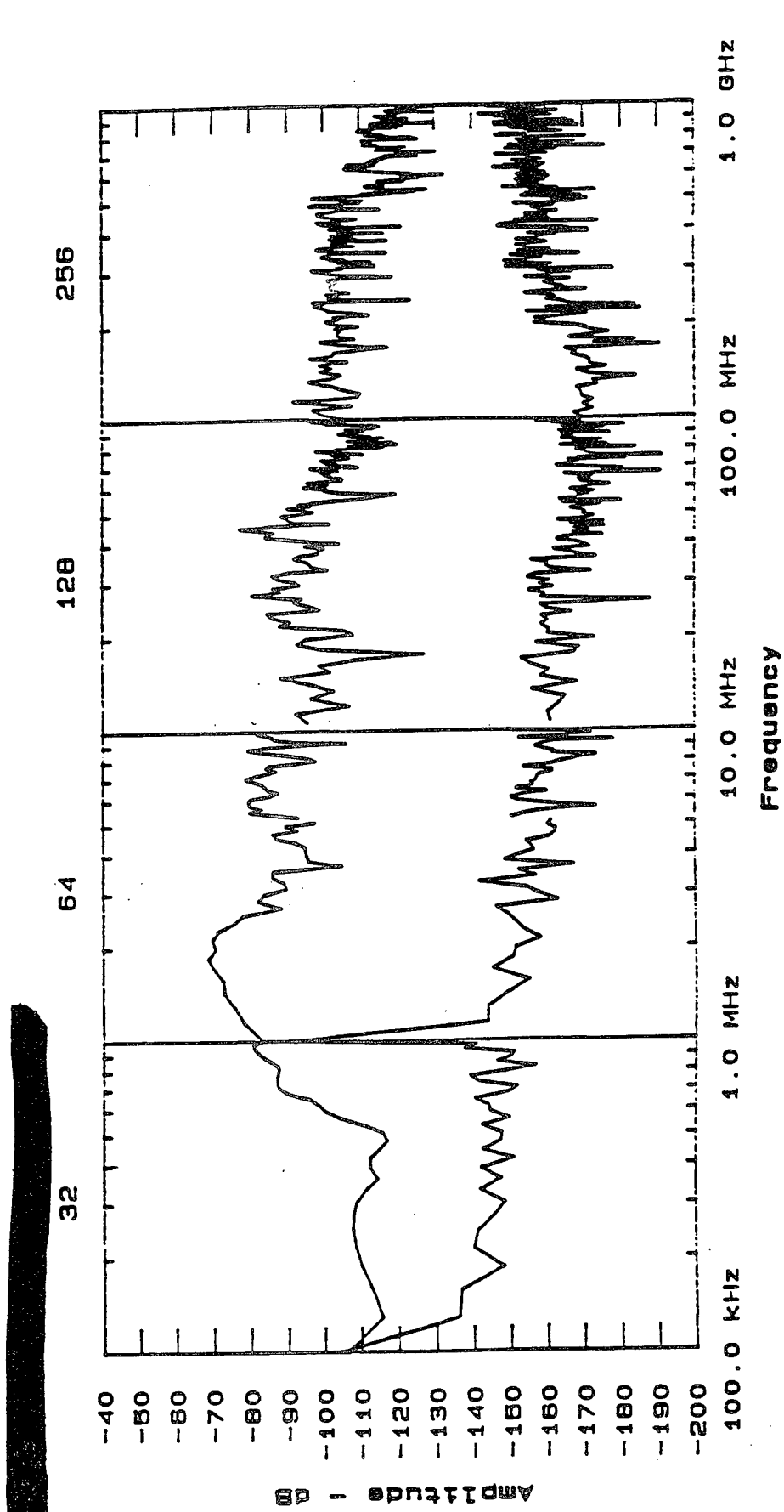


D-21

Signal to Noise Report

4:09 PM TUE.: 16 JUNE. 1992

Test Point	H091	Freq:	Min	100.00 kHz	Inst Link
Test Type	Wide Area	Max	1000.0 MHz	Noise Set	
Facility	THE HOUSE	Amp1:	Min	-191.13 dB	S1g Attten
Test Time	06-16-92 15:54	Max	-68.59 dB	Bandwidth	
Sig Probe	IC39			-12.0 dBm	Source Amp1



D-22

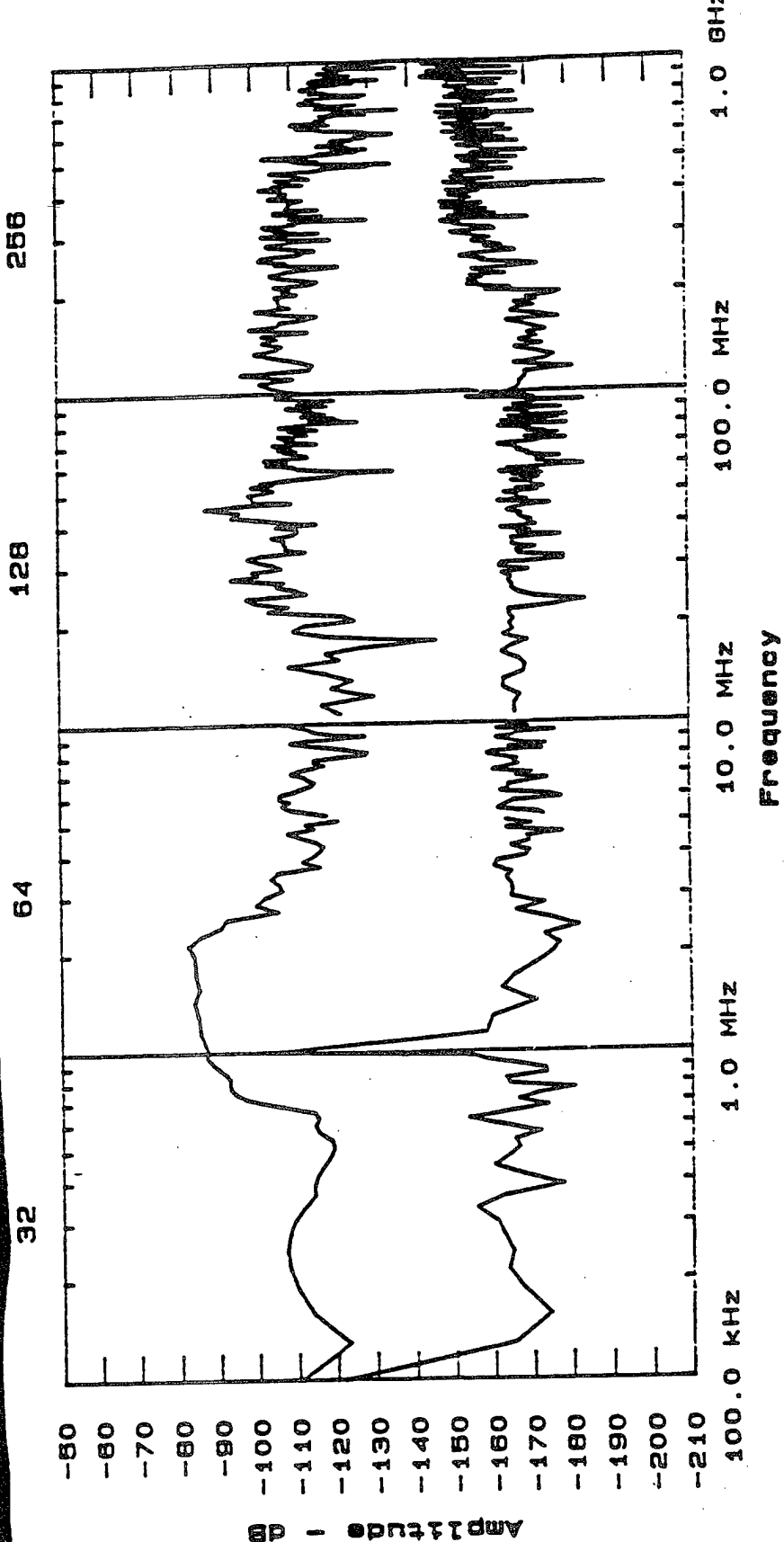
Signal to Noise Report

4: 12 PM TUE.. 16 JUNE. 1992

Test Point H092
 Test Type Wide Area
 Facility THE HOUSE
 Test Time 06-16-92 16:55
 Sig Probe IC39

Freq: Min 100.00 kHz
 Max 1000.0 MHz
 Amp 1: Min -189.63 dB
 Max -82.46 dB
 Inst Link V092
 Noise Set 0.0 dB
 S1G Atten 10 Hz
 Bandwidth 102.0 dBm
 Source Amp 1

[REDACTED]



D-23

Signal to Noise Report

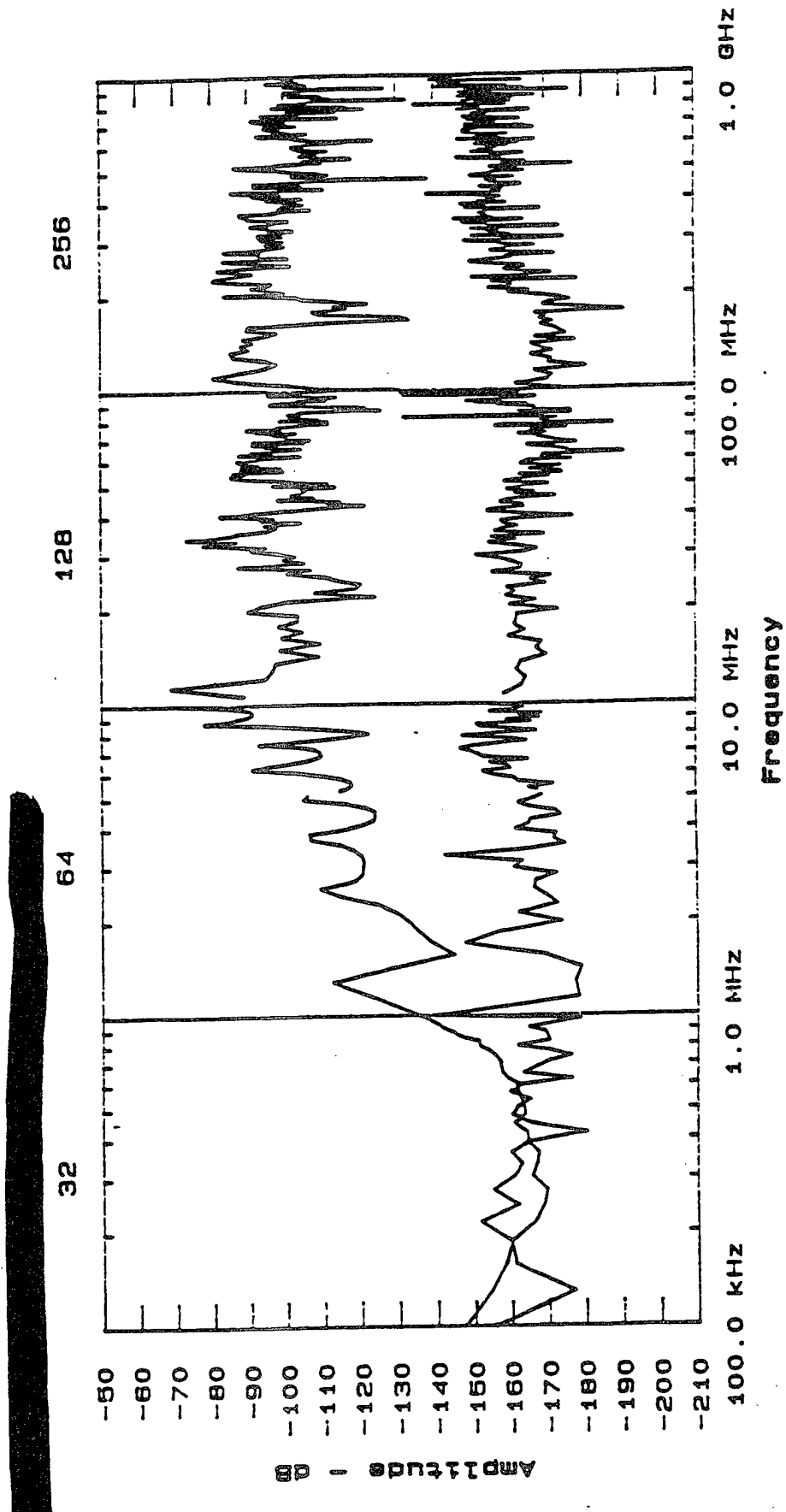
3: 39 PM WED.. 3 JUNE, 1992

Test Point V101
Test Type Wide Area
Facility THE HOUSE
Test Time 06-03-92 16: 38
S19 Probe IC39

Freq: Min 100.00 kHz
Max 1000.0 MHz
Amp1: Min -191.21 dB
Max -69.14 dB

Inst Link
Noise Set
S19 Atten
Bandwidth
Source Amp 1

V101
0.0 dB
10 Hz
-12.0 dBm



D-24

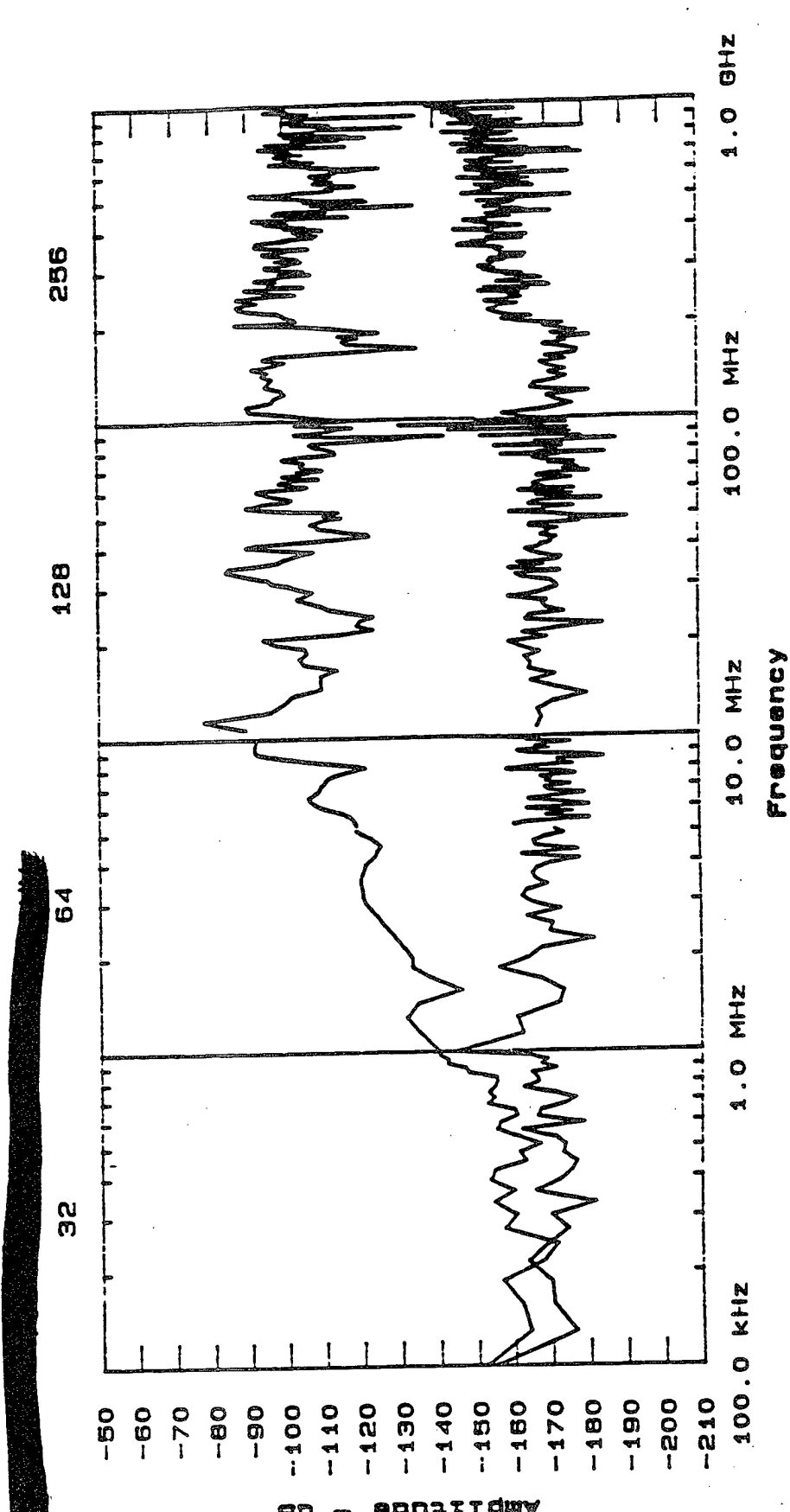
Signal to Noise Report

3: 42 PM WED..

3 JUNE. 1992

Test Point V102
Test Type Wide Area
Facility THE HOUSE
Test Time 06-03-92 15: 39
Sig Probe 1C39

Test Point	V102	Freq:	Min	100.00 kHz	Inst Link	V102
Test Type	Wide Area		Max	1000.0 MHz	Noise Set	0.0 dB
Facility	THE HOUSE	Amp1:	Min	-191.00 dB	Sig Atten	10 Hz
Test Time	06-03-92 15: 39		Max	-78.14 dB	Bandwidth	-12.0 dBm
Sig Probe	1C39				Source Amp1	



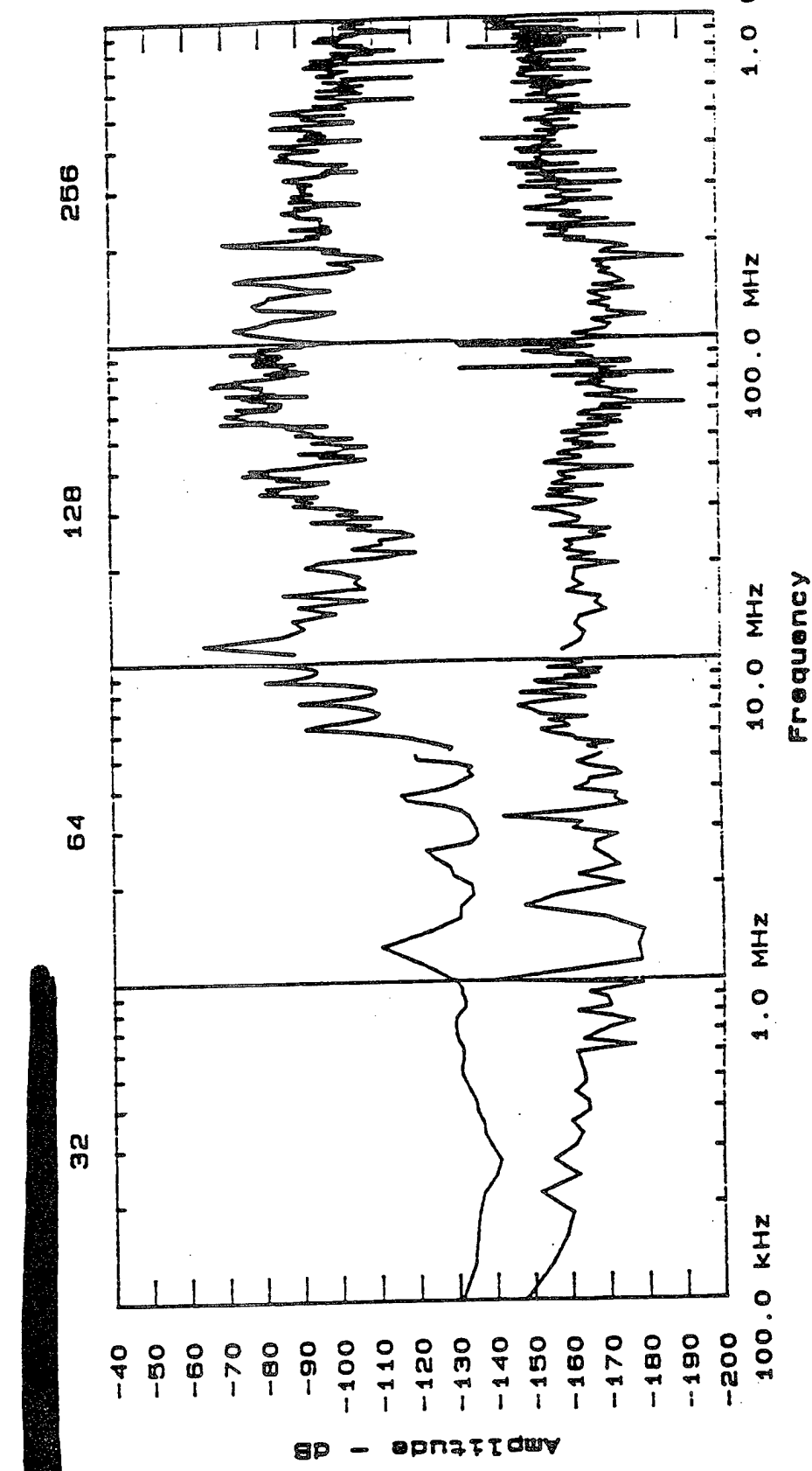
D-25

Signal to Noise Report

4: 14 PM TUE .. 16 JUNE. 1992

Test Point H104
 Test Type Wide Area
 Facility THE HOUSE
 Test Time 06-16-92 15: 66
 Sig Probe IC38

H104	Freq:	Min	100.00 kHz	Inst Link
Wide Area		Max	1000.0 MHz	V101
THE HOUSE	Amp1:	Min	-191.21 dB	Noise Set
06-16-92 15: 66		Max	-64.42 dB	Sig Attenuation
IC38				Bandwidth
				Source Amp1
				-12.0 dBm

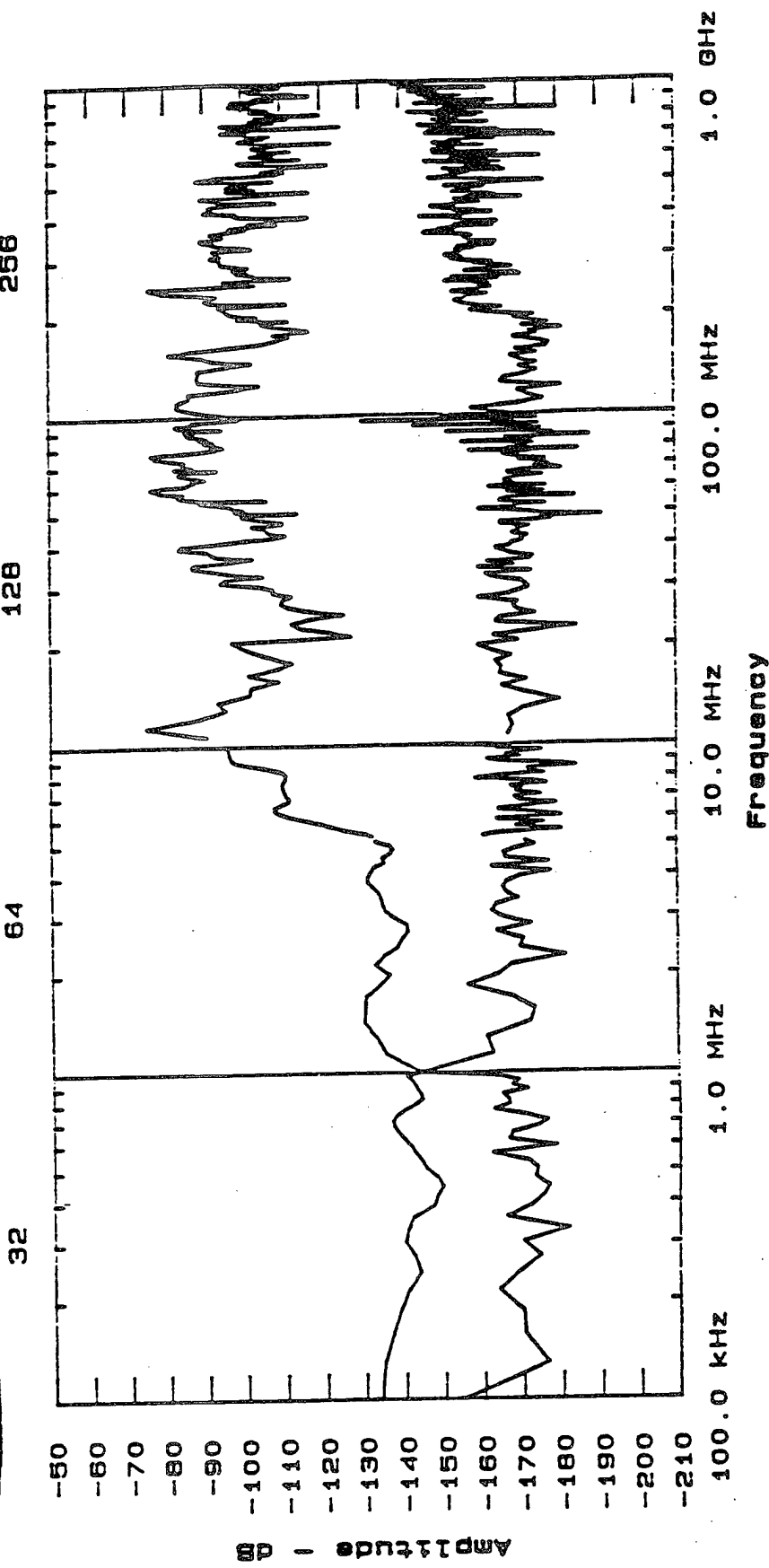


D-26

Report to Noise Pollution Committee

4: 17 PM TUE : 16 JUNE, 1992

H102 Point Wide Area THE HOUSE 06-16-92 15: 57
IC39 Probe



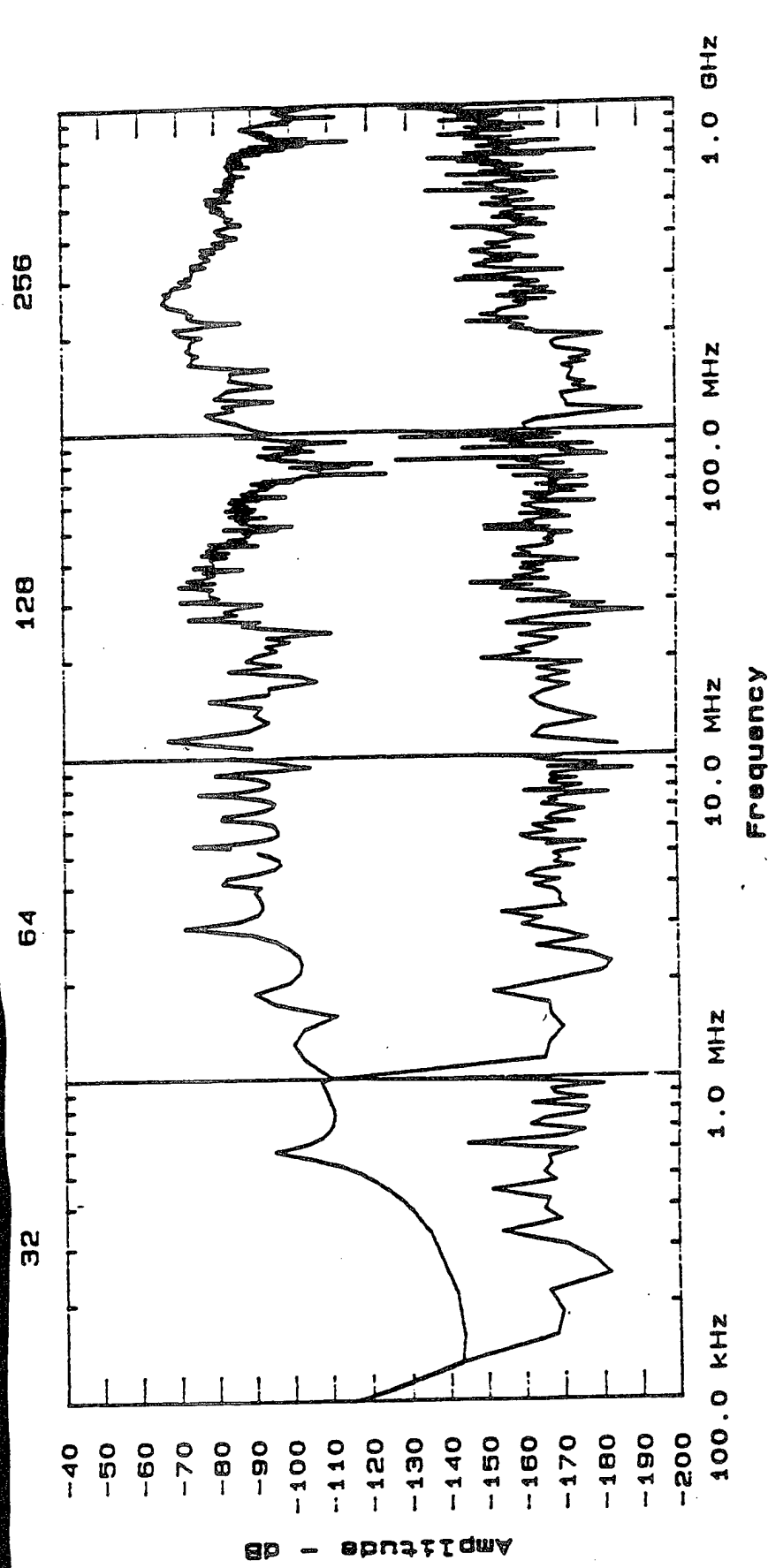
Signal to Noise Report

3: 44 PM WED. 3 JUNE. 1992

Test Point
Test Type
Facility
Test Time
Sig Probe

V111
Wide Area
THE HOUSE
06-03-92 18:40
IC39

Freq: Min 100.00 kHz
Max 1000.0 MHz
Amp1: Min -191.36 dB
Max -68.46 dB
Inst Link V111
Noise Set 0.0 dB
S1g Atten 10 Hz
Bandwidth 100.0 dBm
Source Amp1

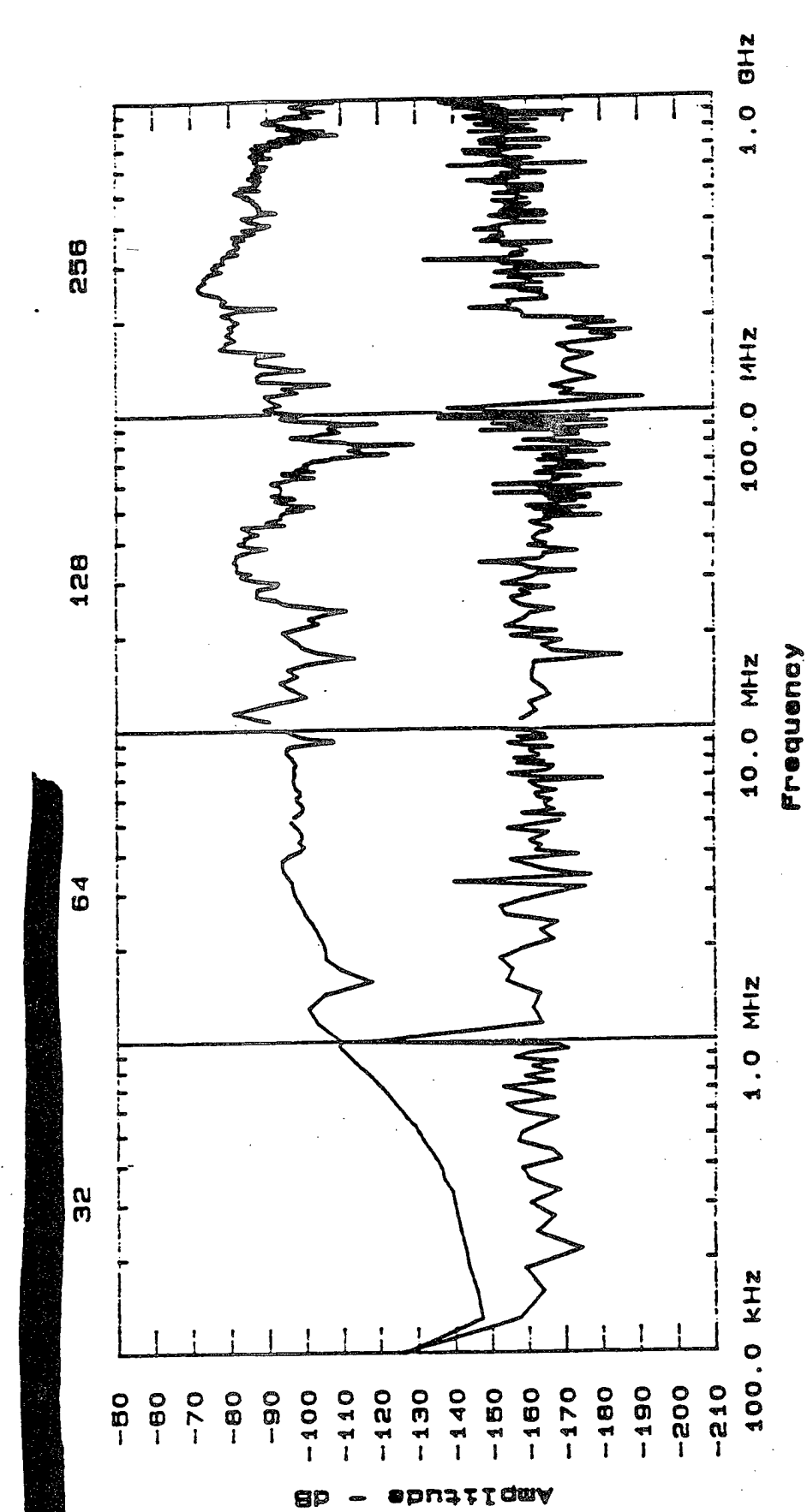


D-28

Signal to Noise Report

3: 47 PM WED.. 3 JUNE. 1992

Test Point	V412	Wide Area	Inst Link
Test Type	THE HOUSE	Noise Set	V412
Facility	06-03-92 15: 41	SIG Atten	0.0 dB
Test Time	IC39	Bandwidth	10 Hz
SIG Probe		Source Amp 1	-12.0 dB



D-29

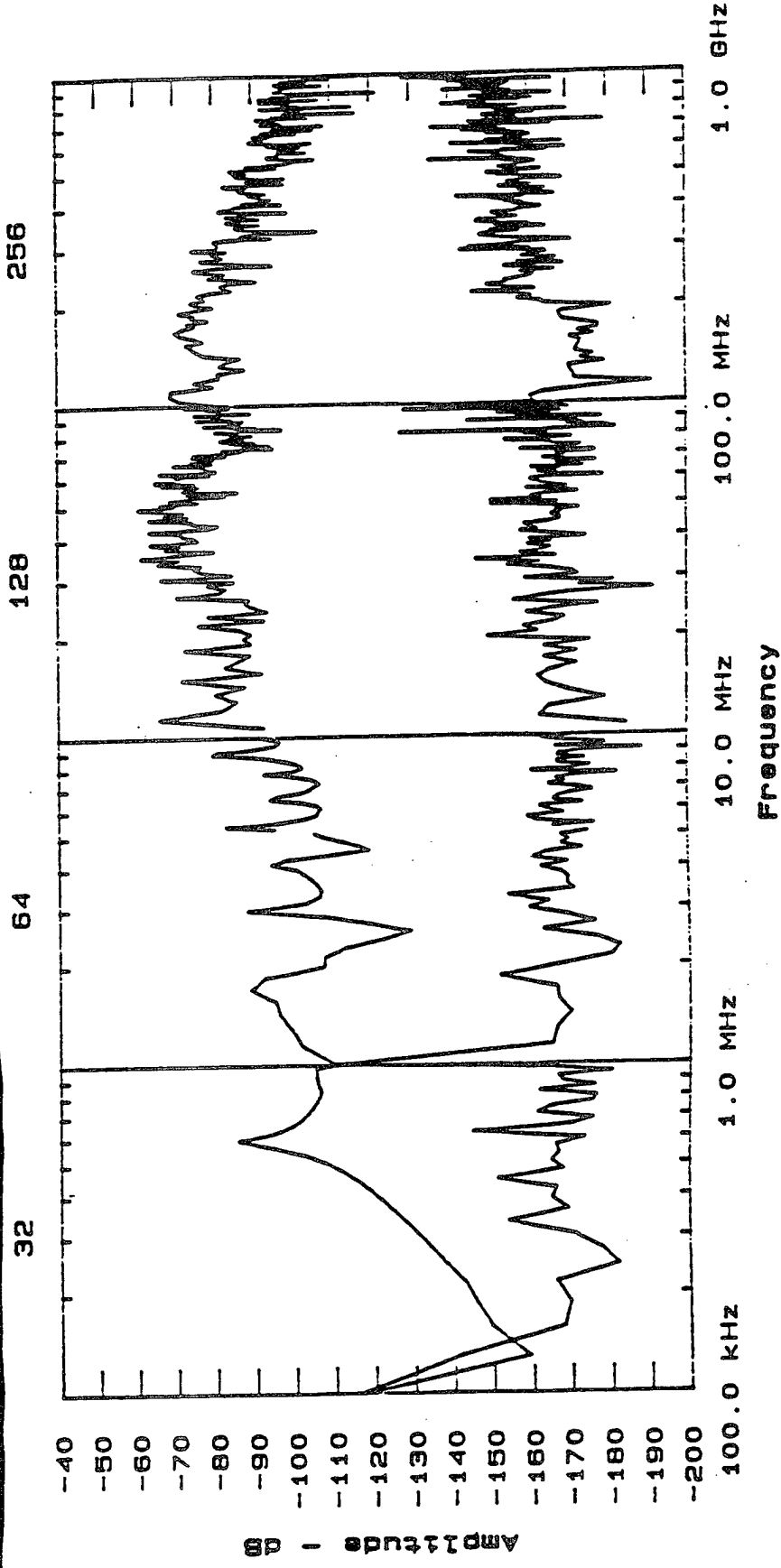
Signal to Noise Report

4:04 PM TUE.. 16 JUNE. 1992

Test Point H111
Test Type Wide Area
Facility THE HOUSE
Test Time 06-16-92 15:52
Sig Probe IC39

H111 Freq: Min 100.00 kHz
Wide Area Max 1000.0 MHz
Test Type Amp1: Min -191.36 dB
Facility Max -60.88 dB
Test Time Source Amp1 -12.0 dBm

[REDACTED]

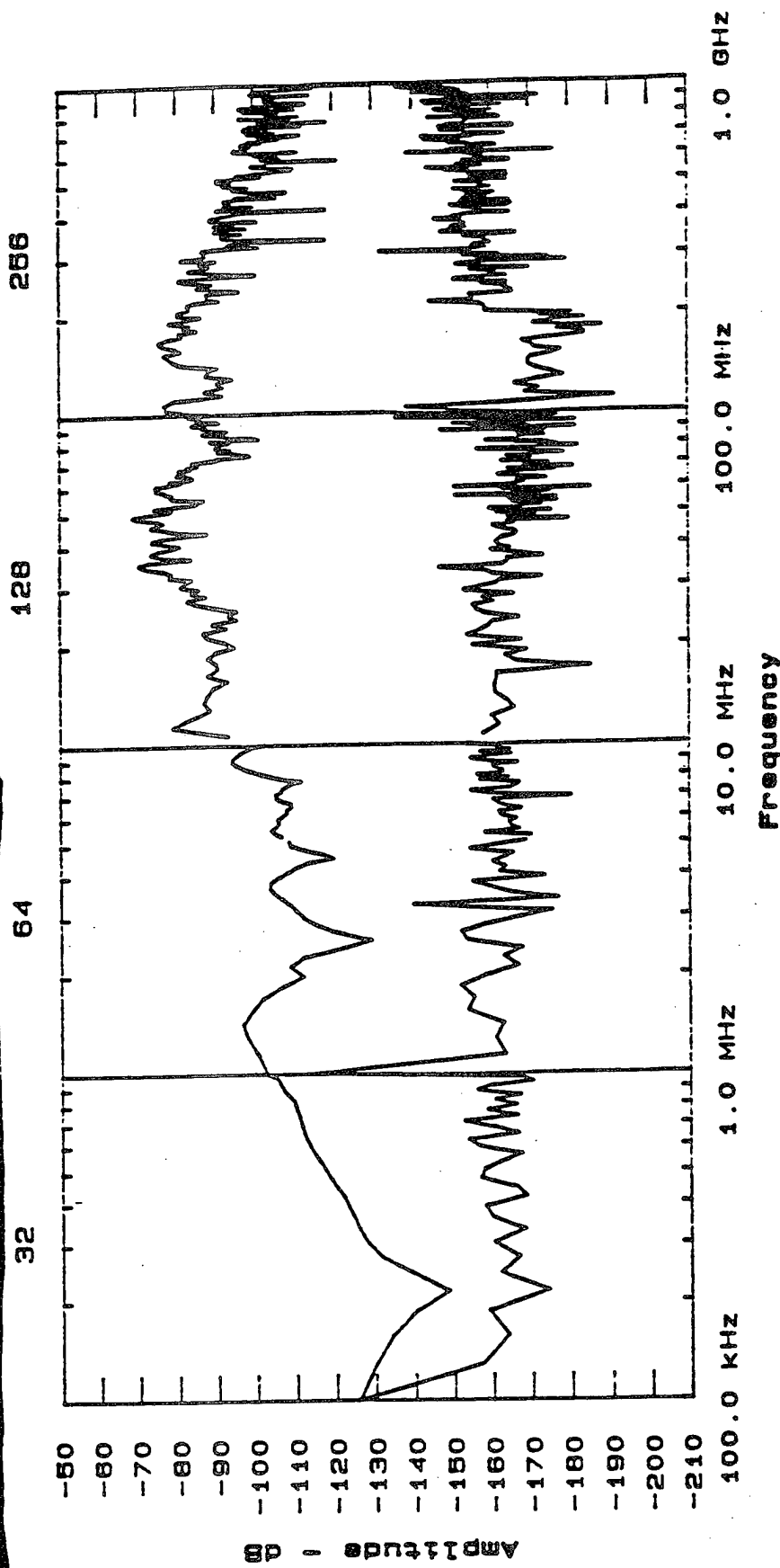


Signal to Noise Report

4: 06 PM TUE.. 16 JUNE, 1992

Test Point H112
 Test Type Wide Area
 Facility THE HOUSE
 Test Time 08-16-92 15: 53
 S1g Probe IC39

Freq: Min 100.00 kHz
 Max 1000.0 MHz
 Amp1: Min -191.24 dB
 Max -69.10 dB
 Inst Link V112
 Noise Set 0.0 dB
 S1g Atten 10 Hz
 Bandwidth -12.0 dBm



D-31